TAMPEREEN TEKNILLINEN YLIOPISTO
TAMPERE UNIVERSITY OF TECHNOLOGY

Markus Takala

Electrical Insulation Materials towards Nanodielectrics

Julkaisu 928 • Publication 928

Tampere 2010

Tampereen teknillinen yliopisto. Julkaisu 928
Tampere University of Technology. Publication 928

Markus Takala

Electrical Insulation Materials towards Nanodielectrics

Thesis for the degree of Doctor of Science in Technology to be presented with due permission for public examination and criticism in Sähkötalo Building, Auditorium S4, at Tampere University of Technology, on the 24th of November 2010, at 12 noon.

Tampereen teknillinen yliopisto - Tampere University of Technology
Tampere 2010

Supervisors

Adjunct Professor Kari Kannus
Department of Electrical Energy Engineering
Tampere University of Technology

Professor Seppo Valkealahti
Department of Electrical Energy Engineering
Tampere University of Technology

D. Sc. (Tech.) Kari Lahti
Department of Electrical Energy Engineering
Tampere University of Technology

Pre-examiners

Professor Stanislaw Gubanski
Department of Materials and Manufacturing Technology
Chalmers University of Technology

Assistant Professor Masahiro Kozako
Department of Electrical Engineering and Electronics
Kyushu Institute of Technology

Opponents

Professor Stanislaw Gubanski
Department of Materials and Manufacturing Technology
Chalmers University of Technology

Professor John Fothergill
Department of Engineering
University of Leicester

Tampere University of Technology
Faculty of Computing and Electrical Engineering
Department of Electrical Energy Engineering

ISBN 978-952-15-2460-8 (printed)
ISBN 978-952-15-2485-1 (PDF)
ISSN 1459-2045

Abstract

New insulation materials can be tailored by compounding nanofillers and polymer materials. The advantageous changes in properties of polymer nanocomposites can be explained by the large interface area of the nanofillers. Theoretical models developed in the field of nanodielectrics concentrate on the analysis of the interface volume. Dielectric breakdown strength (DBS) is one of the most important properties of an insulation material. The DBS of nanocomposites depends heavily on the nanofiller content and even small quantities can cause improvement. This is linked to the maximum interface volume achieved even at low nanofiller concentrations. Homogeneous nanodispersion is the key for DBS increase and reliable results. Often the most profitable nanofiller quantities are below 5 wt-%. A similar observation was made with relative permittivity and dielectric losses of nanocomposites. At low nanofiller concentrations the relative permittivity and dielectric losses stay at the reference level or are even lower. With increasing nanofiller content relative permittivity and dielectric losses start to increase. This is related to the overlapping of interfacial zones of nanoparticles. The overlapping of the interfacial zones also depends on the nanofiller size and dispersion. The treeing growth and partial discharge (PD) endurance of nanocomposites was found to have a partly different kind of behaviour. Surface PD endurance of nanocomposites is strongly a mass related phenomenon, but treeing growth is more complex. It is related to large interface volume of nanocomposites having similar behaviour as observed with short-time DBS.

In this dissertation the above mentioned dielectric properties are studied experimentally, concentrating on silica (SiO_2)-polypropylene (PP), polyhedral oligomeric silsesquixane (POSS)-PP and POSS-epoxy (EP) nanocomposites. The dielectric properties are verified for sheet samples. In DBS measurements ac, dc and lightning impulse (LI) voltage shapes are used. Relative permittivity and dielectric losses are measured with insulation diagnosis analyzer (IDA) or with arbitrary waveform impedance spectroscopy (AWIS). PD endurance of nanocomposites is investigated with rounded rod- or conical rod-plane electrode setups.

Proper nanodispersion is reflected in improved dielectric behaviour of 5 wt-% SiO_2-PP nanocomposite. 5 wt-% SiO_2-PP nanocomposite showed a promising combination of dielectric properties especially considering ac and dc power capacitors. The ac and dc breakdown strength of 5 wt-% SiO_2-PP nanocomposite increased 20 % and 52 % respectively. It is equally important that with both ac and dc voltages the β value in the Weibull probability function is higher with the nanocomposite than with the reference PP, indicating a smaller standard deviation and more homogeneous material. These results have an interesting impact on insulation system design, because safety margins and insulation thicknesses could be reduced. With 5 wt-% SiO_2-PP nanocomposite dielectric losses remained comparable to reference PP. Capacitance did decrease with both materials until 80 °C. This is important, considering e.g. power capacitors, which operate in the 50-60 °C temperature region. There is no capacitance change compared to reference PP and no additional heat is produced due to low loss factor. In PD endurance measurements the average lifetime of 5 wt-% SiO_2-PP nanocomposite was 9 times longer than with reference PP. Also, at the same voltages the PD levels were higher for reference PP than for 5 wt-% SiO_2-PP nanocomposite. Surface analysis of the films revealed that a layer of silicon oxides

formed on the surfaces of the 5 wt-% SiO_2-PP nanocomposite during PD stress. The layers may protect this nanocomposite from degradation and lengthen the lifetime of the sample. This shielding behaviour is significant because the layers are formed due to PD stress to critical spots of insulation.

With respect to the properties of nanodielectrics studied possible applications could be e.g. capacitors, cables, dry transformers, rotating machines, switchgear and outdoor insulations. Although the future of nanodielectrics is promising, there are many questions to be resolved. Manufacturing processes must be optimized and up-scaled to larger volumes. Promising results have mainly been achieved with short-term measurements and work has been done to understand mechanisms behind the functionality, which is important. Full scale models of applications should be produced and long-term measurements conducted in operating conditions. Long-term measurements for real components will finally reveal the actual benefits and possible drawbacks of nanocomposites compared to the insulation materials used at the moment. In addition to dielectric properties, the thermal, mechanical, chemical and ageing properties critical for each component must be verified. This means that the industry should be intensively linked to develop actual new products.

Preface

This dissertation work was carried out in the Department of Electrical Energy Engineering, Tampere University of Technology (TUT), Finland during the period 2005-2010. It was conducted under the supervision of Adjunct Professor Kari Kannus, Doctor Kari Lahti and Professor Seppo Valkealahti, to whom I would want to address my deepest gratitude. Without their guidance and support, this work could not have been done.

I would like to acknowledge the co-authors of my publications for their valuable contributions. I am also grateful to all colleagues who worked and are working in the High Voltage Laboratory at TUT especially to Lasse Linnamaa M. Sc., Pekka Nevalainen M. Sc., Dr. Pertti Pakonen, Hannes Ranta M. Sc., Tiila Sallinen M. Sc. and Pauliina Salovaara M. Sc. for all the scientific comments, discussions and encouragements. Furthermore, I sincerely thank Merja Teimonen and Marja Oksavuori, the department secretaries, who helped with all administrative matters.

I am grateful for co-operation with the Technical Research Centre of Finland (VTT) for supplying all the materials for dielectric measurements. Dr. Martin Albers, Harri Joki M. Sc., Mikko Karttunen Lic. Tech., Satu Kortet M. Sc., Dr. Tony Munter, Dr. Mika Paajanen, Jani Pelto M. Sc. and Lisa Wikström M. Sc. are gratefully acknowledged. Co-operation with the University of Jyväskylä (JyU) has also been fruitful, with Susanna Ahonen M. Sc., Viivi Koivu M. Sc., Prof. Mika Pettersson and Suvi Virtanen M. Sc.

From my research exchange period at Chalmers University of Technology (Chalmers), Gothenburg, Sweden I would like to thank Björn Sonerud PhD, Prof. Stanislaw Gubanski and the other researchers working in the High Voltage Group, for providing assistance in conducting research abroad and in life in general. From my research exchange period to Kitami Institute of Technology (KIT), Kitami, Japan, I would like to thank Prof. Noriyoshi Sugawara for assistance in conducting the inclined plane tests for epoxy nanocomposites.

Thanks also to the Steering Group members of the POMSU, HYDSO, NANOCAPO, Forest-SAX and NANOCOM Tekes projects. The discussions have been useful in guiding this research work and also in linking it to industrial needs.

The financial support from the TUT Graduate School, the Finnish Funding Agency for Technology and Innovations (Tekes), the Fortum Foundation, the Finnish Foundation of Technology, the Emil Aaltonen Foundation, the Walter Ahlström Foundation, the Ulla Tuominen Foundation, the Scandinavia-Japan Sasakawa Foundation, the Technical Society of Tampere are gratefully acknowledged.

Virginia Mattila of the University of Tampere is acknowledged for improving my English and proofreading all my publications and this dissertation.

Thanks to my mother and dad, Kaisa and Josu, and brother, Tuomas for supporting me during my studies.

Finally, I thank my wife, Johanna and daughters, Pihla and Venla for letting me visit Sweden and Japan. I also want to thank them for their support and patience during my studies.

Tampere, September 28th 2010

Markus Takala

Table of Contents

Abstract i
Preface iii
Table of Contents v
List of publications vii
Author's contribution viii
List of abbreviations and symbols x
1 . Introduction 1
1.1 Motivation and target 1
1.2 Research problem and structure of the dissertation 2
2 . Nanotechnology and dielectric materials 3
2.1 Background – from micro to nanofillers 3
2.2 Nanocomposites – functional materials 3
2.3 Theoretical models 8
2.4 Processing of nanocomposites 10
2.5 Dielectric properties of nanocomposites 11
3 . Dielectric breakdown strength 13
3.1 Experimental measurements 13
3.2 Affecting factors 14
3.3 Effect of the voltage shape 17
3.4 Summary 20
4 . Relative permittivity and dielectric losses 23
4.1 Experimental measurements 23
4.2 Affecting factors 24
4.3 Frequency and temperature dependency 30
4.4 Humidity and functionalization dependence 31
4.5 Summary 33
5 . Treeing growth and partial discharge endurance 36
5.1 Experimental measurements 36
5.2 Affecting factors 37
5.3 Bulk and surface degradation phenomena 42
5.4 Summary 43

6 . Discussion 46
6.1 Future trends and challenges 46
6.2 Applicability of nanocomposites 47
7 . Conclusion 50
References 53
Publications 64

List of publications

[P1] M. Takala, P. Salovaara, T. Keikko, K. Kannus, FEM Modeling of Polypropylene and PANI-EB Layer Structure, *International Review of Electrical Engineering*, Vol. 1, No. 5, pp. 613-618, (2006)

[P2] M. Takala, S. Kortet, P. Salovaara, M. Karttunen, K. Kannus, AC Breakdown Strength of Polypropylene-Calcium Carbonate Compounds, In *Proceedings of Nordic Insulation Symposium* (NORD-IS07), Copenhagen, Denmark, June 11-13, pp. 123-126, (2007)

[P3] M. Takala, M. Karttunen, P. Salovaara, S. Kortet, K. Kannus and T. Kalliohaka, Dielectric Properties of Nanostructured Polypropylene-Polyhedral Oligomeric Silsesquioxane Compounds, *IEEE Transactions on Dielectrics and Electrical Insulation*, Vol. 15, No. 1, pp. 40-51, (2008)

[P4] M. Takala, T. Sallinen, P. Nevalainen, J. Pelto and K. Kannus, Surface Degradation of Nanostructured Polypropylene Compounds Caused by Partial Discharges, In *Proceedings of IEEE International Symposium on Electrical Insulation* (ISEI 2008), Vancouver, Canada, June 8-11, pp. 205-209, (2008)

[P5] M. Takala, M. Karttunen, J. Pelto, P. Salovaara, T. Munter, M. Honkanen, T. Auletta and K. Kannus, Thermal, Mechanical and Dielectric Properties of Nanostructured Epoxy-Polyhedral Oligomeric Silsesquioxane Composites, *IEEE Transactions on Dielectrics and Electrical Insulation*, Vol. 15, No. 5, pp. 1224-1235, (2008)

[P6] M. Takala, H. Ranta, J. Pelto, S. Virtanen, V. Koivu, M. Pettersson and K. Kannus, Dielectric Properties of Polypropylene-Silica Nanocomposites, In *Proceedings of Nordic Insulation Symposium* (NORD-IS09), Gothenburg, Sweden, June 15-17, pp. 31-35, (2009)

[P7] M. Takala, B. Sonerud, H. Ranta, J. Pelto, S. Ahonen, M. Pettersson and K. Kannus, Effect of Low Amount of Nanosilica on Dielectric Properties of Polypropylene, In *Proceedings of IEEE International Conference on Solid Dielectrics* (ICSD 2010), Potsdam, Germany, July 4-9, pp. 187-191, (2010)

[P8] M. Takala, H. Ranta, P. Nevalainen, P. Pakonen, J. Pelto, M. Karttunen, S. Virtanen, V. Koivu, M. Pettersson, B. Sonerud and K. Kannus, Dielectric Properties and Partial Discharge Endurance of Polypropylene-Silica Nanocomposite, *IEEE Transactions on Dielectrics and Electrical Insulation*, Vol. 17, No. 4, pp. 1259-1267, (2010)

Author's contribution

The author wrote all the publications and this dissertation. The material processing and morphology analysis chapters in the publications were written by Mikko Karttunen Lic. Tech., Dr. Tony Munter and Jani Pelto M. Sc. of VTT and Viivi Koivu M. Sc., Dr. Mika Pettersson and Suvi Virtanen M. Sc. of the University of Jyväskylä. The materials for all the studies were processed at VTT by Mikko Karttunen Lic. Tech., Satu Kortet M. Sc., Dr. Tony Munter and Jani Pelto M. Sc.

In publication P1 the author has conducted the dielectric measurements with Pauliina Salovaara M. Sc. and the FEM modeling with Dr. Tommi Keikko.

In publication P2 the author conducted the measurements and statistical analysis of the results.

In publication P3 the author conducted the ac and lightning impulse (LI) breakdown strength and dielectric spectroscopy measurements and the statistical analysis of the results. Scanning electron microscope (SEM) characterization and discharging time measurements were conducted at VTT and Raman-atomic force microscope (Raman-AFM) spectroscopy at WiTEC GmbH by Mrs. Andrea Jauss and at Cheos Oy by Mr. Kim Grundström.

In publication P4 the author conducted the surface degradation measurements with Pekka Nevalainen M. Sc. and Tiila Sallinen M. Sc. The author conducted the surface analysis with optical profilometer and analysis of the results. Transmission electron microscope (TEM) spectroscopy was conducted by Jani Pelto M. Sc.

In publication P5 the author conducted the ac and LI breakdown strength and dielectric spectroscopy measurements and statistical analysis of the results. The morphology studies with SEM and AFM, differential scanning calorimeter measurements and mechanical testing were done at VTT by Mikko Karttunen Lic. Tech. and Jani Pelto M. Sc. The TEM characterization was conducted at TUT in the Department of Materials Science by Mari Honkanen M. Sc.

In publication P6 the author conducted the ac and dc breakdown strength and dielectric spectroscopy measurements and statistical analysis of the results. The morphology studies with micro-Raman, X-ray and TEM were conducted at the University of Jyväskylä by Viivi Koivu M. Sc., Dr. Mika Pettersson and Suvi Virtanen M. Sc.

In publication P7 the author conducted the dc breakdown strength measurements and statistical analysis of the results. Dielectric response measurements were conducted with Björn Sonerud PhD at Chalmers University of Technology and TEM characterization was carried out at the University of Jyväskylä by Susanna Ahonen M. Sc. and Dr. Mika Pettersson.

In publication P8 the author conducted the ac and dc breakdown strength and PD endurance measurements and statistical analysis of the results. Dielectric response measurements were conducted with Björn Sonerud PhD at Chalmers University of

Technology and morphology and surface analysis were carried out at the University of Jyväskylä by Dr. Mika Pettersson and Suvi Virtanen M. Sc.

List of abbreviations and symbols

ac	alternating current
AFM	atomic force microscopy
Al_2O_3	alumina
ATH	aluminatrihydrate (microfiller)
AWIS	arbitrary waveform impedance spectroscopy
$BaTiO_3$	barium titanate
$CaCO_3$	calcium carbonate
CIGRE	International Council on Large Electric Systems
DBS	dielectric breakdown strength
dc	direct current
EP	epoxy
EVA	ethylene vinyl acetate
FEM	finite element method
HYDSO	abbreviation for research project “Hybrid materials and their applications”
IDA	Insulation Diagnosis Analyzer
IEC	International Electrotechnical Commission
IEEE	Institute of Electrical and Electronics Engineers
JyU	University of Jyväskylä
KIT	Kitami Institute of Technology
LDPE	low density polyethylene
LFD	low-frequency dispersion
LFS	liquid flame spray
LI	lightning impulse
LS	layered silicate
Forest-SAX	abbreviation for research project “High voltage covered conductor line for forest areas”
MgO	magnesia
MMT	montmorillonite
NANOCAPO	abbreviation for research project “Nanocomposite polymer capacitor film”
NANOCOM	abbreviation for research project “Novel methods to formulate polymer nanocomposites and tailor their dielectric properties”
NMMC	nano- and microfiller mixture composite
PA	polyamide
PANI	polyaniline
PD	partial discharge
PE	polyethylene
PEI	polyetherimide
PI	polyimide
POMSU	abbreviation for research project “Potential new applications of polymers in high voltage technology”
POSS	polyhedral oligomeric silsesquioxane
PP	polypropylene
PVDF	polyvinylidenefluoride
QDC	quasi-dc conduction

RMS	root mean square
SEM	scanning electron microscopy
SiC	silicon carbide
SiO_2	silica
SR	silicone rubber
Tekes	The Finnish Funding Agency for Technology and Innovations
TEM	transmission electron microscopy
TiO_2	titania
TSC	thermally stimulated current
TUT	Tampere University of Technology
VTT	Technical Research Centre of Finland
XLPE	cross-linked polyethylene
ZnO	zinc oxide

α	scale parameter in Weibull distribution
β	shape parameter in Weibull distribution
C_e	edge capacitance
C_p	parallel capacitance
C_0	vacuum capacitance
d	thickness
dif	difference between the mean values
E	electric field strength
ε_r	relative permittivity
ε'	real part of relative permittivity
ε''	imaginary part of relative permittivity
n	power law exponent
ω	angular frequency
R_p	parallel resistance
s	standard deviation
s_{ave}	average standard deviation
$\tan\delta$	dissipation factor
T_g	glass transition temperature

1 . Introduction

Electricity and its distribution to customers are in a key role in ensuring human well-being. Insulation materials are a vital part of the components used in a electrical energy distribution network. In recent years interest in advanced materials e.g. nanodielectrics has been growing. The use of nanotechnology in insulation materials is a new way to develop dielectric materials. In the past, the target was to produce as pure as possible dielectric material, and thus ensure the optimal performance of the component. By contrast, nanodielectrics are dielectric materials mixed with inorganic particles size 1 to 100 nm. The idea of nanocomposites is to use small mass amounts of nanofillers to produce a large interfacial area between the matrix polymer and nanofillers. It is possible to tailor the properties of a dielectric. A homogeneous dispersion of nanoparticles is a prerequisite for improved dielectric properties. The aim of this dissertation is to improve the performance of the nanodielectrics and thus develop better insulation materials for electricity distribution components.

1.1 Motivation and target

Insulating materials are used to isolate components of higher potential from places where it is undesired. They are applied in every electrical application and have been developed for decades. In many electrical applications insulation is in the key role in ensuring the functionality of the equipment. Knowledge of the insulation material helps us in planning investments in the power system and the insulation material developers can choose the best possible option for each application. It is also possible to optimise the insulation further. Insulation structures used are often thick because of the risk-free planning. With new nanomaterials it is possible to achieve more applicable and economical insulation structures.

The development of nanodielectric materials offers advantages for electrical equipment manufacturers. The ideas of long-term thinking and life-cycle analysis have increased in recent years, including in energy engineering. Environmental issues are also becoming more and more important. A symptom of this is the increasing interest in the field of distributed power generation. The idea is to go towards more sustainable power generation and delivery. This dissertation work supports the same goals by improving energy efficient, economical and environmentally friendly electrical power applications by insulation material development.

One good example to demonstrate the importance of insulation materials in components, is the power capacitor. An important improvement for capacitors would be to increase the electric field strength of the insulation material. The reactive power of a capacitor is proportional to the square of the used electric field strength in insulation material. If material can sustain higher electric field, insulation thickness can be reduced to achieve the same reactive power as before. The same can be stated for power cables.

1.2 Research problem and structure of the dissertation

In this dissertation the main objective has been to develop and verify the dielectric properties of new insulation materials. The applicability of the results achieved has been placed in a bigger context in this dissertation.

The research problem can be divided into the following four hypotheses,

1. The electrical properties of a pure base polymer will be enhanced by compounding with nanofillers
2. The comprehensive characterization of the nanocomposites developed will enable their use in different power engineering applications
3. The comprehensive characterization of the nanocomposites developed will provide advantages in the optimization of insulation structures
4. The electrical properties of nanocomposites can be tailored via an understanding of the nanoscale characteristics of the compounds.

The dissertation is a summary of four peer-reviewed publications and four conference proceeding publications, which are presented in the research context in Figure 1.

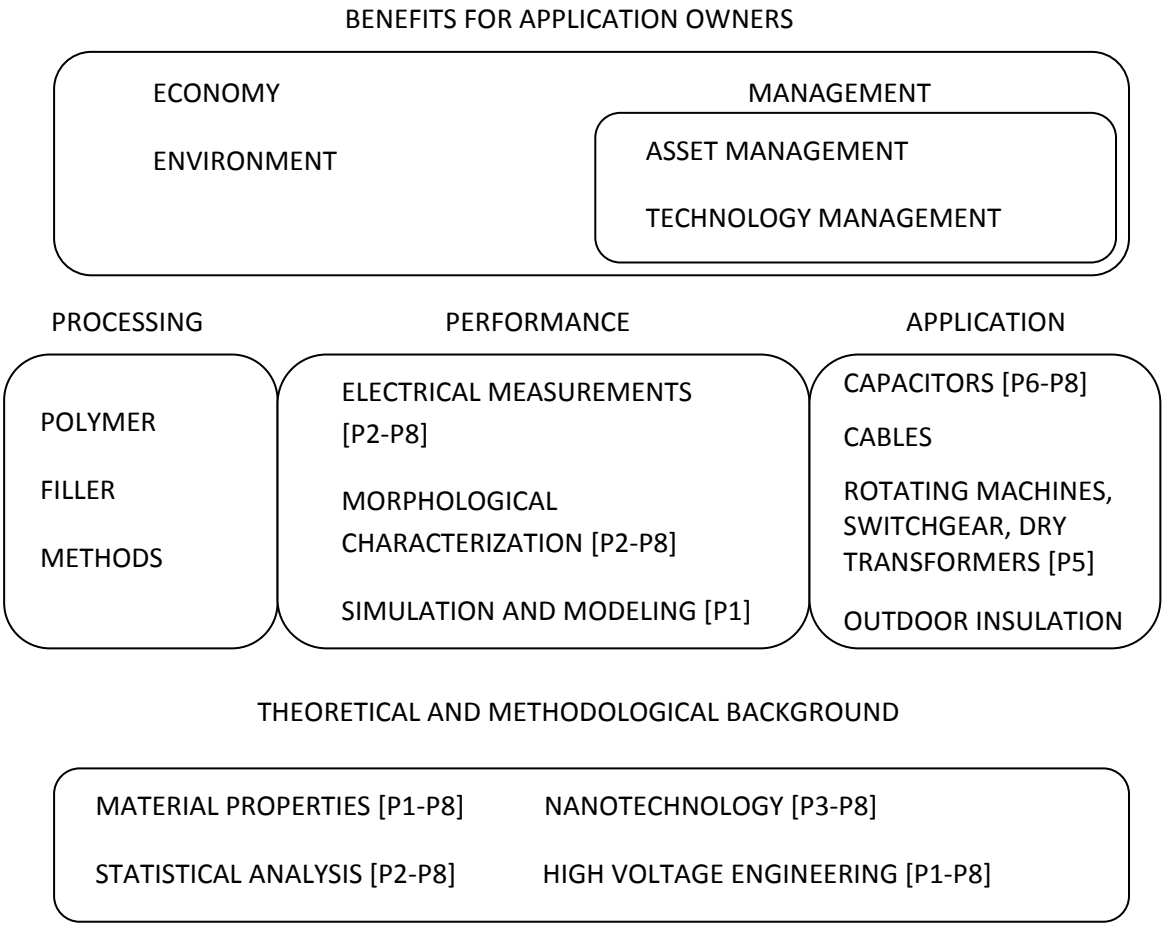

Figure 1. Position of the publications in the research context.

2 . Nanotechnology and dielectric materials

2.1 Background – from micro to nanofillers

Nanofillers or nanoadditives are defined as material having one dimension less than 100 nm. In the field of insulation the word “nanofiller” is mostly used. Polymer nanocomposites are defined as polymers with a small amount (0.1 to 10 wt-%) of nanofillers. Fillers should be homogeneously dispersed in the polymer matrix to form a nanodielectric material [Tan05a, Tan06a]. The mostly used polymers in nanodielectrics research are polyamide (PA), polyethylene (PE), polypropylene (PP), ethylene vinyl acetate (EVA), epoxy resins (EP) and silicone rubbers (SR). Polymers are combined with inorganic nanofillers such as layered silicate (LS), silica (SiO_2), titania (TiO_2), alumina (Al_2O_3), magnesia (MgO).

The short history of nanodielectrics dates back to 1994. The first paper using nanodielectrics was published by John Lewis in the Transactions on Dielectrics and Electrical Insulation (Institute of Electrical and Electronics Engineers, IEEE). The paper is entitled “Nanometric Dielectrics” and discusses the future of insulation materials [Lew94]. After a fairly slow start in the 1990’s nanodielectrics research has increased rapidly in this millennium, which can be seen in the increasing number of publications and group activities in the International Council on Large Electric Systems (CIGRE) and IEEE. The history and development of nanodielectrics have been described more closely in [Dan09, Dis04, Fré01, Fré06a, Fré09, Nel02, Nel06, Nel07, Phi04, Tan05a, Tan06a].

Polymer nanocomposites are the second generation of filled dielectrics in insulation engineering. The first generation of filled dielectrics is microcomposites, which consist of polymers filled with a large amount (of the order of 50-60 wt-%) of micron-sized inorganic fillers (from 100 nm to 100 μm). If the filler weigth content of nano- and microfillers is the same in the matrix, the interfacial surface (area/volume) between the inorganic fillers and the polymer matrix is larger (typically three orders of magnitude) in nanocomposites than in microcomposites [Rae05]. The weight content of the nanoparticles is usually quite low (less than 10 wt-%) because of the low percolation threshold. When nanoparticle content increases beyond the percolation threshold, the nanocomposite may lose its beneficial dielectric properties [Dan09]. The small filler amounts in nanocomposites ensure that inherent polymer properties, e.g. density, remain almost unchanged. The size difference in nano- and microfillers leads to nine orders of magnitude difference in the number of particles at the same filler weight content if the densities and volume contents of fillers are the same. Therefore the distances between neighbouring fillers are much smaller (nanometers) in nanocomposites than in conventional microfilled polymers, if fillers are homogeneously dispersed. More comprehensive discussions on nano-and microcomposites have been published in [Fle08, Fot04, Nel05, Rae05, Sin08a, Tan04].

2.2 Nanocomposites – functional materials

Nanocomposites can be considered to be functional materials. The functionality of nanocomposites is based on large interfacial volume or “interaction zones” [Fot04, Lew04a, Lew04b, Lew05, Mon04, Nel02, Nel03, Nel06, Nel07] in the composite which originates from

large surface to volume ratio of nanofillers. Functionality means that material properties can be improved and tailored by the addition of nanofillers. The increased interfacial volume in nanocomposite changes the structure of the polymer. The properties of interfacial layers (10-20 nm [Smi08]) do not match the properties of polymer matrix or nanofillers. To achieve large interfacial volume, enough filler needs to be used and it should be homogeneously dispersed. A homogeneous dispersion of 1 wt-% octaglycidyldimethylsilyl POSS in EP is presented in atomic force microscopy (AFM) phase images in Figure 2 [P5, Rae05, Roy05]. Figure 2 indicates that there are two slightly different nanostructured phases in the sample. The bright-contrast phase appears to consist of approximately 20 nm interconnected round areas. The large interfacial volume in nanocomposites leads to changes in dielectric properties.

Nanoparticles and their interfaces with the matrix polymer create changes in polymer structure. A highly immobilized layer develops near the surface of the nanofiller through e.g. bondings between polymer and nanofiller. This bound layer influences the region surrounding the particle. The size of the bound layer affects the properties of nanocomposites such as local charge distribution, mobility of polymer chains, chain

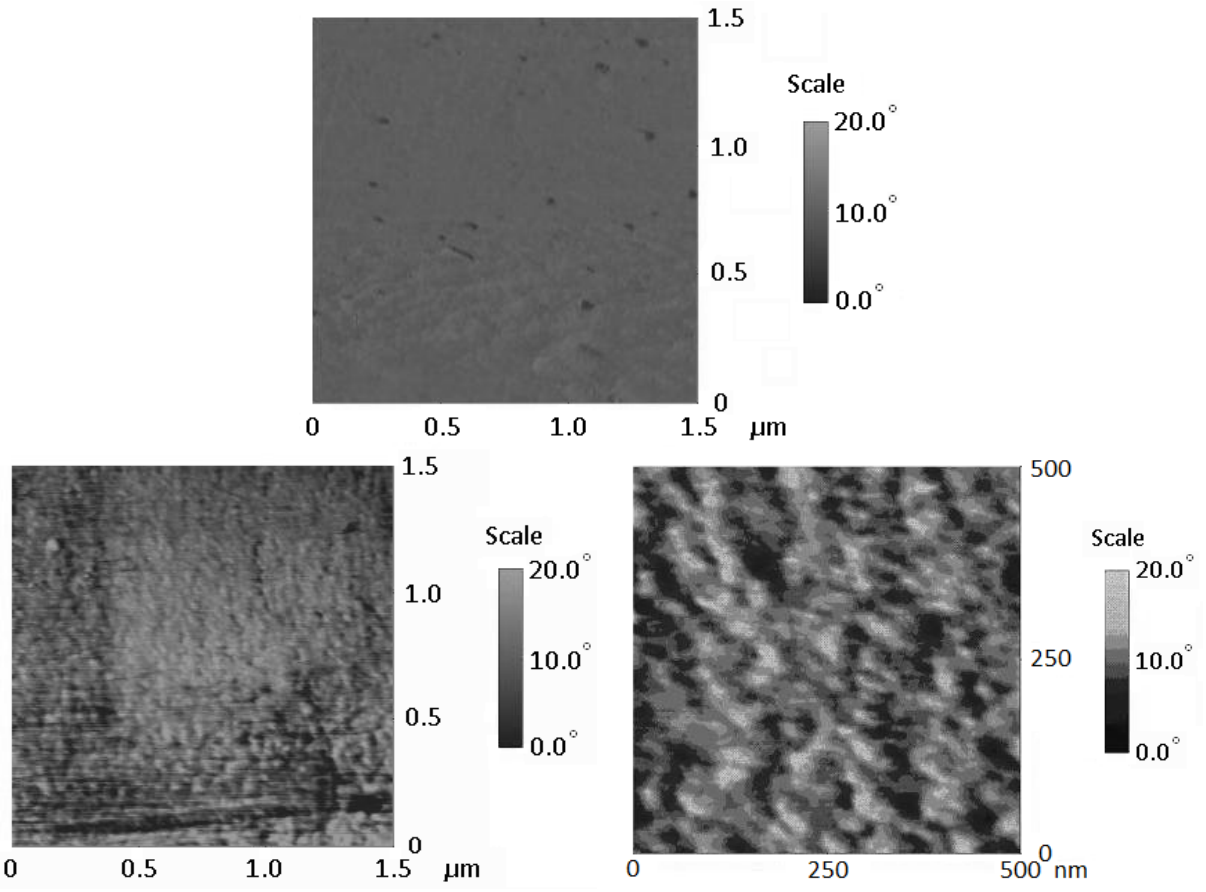

Figure 2. AFM phase images of the reference epoxy (up in centre), 1 wt-% octaglycidyldimethylsilyl-POSS epoxy nanocomposite 1500 nm scan (lower left corner) and 500 nm scan (lower right corner) [P5].

conformation, molecular weight, chain entanglement density, free volume, crystallinity, crosslink density and trap site density and depth [Roy05, Smi08]. Although these changes in properties are evident, the extent to which they will influence dielectric properties will depend on the system (matrix polymer and nanofiller) and the nature of the interaction zone [Nel02, Nel05, Nel06].

Local conductivity regions can be created around the nanofillers. These regions reduce charge accumulation (space charge) [Fot04, Nel04a, Roy07] and thus help in controlling electric field distribution and dielectric breakdown strength. This local conductivity region or "quasi-conductive" region is formed around the nanoparticles that overlap partially and allow charge dissipation (Figure 3). If the percolation threshold [Li07] has not been exceeded and dispersion is in nanoscale, the bulk conductivity remains unaffected. In nanocomposites the interfacial interaction shifths the percolation threshold towards lower weight fractions. Roy et al. conclude that because of the low concentration (5 wt-%) of filler in SiO_2-cross-linked polyethylene (XLPE) nanocomposite the local conductivity regions do not overlap and cause a total breakdown of the nanocomposite [Roy07].

Nanofillers can change the crystallinity of the material [Roy05, Zou07]. The large surface area can also lead to changes in the morphology of semicrystalline polymers. The breakdown strength of the intraspherulitic regions is higher than that of the interspherulitic regions and a change in the disorder within the spherulites or of the interspherulitic region can affect the breakdown strength. This was also discussed in the case of POSS-PP and

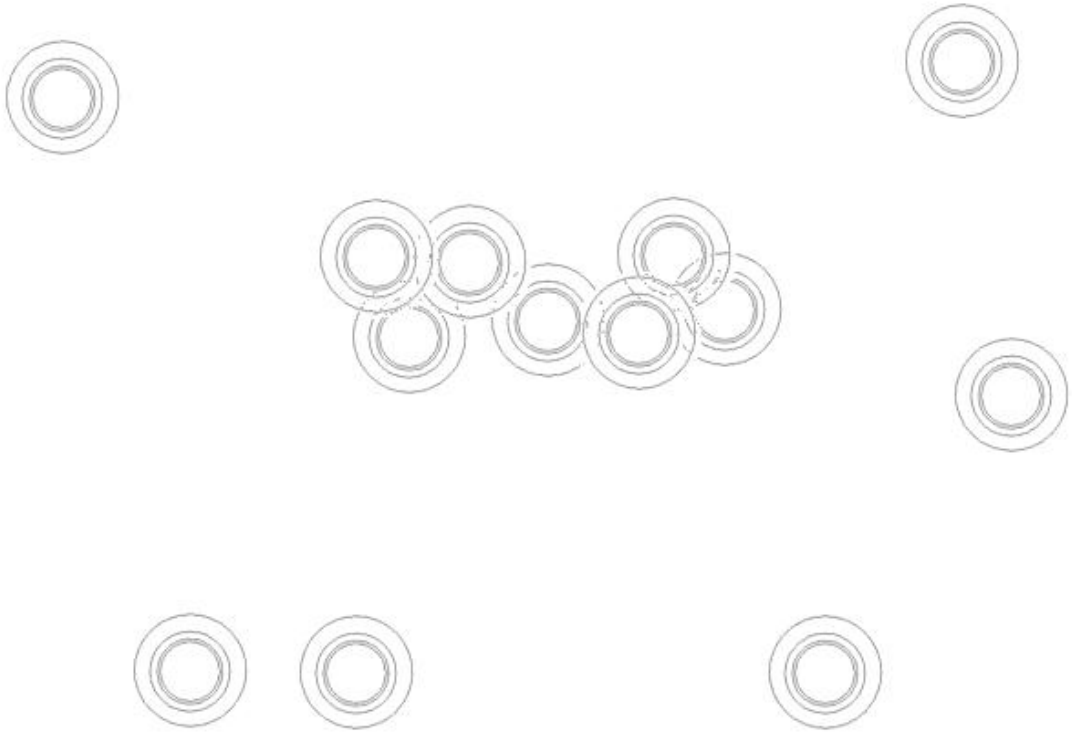

Figure 3. Nanoparticles in polymer matrix. The local conductivity region is formed around the nanoparticles that overlap partially.

calcium carbonate ($CaCO_3$)-PP composites [P2, P3]. LS acts as a nucleating agent in PA matrix and crystalline areas are formed around the fillers. This leads to high crystallinity but the size of the crystals is also smaller than without nanofillers [Koz03, Koz04a, Koz04b, Koz05]. The crystallinity of polymer has an effect on the DBS of the nanocomposite, though Roy et al. concluded that with SiO_2-XLPE nanocomposites changes in crystallinity were not the primary mechanism controlling dielectric breakdown [Roy07]. On the contrary, Bamji et al. report that the slightly lower ac and dc DBS of 4 wt-% LS-PP compared to 2 wt-% LS-PP, could originate from the decrease in spherulite size and density and poorer dispersion of the nanoparticles [Bam05]. LSs are known to be efficient nucleating agents for the crystallization of PP. Charges could be trapped at the LS-PP interfaces and thus decrease the probability of breakdown [Bam05].

Traps are regions of lower potential energy in material volume. The density and depth of trap sites are altered in nanocomposites. Charge carriers are more easily and more often trapped in trap sites than in reference matrix material. Due to this charge carriers are accelerated over shorter distances and have reduced mobility and kinetic energy. This mechanism can be also thought of as a scattering mechanism. The energy of charge carriers is distributed more evenly in the polymer and thus causes less damage in the material and prolongs the lifetime of the polymer. This scattering mechanism decreases the electric field at the electrodes [Nel06, Roy05] and increases the voltage required for charge injection. In Figure 4 octamethyl and isooctyl POSS cage structures are presented [P3]. In normal conditions octamethyl POSS is in solid state and isooctyl in liquid state. In Figure 5 the paraffin oil, isooctyl and octamethyl POSS sample potentials as a function of time are presented [P3]. The measurements were done according to IEC standard 61340-2-1 [IEC00]. The sample was pressured against a charging chamber with an earthed ring. The sample was charged by corona discharge. The charging voltage was 8 kV and the charging time was 100 ms. Potential was measured with the electrostatic voltmeter Trek Model 347. The test temperature was 25 °C. The diameter of the sample area was 100 mm and the depth was 0.5 mm. The corona discharging tests indicated that the discharge time of octamethyl and isooctyl POSS is much longer than that of paraffin oil. Firstly, both POSS materials take a much higher charge than paraffin oil. Secondly, the charge stays longer in both POSS materials. Octamethyl POSS powder especially seems to be stable in this test. The reason for the faster charge decline in isooctyl POSS is that particle interfaces are not apparent like in octamethyl POSS. The measured ac breakdown strength correlated with the charge decline measurements. Charge stays in traps of octamethyl POSS longer than in isooctyl POSS and due to this higher ac breakdown strength results are achieved with octamethyl POSS-PP nanocomposite than with isooctyl POSS-PP nanocomposite.

Ambid et al. [Amb04] also report that LS nanofillers modify the trapping property of both isotactic and syndiotactic PP. Roy et al. [Roy07] report that deep trap sites have been found in SiO_2-XLPE nanocomposites through thermally stimulated current (TSC) measurements. Roy et al. also conclude that the lowest mobilities are achieved with the functionalized materials that also provide deep trap sites. The reduced mobility could affect increased breakdown strength. Murakami et al. suggest that in MgO- low density polyethylene (LDPE) nanocomposite the charge is trapped in the vicinity of the electrode under high electric field and leads to improved breakdown strength with the aid of scattering mechanism [Mur08].

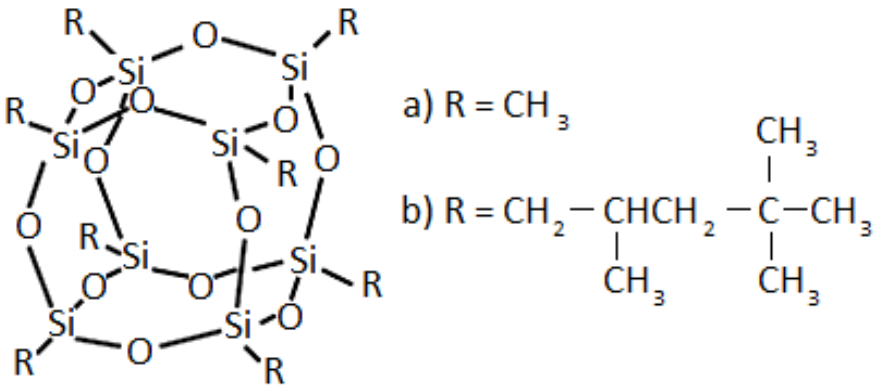

Figure 4. a) octamethyl b) isooctyl POSS cage structures [P3].

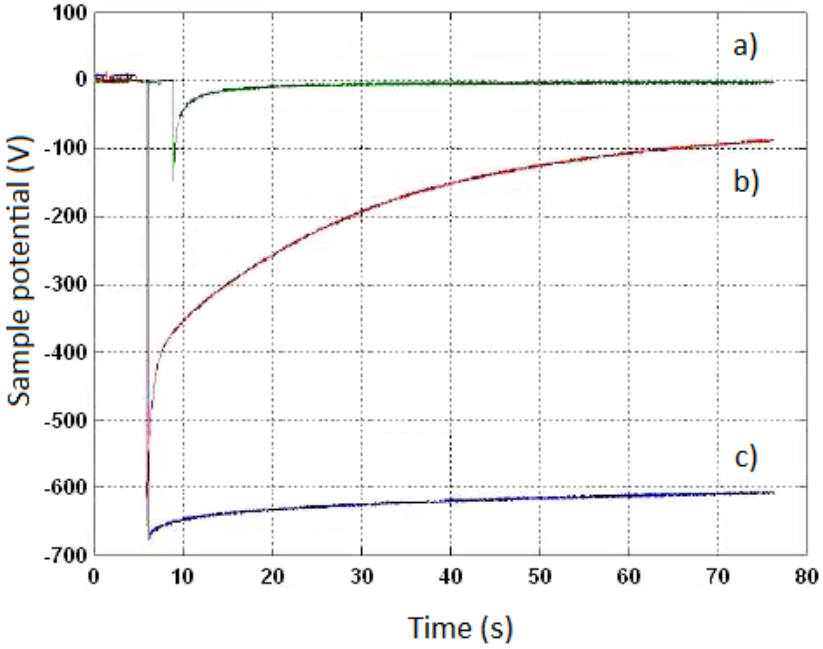

Figure 5. Sample potential as a function of time in a) paraffin oil, b) isooctyl POSS and c) octamethyl POSS [P3].

These mechanisms, which are all related strongly to the interaction zone, lead to the idea of tailoring functional materials by nanofiller addition and surface modification of the nanofillers [And09a, Nel02, Nel06, Nel07, Roy05, Roy07, Smi08]. The target is to increase the compatibility of the matrix polymer and nanofillers to avoid agglomerates. The bonding of the nanofillers can be engineered to increase the degree of self assembly and provide a way to tailor material properties in a desired direction. The coverage of a surface modification is a key factor in the process. One example of surface modification is POSS, which can have 100 different sidegroups (Figure 4). The dielectric properties of POSS-PP and POSS-EP nanostructured composites are presented in P3 and P5. Roy et al. [Roy07] conclude that covalent bonding between vinylsilane functionalized SiO_2 nanoparticles and XLPE was one of the keys to the improved voltage endurance. Zou et al. reported on the functionalization of hydrophobic SiO_2 nanoparticles into EP [Zou07, Zou08]. By

functionalization the water uptake of the SiO_2-EP nanocomposite can be reduced. It offers an advantage against ageing in dielectric applications. Horwarth et al. also prepared samples by grafting POSS particles onto EP matrix to increase ac breakdown strength and corona endurance [Hor05, Hor06].

2.3 Theoretical models

Theoretical models of the nanocomposite behaviour have been developed to interpret the property changes due to addition of nanofillers [Nel07, Phi04, Smi08]. As described earlier, understanding the interface phenomena is the key to the property changes. Models developed by Tanaka et al. [Tan05a] and Raetzke et al. [Rae09] both concentrate on the interpretation of the interface phenomena.

The multi-layered core model presented by Tanaka et al. [Tan05a, Tan05b, Tan06a, Tan06b, Tan07b] is based on colloid chemistry, polymer chemistry and solid state physics (Figure 6). The multi-layered core model is actually a three-core model. It consists of a bonded layer, a bound layer and a loose layer. The thickness of the first layer is of the order of 1 nm and is tightly bonded to both nanofiller and matrix polymer by coupling agents. The second layer is about 10 nm in thickness consisting of polymer chains bound or interacting to the first layer and the surface of the nanofiller. The third layer is several tens of nm in thickness and is characterized by chain conformations, chain mobility and free volume or crystallinity from the polymer matrix. The thickness of the layers depends on the strength of the polymer-nanofiller interaction. In addition, a Gouy-Chapman diffuse layer overlapps the three layers of the multi-layered core model. The nanoparticles are charged positively or negatively when the polymer has mobile charge carriers. The charge is distributed over the interface in such a way that the counter charge carriers with the opposite polarity are diffused outward from the contact surface. In the Gouy-Chapman diffuse layer the charge declines exponentially with distance and Debye shielding length is approximately 30 nm. Experimental measurement data can be analysed with the aid of multi-layered core model. Tanaka et al. conclude that the model can be applied e.g. to explain PD resistance characteristics of LS-PA nanocomposites, but further study is needed to establish a more precise model.

The interphase volume model presented by Raetzke et al. [Rae09] estimates the volume fraction of interphase in polymer due to addition of nanofillers. In the model the nanoparticle diameter (spherical) and the mass densities of matrix material and filler material are needed as input parameters. The model assumes that the spherical nanoparticles are uniformly dispersed in the matrix polymer. With interphase volume model a maximum interphase volume can be formed at low filler contents. Raetzke et al. conclude that different matrix polymers have a different chemical character and the interaction strongly depends on this. Therefore the results can be compared only within the same matrix polymer. In Figure 7 the interphase volume in silicone matrix as a function of SiO_2 weight content and interphase thickness with two particle sizes according to the interphase volume model are presented.

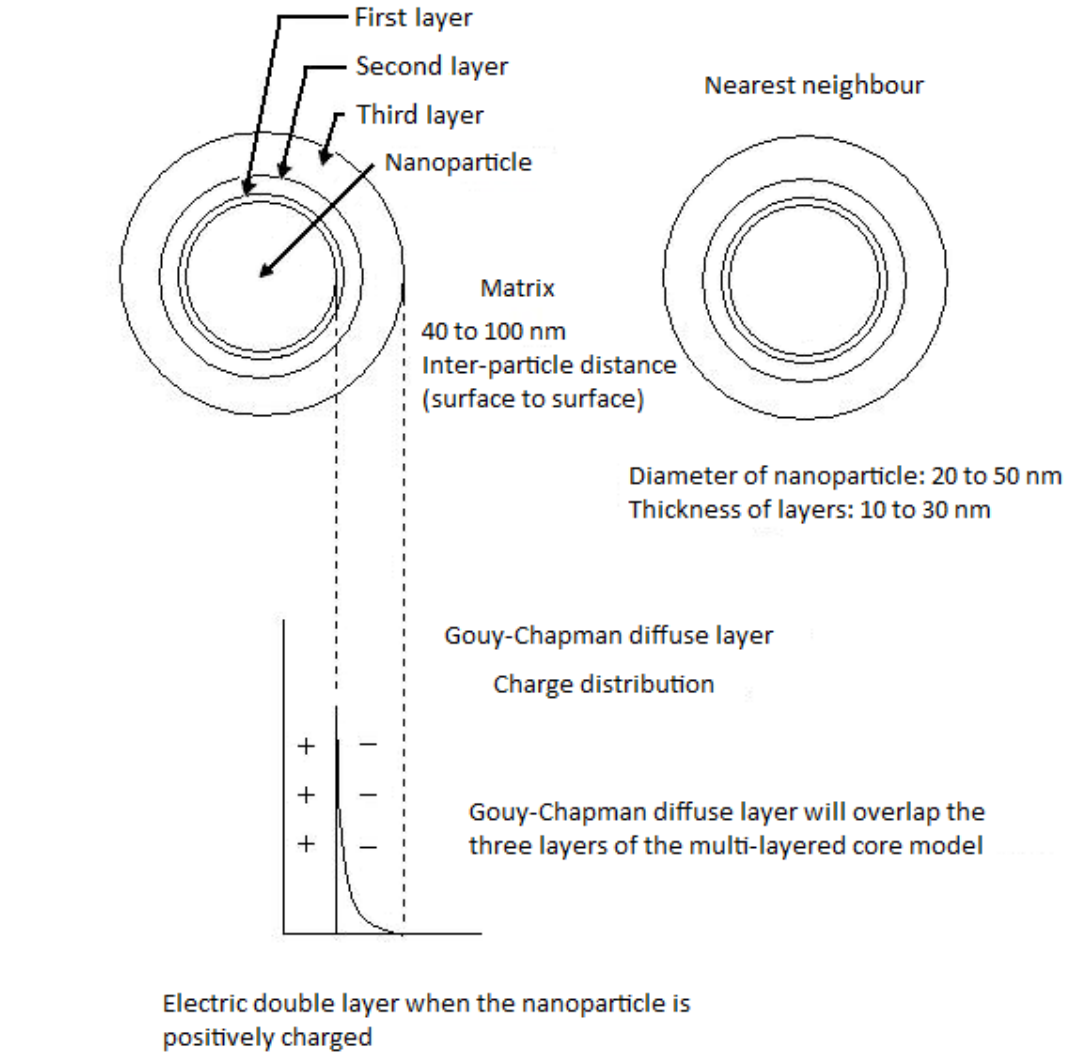

Figure 6. Multi-layered core model for nanoparticle-polymer interfaces [Tan05b].

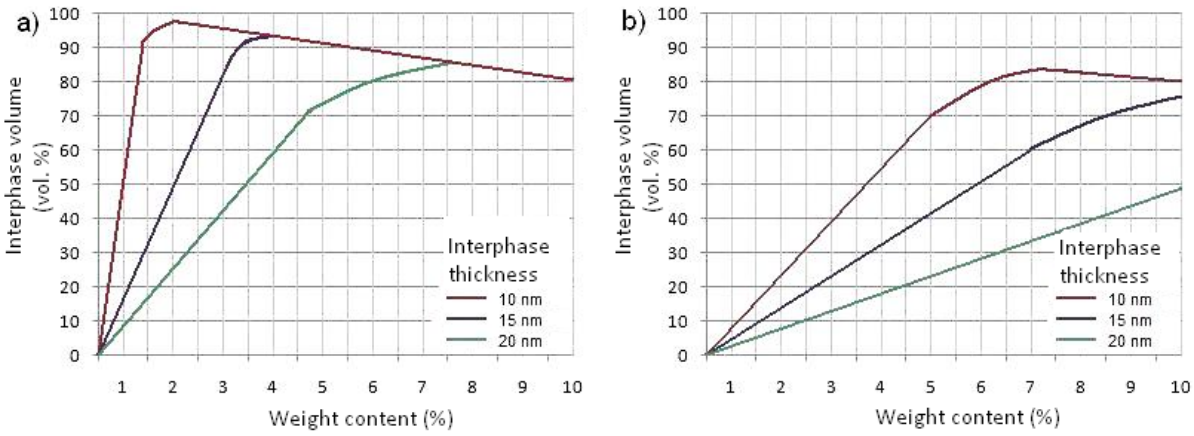

Figure 7. Interphase volume in silicone matrix as a function of SiO_2 weight content and interphase thickness with a) for a particle of diameter 20 nm and b) for a particle of diameter 40 nm according to the interphase volume model [Rae09].

2.4 Processing of nanocomposites

The main aim in the processing of nanocomposites is to ensure proper nanodispersion in the material [Nel07]. Dispersion has a strong effect on the material properties and is clearly the main reason for deviations in the measurements [Cas06, Hoy08]. In the processing of nanocomposites there are a couple of essential steps. The first step is nanoparticle drying in a vacuum. Nanoparticles can also be separated using shear force or by increasing chemical and physical forces between nanofillers and polymer matrix [Bro04, Tan05a, Tan06a]. The second step is to compound the nanoparticles with the matrix polymer and cross-linking agent if used. The third step is to cast, mold or extrude the material into the final form. Orientation may be used to achieve thin film samples (10 µm range in thickness). The fourth step is to remove unwanted byproducts which would impair the electrical properties. The compounding step usually requires high shear stress [Fot04, Rae05] with twin-screw extruder, melt mixer or ultrasonic wand and also optimal processing parameters. The fifth step is to check the homogeneity of nanodispersion by electron microscopy [Tan06a]. In Figure 8 the transmission electron microscopy (TEM) micrographs of 5 wt-% SiO_2-PP nanocomposite are presented [P6, P8]. It can be seen that the nanoparticles are gathered together to form clusters of a few tens up to hundreds of particles. The agglomerates are nevertheless mostly smaller than 100 nm in diameter. These clusters are dispersed evenly in the polymer matrix.

When increasing the nanofiller amount in nanocomposite, the probability for agglomerates increases. The agglomerates act as impurities or defects and decrease the DBS of microcomposites, like Wu et al. describe for Al_2O_3-polyimide (PI) nanocomposites [Wu05].

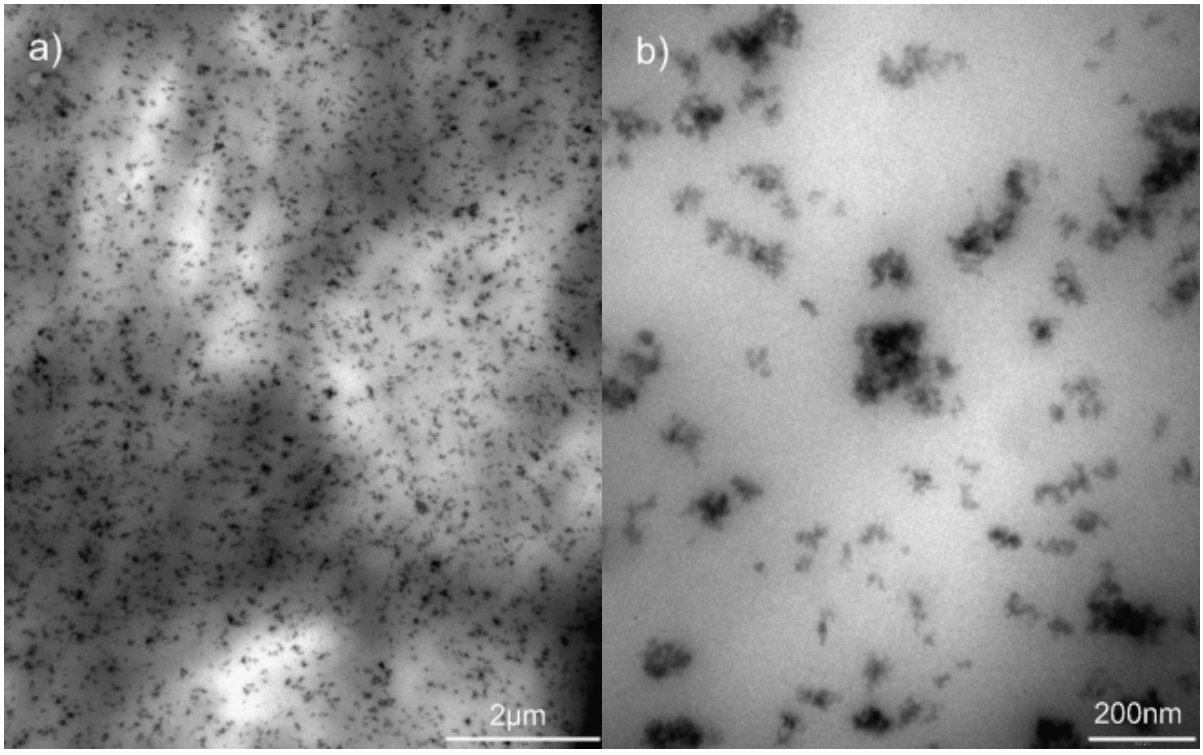

Figure 8. TEM micrographs of ultrathin sections of 5 wt-% SiO_2-PP nanocomposite [P6, P8].

This critical effect has also been observed by Imai et al. for TiO_2-EP nanocomposites [Ima06a], by Vaughan et al. for montmorillonite (MMT)-PE nanocomposites [Vau05] and by Raetzke et al. for SiO_2-SR and Al_2O_3-SR nanocomposites [Rae05]. One reason for using small quantities of 0.1 to 5 wt-% of nanofillers instead of higher amounts is the increasing probability of agglomerates with increasing nanofiller loadings.

2.5 Dielectric properties of nanocomposites

The properties usually studied in the field of insulation with nanocomposites are DBS, relative permittivity and dielectric losses, treeing growth and PD endurance, free volume, conduction at low and high fields, space charge accumulation, TSC, electroluminescence, resistance to tracking and arcing, glass transition temperature (T_g) and thermal conductivity [Tan04, Tan05a]. Out of these properties DBS [P2, P3, P5-P8], relative permittivity and dielectric losses [P1, P3, P5-P8] and treeing growth and PD endurance [P1, P4, P8] are more closely studied in Chapters 3, 4 and 5.

Nanofillers with high surface energy prevent contact between the fillers and matrix polymer. This results in a low density interlayer around the nanofillers i.e., the volume fraction of the outer loose layer is greater than that of the inner bound layer. Thus the free volume of nanocomposite insulations can be higher than with reference matrix polymer [Tan05a]. Higher free volume also results in lower relative permittivity values of the nanocomposites.

Nanofillers can act as ion scavengers and due to that introduce ionic carriers into the material [Tan05a]. Thus low field conductivity increases. The phenomenon may be related to quasi-conductive regions around nanoparticles, which can be explained by the overlapping of neighbouring third layers of the nanoparticles (Figure 3). This is closely related to the increase in low frequency relative permittivity and dielectric losses of nanocomposites. High field conduction mechanisms are not specific for nanocomposites. Either high field conduction is related to thermally assisted ionic-hopping current or space charge limited current, as in conventional polymers [Tan05a]. Based on the charge mobility and trap depth in the vicinity of nanofillers a new trap band and distribution structure is created [Tan05a]. A shallow trap band leads to reduced space charge accumulation and higher mobility of charge carriers. This may result from interfaces of nanoparticles interacting electrostatically with each other by far-distance effect of Gouy-Chapman diffuse layer (Figure 6). Reduced space charge accumulation is important with respect to applications, especially power cables. Space charges cause an increase of electric field and during polarity reversal additional stress to insulation material.

From TSC measurements of TiO_2-EP and SiO_2-PI nanocomposites it can be concluded that deep traps can be formed in the second layer of the multi-layered core model [Tan05a]. The TSC peak shifts to higher temperatures due to the addition of nanofillers. This may indicate that increased operation temperatures in applications are possible with nanocomposite materials. The EL measurements of TiO_2-EP nanocomposites indicate that homo charge is likely to form at the electrode tip, which reduces the resulting electric field [Tan05a]. Homo charge can be formed due to group effect of multi-layered nanoparticles, which contribute

to an increase of traps in the second layer of the multi-layered core model. Fast response on the removal of the voltage has also been observed, possibly due to the overlapping of interaction zones.

Silicone rubber (SR) is used for outdoor insulation applications. In these applications increase of resistance to tracking and arcing could be useful. Only a few publications deal with these properties of SR nanocomposites [Rae09, Tan04, Tan05a, Ven09], but similar phenomena are present as in PD resistance and dielectric breakdown. Improvement in T_g originates from tight bondings between nanofillers and matrix polymer. Both decreases and increases of T_g have been measured from EP nanocomposites [P5, Tan05a]. Thermal conductivity has been measured to increase in SiO_2-PI nanocomposites [Tan05a].

3 . Dielectric breakdown strength

3.1 Experimental measurements

The dielectric breakdown strength (DBS) of a dielectric material can be defined for ac, dc and lightning impulse (LI) voltage shapes. DBS measurements are also affected by the voltage ramp rate used and type of voltage increase. ac or dc voltage is increased with direct increase according to IEC Standard 60243-1 short-time test [IEC98]. For cast film samples (thickness 400-700 µm) in [P2-P3, P5], a voltage ramp rate of 2 kV/s was used, but for thin biaxially oriented samples (thickness 10-25 µm) in [P6-P8], a ramp rate of 400 V/s was used. Direct increase until breakdown was used, which corresponds to the short-time (rapid-rise) test [IEC98]. The wave shape of the impulse voltage was 1.2/50 µs defined according to IEC Standard 60060-1 [IEC89]. In LI DBS measurements the output voltage of the impulse generator was raised 2 kV after each impulse until breakdown occurred. Negative impulses were used and the time interval between impulses was 10-20 s. The thickness of the EP nanocomposites in LI tests was 400-600 µm [P5].

The measurements were performed at room temperature (~20 °C). Rod-like electrodes having a diameter of 12 mm and made of stainless steel were used in the measurements. With biaxially oriented samples (thickness 10-25 µm) graphite layers between the samples and steel electrodes were used to smooth the contact to the sample. The samples were manually fixed to the electrode setup (Figure 9). The measurements were performed by immersing the sample and the electrodes in mineral oil (Shell Diala DX) in order to avoid flashovers and surface discharges. The edges of the electrodes were also rounded to get more equal electric field distribution. For example, PP is known to swell in oil so it is important to avoid oil penetrating into the sample. Due to this the DBS tests were carried out minimizing the oil immersion time. Sets of 10 or 20 parallel test samples were used.

The breakdown field and the film thickness follow the so-called power law equation

$$E_2 = E_1\left[\frac{d_2}{d_1}\right]^{-n}, \qquad (1)$$

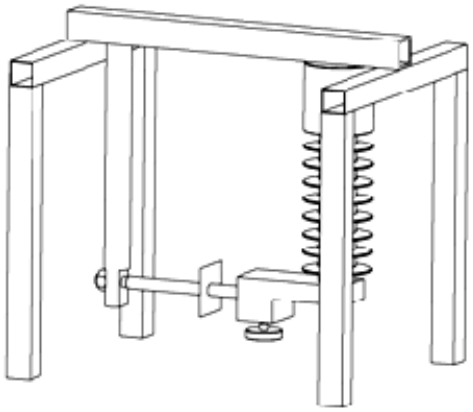

Figure 9. Measurement bench for dielectric breakdown strength measurements.

where E_2 is the breakdown strength of a film with thickness d_2, E_1 is the breakdown strength of a film with thickness d_1 and n is the power law exponent [IEE05]. The power law equation can be used to obtain comparable results from samples with varying thicknesses. The DBS measurement results of biaxially oriented PP nanocomposites were converted to correspond to the breakdown strength of 9 µm thick film using the power law relationship. The power law exponent was fitted for the materials studied and n value of 0.4 was used [P6-P8].

Statistical analysis was applied to the DBS measurements. Results were calculated according to the IEEE Standard 930: IEEE Guide for the Statistical Analysis of Electrical Insulation Breakdown Data [IEE05] using Microsoft Excel and Matlab programs. The dielectric breakdown voltage data was plotted on the Weibull probability plots according to a two-parameter Weibull distribution, stating a zero location parameter. The 2-parameter Weibull cumulative distribution function is related to the probability of failure occurring in certain field strength x as follows

$$F(x) = 1 - \exp\left\{-\left[\frac{x}{\beta}\right]^{\alpha}\right\}. \quad (2)$$

The shape parameter β is related to the width of the distribution. The spread of the measured breakdown strengths decreases with increasing value of β. Accordingly the scattering of the dielectric strength values decreases and consequently the reliability of the measured dielectric behaviour of the material increases when the shape parameter increases. Scale parameter α is related to the 63.2 % probability for the sample to break down at electric field strength α [Hau92].

Statistical differences between two materials can be compared by average standard deviation (s_{ave}), which is the weighted average value of the two standard deviations of the materials. The difference between the mean values of the breakdown strength of the materials (dif) is compared with relevant sectors. These sectors are: not significant ($dif \leq 1.96 \times s_{ave}$), almost significant ($1.96 \times s_{ave} < dif \leq 2.58 \times s_{ave}$), significant ($2.58 \times s_{ave} < dif \leq 3.29 \times s_{ave}$) and highly significant ($dif > 3.29 \times s_{ave}$). With these quantiles statistical significance levels can be calculated and differences between the materials evaluated [Hau92, IEE05].

3.2 Affecting factors

DBS is one of the most important properties of an insulation material. As discussed earlier, the properties of polymer nanocomposites are mainly explained by a large interfacial area of nanofillers. This interfacial area is responsible for the interaction of the electrical field between the matrix polymer and nanofiller [Gua06a, Nel04a, Nel06, Vau05]. The DBS of the nanocomposites depends heavily on the nanofiller content and even small quantities can cause improvement. Often the most profitable nanofiller quantities are below 5 wt-%, as has been noted in [P3, P5-P8]. At the top in Figure 10 the ac breakdown strength of PP as a function of the octamethyl POSS content is presented. Below is the Weibull probability plot as a function of ac breakdown strength of the reference PP and 3 wt-% octamethyl POSS-PP composite. The ac DBS of 3 wt-% octamethyl POSS-PP composite increased 22 % compared

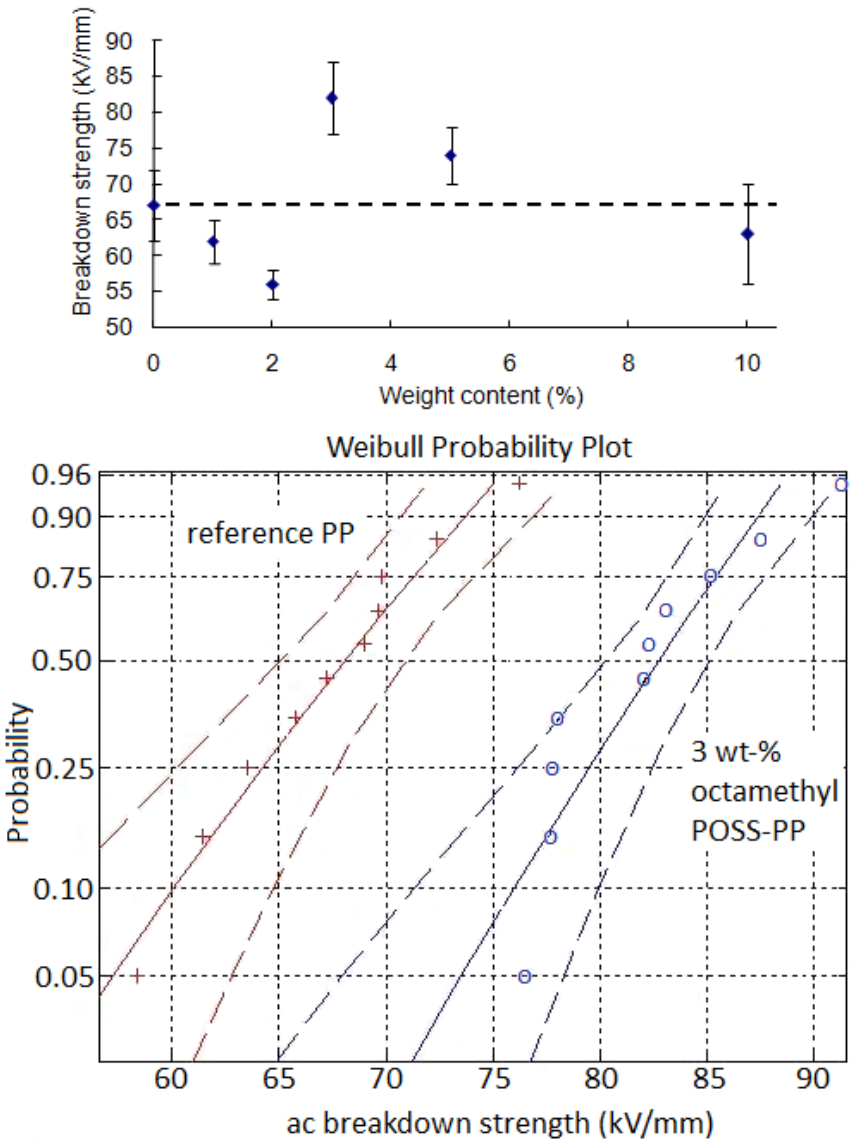

Figure 10. At the top is the measured ac breakdown strength of PP as a function of the octamethyl POSS content. Below is the Weibull probability plot as a function of the ac breakdown strength of the reference PP and 3 wt-% octamethyl POSS-PP composite. Crosses and circles are the measurement points, solid lines are Weibull fittings and broken lines are 90 % confidence intervals [P3].

to the reference PP. The Weibull probability plot shows that for 3 wt-% octamethyl POSS-PP composite DBS values are shifted to higher electric field strengths.

At the top of Figure 11 the LI breakdown strength of EP as a function of the octaglycidyldimethylsilyl POSS content is presented. Below is the Weibull probability plot as a function of LI breakdown strength of the reference EP and 1 wt-% octaglycidyldimethylsilyl POSS-EP nanocomposite. The LI DBS of 1 wt-% octaglycidyldimethylsilyl POSS-EP nanocomposite increased 26 % compared to the reference EP. These changes are linked to the ability of POSS particles to trap charges (Figure 5) [P3] and to the maximum interfacial

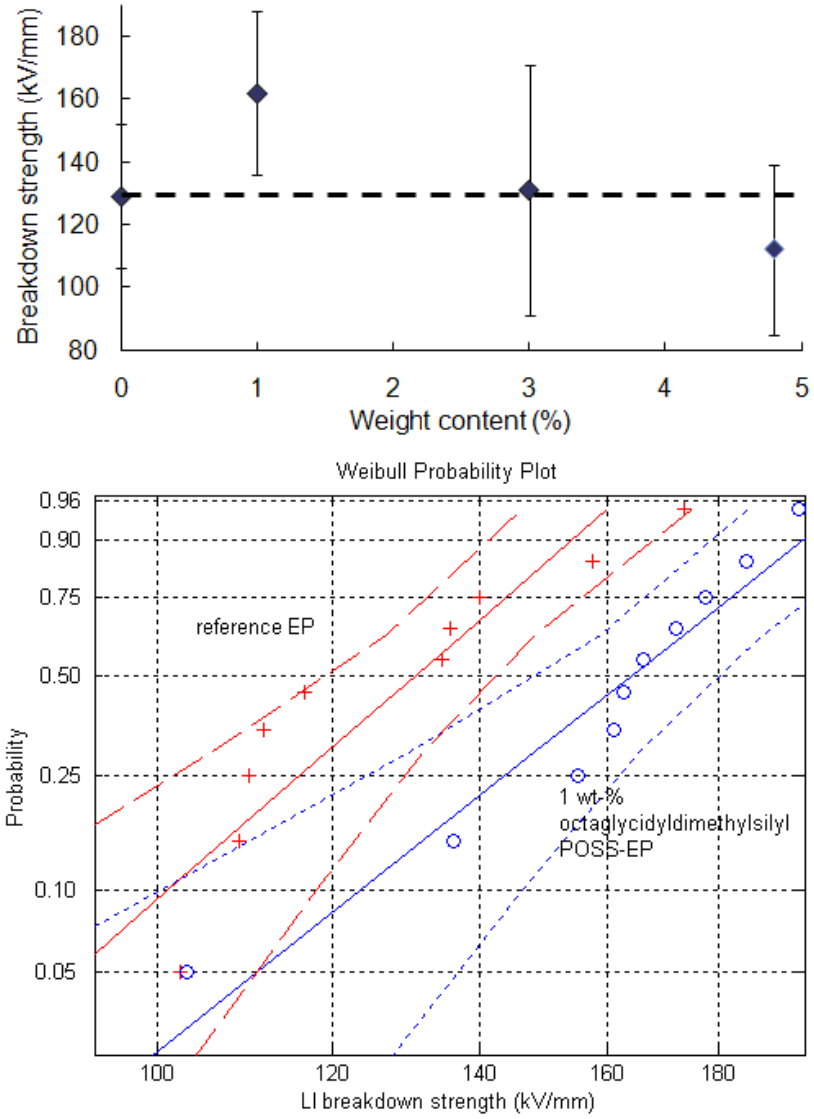

Figure 11. At the top is the measured LI breakdown strength of EP as a function of the octaglycidyldimethylsilyl POSS content. Below is the Weibull probability plot as a function of LI breakdown strength of the reference EP and 1 wt-% octaglycidyldimethylsilyl POSS-EP composite. Crosses and circles are the measurement points, solid lines are Weibull fittings and broken lines are 90 % confidence intervals [P5].

area achieved already at low nanofiller concentrations (Figure 7) [Rae09]. Good homogeneous nanodispersion is the key to DBS increase and reliable results (Figures 2 and 8) [Roy07]. The risk of agglomerates increases with nanofiller content. Agglomerates decrease the DBS as in microcomposites.

The DBS behaviour of nanocomposites may be reflected in changes in the space charge distribution, reduction in the internal electric field caused by the nanofiller size and changes in the polymer morphology [Roy07]. Nelson also emphasizes the effects of the scattering of electrons in high field regions, electron trapping and free volume within the polymer

structure [Nel04a, Nel06]. When the layers of nanoparticles are connected (multi-layered core model, Figures 3 and 6), paths of high conductivity may form. These local short circuit paths lead to faster recombination of space charges in nanocomposites. These effects result in lower space charge accumulation and lower local internal fields due to space charges in nanocomposites. Scattering of electrons decreases the kinetic energy preventing ionization and the deep traps reduce the mobility of charge carriers [Hu06].

Vaughan et al. suggest that the addition of nanofillers changes the crystal growth mode in MMT-PE nanocomposite [Vau05]. The crystals can be smaller if the growth centres (e.g. nanoparticles) are close to each other. However, the crystallinity degree has been observed to increase with mica-PA nanocomposite [Fus08]. Roy et al. conclude that crystallinity is not as such a significant factor in controlling DBS, the nanoparticles in the crystalline phase may disrupt the path provided to the charge carriers and lead to an increase in DBS [Roy07]. In [P2] it is also suggested that the increase of ac DBS in $CaCO_3$-PP composites may be due to the high melting point of $CaCO_3$ (1340 °C) and strengthening of weak areas between spherulites. Murakami et al. also suggest that in MgO-LDPE nanocomposite the increase in dc DBS is related to thermal processes [Mur08].

The general idea in DBS measurements is to compare the matrix polymer with nanofillers to the reference polymer matrix. Stabilizers are also commonly used e.g. against ultra violet radiation ageing. The effect of stabilizers on the DBS of reference polymer can be defined by measuring reference material with and without stabilizers, although this may be difficult in practice. It is important to maintain stable measurement conditions during the DBS measurements. Air pressure, humidity and temperature all affect the measured properties and materials. The temperature effect of nanocomposite DBS has been studied in [Roy07]. Roy et al. conducted dc DBS measurements at four different temperatures 25 °C, 60 °C, 70 °C and 80 °C and for four different SiO_2 surface treatments. DBS decreased as a function of temperature with all compositions and with the reference material. The DBS behaviour of nanocomposites is affected by environmental condition but the actual effect in each case also depends on the voltage shape used (ac, dc, LI) and the matrix polymer and nanofiller. Thus, the importance of each factor varies case by case.

3.3 Effect of the voltage shape

As indicated in Chapter 3.2, there are mechanisms related to nanocomposites which increase the short-term breakdown voltage. These mechanisms are dependent on the voltage shape used in the DBS measurements. The ac and LI DBS of nanocomposites are usually harder to increase than the dc DBS, as has been noted in [P3, P5-P8]. On the left in Figure 12 are the measured ac and dc breakdown strengths of the reference PP and 5 wt-% SiO_2-PP nanocomposite with their 95 % confidence limits. On right are the Weibull probability plots as a function of ac and dc breakdown strength of the reference PP and 5 wt-% SiO_2-PP nanocomposite. The mean values of ac and dc DBS of 5 wt-% SiO_2-PP nanocomposite increased 20 % and 52 % respectively compared to the reference PP. The Weibull probability plots show that for 5 wt-% SiO_2-PP nanocomposite the ac and dc DBS values are shifted to higher electric field strengths. The shift with dc voltage is greater than with ac voltage.

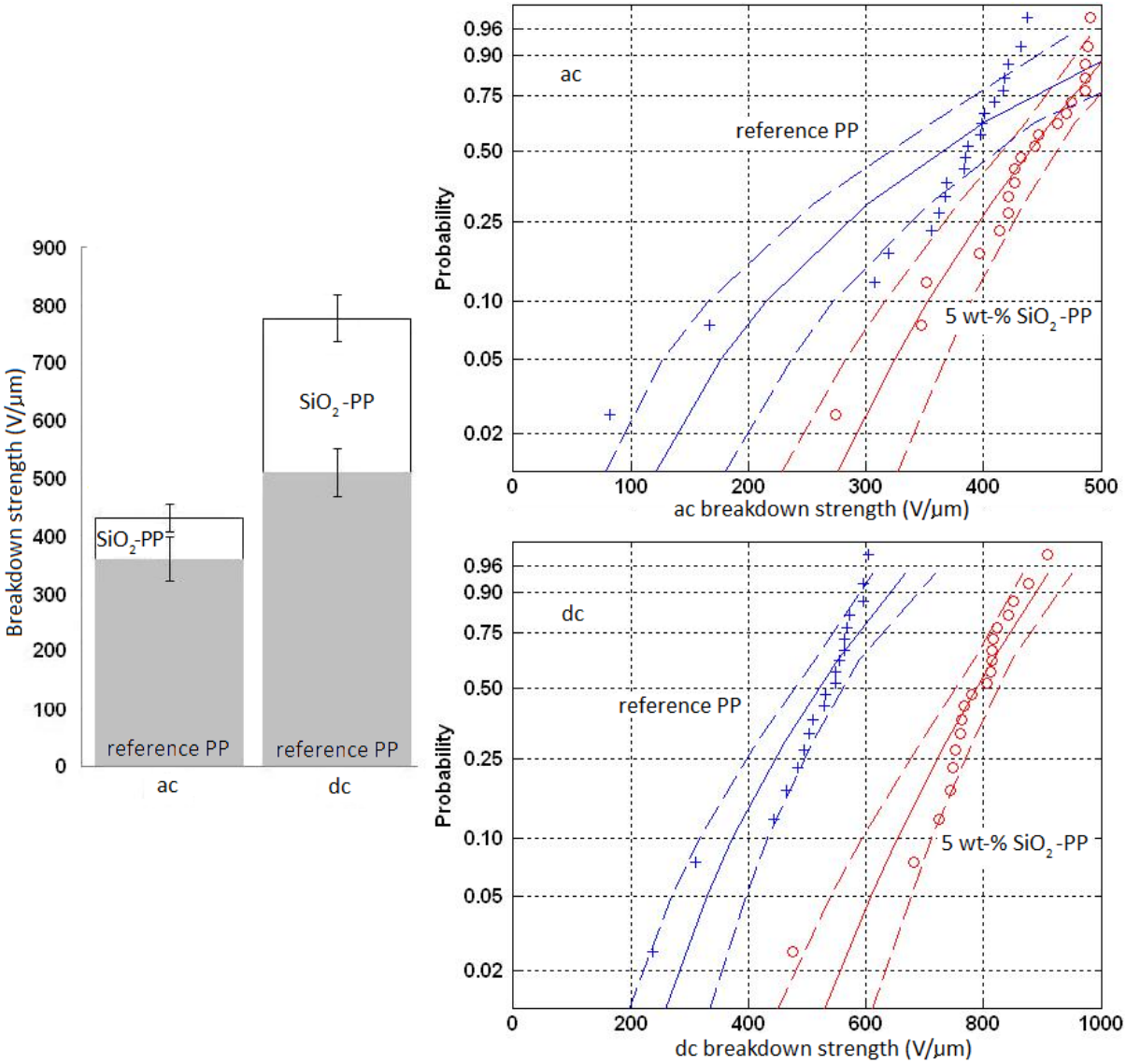

Figure 12. Measured ac and dc breakdown strengths of the reference PP and 5 wt-% SiO_2-PP nanocomposite with their 95 % confidence limits (on the left). On the right are the Weibull probability plots as a function of ac and dc breakdown strength of the reference PP and 5 wt-% SiO_2-PP nanocomposite (ac upper, dc lower). Crosses and circles are the measurement points, solid lines are Weibull fittings and broken lines are 90 % confidence intervals [P6, P8].

As Danikas et al. [Dan09] concluded, reduction of space charge accumulation improves dc voltage performance and scattering mechanism is the reason for improved ac and LI voltage performance. This has also been supported by Hu et al. [Hu06]. Roy et al. emphasize that the increased dc DBS is a common property for all nanocomposites [Roy07]. Smith et al. also report that dc DBS measurements provided higher breakdown strength values with SiO_2-XLPE nanocomposites than the peak values of the ac DBS measurements and the surface modification of SiO_2 nanoparticles had a positive effect [Smi08]. The accumulation of shielding space charge is a process which needs time to develop. Thus, in ac or in fast impulse voltage DBS measurement (1.2/50 µs), the effect of shielding space charge disappears. The large interfacial area creates opportunities for a scattering mechanism.

During ac and LI conditions, this may become the primary mechanism for the increase in the DBS of nanocomposites.

Usually the DBS values of the nanocomposites fit into the Weibull distribution. A common conclusion for the DBS results with ac and dc voltage shapes is that breakdown probability at 62.3 % (α) increases or remains at the reference level, but scattering of the data decreases (β increases) [Gua06a, Hu06, Mon04, Mon05, P3, P5-P8]. This was noticed in the case of 1 wt-% SiO_2-PP nanocomposite (Figure 13) [P8]. Nanocomposites have smaller scattering for DBS values. The breakdown phenomenon in homogeneous nanocomposites is more stable than in the reference matrix polymer. The phenomenon has a positive impact on insulation system design, where safety margins may be reduced. It is actually as important as increase of α. Hoyos et al. concluded that SiO_2-LDPE and LS-LDPE nanocomposites are defect-free as regards electrically weak spots [Hoy08]. This improvement in β values is a good sign of proper nanodispersion in nanocomposites. These phenomena led to the idea of controlled filling of nanocomposites, as Imai et al., Lu and Nelson et al. have already suggested [Ima08, Lu08a, Nel04a].

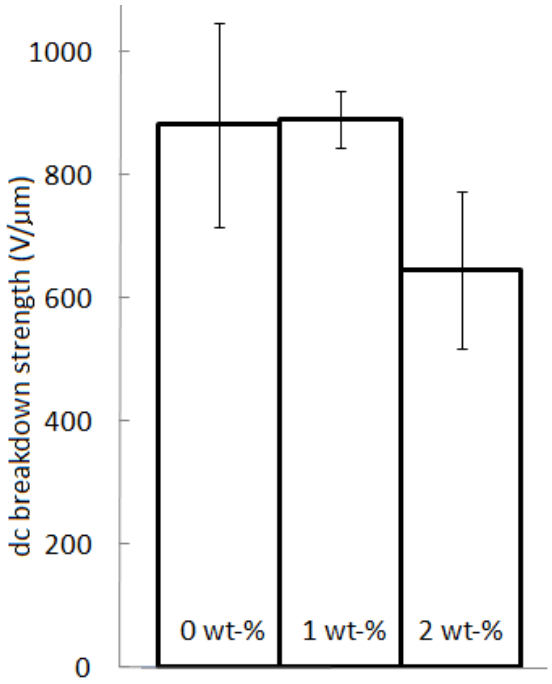

Figure 13. dc breakdown strength mean and standard deviation of reference PP and 1 and 2 wt-% SiO_2-PP nanocomposites [P8].

3.4 Summary

Figure 14 presents the variables and factors affecting the DBS of nanocomposites. DBS depends on many variables and factors which also depend on each other. They all need to be considered when conducting DBS measurements and analysing the results. Figure 15 presents third order polynomial fittings for the DBS results of nanocompostites as a function of nanofiller content. It shows that the same kind of behaviour with different voltage shapes can be achieved with nanocomposites, but with dc voltage the increase is bigger. The difference between the dc vs. ac DBS values is in the order of √2, because ac DBS is given as root mean square (RMS) value. The peaks of the fittings are approximately in the same position with respect to nanofiller content. DBS has a maximum value with respect to nanofiller amount and decreases thereafter. Filler quantities around 5 wt-% and even lower are the most attractive considering DBS of nanocomposites. This kind of behaviour is similar to the interphase volume model presented by Raetzke (Figure 7) [Rae09]. In Table 1 the DBS results of nanocomposites are presented.

In this dissertation the main contributions considering the DBS of nanocomposites are:

1. The ac DBS of 3 wt-% octamethyl POSS-PP nanocomposite increased 22 % compared to the reference PP [P3].

2. The LI DBS of 1 wt-% octaglycidyldimethylsilyl POSS-EP nanocomposite increased 26 % compared to the reference EP [P5].

3. The dc breakdown strength of 1 wt-% SiO_2-PP nanocomposite was slightly higher than with reference PP. The β value in the Weibull probability function of the nanocomposite is higher than in the reference PP, an indicator of smaller standard deviation and homogeneous material [P7].

4. The ac and dc breakdown strength of 5 wt-% SiO_2-PP nanocomposite increased 20 % and 52 % respectively. It is equally important that with both voltage shapes the β value of the nanocomposite is higher than with the reference PP. These results have an interesting impact on insulation system design, because safety margins and insulation thicknesses may be reduced [P8].

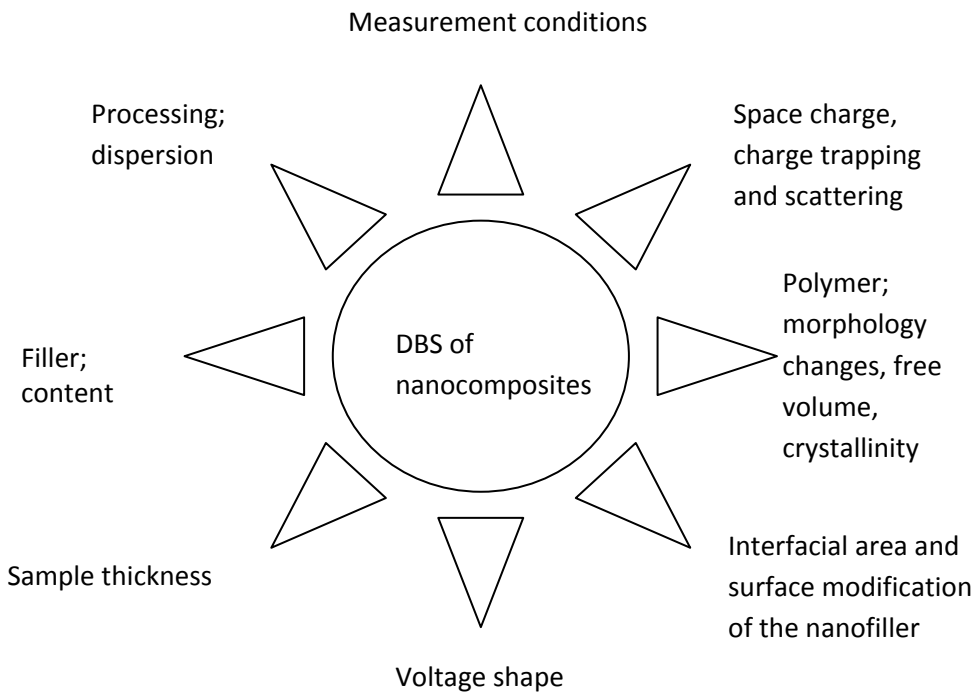

Figure 14. Variables and factors affecting the DBS of nanocomposites.

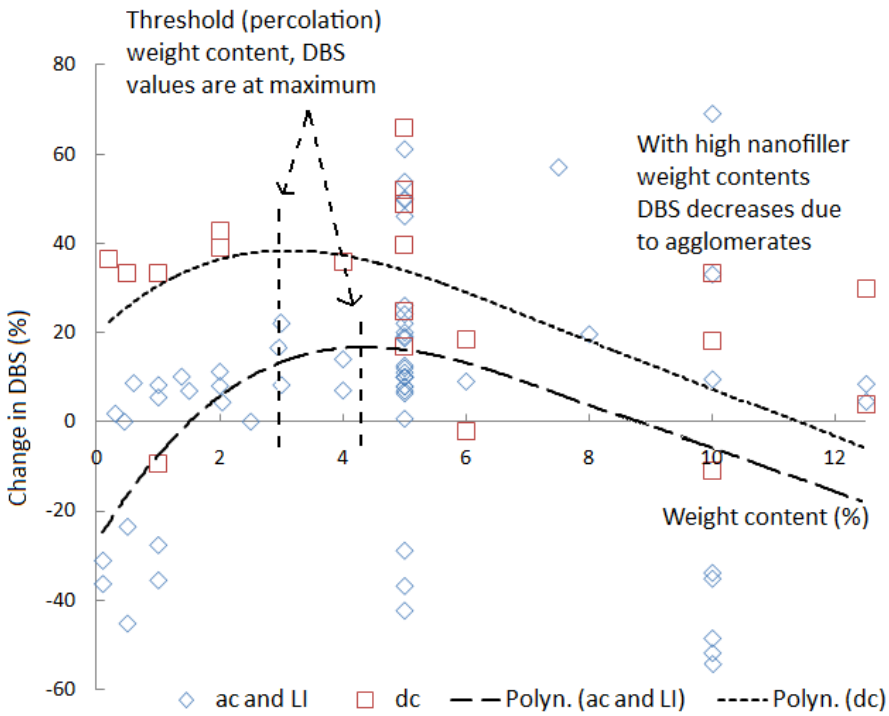

Figure 15. DBS of the nanocomposites as a function of filler content. Diamonds are the measurement results for ac and LI voltages and squares for dc voltage. Third order polynomial fittings are presented with broken lines [Bam05, Gre08, Gua06a, Gua08, Gua09, Hoy08, Hu06, Ima04, Ima06a, Ima06b, Ima08, Kur06, Mon04, Mon05, Mur08, Nel04a, Pél06, Roy07, Shi04, Sin06, Sin08a, Smi08, Tun09, Vau05, P2, P3, P5-P8].

Table 1. Relative change of ac, dc and LI DBS of nanocomposites with respect to the reference material in various experimental studies.

DBS	Matrix	Nanofiller	Weight content (%)	Change (%)	Publication
ac	PP	SiO_2	5	20	P6, P8
	PP	octamethyl-POSS	3	22	P3
	PP	isooctyl-POSS	5	11	P3
	PE	MMT	2, 4, 8	11, 14, 20	Gre08
	LDPE	SiO_2	5	8	Gua06a
	LDPE	MMT	5	24	Gua09
	LDPE	MgO	1, 5, 10 (phr)	5, 13, 28	Kur06
	LDPE	MMT	5	54	Hoy08
	LDPE	MMT (washed)	5	61	Hoy08
	EP	glycidyl-POSS	1, 3	8, 8	P5
	EP	LS	5	10	Ima06a
	EP	SiO_2	5	22	Ima06a
	EP	TiO_2	5	50	Ima06a
	EP	LS	5	12	Ima08
	EP	SiO_2	5	26	Ima08
	EP	TiO_2	5, 7.5, 10	46, 57, 69	Ima08
dc	PP	SiO_2	5	52	P6, P8
	PP	organosilicate	2, 4	39, 36	Bam05
	XLPE	SiO_2	5	17	Roy07
	XLPE	silane treated SiO_2	5	49	Roy07
	XLPE	silazane treated SiO_2	5	25	Roy07
	XLPE	silane treated SiO_2	5	66	Roy07
	XLPE	SiO_2	12,5	4	Smi08
	XLPE	silane treated SiO_2	12,5	30	Smi08
	LDPE	MgO	0.2, 0.5, 1, 2, 5, 10	37, 33, 33, 43, 40, 33	Mur08
LI	PP	octamethyl-POSS	10	13	P3
	XLPE	SiO_2	12,5	22	Smi08
	XLPE	silane treated SiO_2	12,5	31	Smi08
	EP	octaglycidyldimethylsilyl-POSS	1	26	P5
	EP	TiO_2	10	2	Hu06

4 . Relative permittivity and dielectric losses

4.1 Experimental measurements

The dielectric spectroscopy measurements were conducted with insulation diagnosis analyzer (IDA) [P3, P5, P6] or with arbitrary waveform impedance spectroscopy (AWIS) [P7, P8]. With IDA measurements the used frequency range was from 0.1 Hz to 1 kHz at 140 V. The real part of the relative permittivity (ε') was calculated as follows

$$\varepsilon' = \frac{C_P}{C_0} - \frac{C_e}{C_0}, \tag{3}$$

where C_P is the measured parallel capacitance at the measurement frequency when the specimen is represented in terms of equivalent parallel circuit, C_0 the vacuum capacitance of the measurement setup and C_e the edge capacitance according to the IEC standard 250 [IEC69]. The imaginary part of the relative permittivity (ε'') was calculated as follows

$$\varepsilon'' = \frac{1}{R_P C_0 \omega} - \frac{C_e}{C_0}, \tag{4}$$

where R_P is the measured parallel resistance at the measurement frequency when the specimen is represented in terms of equivalent parallel circuit and ω the angular frequency. The relative permittivity (ε_r) was calculated from the results of Equations 3 and 4 as follows

$$\varepsilon_r = \sqrt{\varepsilon'^2 + \varepsilon''^2} \ . \tag{5}$$

The dissipation factor ($\tan\delta$) was calculated according to relationship

$$\tan\delta = \frac{\varepsilon''}{\varepsilon'} \approx \frac{1}{R_P C_P \omega} \quad , C_e << C_P \, . \tag{6}$$

The area of PP nanocomposite samples was approximately 9 cm x 9 cm and thickness 400-700 µm and the area of EP nanocomposites 5 cm x 5 cm and thickness 400-600 µm. Aluminum foil electrodes attached to the samples with a negligible amount of silicone grease were used. Three parallel measurements were conducted on the samples and average values were used.

Dielectric response of the SiO_2-PP nanocomposites was measured using AWIS presented in [Son08]. The measurement system was designed to measure dielectric response using arbitrary repetitive voltage signals. Both the applied voltage signal and the current response were measured by a data acquisition card and Fourier transformed into the frequency domain where a dielectric response spectrum can be extracted. The system demands careful calibration procedures to be accurate [Son08]. In P7 and P8, AWIS was used as a low voltage frequency domain spectroscopy instrument in order to perform dielectric response

measurements on low impedance (i.e. high capacitance) and low loss test samples. Silver electrodes with a diameter of 3 cm were painted on film samples with approximately thickness of 20 µm in order to ensure good contact to the material. After painting the electrodes the samples were heat treated at 60 °C for 18 h under compressive stress in order to avoid creasing of the film. Creasing of the film can cause cracking of the silver paint layer, distorting the measurements. One advantage of the heat treatment is also to exclude the moisture from the insulation. Three samples of each material were measured and three data points were collected at each frequency and temperature. The measured frequency range was from 43 Hz to 43 kHz and temperatures 22 °C, 40 °C, 60 °C, 80 °C and 100 °C. A peak voltage of 4 V (ac) was used.

4.2 Affecting factors

Relative permittivity is connected to polarization mechanisms. Polarization mechanisms can be divided into electronic, ionic, dipolar, interfacial (space charge) and hopping charge polarization [Lu08a]. Each polarization mechanism has a characteristic relaxation frequency. With increasing frequency the slower mechanisms are neglected and relative permittivity decreases. In microcomposites (filler content 50-60 wt-%), relative permittivity usually increases with increasing filler content due to the strong presence of Maxwell-Wagner interfacial polarization [Tan05a]. On the other hand, in nanocomposites relative permittivity also tends to increase with increasing nanofiller content, but lower relative permittivity values than with reference are also possible, especially with low nanofiller content. Actually lower relative permittivity values than with reference can be considered as a sign of a good nanocomposite, but increase in relative permittivity is also possible, especially at higher nanofiller loadings [P5, Nag08].

Figure 16 presents the relative permittivity and dielectric losses of glycidyl POSS-EP nanocomposites. The 1 wt-% of glycidyl POSS-EP nanocomposite gives lower relative

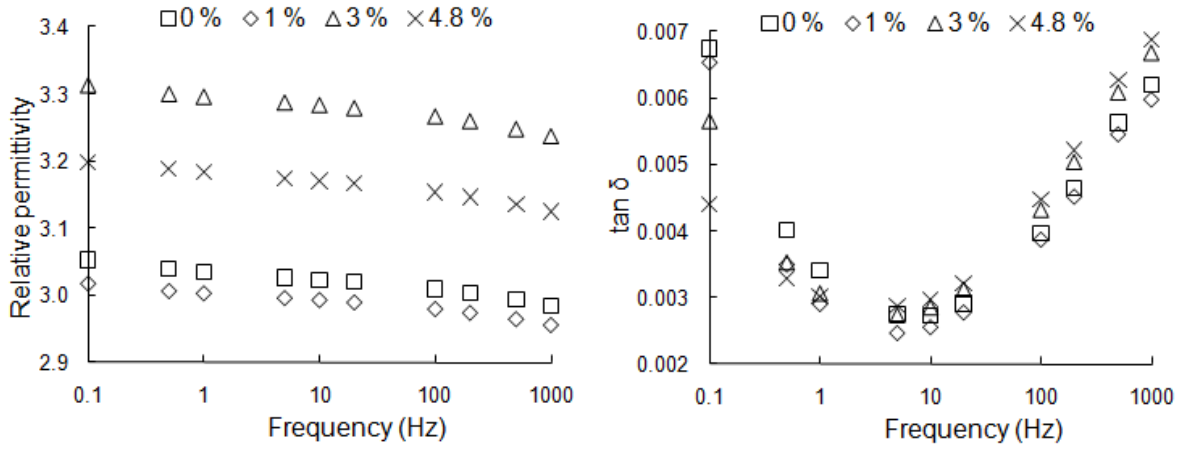

Figure 16. Relative permittivity and dielectric losses of epoxy as a function frequency at different glycidyl POSS contents [P5].

permittivity values than the reference EP. Higher glycidyl POSS content increases the relative permittivity of EP. The dielectric losses of glycidyl POSS-EP nanocomposites remain at the reference level. This means that polarization mechanisms are restricted in nanocomposites with low nanofiller content. Proper nanodispersion is a prequisite for desired changes in relative permittivity as it is for DBS. The changes in relative permittivity are also related to a large interfacial area created by addition of nanofillers [Bro04, Fot04, Lew04a, Tan04]. The restriction of polymer chain movement [Che08, Nel04a, Nel04c, Rae05, Sin06, Tan06a] by nanoparticles and the increase in free volume or reduction in density [Che08, Nel04b, Nel04c, Lee05a, Lee05b, Tan06a] are two phenomena suggested to explain the effect. Lee et al. reported that reduction in the relative permittivity of POSS-PI nanocomposites is due to silsesquioxane cores and increased free volume resulting in a loose structure for PI matrix [Lee05b]. Due to increased free volume highly mobile interlayer or nanovoid can be formed around the nanofiller [Nel04b, Nel04c].

The individual relative permittivities of inorganic nanofillers (ε_r=4-12) are typically higher than with the matrix polymer (ε_r=2-4) [Ima06a, Ima06b, Tun09]. This leads to the conclusion that the lowering of the relative permittivity in nanocomposites cannot originate from the nanoparticles. The reason for the lower relative permittivity in nanocomposites must be related to polarization mechanisms in matrix polymer. Polymer chain mobility has been reported to decrease in nanocomposites systems [Sin08a, Sin08b Tun09]. As Tanaka reports, in the multi-layered core model [Tan05a], a tightly bonded first layer is formed between the nanofiller and the matrix polymer. When these immobile nanolayers are considered in the whole matrix, it leads to restricted mobility of polymer chains and to reduced relative permittivity. The polymer chain entanglements have been reported to impair the mobility of polymer chains and hence relative permittivity [Sin08a, Sin08b]. The immobility and entanglement mechanisms are dependent on nanofiller content and dispersion.

As has been discussed earlier, with low filler content the probability for agglomerates is low and, due to that, interfacial effects in nanocomposites are more pronounced. With low nanofiller content the relative permittivity is determined by the minimum effect of nanofiller permittivity and strong interaction between polymer matrix and nanofiller [Koc09a, Sin08a]. The lowest relative permittivity values are therefore achieved with low nanofiller contents (<5 wt-%, Table 2). With increasing nanofiller content the individual permittivity of the nanofillers will contribute more and more to increasing the relative permittivity of nanocomposite. In this sense, immobilization and nanofiller content effects lead relative permittivity in different directions. The movement of polymer chains is harder and harder with increasing filler content. The greater number of particles with higher relative permittivity than the matrix material raises the relative permittivity value of the nanocomposite.

The nanofiller density will define the number of nanoparticles in the matrix material at each nanofiller content. The number of particles further relates to the interfacial area created by the nanoparticles. Density changes between nanofillers are one reason for the changes in the relative permittivity of nanocomposite with same nanofiller content. It is difficult to separate the effects of immobility, entanglement and nanofiller properties from each other. In general, there is a threshold nanofiller content where these processes have an equal effect. At threshold nanofiller content the relative permittivity is at the same level as the

reference polymer. Actually the threshold nanofiller content can be as low as 0.5-2 wt-%, as was determined in [Hin06, Koc09a, P5, Sin08a] or even as high as 5-10 wt-% [Che08, Koc09b]. The increase of relative permittivity with higher nanofiller content can also be an indication of non-homogeneous dispersion and agglomerates of nanofillers. Impurities in the manufacturing process and residual curing agents and dispersants can also cause increase of relative permittivity in nanocomposites [Rae05, Tan05a].

Dielectric losses consist of conduction and polarization losses. Conductivity depends on temperature, applied frequency and voltage. Polarization losses are due to molecular friction in polarization of a dielectric material in electric field. High tan δ values in microcomposites are explained by the large number of charge carriers due to defects and weak bonding between the microparticles and the matrix polymer [Sin08a]. Dielectric losses of nanodielectrics are usually at the same level as in the reference material (Figure 16). This was also noticed with 5 wt-% SiO_2-PP nanocomposite (Figures 17 and 18). Both studies revealed that the dielectric losses of 5 wt-% SiO_2-PP nanocomposite are at the same level as reference PP. The relative permittivity of 5 wt-% SiO_2-PP nanocomposite was slightly higher than in reference PP. Normalized capacitance did decrease by the same trend with both materials until 80 °C. This is important considering e.g. power capacitors, which operate in 50-60 °C temperature region. There is no capacitance change compared to reference PP and no additional heat is produced due to low loss factor. Actually, even reductions in tan δ have been reported with POSS-PP, SiO_2-PP, SiO_2-PI, SiO_2-EP, LS-EP, TiO_2-EP and Al_2O_3-EP nanocomposites [Cao04, P3, P7, Tan04, Tan05a, Tan06a, Sin08a]. Reduction in tan δ is evident due to an increase in T_g in LS-EP nanocomposites [Tan05a]. Figure 19 presents the dielectric losses of reference PP and 1 and 2 wt-% SiO_2-PP nanocomposites. The dielectric losses of 1 wt-% SiO_2-PP nanocomposite decreased slightly compared to the dielectric losses of reference PP [P7].

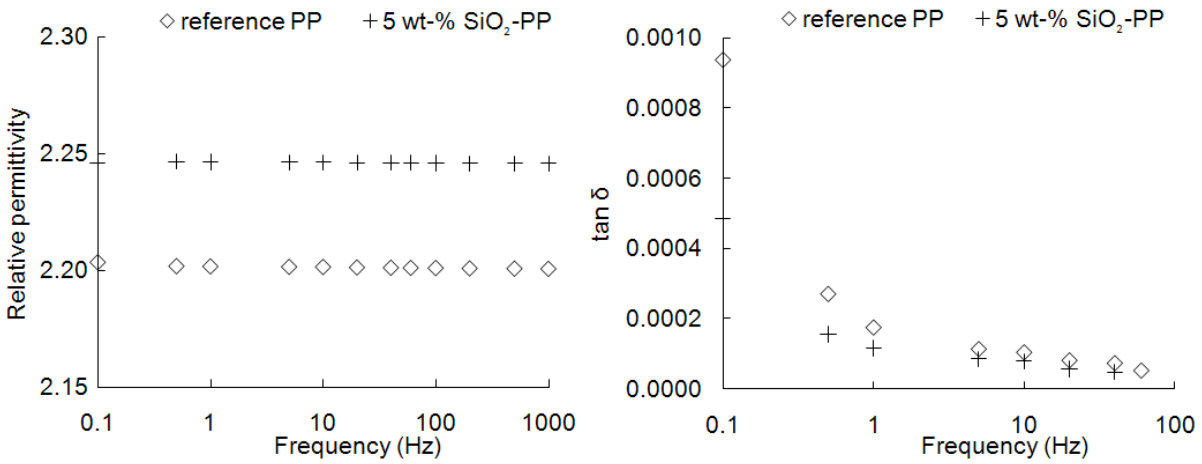

Figure 17. Relative permittivity and dielectric losses of reference PP and 5 wt-% SiO_2-PP nanocomposite as a function of frequency [P6].

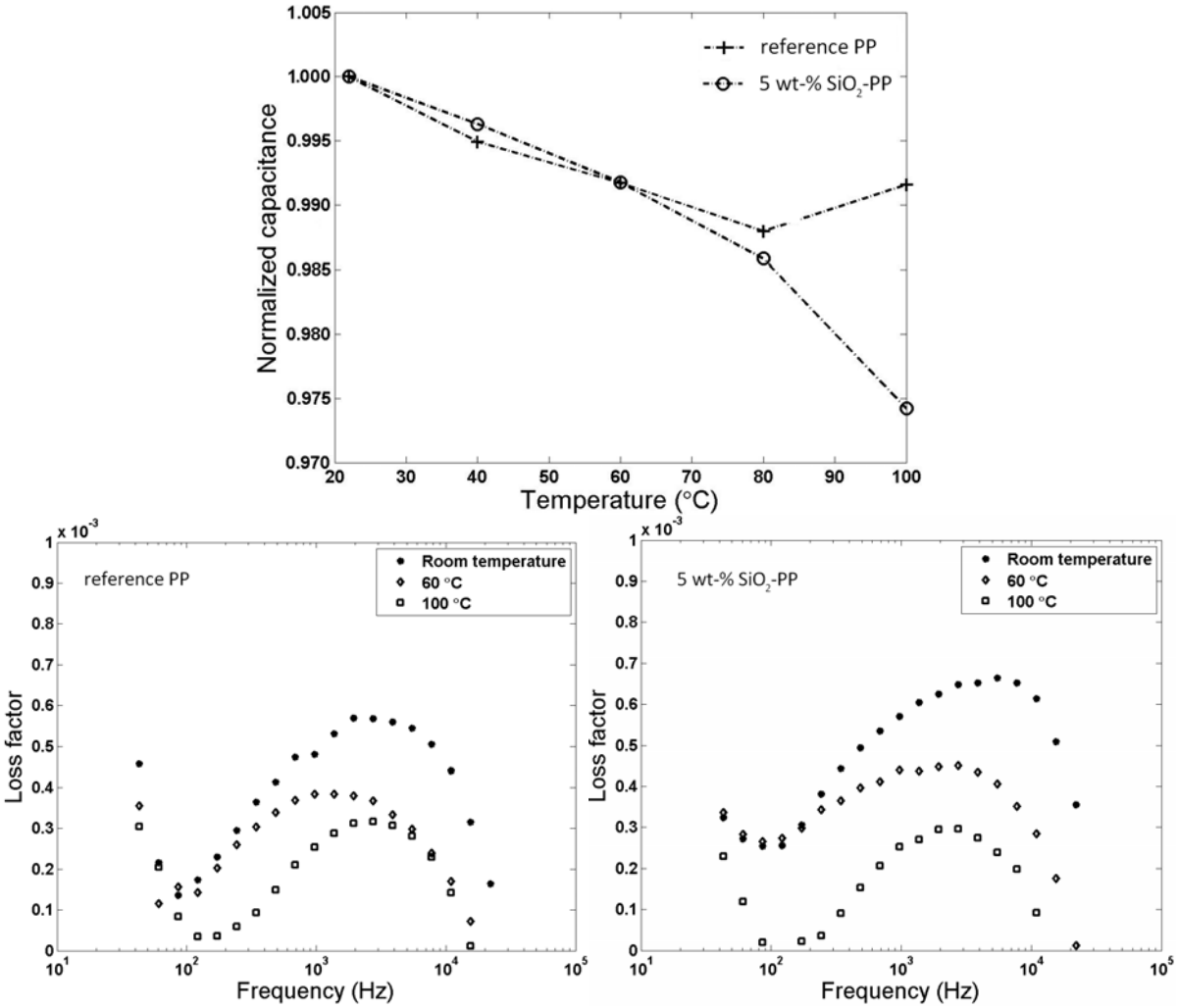

Figure 18. Normalized capacitance (at 43 Hz) of reference PP and 5 wt-% SiO_2-PP nanocomposite as a function of temperature (above). Dielectric losses of reference PP (left below) and 5 wt-% SiO_2-PP nanocomposite (right below) as a function of frequency at different temperatures: RT (22°C), 60 °C and 100 °C [P8].

Lower tan δ values in nanocomposites than in reference material may be also due to lower electrical conductivity. Singha et al. explain that nanoparticles act as barriers to charge transport [Sin08a]. At low nanofiller concentrations the large volume fraction of interfaces and polymer chain entanglements decreases the motion of charge carriers and causes reduction in electrical conductivity. In fact, the strong and stable bonding between the nanofiller surface and the polymer matrix can lead to fewer defects and fewer free charge carriers. The hindered motion and smaller amount of charge carriers together cause a reduction in dielectric losses. This phenomenon is quite similar to the decreased relative permittivity with increased immobility and entanglements of polymer chains. With higher nanofiller concentrations there is larger number of nanoparticles and inter-particle distances are lower. Nanoparticles may also be in contact with each other and the number

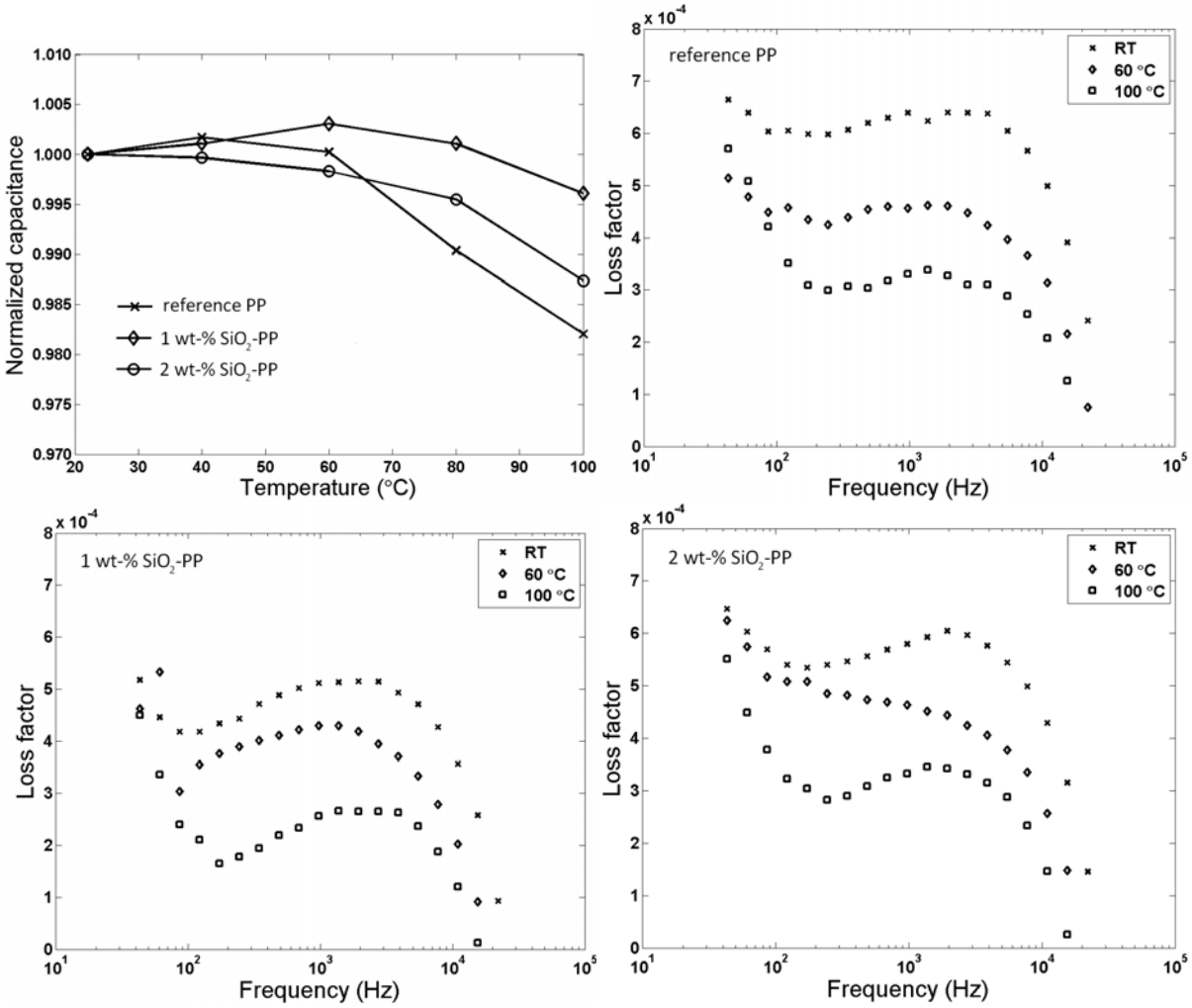

Figure 19. Normalized capacitance (at 43 Hz) of reference PP and 1 wt-% and 2 wt-% SiO_2-PP nanocomposites as a function of temperature (left upper corner). Dielectric losses of reference PP (right upper corner) and 1 wt-% (left lower corner) and 2 wt-% (right lower corner) SiO_2-PP nanocomposites as a function of frequency at different temperatures: RT (22°C), 60 °C and 100 °C [P7].

of free charge carriers is also higher. When the interfacial zones of nanoparticles overlap at high filler concentrations (>5-10 wt-%, Figure 3), the possibility for mobility of charge carriers increases. The overlapping of the interfacial zones also depends on nanofiller size and dispersion. With smaller nanoparticle diameter overlapping is achieved with lower nanofiller content. The possible overlapping increases charge transfer in nanocomposite. Figure 20 presents the dielectric losses of octamethyl POSS-PP composites. There is a threshold level between nanofiller content of 2 and 3 wt-%. With TiO_2-EP nanocomposites 10 wt-% nanofiller content has been observed to increase the tan δ values higher than reference EP [Sin08a].

This same overlapping phenomenon is called quasi-dc conduction (QDC) by Jonscher or low-frequency dispersion (LFD) by Dissado and Hill [Fot04, Lew04a, Nel04a, Nel04b, Nel05,

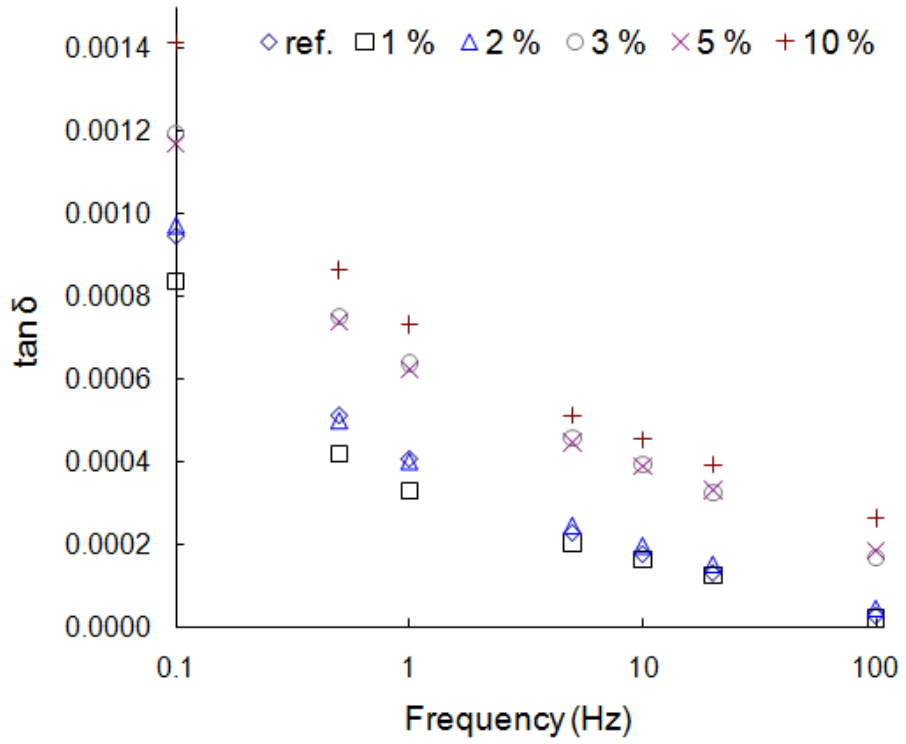

Figure 20. Effect of octamethyl POSS content on the dielectric losses of PP as a function of frequency [P3].

Roy07, Smi08, Zou06a]. Relative permittivity starts to increase at low frequencies (< 0.1 Hz) due to quasi-dc conduction. Lewis has explained that the phenomenon is due to the efficient transfer of charge carriers in quasi-conductive paths formed by partially overlapping charge layers (Figure 3) [Lew04a]. At low frequency electric field induces polarization at the interfacial volume around nanoparticle and a large dipole forms. This leads to high relative permittivity at low frequency. QDC also explains the improved DBS in dc voltage [Fot04, Nel04b]. When the quasi-conductive overlapping regions are formed around the nanoparticles, charge accumulation is smaller and withstand voltage is higher. Tan δ remains at a low level because charge carriers have only limited movement through partially connected interaction zones. Thus QDC does not affect bulk conductivity. All overlapping is dependent on nanofiller content and size and dispersion. Fothergill et al. suggest that few wt-% of nanofiller is needed for interaction zones to overlap [Fot04].

The relative permittivity of the nanofillers has also a minimal effect on the dielectric losses, as has been observed with zinc oxide (ZnO)-EP and TiO_2-EP nanocomposites [Sin08a]. High relative permittivity nanofillers, like TiO_2 (ε_r=5-15 depending on shape), introduce free charges into the polymer matrix. From the nanocomposite studies it can be seen that, with filler quantities of 5-10 wt-% and higher, the dielectric losses start to increase (Table 2). It may be assumed that there is also a threshold level for dielectric losses. Actually the threshold level can be as low as 1-3 wt-%, as was determined in [Hin06, P3, P5]. With increasing amount of nanofiller the probability for aggregates increases and local conduction paths become more pronounced [Sin08a]. These phenomena indicate that low dielectric losses of nanodielectrics are also a measure of dispersion in the material. MMT

nanofillers have been observed to increase tan δ values in PE [Gre08]. Although the DBS of the MMT-PE nanocomposites increased, the dielectric losses also increased with nanofiller content. A slight increase in tan δ has also been observed with LS-SR nanocomposites at 50 Hz [Tan04].

4.3 Frequency and temperature dependency

Relative permittivity and dielectric losses are frequency and temperature dependent [And09a, Fot04, Fré08, Koc09a, Sin08a]. As frequency increases, relative permittivity decreases. Interfacial or space charge polarization and large molecules cannot keep the phase of the applied electric field and contribute to polarization. At higher temperatures a shift in the interfacial processes with respect to frequency has been observed with LS-EP nanocomposites [Fré08]. Dang et al. conclude that enhanced relative permittivity is observed at low frequencies with barium titanate ($BaTiO_3$)- polyvinylidenefluoride (PVDF) nanocomposite, actually ε_r values are 10 times larger at 0.1 Hz than at 10^6 Hz [Dan07]. The polarization relaxation (interfacial and dipole polarization) in $BaTiO_3$-PVDF nanocomposite is easier than with corresponding microcomposite and the nanosize ceramic particles will be charged. With larger $BaTiO_3$ particle size, ε_r decreases in the low frequency region. Ambid et al. suggest that the change in relaxation processes with respect to frequency can be matrix or nanofiller related phenomenon in PP [Amb04]. Layered silica may affect the crystallisation of PP matrix or the interface between nanofiller and matrix may act as a charge trap.

Temperature effect has been studied with SiO_2-PP and TiO_2-EP nanocomposites (Figures 18 and 19) [Nel05, P7, P8]. All the SiO_2-PP nanocomposites maintained the capacitance with respect to increasing temperature, the 1 wt-% SiO_2-PP nanocomposite being the most stable. The capacitance of 1 and 2 wt-% SiO_2-PP nanocomposites remain higher at 80 °C and 100 °C compared to the reference PP. The restriction of polymer chain movement seems to stabilize dielectric properties at higher temperatures. The dielectric losses decreased with increasing temperature. Approximately the same range of changes could be seen between different material compositions [P7]. Nelson and Hu observed two patterns in the $\tan \delta$ behaviour of TiO_2-EP nanocomposites. Below 70 °C $\tan \delta$ is increasing with temperature without any peaks, but above 85 °C $\tan \delta$ exhibits broad peaks. These peaks shift to higher frequencies with increasing temperature. This indicates that relaxation processes are activated above T_g in TiO_2-EP nanocomposite. Above T_g the TiO_2-EP nanocomposite matrix has more mobility and an increase in free volume is observed [Nel05]. Imai et al. also report that with LS-EP nanocomposite, ε_r and $\tan \delta$ stay at low values up to 140 °C compared to reference EP [Ima02]. It has also been noted that alkylammonium ions may serve as charge carriers and have an effect on the relative permittivity and dielectric losses of LS-EP nanocomposite with increasing temperature [Ima06a, Ima06b]. Alkylammonium ions are used to modify LS nanofillers before mixing with EP.

4.4 Humidity and functionalization dependence

The control of humidity is important for dielectric measurements since nanocomposites absorb more moisture than microcomposites because of the increased free volume [Koc09a, Per06, Sin08a, Zou06a, Zou06b, Zou08]. The use of nanoparticles usually introduces a water sensitive component into the polymer matrix and leads to an increase in ε_r and $\tan\delta$ values [Zou08]. The measurement environment should be kept constant with respect to temperature and humidity. Changes in the $\tan\delta$ behaviour of nanocomposites with respect to absorbed water have been studied with Al_2O_3-EP nanocomposites [Zha06]. Zhang et al. conclude that the location and mobility of water in nanocomposites reflect the dielectric response, but after drying no changes could be seen between Al_2O_3-EP nanocomposite and reference EP. The SiO_2-PP nanocomposites were heat treated at 60 °C for 18 h to avoid the effect of water on measurements (Figures 18 and 19) [P7, P8]. Andritsch et al. and Kochetov et al. dried the EP nanocomposites for two days in 120 °C and 140 °C before measurements in N_2 atmosphere [And09b, Koc09a].

Zou et al. conclude that water surrounds hydrophilic SiO_2 nanoparticles in EP [Zou06b]. The overlapping of water layers around nanoparticles can provide paths for charge carriers and QDC behaviour occurs [Zou08]. With high nanoparticle contents and shorter distances, less water and lower temperatures are required for overlapping of the water layer around the nanoparticles. This leads to weakness with respect to mechanical, dielectric and ageing properties. The water uptake of nanocomposites can be reduced with better interfacial adhesion between the matrix polymer and the nanoparticles. Thus, higher density around the nanoparticles can be achieved and less water can be absorbed in the composite. Another solution is to change the surface of the nanoparticle to a hydrophobic one. Hydrophobic SiO_2 nanoparticles can reduce the water absorption in nanocomposites [Zou08]. With 3 wt-% of hydrophobic SiO_2 in EP, the water uptake can be even less than with reference EP, but the samples are difficult to prepare.

Functionalization of the nanofiller surfaces can also lead to changes in interfacial polarization, which is suggested to be less pronounced with coated nanofillers [And09b, Sin08a]. Though, interfacial or space charge polarizations occur at low frequencies (< 100 Hz), when space charge accumulation at interface boundaries is possible. Actually the fillers can have functionalities as such. The relative permittivity of polyaniline emeraldine base (PANI-EB) can change as a function of ac electric field (Figure 21) [P1, Sal06]. Electric field strength calculations for insulation structure with defects are presented in P1. The field grading property leads to lower electric field stresses in possible applications e.g. in power capacitors (Figure 22). The operation is similar to metal-oxide varistors used in overvoltage protection. The curing agent used in epoxy casting also has an effect on nanocomposite relative permittivity. Tagami et al. conclude that with amine-cured LS-EP nanocomposites relative permittivity is lower than with anhydride-cured epoxy nanocomposites [Tag08]. Amine-cured samples have OH-bonds, which cause strong interaction with nanofiller. Strong interaction with nanofiller restricts the chain movement. Cao et al. also report that silicon carbide (SiC), $BaTiO_3$ and ZnO composites have been employed as field grading materials because their conductivity and/or relative permittivity are heavily dependent on electric field, unless the DBS of the composites is weak [Cao04].

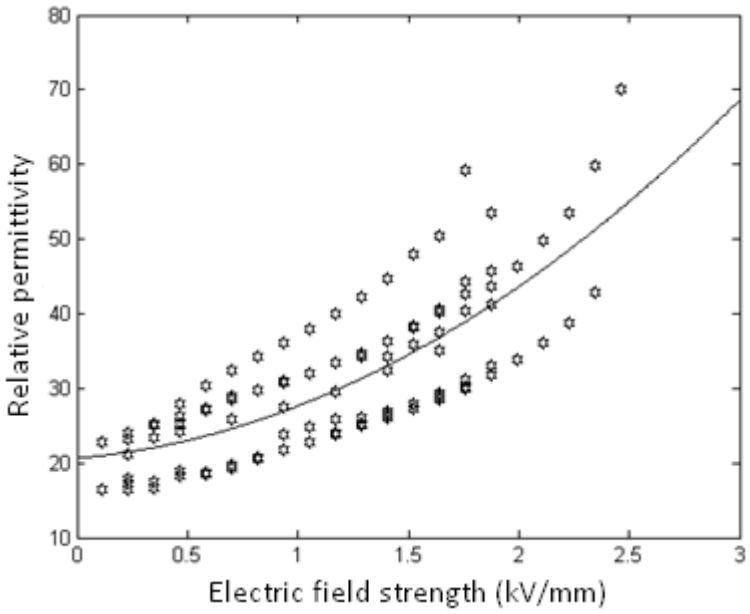

Figure 21. Relative permittivity of PANI-EB as a function of electric field strength. Stars are the measurement points and the solid line is the fitting for relative permittivity of PANI-EB [P1].

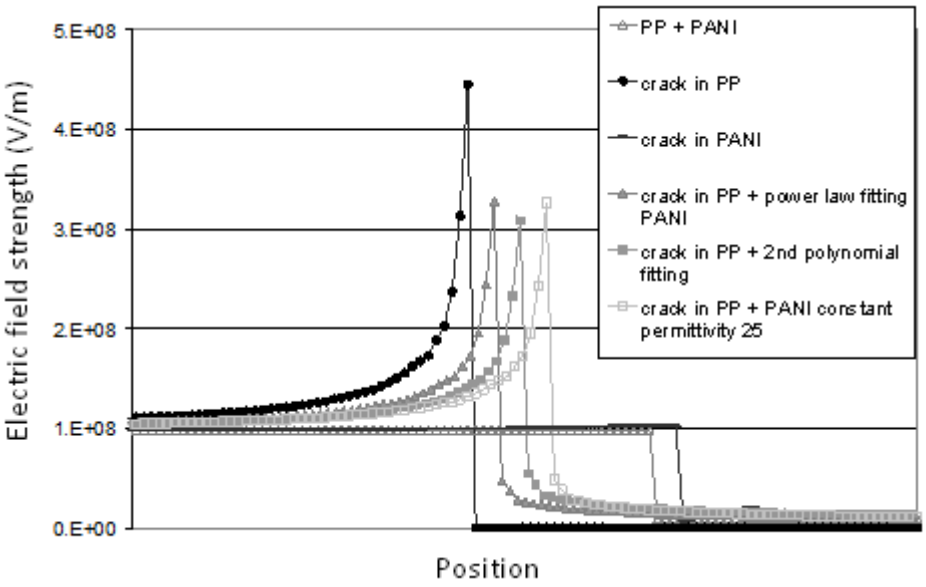

Figure 22. Electric field strengths for insulation structure with defects. The curves are shifted along the Position-axis. The electric field strength is highest at the tip of the defect [P1].

4.5 Summary

Figure 23 presents the variables and factors affecting the relative permittivity and dielectric losses of nanocomposites. Many of the factors presented are interdependent. In Figure 24 a schematic drawing of the relative permittivity and dielectric losses of nanocomposites as a function of nanofiller content is presented. With increasing nanofiller content, the relative permittivity and dielectric losses have a threshold nanofiller content. Both relative permittivity and dielectric losses start to increase after that level. Behaviour is the same as with microcomposites. However, at low filler contents the relative permittivity of nanocomposites tend to decrease and dielectric losses remain at the reference level or even decrease. Table 2 presents the threshold of the nanofiller content in relative permittivity and dielectric losses of nanocomposites.

In this dissertation the main contributions considering the relative permittivity and dielectric losses of nanocomposites are:

1. Measurements of PANI-EB and the model calculations indicate that PANI-EB may lower the electric field stress, especially in higher electric field regions like defects in capacitor insulation [P1].

2. Higher permittivity values were obtained with octamethyl POSS compounds than with the reference PP. With higher octamethyl POSS quantities the loss factor increased, but with small quantities the loss factor remained at the same level as with the reference PP. Octaglycidyldimethylsilyl POSS did not affect the relative permittivity or loss factor of EP [P3, P5].

3. The capacitance of 1 and 2 wt-% SiO_2-PP nanocomposites remains higher at 80 °C and 100 °C compared to the reference PP. It also seems that the measured loss factor of 1 wt-% SiO_2-PP nanocomposite is lower than with the reference PP [P7].

4. With 5 wt-% SiO_2-PP nanocomposite dielectric losses remained comparable to the reference PP. Normalized capacitance did decrease by the same trend with both materials until 80 °C. There is no capacitance change compared to the reference PP and no additional heat is produced due to low loss factor [P6, P8].

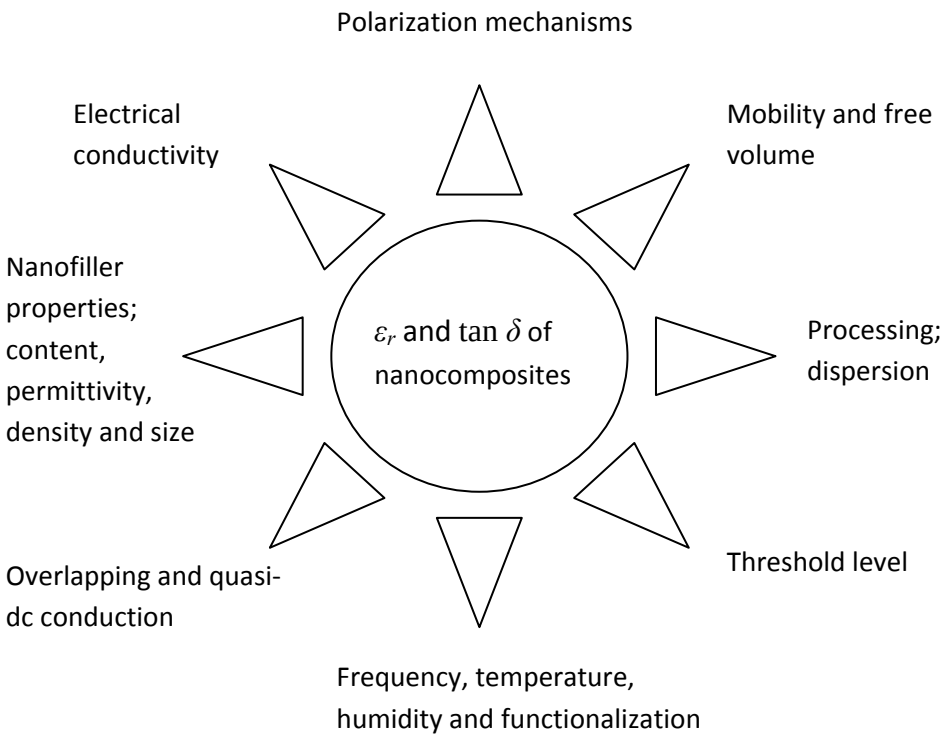

Figure 23. Variables and factors affecting the relative permittivity and dielectric losses of nanocomposites.

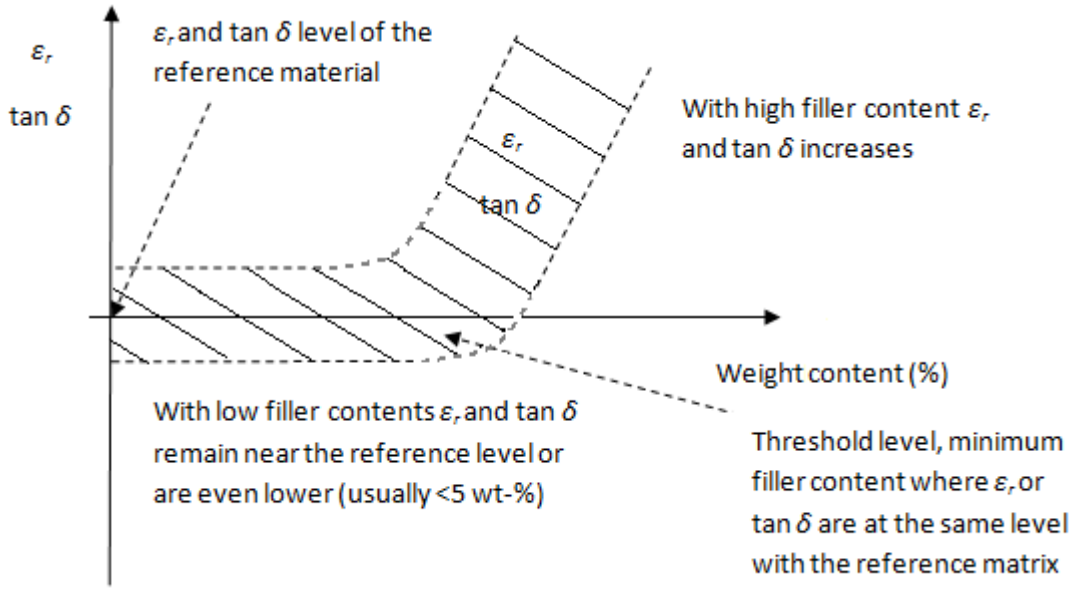

Figure 24. Relative permittivity and dielectric losses of nanocomposites as a function of filler content [Che08, Fus04, Fus08, Ima02, Jia07, Koc09a, Koc09b, Nag08, Roy05, Shi04, Sin08a, P3, P5-P8].

Table 2. Threshold of the nanofiller content in nanocomposites, where relative permittivity and dielectric losses are at the same level as the reference matrix.

	Matrix	Nanofiller	Weight content (%)	Effect compared to reference	Threshold weight content (%)	Publication
ε_r	PP	octamethyl-POSS	1, 2, 3, 5, 10	increase		P3
	PP	SiO_2	5	no difference		P6, P8
	LDPE	MgO	1, 5, 10 (phr)	decrease and increase	between 1 and 5	Nag08
	LDPE	MgO	1, 2, 5, 10 (phr)	decrease and increase	between 1 and 2	Hin06
	XLPE	SiO_2	5	decrease		Roy05
	XLPE	vinylsilane-treated SiO_2	5	no difference		Roy05
	PEI	SiO_2	5, 10, 15	decrease		Che08
	PA	mica (silicate)	2, 4, 5	decrease		Fus08
	EP	glycidyl-POSS	1, 3, 4.8	decrease and increase	between 1 and 3	P5
	EP	octaglycidyldimethylsilyl-POSS	1, 3, 4.8	no difference		P5
	EP	SiO_2	3	increase		Jia07
	EP	LS	6	decrease		Ima02
	EP	aluminum nitride (AlN)	0.5, 2, 5, 10	decrease and increase	between 0.5 and 2	Koc09a
	EP	boron nitride (BN)	0.5, 2, 5	decrease and increase	between 2 and 5	Koc09a
	EP	Al_2O_3	0.5, 2, 5, 10	decrease and increase	between 5 and 10	Koc09b
	EP	LS	6	decrease		Shi04
	EP	TiO_2	0.1, 0.5, 1, 5, 10	decrease and increase	between 0.5 and 1	Sin08a
	EP	ZnO	0.1, 0.5, 1, 5	decrease and increase	between 1 and 5	Sin08a
	SR	LS	5	no difference		Tan04
tan δ	PP	octamethyl-POSS	1, 2, 3, 5, 10	decrease and increase	between 2 and 3	P3
	PP	SiO_2	1, 2	decrease or no difference		P7
	PP	SiO_2	5	no difference		P6, P8
	XLPE	SiO_2	5	decrease		Roy05
	XLPE	vinylsilane-treated SiO_2	5	decrease		Roy05
	PA	mica (silicate)	2, 4, 5	no difference		Fus08
	EP	glycidyl-POSS	1, 3, 4.8	decrease and increase	between 1 and 3	P5
	EP	octaglycidyldimethylsilyl-POSS	1, 3, 4.8	no difference		P5
	EP	LS	6	decrease		Ima02
	EP	SiO_2	3	decrease		Jia07
	EP	aluminum nitride (AlN)	0.5, 2, 5, 10	increase		Koc09a
	EP	boron nitride (BN)	0.5, 2, 5	no difference		Koc09a
	EP	Al_2O_3	0.5, 2, 5, 10	no difference		Koc09b
	EP	LS	6	decrease		Shi04
	EP	TiO_2	0.1, 0.5, 1, 5, 10	decrease and increase	between 1 and 5	Sin08a
	EP	ZnO	0.1, 0.5, 1, 5	decrease	over 5	Sin08a
	SR	LS	5	no difference		Tan04

5 . Treeing growth and partial discharge endurance

5.1 Experimental measurements

This chapter combines treeing growth and partial discharge (PD) studies conducted for nanocomposites in various measurement setups. Measurement conditions (temperature, humidity), used voltage level and shape and frequency of the voltage have an effect on these properties. Measurements are conducted with different electrode geometries, e.g. cylinder, rod and needle plane, providing different electric field distributions. In P4 rounded rod electrodes and in P8 conical rod electrodes were used (Figure 25). A rounded rod electrode in P4 was chosen to cause even erosion to the material for a round shape area with a diameter of 2-3 cm. A conical rod electrode in P8 was chosen to simulate small, puncture-like flaws in the insulation material or in the electrodes. Those weak spots determine e.g. the electric fields used in capacitors and in general impair the reliability of insulation systems. The effect of puncture-like flaws in a similar electrode setup has been simulated in P1.

The methods used to analyse experiments vary in the literature. Treeing growth is studied with total failure time at different voltage levels, the length of an electrical tree, tree inception time and voltage and with type of tree (branch or bush). Surface degradation is studied with quantities as PD level [P4, P8], PD pattern and PD inception voltage, light intensity, surface roughness [P4], erosion depth and speed [P8], eroded mass and time to failure [P8]. Material samples and surfaces are characterized after degradation with optical microscopy [P8], profilometer [P4] and electron microscopy. In Figure 26 a photograph of PANI-PP material is presented. After 4 h of PD degradation the surface of the material is

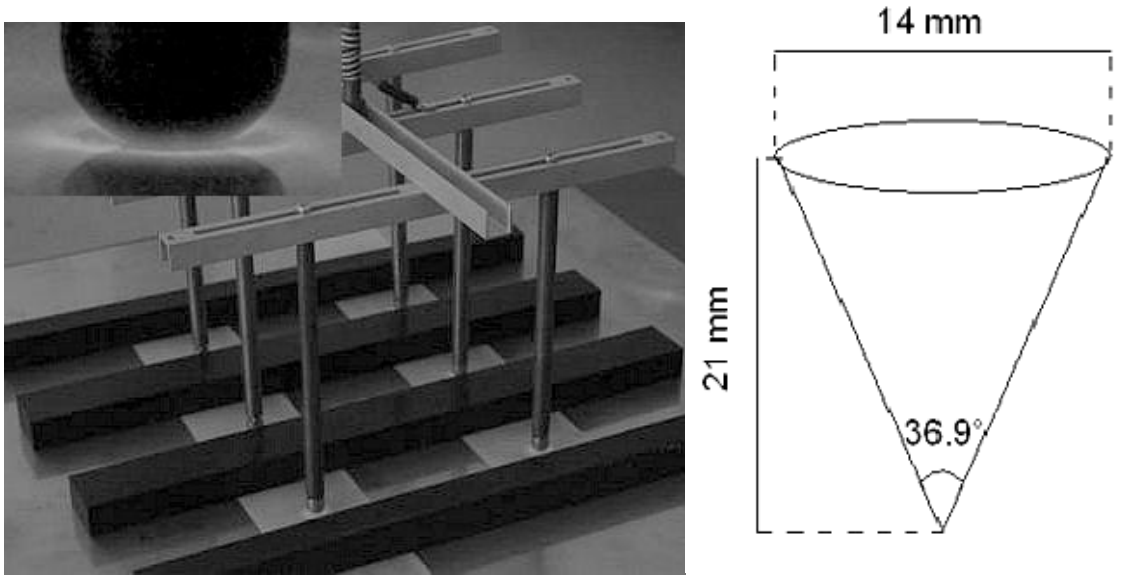

Figure 25. Surface degradation test with partial discharges around six electrodes and the material sheet (on left) [P4]. *Sketch of the conical rod electrode used in PD endurance measurements* [P8].

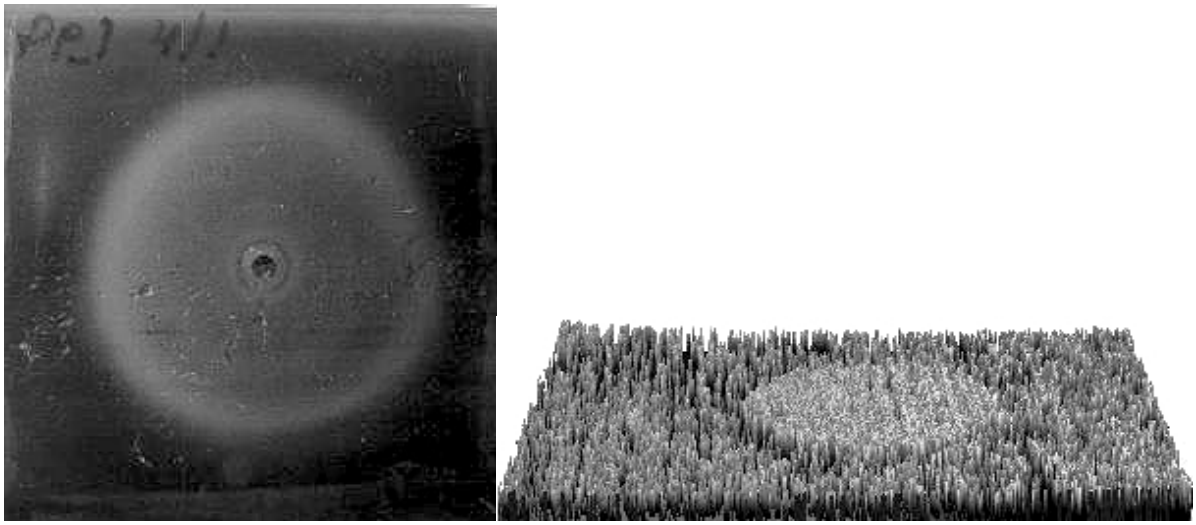

Figure 26. Photograph of PANI-PP material sample after 4 hours of PD degradation test (on left). Three dimensional surface profile of the sample centre (on right) [P4].

eroded. There are common factors and mechanisms affecting treeing growth and PD endurance of nanocomposites.

5.2 Affecting factors

The time scale of the treeing growth and PD endurance measurements is clearly longer than the short-time DBS measurements discussed in Chapter 3. The correlation between the results from short-term DBS and treeing growth and PD endurance measurements of nanocomposites has been found to be good [Hor05, Hor06, Ima04, Ima06a, Ima06b, Ima08, Kur06, Mon05, P8]. In general, this means that the materials with increased short-time DBS also have better resistance to treeing growth or PD endurance. In some cases these properties even correlate with the filler amount [Ima06a, Ima06b, Ima08, Kur06].

Bonding strength between nanofillers and matrix polymer has been claimed to be important in various studies [Fus08, Iiz07, Iiz08, Koz04a, Koz05, Mai08a, Mai08b, Mon05, Nel06, Pei03, Rae05, Rae09, Smi08, Tan06a, Tan08, Tie09, Ven09]. Strong bonding (such as ionic or covalent) and interaction between matrix and nanofiller promotes the endurance of the nanocomposite because the interface volume in nanocomposite is large. Strong bonds and interaction between nanofillers and polymer matrix lead to restricted molecular motion, as discussed in Chapter 4. When the bonds are strong between the nanoparticle and polymer matrix, the nanofiller is not easily dislodged under PD stress. The size of the particles and dispersion determine the endurance of nanocomposites. Various studies indicate that it matters little which nanoparticles are used [Dan09, Fus08, Gua06a, Gua08, Koz05, Mai08a, Pre09, Rae05, Tan08, Tie08]. If the diameter of the particles is reduced from 1 µm to 100 nm, the number of the particles would rise by a factor of 1000, when keeping the weight content constant [Din04]. Considering the tree channel interacting with many nanoparticles compared to few microparticles, higher energy is consumed. Figure 27 presents the PD degradation of micro- and nanocomposites. In surface degradation, smaller particle size

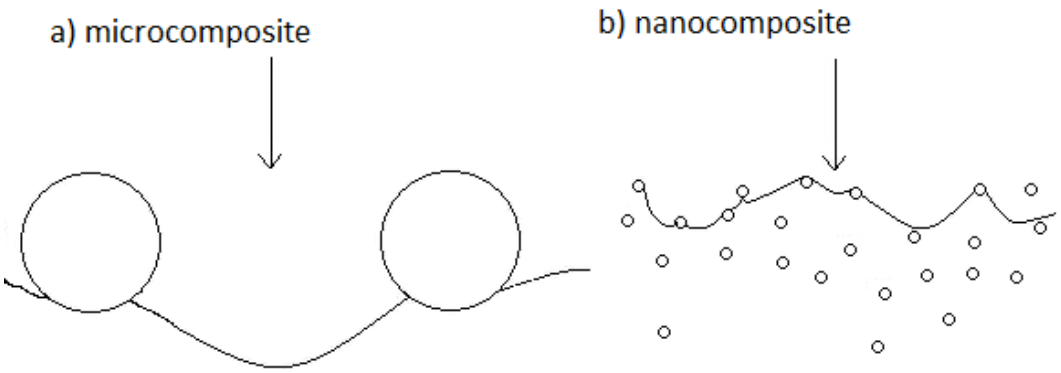

Figure 27. PD degradation of a) microcomposite, b) nanocomposite. PD stress direction marked with an arrow.

leads to lower erosion of the polymer matrix because of increased surface area and smaller amount of matrix material between the nanoparticles [Mai08a, Zha03].

The strength of the nanocomposites is not determined by the shape of the particle under surface degradation. Particles or layer shape nanofillers both give improved treeing growth and PD endurance [Fré05, Fré08, Mai08b]. However, Guastavino et al. conclude that ordered structure (intercalated) of LS nanofiller seems to behave better than random structure (exfoliated) of LS in EVA treeing experiment [Gua06b]. Functionalization [Fré06a, Iiz07, Mai08b, Min04, Nel07, Tan07a] of the nanofillers is beneficial and has effects on the chemical bondings. As presented in [Iiz07], silane treatment provides coupling between nanoparticles and EP. Roy et al. conclude that the lifetime of surface treated nanofiller composites is related to the formation of chemical bonds, which in turn reduce particle surface wetting and the formation of interfacial defects [Roy05]. The positive effect of functionalization has also been noticed in corona endurance of SiO_2-PI nanocomposite [Min04].

Inter-filler space or matrix volume surrounding nanoparticles should be minimized (distances from tens of nanometers up to parts of micrometers). Matrix material is the weak part under electrical degradation [Ala08, Ala09, Fus08, Ima06b, Koz04a, Koz05, Mai08a, Pre09, Tan06a, Tan08]. This manifests as smaller cavity sizes measured after surface degradation from 5 wt-% SiO_2-PP nanocomposite compared to reference PP in P8. Fuse et al. conducted scanning electron microscopy (SEM) and TEM analysis of the cavity sizes in mica-PA nanocomposites [Fus08]. The cavity sizes in nanocomposite were of the same order as inter-filler distance as they were 10-20 times larger in reference PA than in mica-PA nanocomposite. Nanofillers make it difficult for PD to create bigger cavities than the inter-particle distance (Figure 27). Imai et al. also noted that the treeing in LS-EP nanocomposite is arrested and separated into several branches by the silicate layers [Ima04]. Due to this the electric field strength around the tips of the branched treeings is decreased. Branching of electrical tree into bush shape pattern is noted in [Shi04] with the same LS-EP system. Actually, Maity et al. conclude that the degradation channels are located in the inter-filler regions and the width and depth are determined by the size of the nanofiller and the interface region surrounding each nanofiller in Al_2O_3-EP and TiO_2-EP nanocomposites [Mai08a].

In PD endurance measurements the erosion speeds for reference PP were 8.2, 2.6, 7.0 and 68 times higher than for the 5 wt-% SiO_2-PP nanocomposite at 2, 3, 3.5 and 4 kV respectively (Figure 28) [P8]. The corresponding PD levels were on average 1940 pC, 3910 pC, 4780 pC

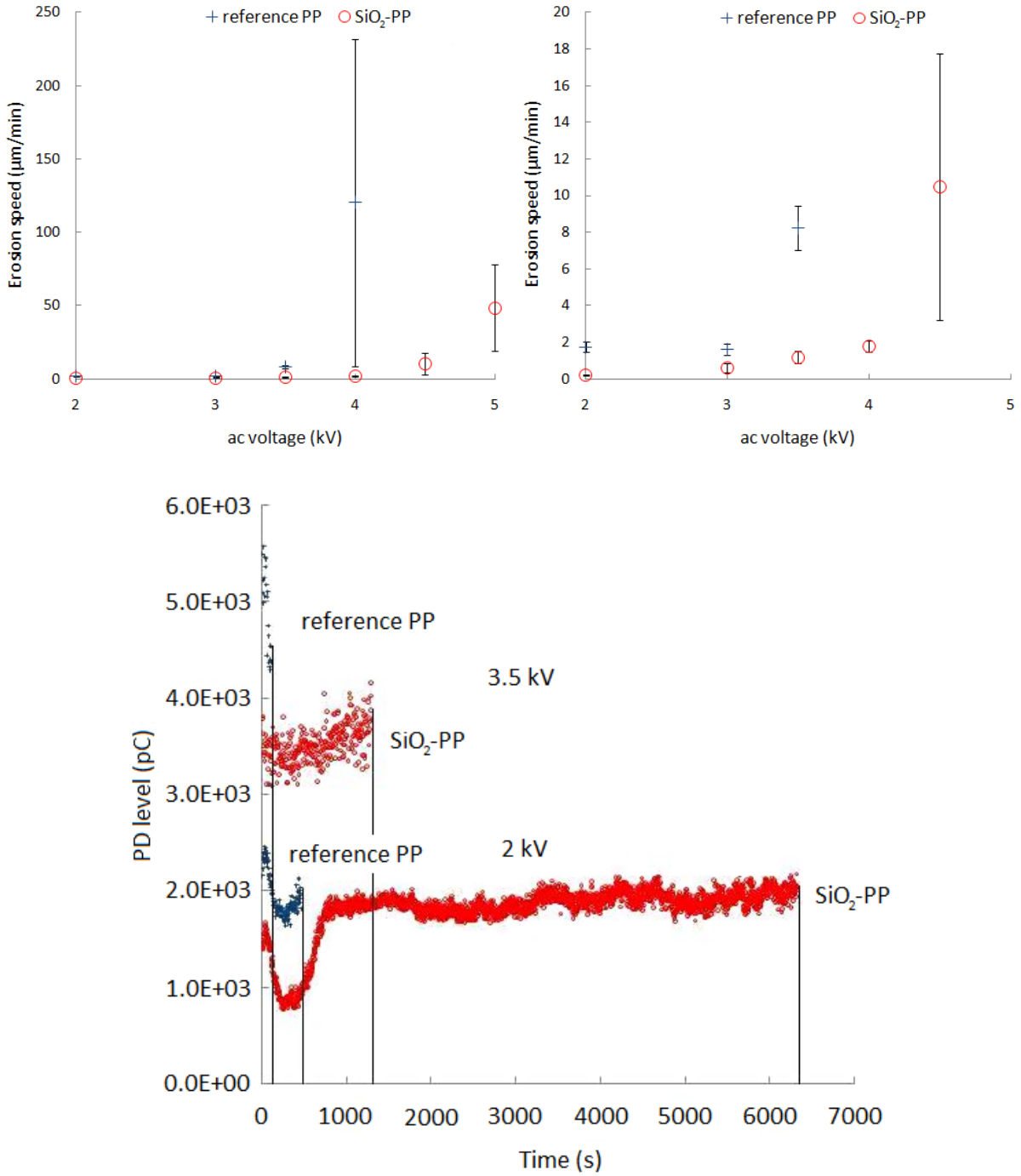

Figure 28. Erosion speeds under voltage stress and 95 % confidence limits of reference PP and 5 wt-% SiO_2-PP nanocomposite as a function of voltage (above). Partial discharge levels of reference PP and 5 wt-% SiO_2-PP nanocomposite as a function of time at 2 kV and 3.5 kV ac voltages (below) [P8].

and 12400 pC for reference PP. The PD levels for 5 wt-% SiO_2-PP nanocomposite were on average 1800 pC, 4620 pC, 3530 pC, 8070 pC, 9520 pC and 19420 pC at 2, 3, 3.5, 4 kV, 4.5 kV and 5 kV respectively. At the beginning of the tests a clear difference can be seen in PD levels of reference PP and 5 wt-% SiO_2-PP nanocomposite, but during the tests the PD levels tended to increase until final breakdown. Surface analysis of the films revealed that a layer of silicon oxides formed on the surfaces of the 5 wt-% SiO_2-PP nanocomposite during PD stress (Figure 29). The layers may protect the 5 wt-% SiO_2-PP nanocomposite from degradation and prolong the lifetime of the sample. This shielding behaviour is significant because the layers are formed due to PD stress on critical spots of insulation.

Kozako et al. studied the surface degradation of LS-PA nanocomposites [Koz04a]. Only a small fraction of pure PA is apparent, because spherulites are grown from the LS nanofillers (rectangular sheet shape). When pure PA is eroded spherulites and LS layers emerge and pile up on the surface. The same piling up mechanism has also been observed in P8 with 5 wt-% SiO_2-PP nanocomposite (Figure 29) and in [Fus08, Gua06a, Koz05, Mai08a, Mon05]. A protecting shield of Si-O has been reported to form during surface degradation of SiO_2-EP, POSS-PP and POSS-EP nanocomposites [Fab09, Hor02, Hor05, Hor06]. If some of the nanoparticles are removed from the surface there is less matrix material to be eroded before a new layer of particles emerges (Figure 27). Therefore Maity et al. presume that Al_2O_3-EP and TiO_2-EP nanocomposites have constant surface degradation rates [Mai08a]. This result is related to the homogeneous dispersion of nanoparticles, which was observed in Chapter 3 to increase β values in DBS measurements of nanocomposites. With microcomposites the degradation channels are wider and deeper because the inter-filler distance is larger and it takes longer to reach new microparticles to arrest degradation (Figure 27). As the nanofiller loading increases the inter-filler space decreases. Thus, the surface roughness of nanocomposites has been measured to decrease due to the addition of nanofillers [Pre09, Tan04].

The morphology of the inter-filler space affects the degradation of polymer nanocomposites [Fus04, Fus08, Gua09, Hor02, Koz03, Koz04a, Koz05, Tan06a, Tan08, Tie08]. It is not only a question if the crystallinity degree is increased or decreased compared to the reference material due to the addition of nanofillers. It is also a matter of the size of the crystalline areas and if small or large crystals give better performance under PD stress. Fuse et al. conclude that the crystallinity of 2 wt-% mica-PA nanocomposite increased to 42.8 % from 20.0 % for reference PA matrix [Fus08]. Mica nanofillers effectively create small crystals in PA matrix. Increase of crystallinity degree improves PD resistance, but also leads to an improved gas barrier property of the mica-PA nanocomposites. Thus, oxidation of the matrix is reduced [Fus08, Tan08]. Guastavino et al. also reported modifying the crystallinity of LDPE with MMT and sepiolite nanofillers [Gua09]. These two fillers alone did not perform well in electrical ageing tests, but when compounded together with LDPE, longer lifetime was achieved. MMT nanofillers enhanced the DBS and sepiolite increased the homogeneity of the nanocomposite.

Nanofillers and the surrounding interface volume can also trap charges [Nel06, P3, Rae08], as has been concluded with POSS-PP nanocomposites (Figure 5) and also with MgO-LDPE nanocomposite [Kur06, Mas07]. The number of particles and the interface volume is large even with low filler content in nanocomposites. The large interface volume provides traps

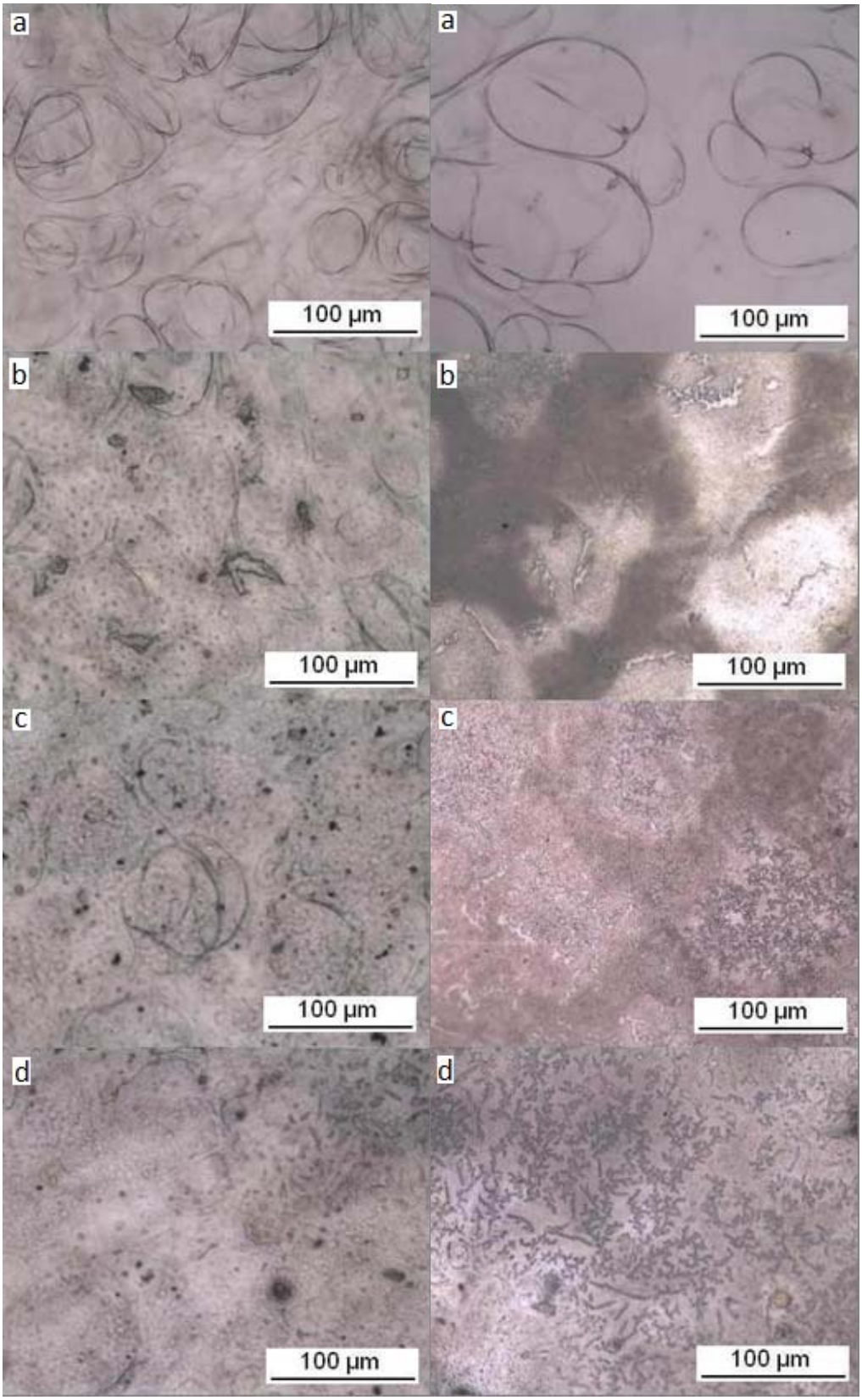

Figure 29. Optical microscope pictures from reference PP (on left) and 5 wt-% SiO_2-PP nanocomposite (on rigth). a) from non-stressed area, b) at 2 kV stressed area, c) at 3 kV stressed area and d)at 4 kV stressed area [P8].

for charges and electron energies are therefore decreased in high electric field conditions [Nel06]. Decrease of PD level and/or increase of inception voltage has been reported with 5 wt-% SiO_2-PP nanocomposite in P8 (Figure 28) and in [Gua08, Min04, Nel05, Pre09, Tie08]. The PD level at the same voltages was higher with reference PP than with 5 wt-% SiO_2-PP nanocomposite (Figure 28). Mingyan et al. suggested that charge transfer reduced charge accumulation and increased the initial corona voltage [Min04]. As discussed earlier in Chapter 4, inorganic nanofillers have higher relative permittivity than the polymer matrix [Ala08, Ala09, Ima06a, Ima06b, Tan04, Tan08, Tun09]. The tree growth follows the interface region of the nanoparticle until the electric field compels it to grow towards the next nanoparticle. Thus the tree pattern tends to be bushy and propagation time increases. In surface degradation more energy is concentrated on the nanoparticles which are more resistant to degradation than the surrounding polymer matrix.

One important factor affecting the treeing growth and PD endurance of nanocomposites is the amount of nanofiller. Kurnianto et al. and Nagao et al. suggest in their treeing studies that the movement of electrons is damped due to collisions with MgO nanoparticles in LDPE matrix [Kur06, Nag08]. Increase of the nanofiller content increases the number of collisions and hindrance of electron mobility in the nanocomposite. There are also indications that combined nano- and microparticles give improved treeing performance in EP matrix, as they form a “densely-packed structure” [Ima06b, Tan08]. When nanoparticles are mixed with conventionally filled epoxy, the collisions of electrons increase [Ima06b, Ala08, Ala09]. Imai et al. call this type of composite nano- and microfiller mixture composite (NMMC). Thermally stable Al_2O_3-nanofillers form a densely packed structure and only small regions of matrix material are exposed to PD [Ven09]. This is advantageous, because tracking and erosion are related to thermal degradation. Venkatesulu et al. conclude that in an inclined plane test for tracking and erosion the same results were achieved with 30 wt-% alumina trihydrate (ATH) microfiller and 4 wt-% Al_2O_3 nanofiller SR composites [Ven09]. Fréchette et al. conclude that a combination of micrometric and nanometric SiO_2 particles is advantageous with respect to surface degradation [Fré04]. Because micrometric particles have a large volume, more energy is needed to dig them out from the EP matrix. These results relate to the mass effect in the surface degradation process, which seems also to be advantageous with nanocomposites. However, nanofillers are not able to compete with microfillers with mass. The usual microfiller rates of 50-60 wt-% are hard to beat with a small amount of nanofillers (under 5 wt-%); a bigger amount (over 10 wt-%) with homogeneous dispersion is needed.

5.3 Bulk and surface degradation phenomena

Short-time breakdown and electrical treeing are considered to take place in bulk polymer. The mechanisms involved in these two phenomena lead to different directions. Good nanodispersion is the most critical parameter in DBS behaviour. Even a small number of nanoparticles increases the DBS of polymers. Considering the treeing mechanism, more obstruction is needed to inhibit tree growth. With increasing nanofiller content there comes a limit where the probability for agglomerates increases and DBS decreases. When the voltage is high enough, even smaller agglomerates become weak parts of the system. This can lead to a crossover phenomenon, which has been identified in [Iiz07, Rae08, Tie08,

Tan08]. Crossover phenomenon means that after increasing the voltage over a certain limit, nanocomposites start to lose good treeing properties over base polymer. At lower electric field strengths the lifetime of the nanocomposite is extended in a treeing experiment. This is important for the insulation design in reality. The crossover phenomenon is related to the overlapping of interaction zones and depends on the nanofiller loading and dispersion and on the electric field if the treeing endurance of the nanocomposite is weak. Similar behaviour has been reported in short-time DBS measurements at high filler loadings (Figure 15). Iizuka et al. conclude that treeing lifetime is highly structure sensitive (dispersion and filler content) and surface PD resistance is less structure sensitive [Iiz07].

Surface PD resistance is enhanced due to the segmentation of polymer matrix [Tan08]. Nanosegmentation means that the remaining polymer matrix regions are narrow and thus separation of nanofillers from matrix polymer is difficult. This mechanism means that even higher nanofiller loadings would be advantageous with respect to surface degradation, because the matrix polymer is the weak part of the degradation process. This indicates that PD resistance is less structure sensitive. Good surface endurance properties have also been achieved with high loadings of microfillers [Ven09]. The above mentioned processes lead to the ideas of NMMCs, coatings and layer structures.

5.4 Summary

Figure 30 presents the variables and factors affecting the treeing growth and PD endurance of nanocomposites. As mentioned, the correlation between short-term DBS measurements and these endurance measurements is strong. These properties are connected because the affecting mechanisms are partly the same. Figure 31 presents a schematic drawing of the treeing growth and PD endurance of nanocomposites as a function of nanofiller content. The surface PD endurance of nanocomposites is strongly a mass related phenomenon, but treeing growth is a more complex phenomenon. It is related to large interface volume of nanocomposites and has similar behaviour as that observed in short-time DBS (Figure 15). In the context of treeing this is called the crossover phenomenon. Table 3 shows the treeing growth, PD endurance, tracking and arcing of nano- and microcomposites.

In this dissertation the main contributions regarding the PD endurance of nanocomposites are:

1. In PD endurance measurements the average lifetime of 5 wt-% SiO_2-PP nanocomposite was 9 times longer than with reference PP [P8].

2. The PD levels at the same voltage level were higher for reference PP than for 5 wt-% SiO_2-PP nanocomposite. At the beginning of the tests a clear difference could be seen in the PD levels of reference PP and 5 wt-% SiO_2-PP nanocomposite, but during the tests the PD levels tended to increase until final breakdown [P8].

3. Surface analysis of the films revealed that a layer of silicon oxides formed on the surfaces of the 5 wt-% SiO_2-PP nanocomposite during PD stress. The layers may protect the 5 wt-% SiO_2-PP nanocomposite from degradation and lengthen the

lifetime of the sample. This shielding behaviour is significant because the layers are formed on critical spots of insulation due to PD stress [P8].

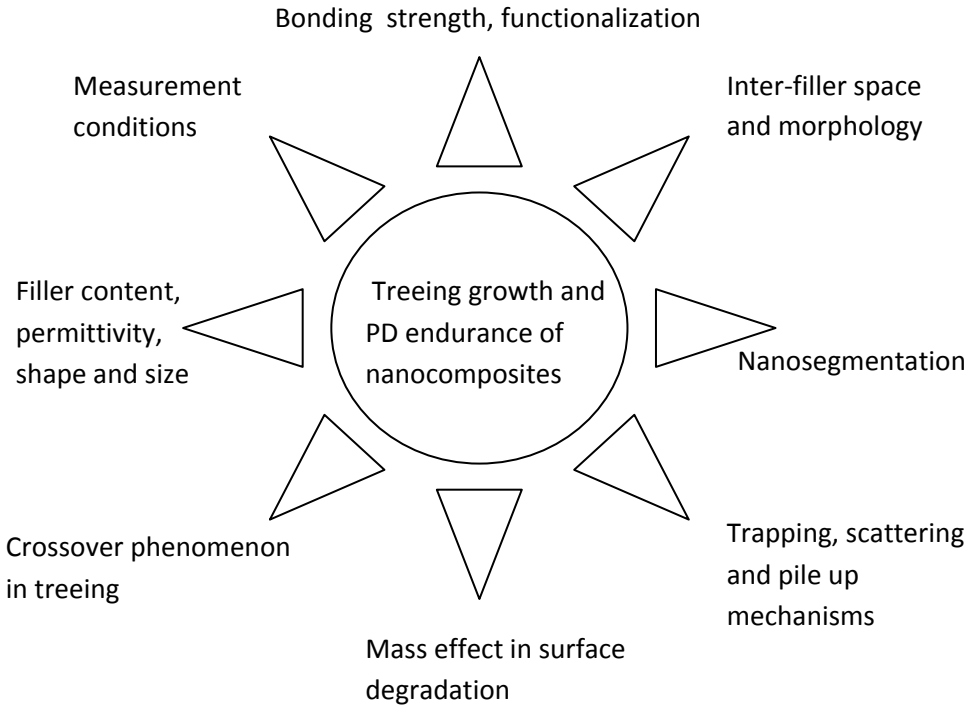

Figure 30. Variables and factors affecting the treeing growth and PD endurance of nanocomposites.

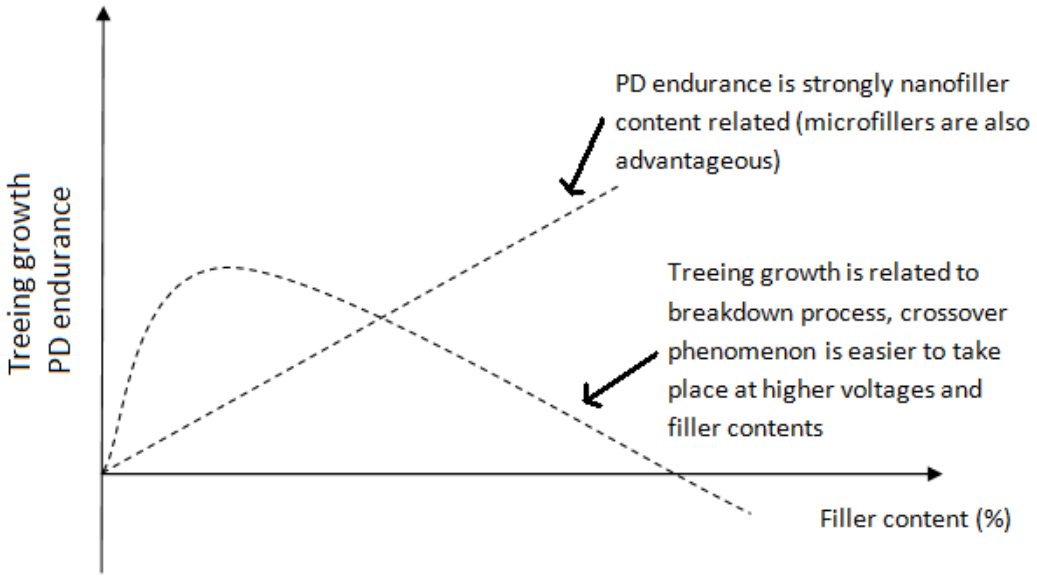

Figure 31. Treeing growth and PD endurance of nanocomposites as a function of filler content [Fus08, Hen99, Ima06b, Kur06, Min04, Nag08, Pre09, Rae09, Tan04, Tan07a, P8].

Table 3. Treeing growth, PD endurance, tracking and arcing of nano- and microcomposites with respect to the reference material.

	Matrix	Nanofiller	Filler content (%)	Effect	Variable vs. nanofiller content behaviour	Publication
Treeing growth	LDPE	MgO	1, 5, 10 (phr)	2.8 times longer time to breakdown	increase with filler content (best result 10)	Kur06, Nag08
	XLPE	SiO_2	5	100 times longer time to breakdown		Roy07
	EP	TiO_2	10	33 times longer time to breakdown		Ima08
	EP	nanofiller	5, 10	length of electrical tree reduced to 1/15 (5 wt-%)	increase with filler content (best result 10)	Tan07b
	EP	LS	0.5, 2.5	24 times longer time to breakdown	2.5 wt-% gives best result	Ima06b
PD endurance	PP	SiO_2	5	9 times longer time to breakdown		P8
	PA	LS	2, 4, 5	erosion depth decreases to 1/4	4 and 5 wt-% give best results	Fus08
	PA	LS	2, 4, 5	surface roughness decreases to 1/8	4 and 5 wt-% give best results	Tan04
	PI	SiO_2	5, 6, 7, 8	5.5 times longer time to breakdown between 8 and 5 wt-% samples	increase with filler content (best result 8)	Tan04
	PI	SiO_2	8	12 times longer time to breakdown		Tan04
	PI	SiO_2	3, 5, 6, 8, 10	3.5 times longer time to breakdown between 10 and 3 wt-% samples	increase with filler content (coupling agent better)	Min04
	LDPE	MgO	1, 5, 10 (phr)	erosion depth decreases to 1/3	increase with filler content (best result 10 phr)	Nag08
	EP	nano-SiO_2 vs. micro-SiO_2	5	erosion depth decreases to 1/5		Tan04
	EP	SiO_2	1.8, 3.6, 4.8, 7.2, 8.5, 9	13 times longer time to breakdown	increase with filler content (best results 8.5 and 9)	Hen99
	EP	Al_2O_3	0.1, 1, 5	surface roughness decreases to 3/5	increase with filler content (best result 5)	Pre09
Tracking	SR	LS	5	endurance time 2 times longer		Tan04
	SR	ATH (microfiller)	40	endurance time 2 times longer		Tan04
	SR	LS	5	erosion depth decreases to 1/3		Tan04
	SR	ATH (microfiller)	40	erosion depth increases by 1/4		Tan04
Arcing	SR	SiO_2 precipitated	0.1, 0.2, 0.5, 1, 2, 5, 10, 15	arcing time 3 times longer (5 wt-% sample)	after 5 wt-% decrease in arcing time	Rae09
	SR	SiO_2 fumed	2, 5, 10	arcing time 1.5 times longer	increase with filler content (best result 10)	Rae09

6 . Discussion

The future of nanodielectrics is bright, but there are evident challenges in using this technology in electrical applications. The future of nanodielectrics has been discussed in [Cao04, Dan09, Fré06b, Nel07, Nel08, Tan04, Tan05a, Tan07a]. As shown in the earlier chapters, the dielectric properties of polymers can be tailored with nanofillers. Tailoring of dielectric properties of nanocomposites is a reasonable research target in the future. The mechanisms and phenomena behind the properties of nanodielectrics must be thoroughly known. Even small nanofiller content creates large interfacial areas between the nanofillers and polymer matrix. This is one foreseen advantage in applying nanotechnology in dielectric materials, which can lead to lower costs after up-scaling of processes [An06, Ima06b, Zou06a].

The insulation technology needs efficient, reliable and compact products. Improvement of dielectric properties leads to cost savings and superior products. On the other hand improved energy quality and energy savings are also wanted. Reliability would result in lower maintenance costs. There is a need for insulation for higher voltages as the transmission voltages are increasing. The use of dc voltage in power transmission is becoming more important. Environmental and health aspects also have to be taken into account. The whole life-cycle of materials used and applications has to be considered, including ultimate recycling. One environmental option is to get rid of SF_6 gas (a greenhouse gas) in switchgear [Ima08, Tag08]. One application is to develop more heat resistant thermoplastic nanocomposites and replace thermoset resins, which cannot be recycled. The price of nanoparticles is decreasing and availability is becoming easier, especially because the processing of nanoparticles is advancing rapidly.

6.1 Future trends and challenges

With increasing interest in the functionalization of nanofillers the target in future is to manufacture self-assembled nanodielectrics with controlled filler dispersion [Nel04a, Nel06, Ima08]. This target is achievable if the matrix can be made chemically so attractive to the nanofiller (chemical hooks) that agglomerates are minimized and nanofillers are located at even distances in the matrix. Improved dispersion leads to small number of agglomerates with higher nanofiller contents. Thus, even lower threshold levels are possible as the dispersion of nanofillers is a key factor affecting dielectric properties. Possible ways of functionalization are nanocoating of insulation with flame spraying (LFS, liquid flame spray) or solution [Wu07, Wu08]. Superhydrophobic nanocoatings would increase resistance to tracking and erosion on SR and EP, although the effect on the self-recovery of hydrophobicity of SR needs to be studied further. Highly ordered layer structures could also be designed. One future trend could also be nanostructured layers with different functionalities e.g. a layer of high permittivity combined with a layer of high DBS [P1, Sal06]. Saha has concluded that a nanocapacitor with giant capacitance can be manufactured from metal filaments or conducting polymer chain segments [Sah08]. High capacitance capacitors would be useful for energy storage purposes. Water treeing resistance of

nanocomposites has not been studied. This is an important property, especially considering high voltage cables. The crossover phenomenon has to be thoroughly studied.

Even though the future of nanodielectrics is promising, there are many questions to be resolved. Manufacturing systems must be optimized and up-scaled to larger volumes. Promising results (Tables 1-3) have mainly been achieved with short-term measurements and work has been done to understand the mechanisms behind the functionality, which is important. Full-scale models of applications should be produced and long-term measurements conducted in operating conditions. Long-term measurements for real components will finally reveal the actual benefits and possible drawbacks of nanocomposites compared to the insulation materials currently in use. In addition to dielectric properties, the thermal, mechanical, chemical and ageing properties critical for each component must be ascertained. This means that industry should be more intensively linked to the research activities and actual new products should be developed. This step has been taken in Japan by Maekawa et al. with XLPE dc cable [Nag08] and by Imai et al. with EP connecting conductor and vacuum interrupter [Ima08].

6.2 Applicability of nanocomposites

There is a wide range of possible applications for polymer nanocomposites in the high voltage technology area. For PP capacitors, dc DBS especially has been seen to increase with the addition of nanofillers. This has been noticed especially in case of SiO_2-PP nanocomposite [P6, P8]. A general result related to DBS of nanocomposites is that homogeneous material leads to smaller deviation of the variable (Figures 12 and 13). Reduced deviation in DBS values leads to advantage in insulation design. By increasing nanofiller content over threshold level the dielectric losses increase and DBS increase is saturated or decreased. Higher relative permittivity would be advantageous in capacitors but it seems that larger nanofiller loadings or microparticles are needed to achieve this. This is basically also a typical engineering challenge to find out the material performance optimal for all these properties. The PD endurance measurement also revealed that SiO_2-PP nanocomposite withstands surface PDs better than the reference PP [P8].

From the results of 5 wt-% SiO_2-PP nanocomposite [P6, P8], it can be calculated that an increase of 47 % could be achieved in the reactive power of an ac capacitor. This result should be utilized in high voltage capacitor development by using higher electric field gradient or thinner insulation. There is also a growing need for further development of dc capacitors in industry. A larger increase of 52 % is observed with dc DBS of 5 wt-% SiO_2-PP nanocomposite as discussed in Chapter 3 leading to a 231 % increase in the energy density of the capacitor [P8]. It should be noted that in real applications there are always transients affecting insulation materials. The withstand for transients must also be high. The next steps should be to up-scale things towards manufacturing. Larger areas of PP film should be tested and longer measurement times should be used for results comparable with industrial measurements. The accumulation of space charges at dc voltage should also be studied. Nanocomposite capacitors for electronics have been studied in [Li04, Jia07, Lu08a, Lu08b] and nanocomposite materials could be useful, also at lower voltages.

PE based XLPE for cable insulation is being actively researched. The lower relative permittivity values in nanocomposites than in the reference material may be important in decreasing the reactive current in cables [Nel06, Nel07]. Decay in space charge accumulation is important to decrease local electric field enhancement regarding dc cable application. Dc power transmission is growing rapidly and there is a need for cables rated for higher voltages with reduced insulation thickness. Actually the first 500 kV dc cable has been manufactured in Japan with inorganic fillers added to XLPE [Nag08].

EP insulations are used in rotating machines, dry type and measurement transformers and switchgear casings. Using nanocomposites the size of mold transformers can be more compact and thus they can be installed in smaller spaces. In switchgear and transformers the idea is to replace the use of SF_6 and oil insulation by nanocomposites and thus decrease greenhouse effect and respectively reduce fire risk. In LI DBS measurements of 1 wt-% octaglycidyldimethylsilyl POSS-EP nanocomposite DBS was 26 % higher than in the reference EP [P5]. Compact switchgear with vacuum switches has been developed for 24 kV by using EP nanocomposites [Tan06a]. Connecting conductor and vacuum interrupters have also been molded by NMMCs [Ima08]. Nano- and microfillers are used together in NMMCs to achieve corresponding thermal expansion coefficient with aluminum. Thus, exfoliation of conductor and EP interfaces due to heat-cycling is weaker. The PD resistance of NMMCs is better than with single nanocomposite or microcomposite (mass related phenomenon, Figure 31) [Tan08]. It could be an auspicious way of research to compare the filler size effect in nano- and microcomposites, especially with EP.

SRs are used in high voltage outdoor insulations (surge arresters, post insulators, bushings). Resistance to tracking and erosion can be improved with LS-SR nanocomposites [Den04]. The addition of 5 wt-% of LS nanofillers to SR provided better resistance to tracking and erosion compared to 40 wt-% ATH filled SR [Tan04]. The erosion depth was smaller for nanocomposite than for reference SR and ATH-SR microcomposite. Dielectric losses were slightly higher with LS-SR nanocomposite. The effect of nanoparticles on hydrophobicity recovery of SR needs to be studied with long-term measurements.

Table 4 presents a summary of the analysis of possible applications and future on nanocomposite research.

Table 4. Possible applications of nanocomposites and status and future of the research.

Application	Current status of the research	Current status	Next steps	1. application and timeframe to market
PP Capacitor	Only few publications on PP nanocomposites	5 wt-% SiO_2-PP (ac 20 %, dc 52 %, ε_r/tan δ no effect, 9 times longer time to breakdown under PD stress) 3 wt-% octamethyl-POSS PP (ac 22 %, ε_r/tan δ increase) [P3, P6, P8]	Up-scaling of research activities, measurements for trial capacitors, long-term measurements, temperature and humidity measurements	DC capacitor, over 5 years
XLPE Cable	Active field and more publications than on PP or SR nanocomposites	5 wt-% SiO_2-XLPE (dc 66 %, ε_r/tan δ no effect/decrease, 100 times longer time to breakdown) 12.5 wt-% SiO_2-XLPE (LI 31 %) [Roy05, Roy07, Smi08]	Long-term measurements of full cables, space charge accumulation, thermal conductivity	DC cable, trial cable [Nag08], under 5 years
EP Insulation	Active field and many publications on EP nanocomposites	10 wt-% TiO_2-EP (ac 69 %, 33 times longer time to breakdown) 1 wt-% octaglycidyldimethylsilyl-POSS EP (LI 26 %, ε_r/tan δ no effect) [Ima08, P5]	Long-term measurements of full components, measurements for thermal conductivity	Rotating machines and switchgear, trial components [Ima08, Tan06a], under 5 years
SR Outdoor Insulation	Only few publications on SR nanocomposites	5 wt-% $Si0_2$-SR (arcing time 3 times longer) 5 wt-% LS-SR (ε_r/tan δ no effect, tracking test 2 times longer) [Rae09, Tan04]	Up-scaling of research activities, measurements for trial components, long-term measurements in outdoor circumstances	Post insulator, over 5 years

7 . Conclusion

In this dissertation the main objective was to verify the dielectric properties of new insulation materials. The hypotheses of the research were:

1. The electrical properties of a pure base polymer will be enhanced by compounding with nanofillers
2. The comprehensive characterization of the nanocomposites developed will enable their use in different power engineering applications
3. The comprehensive characterization of the nanocomposites developed will provide advantages in the optimization of insulation structures
4. The electrical properties of nanocomposites can be tailored via an understanding of the nanoscale characteristics of the compounds.

In this dissertation it has been shown that new insulation materials can be tailored by compounding nanofillers and polymer materials. The advantageous changes in the properties of polymer nanocomposites can be explained by the large interface volume of the nanofillers. Theoretical models developed in the field of nanodielectrics concentrate on the analysis of the interface volume. Dielectric breakdown strength (DBS) is one of the most important properties of an insulation material. The DBS of nanocomposites depends heavily on the nanofiller content and even small quantities can achieve improvement. This is linked to the maximum interfacial area already achieved at low nanofiller concentrations. Homogeneous nanodispersion is the key to DBS increase and reliable results. Often the most beneficial nanofiller quantities are below 5 wt-%. A similar observation was made with relative permittivity and dielectric losses of nanocomposites. A threshold nanofiller content can also be found for these properties. At low nanofiller concentrations the relative permittivity and dielectric losses stay at reference level or are even lower. With increasing nanofiller content relative permittivity and dielectric losses start to increase. This is related to overlapping of interfacial zones of nanoparticles. The overlapping of the interfacial zones also depends on the nanofiller size and dispersion. Moreover, the treeing growth and PD endurance of nanocomposites were found to be partly different phenomena. The surface PD endurance of nanocomposites is a decidedly mass related phenomenon, but treeing growth is more complex. It is related to the large interface volume of nanocomposites and similar behaviour as seen with short-time DBS.

In this work, PP and PANI-EB layer structure was modeled with a finite element method. Defects were simulated in the structure and electric field distribution in the structure was studied. The advantage of the PANI-EB layer is not obvious when there is no distortion in the structure, but with some distortion PANI-EB can absorb electric field because its relative permittivity changes as a function of electric field. Measurements of PANI-EB and the model calculations indicate that PANI-EB can lower the electric field stress, especially in higher electric field regions like defects in capacitor insulation.

The ac DBS of 3 wt-% octamethyl POSS-PP nanocomposite increased 22 % compared to reference PP. The results of the relative permittivity and loss factor measurements indicated that octamethyl POSS could have an effect on the dielectric properties of PP. According to the measurements, higher permittivity values were obtained with octamethyl POSS compounds than with reference PP. With higher octamethyl POSS quantities the loss factor increased, but with small quantities the loss factor remained at the same level as with reference PP. Reasonable explanations for the increase in ac breakdown strength are that small size POSS particles are segregated on the boundaries between spherulites and the good ability to scavenge charge leads to good resistance to dielectric breakdown. The LI DBS of 1 wt-% octaglycidyldimethylsilyl POSS-EP nanocomposite increased 26 % compared to the reference EP. Octaglycidyldimethylsilyl POSS did not affect the relative permittivity or loss factor of EP.

In the dissertation, interesting dielectric properties were also measured from 1 wt-% SiO_2-PP nanocomposite. The dc breakdown strength of 1 wt-% SiO_2-PP nanocomposite was slightly higher than with reference PP. It is equally important that the β value in the Weibull probability function of the nanocomposite is higher than in the reference PP, an indicator of smaller standard deviation and homogeneous material. The capacitance of 1 and 2 wt-% SiO_2-PP nanocomposites remained higher at 80 °C and 100 °C compared to the reference PP. It also seems that the measured loss factor of 1 wt-% SiO_2-PP nanocomposite is lower than with reference PP. Thermal stability, increased β value in dc DBS measurements and lower dielectric losses are beneficial to dc capacitors.

In this dissertation it was shown that, proper nanodispersion improves the dielectric behaviour of 5 wt-% SiO_2-PP nanocomposite. 5 wt-% SiO_2-PP nanocomposite showed a promising combination of dielectric properties especially considering ac and dc power capacitors. The ac and dc breakdown strength of 5 wt-% SiO_2-PP nanocomposite increased 20 % and 52 % respectively. It is equally important that with both voltage shapes the β value of the nanocomposite is higher than with reference PP, an indicator of smaller standard deviation and homogeneous material. These results have an interesting impact on insulation system design, because safety margins and insulation thicknesses may be reduced. With 5 wt-% SiO_2-PP nanocomposite dielectric losses remained comparable to reference PP. Normalized capacitance did decrease by the same trend in both materials until 80 °C. This is important considering e.g. power capacitors, which operate in the 50-60 °C temperature range. There is no capacitance change compared to reference PP and no additional heat is produced due to low loss factor. In PD endurance measurements the average lifetime of 5 wt-% SiO_2-PP nanocomposite was 9 times longer than with reference PP. Also, the PD levels at the same voltage level were higher for reference PP than for 5 wt-% SiO_2-PP nanocomposite. Surface analysis of the films revealed that a layer of silicon oxides formed on the surfaces of the 5 wt-% SiO_2-PP nanocomposite during PD stress. The layers may protect the 5 wt-% SiO_2-PP nanocomposite from degradation and prolong the lifetime of the sample. This shielding behaviour is significant because the layers are formed at critical spots of insulation due to PD stress.

With respect to the properties of nanodielectrics studied the possible applications could be capacitors, cables, dry transformers, rotating machines, switchgears and outdoor insulations. Even though the future of nanodielectrics is promising, there are many

questions to be resolved. Manufacturing systems of nanocomposite materials must be optimized and up-scaled to larger volumes. Special effort has to be directed to ensure homogeneous dispersion, also in up-scaled manufacturing systems. Promising results have mainly been achieved with short-term measurements and work has been done to understand the mechanisms behind the functionality, which is important. Full scale models of applications should be produced and long-term measurements conducted in operating conditions. Long-term measurements for real components will finally reveal the actual benefits and possible drawbacks of nanocomposites compared to the insulation materials currently in use. In addition to dielectric properties, the thermal, mechanical, chemical and ageing properties critical for each component must be ascertained. This means that the industry should be more intensively linked to research activities to develop actual new products.

References

[Ala08] S. Alapati and M. J. Thomas, “Electrical Treeing in Polymer Nanocomposites”, National Power Systems Conf. (NPSC), pp. 351-355, 2008.

[Ala09] S. Alapati and M. J. Thomas, “Electrical tree growth in high voltage insulation containing inorganic nanofillers”, Intern. Symp. High Voltage Eng. (ISH), A-25, 2009.

[Amb04] M. Ambid, D. Mary, G. Teyssedre, C. Laurent, G. C. Montanari, D. Kaempfer and R. Mülhaupt, “Effect of Filler Concentration on Dielectric Behaviour and on Charge Trapping in PP/clay Nanocomposites”, IEEE Conf. Electr. Insul. Dielectr. Phenomena (CEIDP), pp. 389-392, 2004.

[An06] A. L. An and S. A. Boggs, “What is “Nano” in the Context of a Filled Dielectric”, IEEE Intern. Sympos. Electr. Insul. (ISEI), pp. 273-276, 2006.

[And09a] T. Andritsch, R. Kochetov, P. H. F. Morshuis and J. J. Smit, “Comparison of the dielectric behavior of epoxy-based Al_2O_3- and SiO_2- nanocomposites”, Nordic Insul. Symp. (NORD-IS), pp. 137-140, 2009.

[And09b] T. Andritsch, R. Kochetov, P. H. F. Morshuis and J. J. Smit, “Comparison of the dielectric response of alumina-epoxy composites with nano- and conventional sized filler”, Intern. Symp. High Voltage Eng. (ISH), A-28, 2009.

[Bam05] S. S. Bamji, M. Abou-Dakka, A. T. Bulinski, L. Utracki and K. Cole, “Dielectric Properties of Polypropylene Containing Nano-Particles”, IEEE Conf. Electr. Insul. Dielectr. Phenomena (CEIDP), pp. 166-170, 2005.

[Bro04] C. Brosseau and P. Talbot, “Effective Permittivity of Nanocomposite Powder Compacts”, IEEE Trans. Dielectr. Electr. Insul., Vol. 11, pp. 819-832, 2004.

[Cao04] Y. Cao, P. C. Irwin and K. Younsi, “The Future of Nanodielectrics in the Electrical Power Industry”, IEEE Trans. Dielectr. Electr. Insul., Vol. 11, pp. 797-807, 2004.

[Cas06] J. Castellon, S. Agnel, A. Toureille, M. Fréchette, K. C. Cole and D. Desgagnés, “Electrical properties analysis of nano-filled epoxy by space charge characterization”, IEEE Conf. Electr. Insul. Dielectr. Phenomena (CEIDP), pp. 345-348, 2006.

[Che08] B-K. Chen, J-U. Du and C-W. Hou, “The Effects of Chemical Structure on the Dielectric Properties of Polyetherimide and Nanocomposites”, IEEE Trans. Dielectr. Electr. Insul., Vol. 15, pp. 127-133, 2008.

[Dan07] Z-M. Dang, H-P. Xu and H-Y. Wang, “Significantly enhanced low-frequency dielectric permittivity in the $BaTi0_3$/poly(vinylidene fluoride) nanocomposite”, Appl. Phys. Lett. 90, pp. 12901-12903, 2007.

[Dan09] M. G. Danikas and T. Tanaka, “Nanocomposites-A Review of Electrical Treeing and Breakdown”, IEEE Electr. Insul. Mag., Vol. 25, pp. 19-25, 2009.

[Den04] C. Dengke, Y. J. Hui, W. Xishan and L. Lei, “Research on characterization of RTV silicone rubber/LS (layered silicate) electrical insulation nanocomposites”, IEEE Intern. Conf. Solid Dielectr. (ICSD), pp. 796-799, 2004.

[Din04] H.-Z. Ding and B. R. Varlow, “Effect of Nano-Fillers on Electrical Treeing in Epoxy Resin Subjected to AC Voltage”, IEEE Conf. Electr. Insul. Dielectr. Phenomena (CEIDP), pp. 332-335, 2004.

[Dis04] L. A. Dissado and J. C. Fothergill, “Editorial: Dielectrics and Nanotechnology”, IEEE Trans. Dielectr. Electr. Insul., Vol. 11, pp. 737-738, 2004.

[Fab09] D. Fabiani, A. Cavallini, G. C. Montanari and L. Testa, “Extraction of Aging Markers for Nanostructured Epoxy Resin Aged under Surface Discharges”, IEEE Electr. Insul. Conf. (EIC), pp. 387-391, 2009.

[Fle08] R. J. Fleming, A. Ammala, P. S. Casey and S. B. Lang, “Conductivity and Space Charge in LDPE Containing Nano- and Micro-sized ZnO Particles”, IEEE Trans. Dielectr. Electr. Insul., Vol. 15, pp. 118-126, 2008.

[Fot04] J. C. Fothergill, J. K. Nelson and M. Fu, “Dielectric Properties of Epoxy Nanocomposites containing TiO_2, Al_2O_3 and ZnO fillers”, IEEE Conf. Electr. Insul. Dielectr. Phenomena (CEIDP), pp. 406-409, 2004.

[Fré01] M. F. Fréchette, M. Trudeau, H. D. Alamdari and S. Boily, “Introductory Remarks on Nanodielectrics”, IEEE Conf. Electr. Insul. Dielectr. Phenomena (CEIDP), pp. 92-99, 2001.

[Fré04] M. F. Fréchette, R. Y. Larocque, R. Veillette and M. L. Trudeau, “Meso and Nano Morphological Changes of an Epoxy Surface Exposed to Low-Intensity Discharges in Air”, IEEE Conf. Electr. Insul. Dielectr. Phenomena (CEIDP), pp. 393-397, 2004.

[Fré05] M. F. Fréchette, R. Y. Larocque, M. L. Trudeau, R. Veillette, K. C. Cole and M.-T. Ton That, “Nanodielectric Surface Performance When Submitted to Partial Discharges in Compressed Air”, IEEE Conf. Electr. Insul. Dielectr. Phenomena (CEIDP), pp. 727-731, 2005.

[Fré06a] M. F. Fréchette and C. W. Reed, “On molecular dielectrics in their role in shaping and controlling nanodielectrics”, IEEE Conf. Electr. Insul. Dielectr. Phenomena (CEIDP), pp. 333-337, 2006.

[Fré06b] M. F. Fréchette and C. W. Reed, “The Emerging Field of Nanodielectrics: an Annotated Appreciation”, IEEE Intern. Sympos. Electr. Insul. (ISEI), pp. 458-465, 2006.

[Fré08] M. F. Fréchette, R. Y. Larocque, M. Trudeau, R. Veillette, R. Rioux, S. Pélissou, S. Besner, M. Javan, K. Cole, M.-T. Ton That, D. Desgagnés, J. Castellon, S.

Agnel, A. Toureille, G. Platbrood, “Nanostructured Polymer Microcomposites: A Distinct Class of Insulating Materials”, IEEE Trans. Dielectr. Electr. Insul., Vol. 15, pp. 90-105, 2008.

[Fré09] M. F. Fréchette, “Innovation in Dielectric Materials: from Macro to Nanoscales”, IEEE Electr. Insul. Conf. (EIC), pp. 514-523, 2009.

[Fus04] N. Fuse, M. Kozako, T. Tanaka, S. Murase and Y. Ohki, “Possible Mechanism of Superior Partial-Discharge Resistance of Polyamide Nanocomposites”, IEEE Conf. Electr. Insul. Dielectr. Phenomena (CEIDP), pp. 322-325, 2004.

[Fus08] N. Fuse, Y. Ohki, M. Kozako and T. Tanaka, “Possible Mechanism of Superior Resistance of Polyamide Nanocomposites to Partial Discharges and Plasmas”, IEEE Trans. Dielectr. Electr. Insul., Vol. 15, pp. 161-169, 2008.

[Gre08] C. D. Green, A. S. Vaughan, G. R. Mitchell and T. Liu, “Structure Property Relationships in Polyethylene/Montmorillonite Nanodielectrics”, IEEE Trans. Dielectr. Electr. Insul., Vol. 15, pp. 134-143, 2008.

[Gua06a] F. Guastavino, A. Ratto, E. Torello, M. Hoyos, N. García, H. Reinecke, E. Benito and P. Tiemblo, “AC electrical strength measurements on LDPE nanocomposites”, IEEE Conf. Electr. Insul. Dielectr. Phenomena (CEIDP), pp. 329-332, 2006.

[Gua06b] F. Guastavino, A. Dardano, G. C. Montanari, F. Deorsola and L. Testa, “Electrical tree growth in EVA-layered silicate nanocomposites”, IEEE Conf. Electr. Insul. Dielectr. Phenomena (CEIDP), pp. 294-297, 2006.

[Gua08] F. Guastavino, E. Torello, A. Dardano, S. Bono, M. Pellegrini and L. Vignati, “A comparison of the short and long term behaviour of nanostructured enamels with the performances of conventional insulation”, IEEE Intern. Sympos. Electr. Insul. (ISEI), pp. 659-662, 2008.

[Gua09] F. Guastavino, A. Dardano, S. Squarcia, P. Tiemblo, J. Guzman, E. Benito and N. Garcia, “Breakdown and Electrical Aging Tests on Different Nanocomposite Materials”, IEEE Electr. Insul. Conf. (EIC), pp. 529-533, 2009.

[Hau92] W. Hauschild and W. Mosch, “Statistical Techniques for High-Voltage Engineering”, Peter Peregrinus Ltd., London, UK, 1992.

[Hen99] P. O. Henk, T. W. Kortsen and T. Kvarts, “Increasing the electrical discharge endurance of acid anhydride cured DGEBA epoxy resin by dispersion of nanoparticle silica”, High Perform. Polym., Vol. 11, pp. 281-296, 1999.

[Hin06] K. Hinata, A. Fujita, K. Tohyama and Y. Murata, “Dielectric Properties of LDPE/MgO Nanocomposite Material under AC High Field”, IEEE Conf. Electr. Insul. Dielectr. Phenomena (CEIDP), pp. 313-316, 2006.

[Hor02] J. Horwath and D. Schweickart, “Inorganic Fillers for Corona Endurance Enhancement of Selected Polymers”, Intern. Power Modulator Symp., pp. 644-647, 2002.

[Hor05] J. Horwath, D. Schweickart, G. Garcia, D. Klosterman and M. Galaska, “Improved Performance of Polyhedral Oligomeric Silsesquioxane Epoxies”, IEEE Conf. Electr. Insul. Dielectr. Phenomena (CEIDP), pp. 155-157, 2005.

[Hor06] J. Horwath, D. Schweickart, G. Garcia, D. Klosterman, M. Galaska, A. Schrand and L. Walko, “Improved Electrical Properties of Epoxy Resin with Nanometer-Sized Inorganic Fillers”, Intern. Power Modulator Symp., pp. 189-191, 2006.

[Hoy08] M. Hoyos, N. García, R. Navarro, A. Dardano, A. Ratto, F. Guastavino and P. Tiemblo, “Electrical Strength in Ramp Voltage AC Tests of LDPE and Its Nanocomposites with Silica and Fibrous and Laminar Silicates”, J. Pol. Sci.: Part B: Pol. Phys., Vol. 46, pp. 1301-1311, 2008.

[Hu06] Y. Hu, R. C. Smith, J. K. Nelson and L. S. Schadler, “Some mechanistic understanding of the impulse strength of nanocomposites”, IEEE Conf. Electr. Insul. Dielectr. Phenomena (CEIDP), pp. 31-34, 2006.

[IEC69] IEC Publication 250: “Recommended Methods for the Determination of the Permittivity and Dielectric Dissipation Factor of Electrical Insulating Materials at Power, Audio and Radio Frequencies Including Metre Wavelengths”, 1969.

[IEC89] IEC Publication 60060-1: “High-voltage Test Techniques. Part 1: General Definitions and Test Requirements”, 1989.

[IEC98] IEC Publication 60243-1: “Electrical Strength of Insulating Materials-Test Methods-Part 1: Test at Power Frequencies”, 1998.

[IEC00] IEC 61340-2-1: “Electrostatics-Part 2-1: Measurement methods in electrostatics-Test methods to measure ability of materials and products to dissipate static electric charge”, 2000.

[IEE05] IEEE Standard 930: “IEEE Guide for the Statistical Analysis of Electrical Insulation Breakdown Data”, IEEE Dielectr. Electr. Insul. Society, 2005.

[Iiz07] T. Iizuka, K. Uchida and T. Tanaka, “Different Voltage Endurance Characteristics of Epoxy/Silica Nanocomposites Prepared by Two Kinds of Dispersion Methods”, IEEE Conf. Electr. Insul. Dielectr. Phenomena (CEIDP), pp. 236-239, 2007.

[Iiz08] T. Iizuka, Y. Ohki and T. Tanaka, “Effects of Coupling Agent and Filler Dispersion on V-t Characteristics of Epoxy/Silica Nanocomposites”, Intern. Symp. Electr. Insul. Mat. (ISEIM), pp. 60-63, 2008.

[Ima02] T. Imai, Y. Hirano, H. Hirai, S. Kojima and T. Shimizu, “Preparation and Properties of Epoxy-Organically Modified Layered Silicate Nanocomposites”, IEEE Intern. Sympos. Electr. Insul. (ISEI), pp. 379-383, 2002.

[Ima04] T. Imai, F. Sawa, T. Yoshimitsu, T. Ozaki and T. Shimizu, “Preparation and Insulation Properties of Epoxy-Layered Silicate Nanocomposite”, IEEE Conf. Electr. Insul. Dielectr. Phenomena (CEIDP), pp. 402-405, 2004.

[Ima06a] T. Imai, F. Sawa, T. Ozaki, Y. Inoue, T. Shimizu and T. Tanaka, “Comparison of Insulation Breakdown Properties of Epoxy Nanocomposites under Homogeneous and Divergent Electric Fields”, IEEE Conf. Electr. Insul. Dielectr. Phenomena (CEIDP), pp. 306-309, 2006.

[Ima06b] T. Imai, F. Sawa, T. Nakano, T. Ozaki, T. Shimizu, M. Kozako and T. Tanaka, “Effects of Nano- and Micro-filler Mixture on Electrical Insulation Properties of Epoxy Based Composites”, IEEE Trans. Dielectr. Electr. Insul., Vol. 13, pp. 319-326, 2006.

[Ima08] T. Imai, G. Komiya, K. Murayama, T. Ozaki, F. Sawa, T. Shimizu, M. Harada, M. Ochi, Y. Ohki and T. Tanaka, “Improving Epoxy-based Insulating Materials with Nano-fillers toward Practical Application”, IEEE Intern. Sympos. Electr. Insul. (ISEI), pp. 201-204, 2008.

[Jia07] K. Jiang, L. Cheng, L. Zheng, Z. Yao, G. Li and Q. Yin, “The Unique Dielectric Behaviour of Nanosilica Epoxy Composites”, IEEE Intern. Conf. Nanot., pp. 1101-1106, 2007.

[Koc09a] R. Kochetov, T. Andritsch, U. Lafont, P. H. F. Morshuis, S. J. Picken and J. J. Smit, “Preparation and Dielectric Properties of Epoxy-BN and Epoxy-AlN Nanocomposites”, IEEE Electr. Insul. Conf. (EIC), pp. 397-400, 2009.

[Koc09b] R. Kochetov, T. Andritsch, U. Lafont, P. H. F. Morshuis, S. J. Picken and J. J. Smit, “The Thermal Conductivity in Epoxy-Aluminum Nitride and Epoxy-Aluminum Oxide Nanocomposite Systems”, Nordic Insul. Symp. (NORD-IS), pp. 27-30, 2009.

[Koz03] M. Kozako, N. Fuse, K. Shibata, N. Hirai, Y. Ohki, T. Okamoto and T. Tanaka, “Surface Change of Polyamide Nanocomposite Caused by Partial Discharges”, IEEE Conf. Electr. Insul. Dielectr. Phenomena (CEIDP), pp. 75-78, 2003.

[Koz04a] M. Kozako, N. Fuse, Y. Ohki, T. Okamoto and T. Tanaka, “Surface Degradation of Polyamide Nanocomposites Caused by Partial Discharges Using IEC (b) Electrodes”, IEEE Trans. Dielectr. Electr. Insul., Vol. 11, pp. 833-839, 2004.

[Koz04b] M. Kozako, R. Kido, N. Fuse, Y. Ohki, T. Okamoto and T. Tanaka, “Difference in Surface Degradation due to Partial Discharges between Polyamide Nanocomposite and Microcomposite”, IEEE Conf. Electr. Insul. Dielectr. Phenomena (CEIDP), pp. 398-401, 2004.

[Koz05] M. Kozako, R. Kido, T. Imai, T. Ozaki, T. Shimizu and T. Tanaka, “Surface Roughness Change of Epoxy/TiO_2 Nanocomposites due to Partial Discharges”, Intern. Symp. Electr. Insul. Mat. (ISEIM), pp. 661-664, 2005.

[Kur06] R. Kurnianto, Y. Murakami, N. Hozumi, M. Nagao and Y. Murata, “Some Fundamentals on Treeing Breakdown in Inorganic-filler/LDPE Nano-composite Material”, IEEE Conf. Electr. Insul. Dielectr. Phenomena (CEIDP), pp. 373-376, 2006.

[Lee05a] Y-J. Lee, J-M. Huang, S-W. Kuo and F-C. Chang, “Low-dielectric, Nanoporous Polyimide Films Prepared from PEO-POSS Nanoparticles”, Polymer, Vol. 46, pp. 10056-10065, 2005.

[Lee05b] Y-J. Lee, J-M. Huang, S-W. Kuo, J-S. Lu and F-C. Chang, “Polyimide and polyhedral oligomeric silsesquioxane nanocomposites for low-dielectric applications”, Polymer, Vol. 46, pp. 173-181, 2005.

[Lew94] T. J. Lewis, “Nanometric Dielectrics”, IEEE Trans. Dielectr. Electr. Insul., Vol. 1, pp. 812-825, 1994.

[Lew04a] T. J. Lewis, “Interfaces and Nanodielectrics are Synonymous”, IEEE Intern. Conf. Solid Dielectr. (ICSD), pp. 792-795, 2004.

[Lew04b] T. J. Lewis, “Interfaces are the Dominant Feature of Dielectrics at the Nanometric Level”, IEEE Trans. Dielectr. Electr. Insul., Vol. 11, pp. 739-753, 2004.

[Lew05] T. J. Lewis, “Interfaces: nanometric dielectrics”, J. Phys. D: Appl. Phys., Vol. 38, pp. 202-212, 2005.

[Li04] D. Li-jie, X. Chuan-xi, C. Juan and N. Ce-wen, “Dielectric Behaviour of $BaTiO_3$/PVDF Nanocomposites In-situ Synthesized by the Sol-Gel Method”, J. of Wuhan Univ. of Tech. –Mater. Sci. Ed., Vol. 19, pp. 9-11, 2004.

[Li07] J. Y. Li, L. Zhang and S. Ducharme, “Electric energy density of dielectric nanocomposites”, Applied Physics Letters 90, pp. 132901-132903, 2007.

[Lu08a] J. Lu, “High Dielectric Constant Polymer Nanocomposites for Embedded Capacitor Applications”, Ph. D. Thesis, Georgia Institute of Technology, 209 p., 2008.

[Lu08b] J. Lu and C. P. Wong, “Recent Advances in High-k Nanocomposite Materials for Embedded Capacitor Applications”, IEEE Trans. Dielectr. Electr. Insul., Vol. 15, pp. 1322-1328, 2008.

[Mai08a] P. Maity, S. Basu, V. Parameswaran and N. Gupta, “Degradation of Polymer Dielectrics with Nanometric Metal-oxide Fillers due to Surface Discharges”, IEEE Trans. Dielectr. Electr. Insul., Vol. 15, pp. 52-62, 2008.

[Mai08b] P. Maity, S. V. Kasisomayajula, V. Parameswaran, S. Basu and N. Gupta, “Improvement in Surface Degradation Properties of Polymer Composites due to Pre-processed Nanometric Alumina Fillers”, IEEE Trans. Dielectr. Electr. Insul., Vol. 15, pp. 63-72, 2008.

[Mas07] S. Masuda, S. Okuzumi, R. Kurniant, Y. Murakami, M. Nagao, Y. Murata and Y. Sekiguchi, “DC Conduction and Electrical Breakdown of MgO/LDPE Nanocomposite”, IEEE Conf. Electr. Insul. Dielectr. Phenomena (CEIDP), pp. 290-293, 2007.

[Min04] Z. Mingyan, Z. Jinghe, W. Kun and F. Yong, “Preparation and Characterization of the Nano-doped Polyimide Film”, IEEE Intern. Conf. Solid Dielectr. (ICSD), pp. 840-843, 2004.

[Mon04] G. C. Montanari, D. Fabiani, F. Palmieri, D. Kaempfer, R. Thomann and R. Mülhaupt, “Modification of Electrical Properties and Performance of EVA and PP Insulation through Nanostructure by Organophilic Silicates”, IEEE Trans. Dielectr. Electr. Insul., Vol. 11, pp. 754-762, 2004.

[Mon05] G. C. Montanari, F. Ciani, L. Testa, F. Guastavino, G. Coletti, R. Mülhaupt, “Electric strength, space charge and surface discharge characterization of nanostructured epoxy-silicate insulating materials”, Intern. Symp. Electr. Insul. Mat. (ISEIM), pp. 206-209, 2005.

[Mur08] Y. Murakami, M. Nemoto, S. Okuzumi, S. Masuda, M. Nagao, N. Hozumi, Y. Sekiguchi and Y. Murata, “DC Conduction and Electrical Breakdown of MgO/LDPE Nanocomposite”, IEEE Trans. Dielectr. Electr. Insul., Vol. 15, pp. 33-39, 2008.

[Nag08] M. Nagao, Y. Murakami, Y. Murata, Y. Tanaka, Y. Ohki and T. Tanaka, “Material Challenge of MgO/LDPE Nanocomposite for High Field Electrical Insulation”, CIGRE D1-301, 2008.

[Nel02] J. K. Nelson, J. C. Fothergill, L. A. Dissado and W. Peasgood, “Towards an Understanding of Nanometric Dielectrics”, IEEE Conf. Electr. Insul. Dielectr. Phenomena (CEIDP), pp. 295-298, 2002.

[Nel03] J. K. Nelson, Y. Hu and J. Thiticharoenpong, “Electrical Properties of TiO_2 Nanocomposites”, IEEE Conf. Electr. Insul. Dielectr. Phenomena (CEIDP), pp. 719-722, 2003.

[Nel04a] J. K. Nelson and J. C. Fothergill, “Internal Charge Behaviour of Nanocomposites”, Nanotechnology, Vol. 15, pp. 586-595, 2004.

[Nel04b] J. K. Nelson, L. A. Utracki, R. K. MacCrone and C. W. Reed, “Role of the Interface in Determining the Dielectric Properties of Nanocomposites”, IEEE Conf. Electr. Insul. Dielectr. Phenomena (CEIDP), pp. 314-317, 2004.

[Nel04c] J. K. Nelson and Y. Hu, “The Impact of Nanocomposite Formulations on Electrical Voltage Endurance”, IEEE Intern. Conf. Solid Dielectr. (ICSD), pp. 832-835, 2004.

[Nel05] J. K. Nelson and Y. Hu, “Nanocomposite Dielectrics-Properties and Implications”, J. Phys. D: Appl. Phys., Vol. 38, pp. 213-222, 2005.

[Nel06] J. K. Nelson, “The Promise of Dielectric Nanocomposites”, IEEE Intern. Sympos. Electr. Insul. (ISEI), pp. 452-457, 2006.

[Nel07] J. K. Nelson, “Overview of Nanodielectrics: Insulating Materials of the Future”, Electrical Insulation Conference and Electrical Manufacturing Expo, pp. 229-235, 2007.

[Nel08] J. K. Nelson, “Editorial: Nanodielectrics”, IEEE Trans. Dielectr. Electr. Insul., Vol. 15, p. 1, 2008.

[Pei03] Z. Peihong, Z. Weiguo, L. Yan, F. Yong and L. Qingquan, “Study on Corona-Resistance of Polyimide-Nano Inorganic Composites”, Intern. Conf. Prop. Appl. Dielectr. Mat., pp. 1138-1141, 2003.

[Pél06] S. Pélissou, S. Besner, M. Fréchette, K. C. Cole and D. Desgagnés, “Preliminary Characterization of a Nanodielectric Material”, IEEE Conf. Electr. Insul. Dielectr. Phenomena (CEIDP), pp. 338-340, 2006.

[Phi04] S. Phillips, T. Haddad and S. Tomczak, “Developments in nanoscience: polyhedral oligomeric silsesquioxane (POSS)-polymers”, Current Opinion in Solid State and Materials Science, Vol. 8, pp. 21-29, 2004.

[Pre09] P. Preetha and M. J. Thomas, “Partial discharge resistant characteristics of alumina filled polymer nanocomposites”, Intern. Symp. High Voltage Eng. (ISH), A-51, 2009.

[Rae05] S. Raetzke and J. Kindersberger, “Erosion Behaviour of Nano Filled Silicone Elastomers”, Intern. Symp. High Voltage Eng. (ISH), C-09, 2005.

[Rae08] S. Raetzke, Y. Ohki, T. Imai, J. Kindersberger and T. Tanaka, “Enhanced Performance of Tree Initiation V-t Characteristics of Epoxy/Clay Nanocomposite in Comparison with Neat Epoxy Resin”, IEEE Conf. Electr. Insul. Dielectr. Phenomena (CEIDP), pp. 528-531, 2008.

[Rae09] S. Raetzke and J. Kindersberger, “Resistance to High Voltage Arcing and the Resistance to Tracking and Erosion for Silicone/SiO_2 Nanocomposites”, Intern. Symp. High Voltage Eng. (ISH), F-10, 2009.

[Roy05] M. Roy, J. K. Nelson, R. K. MacCrone, L. S. Schadler, C. W. Reed, R. Keefe and W. Zenger, “Polymer Nanocomposite Dielectrics - The Role of the Interface”, IEEE Trans. Dielectr. Electr. Insul., Vol. 12, pp. 629-643, 2005.

[Roy07] M. Roy, J. K. Nelson, R. K. MacCrone and L. S. Schadler, “Candidate mechanisms controlling the electrical characteristics of silica/XLPE nanodielectrics”, J. Mater. Sci., Vol. 42, pp. 3789-3799, 2007.

[Sah08] S. K. Saha, “Nanodielectrics with giant permittivity”, Bull. Mater. Sci., Vol. 31, pp. 473-477, 2008.

[Sal06] P. Salovaara, M. Takala and K. Kannus, “Dielectric Properties of Polyaniline Emeraldine Base”, International Review of Electrical Engineering, Vol. 1, pp. 462-467, 2006.

[Shi04] T. Shimizu, T. Ozaki, Y. Hirano, T. Imai and T. Yoshimitsu, “Properties of Epoxy-Layered Silicate Nanocomposites”, CIGRE D1-204, 2004.

[Sin06] S. Singha and M. J. Thomas, “Polymer composite/nanocomposite processing and its effect on the electrical properties”, IEEE Conf. Electr. Insul. Dielectr. Phenomena (CEIDP), pp. 557-560, 2006.

[Sin08a] S. Singha and M. J. Thomas, “Dielectric Properties of Epoxy Nanocomposites”, IEEE Trans. Dielectr. Electr. Insul., Vol. 15, pp. 12-23, 2008.

[Sin08b] S. Singha and M. J. Thomas, “Permittivity and Tan Delta Characteristics of Epoxy Nanocomposites in the Frequency Range of 1 MHz-1 GHz”, IEEE Trans. Dielectr. Electr. Insul., Vol. 15, pp. 2-11, 2008.

[Smi08] R. C. Smith, C. Liang, M. Landry, J. K. Nelson and L. S. Schadler, “The Mechanisms Leading to the Useful Electrical Properties of Polymer Nanodielectrics”, IEEE Trans. Dielectr. Electr. Insul., Vol. 15, pp. 187-196, 2008.

[Son08] B. Sonerud, T. Bengtsson, J. Blennow, and S. M. Gubanski, “Dielectric response measurements utilizing semi-square voltage waveforms”, IEEE Trans. Dielectr. Electr. Insul., Vol. 15, pp. 920-926, 2008.

[Tag08] N. Tagami, M. Okada, N. Hirai, Y. Ohki, T. Tanaka, T. Imai, M. Harada and M. Ochi, “Dielectric Properties of Epoxy/Clay Nanocomposites –Effects of Curing Agent and Clay Dispersion Method”, IEEE Trans. Dielectr. Electr. Insul., Vol. 15, pp. 24-32, 2008.

[Tan04] T. Tanaka, G. C. Montanari and R. Mulhaupt, “Polymer Nanocomposites as Dielectrics and Electrical Insulation perspectives for Processing Technologies, Material Characterization and Future Applications”, IEEE Trans. Dielectr. Electr. Insul., Vol. 11, pp. 763-784, 2004.

[Tan05a] T. Tanaka, “Dielectric Nanocomposites with Insulating Properties”, IEEE Trans. Dielectr. Electr. Insul., Vol. 12, pp. 914-928, 2005.

[Tan05b] T. Tanaka, M. Kozako, N. Fuse and Y. Ohki, “Proposal of a Multi-core Model for Polymer Nanocomposite Dielectrics”, IEEE Trans. Dielectr. Electr. Insul., Vol. 12, pp. 669-681, 2005.

[Tan06a] T. Tanaka and M. Frechette, “Emerging Nanocomposite Dielectrics”, CIGRE Task Force Report D1.16.03, ELECTRA, No. 226, pp. 24-32, 2006.

[Tan06b] T. Tanaka, “Interpretation of Several Key Phenomena Peculiar to Nano Dielectrics in terms of a Multi-core Model”, IEEE Conf. Electr. Insul. Dielectr. Phenomena (CEIDP), pp. 298-301, 2006.

[Tan07a] T. Tanaka, “Polymer Nanocomposites as HV Insulaiton: Superiority and Expectation”, Intern. Symp. High Voltage Eng. (ISH), p. 1, 2007.

[Tan07b] T. Tanaka, “Polymer Nanocomposites: their Superiority in Dielectric Characteristics and Physical Model for Mechanisms to Interpret Various Dielectric Phenomena”, Intern. Symp. High Voltage Eng. (ISH), T3-101, 2007.

[Tan08] T. Tanaka, Y. Ohki, M. Ochi, M. Harada and T. Imai, “Enhanced Partial Discharge Resistance of Epoxy/Clay Nanocomposite Prepared by Newly Developed Organic Modification and Solubilization Methods”, IEEE Trans. Dielectr. Electr. Insul., Vol. 15, pp. 81-89, 2008.

[Tie08] P. Tiemblo, M. Hoyos, J. M. Gómez-Elvira, J. Guzmán, N. Garciá, A. Dardano and F. Guastavino, “The development of electrical treeing in LDPE and its nanocomposites with spherical silica and fibrous and laminar silicates”, J. Phys. D: Appl. Phys., Vol. 41, pp. 1-8, 2008.

[Tun09] E. Tuncer, A. J. Rondinone, J. Woodward, I. Sauers, D. R. James and A. R. Ellis, “Cobalt iron-oxide nanoparticle modified poly(methyl methacrylate) nanodielectrics”, Appl. Phys. A, Vol. 94, pp. 843-852, 2009.

[Vau05] A. S. Vaughan, C. D. Green, Y. Chang and G. Chen, “Nanocomposites for High Voltage Applications: Effect of Sample Preparation on AC Breakdown Studies”, IEEE Conf. Electr. Insul. Dielectr. Phenomena (CEIDP), pp. 732-735, 2005.

[Ven09] B. Venkatesulu and M. J. Thomas, “Erosion resistance of silicone rubber nanocomposite at low filler loadings”, 16th Intern. Symp. High Voltage Eng. (ISH), C-48, 2009.

[Wu05] J. Wu, S. Yang, S. Gao, A. Hu, J. Liu, L. Fan, “Preparation, morphology and properties of nano-sized Al_2O_3/polyimide hybrid films”, European Pol. J., Vol. 41, pp. 73-81, 2005.

[Wu07] J. Wu, B. Heil and A. Schnettler, “Study on durability of nanostructured superhydrophobic insulating surfaces under simultaneous climatic and electrical stresses”, Intern. Symp. High Voltage Eng. (ISH), T4-166, 2007.

[Wu08] J. Wu and A. Schnettler, “Degradation Assesment of Nanostructured Superhydrophobic Insulating Surfaces Using Multi-stress Methods”, IEEE Trans. Dielectr. Electr. Insul., Vol. 15, pp. 73-80, 2008.

[Zha03] M. Y. Zhang, C. Yan, F. Yong and Q. Q. Lei, “Synthesis and Characterization of Corona-resistant Nanocluster-trapped Polyimide/Silica Composites”, Intern. Conf. Prop. Appl. Dielectr. Mat., pp. 753-756, 2003.

[Zha06] C. Zhang and G. C. Stevens, “Dielectric Properties of Epoxy-Alumina Nanocomposites: The Effect of Absorbed Water”, IEEE Conf. Electr. Insul. Dielectr. Phenomena (CEIDP), pp. 325-328, 2006.

[Zou06a] C. Zou, J. C. Fothergill, M. Fu and J. K. Nelson, “Improving the Dielectric Properties of Polymers by Incorporating Nanoparticles”, 10th Intern. Electr. Insul. Conf. (INSUCON), pp. 125-130, 2006.

[Zou06b] C. Zou, M. Fu, J. C. Fothergill and S. W. Rowe, “Influence of absorbed water on the dielectric properties and glass-transition temperature of silica-filled epoxy nanocomposites”, IEEE Conf. Electr. Insul. Dielectr. Phenomena (CEIDP), pp. 321-324, 2006.

[Zou07] C. Zou, “The effect of humidity and surface functionalisation on the dielectric properties of nanocomposites”, Ph. D. Thesis, University of Leicester, 162 p., 2007.

[Zou08] C. Zou, J. C. Fothergill and S. W. Rowe, “The Effect of Water Absorption on the Dielectric Properties of Epoxy Nanocomposites”, IEEE Trans. Dielectr. Electr. Insul., Vol. 15, pp. 106-117, 2008.

Publications

Publication 1

M. Takala, P. Salovaara, T. Keikko, K. Kannus, FEM Modeling of Polypropylene and PANI-EB Layer Structure, *International Review of Electrical Engineering*, Vol. 1, No. 5, pp. 613-618, (2006)

© 2006 Praise Worthy Prize S.r.l. Reprinted, with permission of Praise Worthy Prize S.r.l., from the International Review of Electrical Engineering.

International Review of Electrical Engineering (I.R.E.E.), Vol. 1, No. 5
November-December 2006

FEM Modeling of Polypropylene and PANI-EB Layer Structure

M. Takala[1], P. Salovaara[2], T. Keikko[3] and K. Kannus[4]

Abstract – *This paper presents the results of finite element method (FEM) modeling of polypropylene (PP) and polyaniline emeraldine base (PANI-EB) layer structure. Modeling started with permittivity measurements of pure PANI-EB as a function of electric field. Curve fitting of the electric field dependence of relative permittivity was made for PANI-EB. The actual behavior of the materials was concluded in the model, which consisted PP and PANI-EB layers. Defects were simulated in the structure and electric field distribution in the structure was studied. Modeling of this kind of structure was done to verify the effect of PANI-EB layer on the electric field strength in PP. The target is to find possible ways to lower the stresses which are subjected to PP. The advantage of the PANI-EB layer is not obvious when there is no distortion in the structure, but with some distortion PANI-EB can absorb electric field because its relative permittivity changes as a function of electric field. The results indicate that the idea of using PANI-EB as an electric field dependent permittivity material in stress grading needs to be studied further.* ***© Copyright 2006 Praise Worthy Prize - All right reserved***

Keywords: *FEM modeling, electric field dependent relative permittivity, polyaniline emeraldine base, polypropylene*

I. Introduction

Systems which incorporate nonlinear grading materials require design and measurement of material properties. Zhou and Boggs et al. have published problems and theory considering the measurement of nonlinear grading materials and performance of solid dielectrics in high electric fields [1]-[7].

Carbon black has been widely used in stress grading in polyolefins and rubbers [8]. Other grading materials have also been tested and developed [9]-[12]. Pelto et al. [9] reported of doped ZnO micro-varistor powders, silicon- and boron carbide powder, ferroelectric ceramics e.g. PZT and undoped polyaniline. In paper by Watanabe et al. [10] authors report the use of iron (III) oxide-, copper oxide- and titanium oxide-kaolin as functionally grading materials. Aluminium and titanium oxides have been used to control permittivity in epoxy application [11], [12]. In this paper the functionality of PANI-EB for stress grading is verified with FEM calculations.

In materials there are always some defects which may affect the functionality of the insulation layer, especially in long-term use. Insulation structures are subjected to different kinds of stresses e.g. electric field and temperature. In addition, insulation structures have been decreasing in size. With thin insulation structures defects are more likely to cause problems. The strongest electric field concentrates on the abnormal region of the material. These defects may be either on the surface or in the insulation. E.g. roughness of the aluminium foil in capacitor structures affect electric field disturbance in PP insulation. The manufacturers of the capacitors are interested in enhancing the electric field strength and relative permittivity of PP to achieve larger capacitive power. Smaller structures and larger quantities of power are in scope of the manufacturers.

This study is a continuation of the paper by Salovaara et al. [13], where a more profound dielectric characterization of PANI-EB was made. Previously published articles have been suggesting good prospects for PANI-EB to act as an electric field grading material [9], [14], [15]. Kieffel et al. [15] report that in the case of PANI-EB/EVA (Ethylene Vinyl Acetate) the insulation behaves better than carbon black/EVA in lightning impulse tests. Pelto et al. [9] have also shown that their PANI-EB composites can be used in stress grading. These publications strongly suggest that PANI-EB can be used as a stress grading material in high voltage applications.

This paper presents the results of FEM modeling of PP and PANI-EB layer structure. Modeling started with permittivity measurements of pure PANI-EB as a function of electric field. Curve fitting of the electric field dependence of relative permittivity was performed for PANI-EB. Fitting was used in FEM calculations.

Published on International Review of Electrical Engineering (I.R.E.E.), Vol. 1, No. 5, pp. 613-618, 2006. Quoted with the permission of the Publisher Praise Worthy Prize S. r. l. (http://www.praiseworthyprize.com/; info@ praiseworthyprize.com).

II. Modeling

II.1. PANI-EB Permittivity Curve Fitting

Curve fitting of the relative permittivity of PANI-EB was performed for modeling purposes with Matlab. The measured values were fitted on both power law and 2nd degree polynomial equations with least squares fitting. Power law fitting is calculated only from two separate measurements (Fig. 1) which are the last when the pellet was stressed until breakdown and the other measurement was from the middle of the measurement result curves. The 2nd degree polynomial fitting is based on all measurements of the pellet (Fig. 2). More information on the measurements can be found in [14].

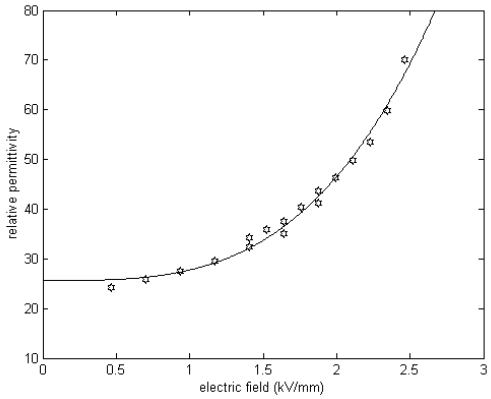

Fig. 1. Fitted power law permittivity curve.

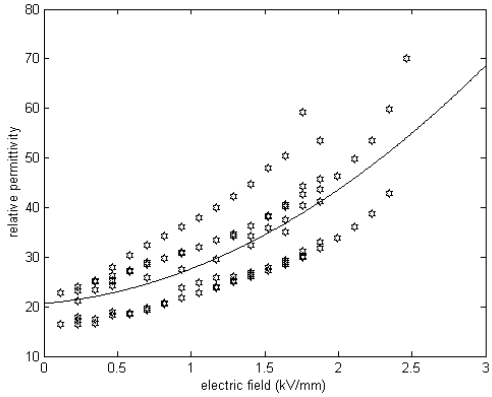

Fig. 2. Fitted 2nd degree polynomial permittivity curves.

The calculated equations of the electric field dependent relative permittivity of PANI-EB are shown below. Equation 1 describes the best fitting for power law and Equation 2 for 2nd degree polynomial fitting. The unit of E is kV/mm.

$$\varepsilon_r = 25.5 + 2.2E^{3.3} \quad (1)$$

$$\varepsilon_r = 20.7 + 2.5E + 4.5E^2 \quad (2)$$

The correlation coefficient of the power law fitting is high, 0.987, so the fitted curve and the two measurement results correlate very well (Fig. 1). It would be lower, only approx. 0.6, if all measurement results had been included in the fitting calculations. The correlation coefficient of the 2nd degree polynomial curve is 0.606 because of the fitting calculation included all the eight measurement results (Fig. 2).

II.2. FEM Modeling

Modeling of the insulation structure was done with Comsol Multiphysics. The calculation model used in this study was an approximate formulation for electrostatics of conducting and dielectric materials. FEM modelling was carried out considering Equation 3

$$-\nabla \cdot \varepsilon_0 \varepsilon_r \nabla V = \rho \,, \quad (3)$$

where ε_0 is vacuum permittivity, ε_r is relative permittivity, V is electric potential and ρ is charge density. A value of $\varepsilon_0\varepsilon_r$ is considered as a fit of the electric field. However, derivatives of the fit are not considered in Equation 3.

The voltage between capacitor electrodes was set at 500 V_{peak} (AC) and it was held constant. With that operation voltage appropriate field strengths would be applied to PP. Actually the electric field strength in PP is 100 kV/mm in reference situation. Fig. 3 presents the insulation structure studied of 5 μm PP and 1 μm PANI-EB (upper part) and elementary mesh.

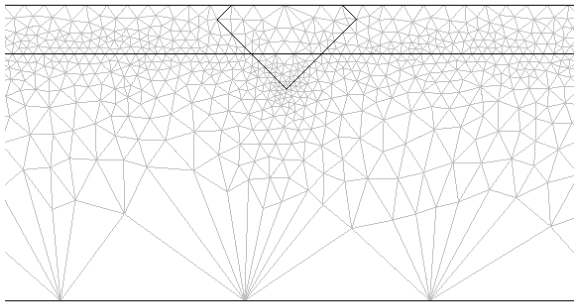

Fig. 3. The structure of PP (5 μm) and PANI-EB (1 μm) model and elementary mesh.

The permittivity of PP was held constant 2.2 [16] during the calculations. The dimensions of the model were also held constant. Small defects were simulated to the structure and the depths of the defects were changed. The effect of the fitting used was also studied. Power law and 2nd degree polynomial fitting of permittivity of PANI-EB layer were used. The voltage was applied to the upper boundary of the Fig. 3 and the lower part was grounded. The width of the examined sample was 10 μm.

Copyright © 2006 Praise Worthy Prize - All right reserved

III. Results

The modeling results are presented in Figures 4-11. In Fig. 4 the electric field norm in the insulation structure is presented. The higher field is located in PP and the lower in PANI-EB sections according to the permittivities of the materials. In Figs. 4 and 5 power law fitting was used. In Fig. 11 the electric field norms of all modeling results are presented. Electric field norms are measured vertically from the edge of PP to the edge of PANI-EB at the defect point. In Fig. 5 a small defect was modeled in PANI-EB layer. The depth of the defect was slightly over 0.5 μm in the PANI-EB layer and the defect was filled with conducting aluminium. Only a small increase in the electric field strengths of both PP and PANI-EB can be seen in Fig. 11 (two lines with no peaks). In Fig. 11 the curves are shifted so that the levels of the electric field norm are easier to find.

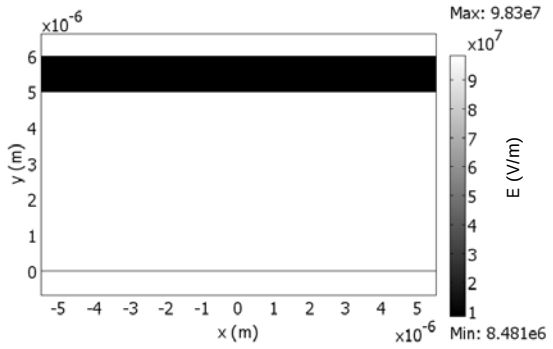

Fig. 4. Layered structure of 5 μm PP and 1 μm PANI-EB and electric field norm.

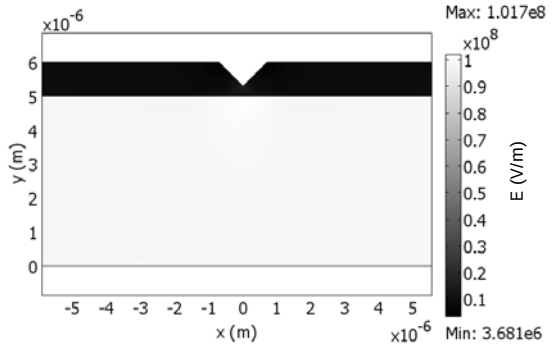

Fig. 5. Defect in the PANI-EB layer and electric field norm.

In Fig. 6 the insulation structure has a small defect in PP. The PANI-EB layer is not present and the black area in the model is aluminium. As a result we can see the rise in the electric field strength at the sharp corner of the defect. Actually the electric field strength is increased 4.5 times compared to earlier situations (Figs. 4 and 5). In Fig. 7 the insulation structure has a defect in the PP layer. The defect is filled with PANI-EB material. As a result we can see that the area with increased electric field strength is smaller when the PANI-EB material is inside the defect. The electric field strength at the top of the defect is also lower than in the previous situation (Fig. 11). It is 3.3 times higher than in the reference situation. Power law fitting is used to determine the permittivity of PANI-EB. In Fig. 8 the insulation structure is presented as in Fig. 7. The only difference is that the permittivity of PANI-EB is presented with 2nd degree polynomial fitting. The results are much the same as earlier. The electric field strength at the top of the defect is lowered to 3.1 times the reference value.

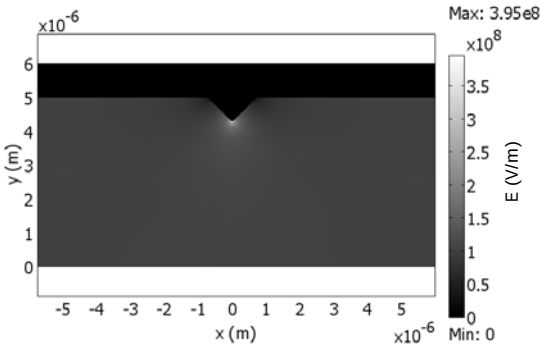

Fig. 6. Defect in the PP layer without PANI-EB layer and electric field norm.

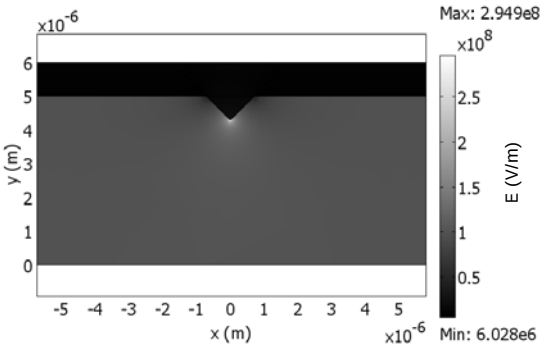

Fig. 7. Defect in PP filled with PANI-EB (power law fitting of permittivity of PANI-EB) and electric field norm.

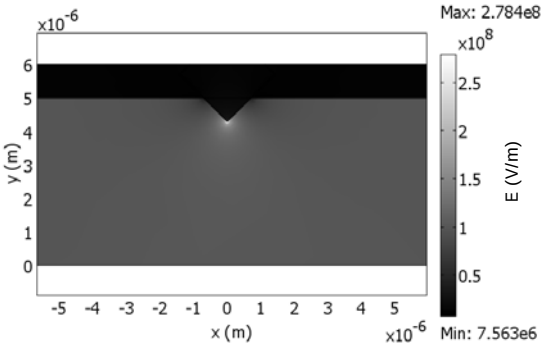

Fig. 8. Defect in PP filled with PANI-EB (2nd degree polynomial fitting of permittivity of PANI-EB) and electric field norm.

Copyright © 2006 Praise Worthy Prize - All right reserved

In Fig. 9 the difference is that now the permittivity of PANI- EB is modeled as constant, 25. This permittivity leads to the same situation in the electric field distribution as presented in earlier situations (Figs. 7 and 8). The electric field strength is 3.3 times higher than in the reference case. With these calculations it is apparent that the permittivity is increased at the top of the defect because of the field dependence of the permittivity of PANI-EB applied in the model. PANI-EB acts as an electric field absorbent having higher permittivity in regions with high electric field strengths.
In Fig. 10 an air gap between PP and PANI-EB layers is modeled. The electric field strength is increased inside the air gap. Partial discharges would be apparent starting from the corners of the gap with highest electric field strengths. The structure would suffer from discharges with increasing probability that the structure may break down completely. It is crucial to succeed in covering the PP film with the PANI-EB layer tightly enough in order to avoid voids where discharges can ignite.

In conclusion, the addition of PANI-EB between the electrode and defected PP decreases the electric field stress from 450 kV/mm to about 330 kV/mm in the defect point. However, if the nonlinearity of the permittivity of PANI were higher, the decrease in field strength would also be greater. Power law fitting, 2nd degree polynomial fitting and constant value of 25 of the relative permittivity of PANI-EB do not cause any significant changes to the electric field strength in PP.

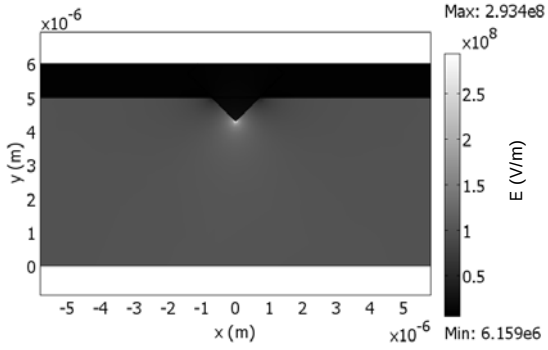

Fig. 9. Defect in PP filled with PANI-EB (permittivity of PANI-EB constant 25) and electric field norm.

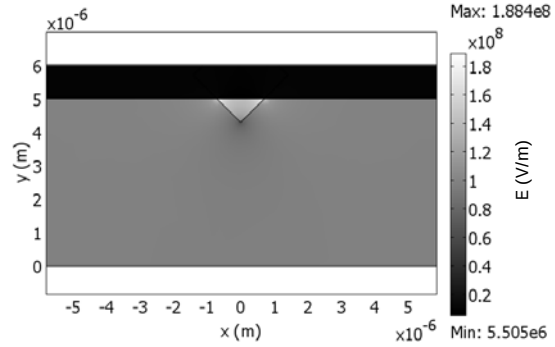

Fig. 10. Defect between PP and PANI-EB layers filled with air and electric field norm.

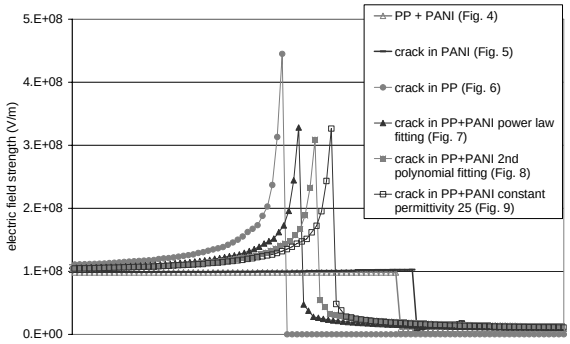

Fig. 11. Electric field norms of the modeling results. The curves are shifted along the x-axis.

IV. Discussion

According to these modeling results it seems that PANI-EB has potential to be used as a material to grade electrical stresses. The advantage is not obvious when there is no distortion in the structure but with some distortion PANI-EB can absorb electric field because its relative permittivity changes as a function of electric field. Especially when electric field is critically increased due to defects in insulation structure, PANI-EB can smooth the stresses.

Modeling was made on a one micrometer thick PANI-EB layer. The real permittivity measurements as a function of electric field were made on material samples two millimeters thick. The real functionality of PANI-EB in micrometer thicknesses is a major issue. In addition, the measurements were problematic because the interesting part of the functionality of PANI-EB is achieved with strongest electric fields. With strong electric fields pure PANI-EB breaks down.

PANI-EB has a useful property of electric field dependent relative permittivity. By changing the applied voltage and thickness of the insulation layers we can adjust PANI-EB to operate with some defined permittivity in the normal operation of the equipment. With thinner layer of PANI-EB we can ensure greater stress for PANI-EB in relation to PP. It is possible that PANI-EB will break down, but the layer thicknesses should be optimized so that in normal operation PANI-

Copyright © 2006 Praise Worthy Prize - All right reserved

EB does not break down easily. And what if PANI-EB breaks down? There is still the PP layer to ensure that the insulation structure will hold. In theory, PP should have suffered lower stresses beforehand in normal operation when PANI-EB is present.

V. Conclusion

The nonlinear behavior of the relative permittivity of PANI-EB as a function of electric field may be useful to smooth the stresses in insulation structures. With the examples modeled and real measurements from pure PANI-EB it seems that PANI-EB can lower the electric field stress, especially in higher electric field regions like defects.

It is very important to use simulations to find, how PANI-EB would act in field grading. This article presents a way to combine theoretical calculation models and very practical data from material measurements. Much more measurement data, also at higher fields (over 2.5 kV/mm), should be available to achieve better fittings for the permittivity of PANI-EB. In this kind of modeling we also have to make some simplifications compared to real applications. In real applications there may be some other dominant factors which cannot even be modeled e.g. the shape of the defect and whether caused by PP or aluminium.

The potential applications for such materials as PANI-EB are evident. This study was undertaken considering capacitor structures, but stress grading materials could also be useful in many other types of electrical apparatus e.g. cable joints and terminations. The future of these materials and composites is promising.

Acknowledgements

This work was done on a research project funded by Tekes (National Technology Agency of Finland), Borealis Polymers S/A, Evox Rifa Ltd., Nokian Capacitors Ltd., Panipol Ltd. and Tervakoski Dielectrics Ltd.

References

[1] S. Boggs, J. Y. Zhou, Dielectric Property Measurement of Nonlinear Grading Materials, *2000 Conference on Electrical Insulation and Dielectric Phenomena,* 2000, pp. 764-767.

[2] J. Y. Zhou, S. Boggs, Dielectric Property Measurement of Nonlinear Dielectric Properties – Effect of Dielectric Dispersion, *2001 IEEE Conference on Electrical Insulation and Dielectric Phenomena,* 2001, pp. 1-4.

[3] J. Y. Zhou, S. Boggs, Dielectric Properties of Three Component Mixtures of Nonlinear, Resistive, and Non-conducting Grains, *2003 Annual Report Conference on Electrical Insulation and Dielectric Phenomena,* 2003, pp. 112-115.

[4] S. Boggs, Very High Field Phenomena in Dielectrics, *IEEE Transactions on Dielectrics and Electrical Insulation*, October 2005, Vol. 12, No. 5, pp. 929-938.

[5] S. Boggs, J. Kuang, High Field Effects in Solid Dielectrics, *IEEE Electrical Insulation Magazine*, November/December 1998, Vol.14, No. 6, pp. 5-12.

[6] S. Boggs, Implications of High Field Conductivity in Solid Dielectrics, *Conference on Electrical Insulation and Dielectric Phenomena*, Pocono Manor, October 1993, pp. 532-537.

[7] S. Boggs, D. H. Damon, J. Hjerrild, J. T. Holboll, M. Henriksen, Effect of Insulation Properties on the Field Grading of Solid Dielectric DC Cable, *IEEE Transactions on Power Delivery*, October 2001, Vol. 16, No. 4, pp.456-461.

[8] G. Lupo, C. Petrarca, L. Egiziano, V. Tucci, M. Vitelli, Numerical Evaluation of the Electrical Field in Cable Terminations Equipped with Non Linear Grading Materials, *Conference on Electrical Insulation and Dielectric Phenomena*, Atlanta, October 1998, pp. 585-588.

[9] J. Pelto, M. Paajanen, K. Kannus, K. Lahti, P. Harju, Nonlinear DC Voltage-Current Characteristics of New Polymeric Composite Materials Based on Semiconductive Polyaniline Emeraldine Base Filler, *2004 International Conference on Solid Dielectrics*, Toulouse, France, 2004, Vol. 2, pp. 825-828.

[10] S. Watanabe, Y. Kim, N. Hayashi, Y. Uchida, D. Lee, D. Dykes, G. Touchard, M. Ieda, Manufacture of Insulating Agents for Electric Field Relaxation Using Functionally Graded Materials, with Electric Field Calculations, *Proceedings of the 5th International Conference on Properties and Applications of Dielectric Materials*, Seoul, Korea, May 25-30, 1997, pp. 519-522.

[11] H. Shumiya, K. Kato, H. Okubo, Fabrication and Prediction Techniques for FGM (Functionally Graded Materials) Application to Solid Insulators, *2005 Annual Report Conference on Electrical Insulation and Dielectric Phenomena*, October 2005, pp. 673-676.

[12] N. Hayashi, K. Kawahara, M. Sumikura, M. Hara, Electric Field Control by Permittivity Functionally Graded Materials and Their Lightning Impulse Withstand Voltages for Surface Breakdown, *Conference Record of the 2002 IEEE International Symposium on Electrical Insulation*, Boston, April 2002, pp. 260-263.

[13] P. Salovaara, M. Takala, K. Kannus, Dielectric Properties of Polyaniline Emeraldine Base, *International Review of Electrical Engineering (IREE)*, 2006, Vol. 1 N. 4, pp. 462-467.

[14] J. Lu, K. Moon, B. Kimt and C. P. Wong, Novel All Organic High Dielectric Constant Polyaniline/Epoxy Composites for Embedded Capacitor Applications, *International Symposium on Advanced Packaging Materials: Processes, Properties and Interface*, 2006, pp. 88-92.

[15] Y. Kieffel, J. P. Travers, D. Cottevieille, Undoped Polyaniline in the High Voltage Domain: Non Linear Behavior and Aging Effects, *2000 Conference on Electrical Insulation and Dielectric Phenomena,* 2000, pp. 52-56.

[16] K. Kannus, P. Harju, K. Lahti, J. Pelto, M. Paajanen, Electrical Properties of Polypropylene and Polyaniline Compounds, *2004 International Conference on Solid Dielectrics*, Toulouse, France, 2004, Vol. 1, pp. 67-70.

Copyright © 2006 Praise Worthy Prize - All right reserved

Authors' information

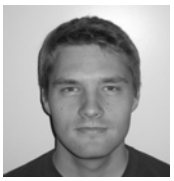

Markus Takala was born in Vaasa, Finland in 1980. He graduated M. Sc. (Eng.) in electrical power engineering, Tampere University of Technology, Tampere, Finland, 2005. His research interests include topics in new electrical insulation materials. Nanostructured epoxy and PP have been the main research topics.

Pauliina Salovaara was born in Mouhijärvi, Finland in 1980. She graduated M.Sc. (Eng.) from the Department of Electrical Power Engineering, Tampere University of Technology, Tampere, Finland, 2004. Since 2004 she has been a researcher in high voltage Laboratory at TUT. She has published articles on dielectric properties of PP compounds. Her research interests include new dielectric material compounds and high voltage engineering.

Tommi Keikko was born in Vammala, Finland, 1970. He received his M.Sc. (Eng.) degree and Dr.Tech. degree in electrical engineering from Tampere University of Technology in 1995 and 2003 respectively. Since January 1995 he has worked as a research engineer at Tampere University of Technology in the Department of Electrical Engineering. At present, he is working in the Institute of Power Engineering as a senior researcher. His areas of interest are electric and magnetic field calculations and technical management of LF electromagnetic fields in living and working environments.

Kari Kannus was born in Längelmäki, Finland, on May 17, 1957. He received his M.Sc. (Eng.), Licentiate of Technology and Doctoral degrees in electrical engineering from Tampere University of Technology (TUT) in 1981, 1987 and 1998 respectively. From 1982 to 1988 he was a teaching and research assistant and from 1988 to 1992 he was a laboratory manager at the Institute of Power Engineering of TUT. From 1993 to 1998 he was a researcher and since 1999 he has been a senior researcher at TUT. Since 2002 he has been a Docent of High Voltage Engineering at TUT. His main research interests are in the field of high voltage technology, especially overvoltage protection and surge arresters, new polymeric materials and environmental testing.

Copyright © 2006 Praise Worthy Prize - All right reserved

Publication 2

M. Takala, S. Kortet, P. Salovaara, M. Karttunen, K. Kannus, AC Breakdown Strength of Polypropylene-Calcium Carbonate Compounds, In *Proceedings of Nordic Insulation Symposium* (NORD-IS07), Copenhagen, Denmark, June 11-13, pp. 123-126, (2007)

© 2007 NORD-IS. Reprinted, with permission, from the proceedings of Nordic Insulation Symposium.

AC Breakdown Strength of Polypropylene-Calcium Carbonate Compounds

M. Takala[1], S. Kortet[2], P. Salovaara[1], M. Karttunen[2] and K. Kannus[1]
[1]*Tampere University of Technology, Tampere, Finland*
[2]*Technical Research Centre of Finland, Tampere, Finland*

Abstract

This study presents the results of AC breakdown measurements conducted on polypropylene-calcium carbonate (PP-$CaCO_3$) polymer compounds. Two different PP matrices and two types and amounts of $CaCO_3$ were used. Thickness of the samples was approximately 600 µm. The measurements were conducted at the high voltage laboratory of Tampere University of Technology. Twenty parallel measurements were taken for each kind of material. Statistical analysis was applied to the results to determine the effects of the additive type and amount on the AC breakdown strength of polypropylene.

1. Introduction

Polymers are widely used as insulating materials. Polypropylene is the most used material e.g. in power capacitor insulation. Because capacitive reactive power is proportional to the square of operating voltage of the capacitor, an increase in operating voltage as a consequence of increase in breakdown voltage in PP, is advantageous.

Deng and Hackam have written about the hydrophobicity [1]-[3] and electrical performance [4], [5] of $CaCO_3$ filled cross-linked polyethylene (XLPE). According to studies by Deng and Hackam the recovery of hydrophobicity on the surface of XLPE depends on filler concentration and the temperature of the saline aqueous solution. Complete recovery was not reached for specimens with 15 and 25 % filler concentrations. Deng and Hackam also suggest that in time to failure measurements XLPE specimens with higher concentrations of $CaCO_3$ can withstand higher temperature due to higher melting point. Therefore $CaCO_3$ offers protection against erosion for longer durations than when either lower concentration of or no filler is used. Koshino et al. [6] studied the deterioration of $CaCO_3$-silicone rubber (SIR) due corona discharges. The performance of SIR depends upon the kinds and amount of the base polymer and fillers. Nitric acid and ozone are generated by the corona discharges. In immersion tests $CaCO_3$-SIR insulator dissolves in nitric acid and actually $CaCO_3$ dissolves in nitric acid and then acid penetrates through the voids in the bulk portion. The surfaces of the specimens are cracked.

These studies show that $CaCO_3$ can be advantageous in time to failure measurements of XLPE but also harmful in immersion tests of SIR.

The aim of this study is to determine the effects of $CaCO_3$ to the AC breakdown strength of polypropylene.

2. Materials

Samples PP1_1 to PP1_4 were based on PP1 polypropylene and samples PP2_1 and PP2_2 were based on PP2 polypropylene. In addition, samples PP1_1 and PP1_2 contain 10 wt-% of $CaCO_3$ mixture 1 and samples PP1_3, PP1_4, PP2_1 and PP2_2 contain 10 wt-% of $CaCO_3$ mixture 2. The w-% of the mixture is calculated from the weight of the polymer. The difference between mixtures 1 and 2 is the amount and particle size of $CaCO_3$ in these masterbatches. Mixture 2 contains 70% $CaCO_3$ and mixture 1 contains 40% $CaCO_3$.

PP and $CaCO_3$ were mixed with twin screw extruder (Berstorff ZE 25x48D) at the Technical Research Centre of Finland. PP1_2 is the same sample run through the extruder as PP1_1. The same processing was done with sample pairs PP1_3, PP1_4; PP2_1, PP2_2. Polymers were extruded with the Brabender Plasticorder single screw extruder (diameter 18 mm) using a flat die. The cast film was usually 0,5-0,7 mm thick.

3. Measurements and statistical analysis

3.1. Measurements

The AC dielectric strength of electrical insulator components made of the blends mentioned above was measured. The measurements were performed at room temperature (~20 °C). The size of the test samples was approximately 4 cm x 4 cm and thickness 500-700 µm. In the measurements rod-like electrodes having a diameter of 12 mm and made of stainless steel were used. The measurement bench is presented in Fig. 1.

The measurements were performed by immersing the sample to be measured and the electrodes in mineral oil (Shell Diala DX) in order to avoid surface discharges and flashovers. The AC breakdown measurements were performed using a high voltage supply (Hipotronics) with a maximum output of 50 kV and 6 A. The applied voltage was AC 50 Hz with 2 kV/s rate of rise according to IEC 60243-1 [7] until breakdown

occurred. A set of 20 test samples was used with each blend.

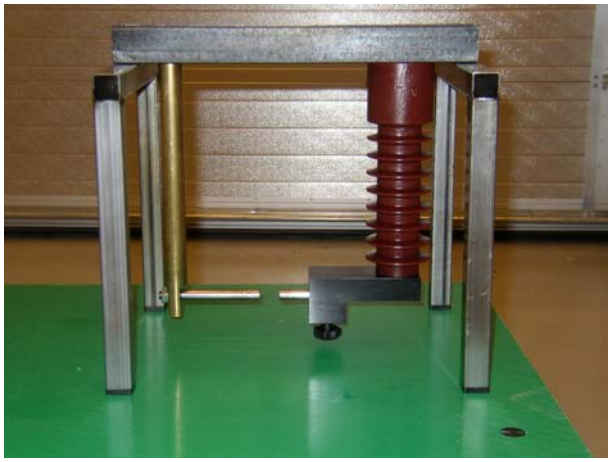

Fig. 1 - Measurement bench.

3.2. Statistical analysis

Statistical analysis was applied to the breakdown test results. Results were calculated according to the IEEE standard "IEEE Guide for the Statistical Analysis of Electrical Insulation Breakdown Data" [8] using Microsoft Excel and Matlab.
Two-parameter Weibull distribution function was used to process data derived from dielectric strength measurements. Distribution parameter estimation is easier and confidence intervals of parameters are smaller with two than with three-parameter Weibull distribution [9]. The quality of data fit was good, even if slight deviations at low or high probability values were sometimes detected [10]. The 2-parameter Weibull cumulative distribution function (1) is related to the probability for failure to occur in certain field strength *x* [11].

$$F(x) = 1 - \exp\left\{-\left[\frac{x}{\beta}\right]^{\alpha}\right\} \qquad (1)$$

The shape parameter α is related to the shape or the width of the distribution. The spread of the breakdown strengths is narrower when the value of α is higher. There is a smaller scattering of the dielectric strength values and consequently higher reliability of the dielectric behavior of the material when shape parameter is high. Scale parameter β is related to the 63.2 % probability for the sample to break down at electric field strength β [10].

4. Measurement results

Table 1 presents the results of the AC breakdown strength measurements. The mean value was calculated from 20 measurement results obtained from the measurements. Uncertainties were estimated with standard deviation using Student's T-distribution 95 % confidence intervals. According to the standard [8] correlation to the data points should be over 0.935 to achieve enough good correlation with 20 measurements using 2-parameter Weibull distribution. With these measurements 3-parameter Weibull distribution gave the same correlation results as 2-parameter Weibull distribution. Correlation values of the Table 1 were calculated using 2-parameter Weibull distribution. With PP2 and PP2_1 the achieved correlation was slightly below 0.935.

Table 1 - AC breakdown measurement results.

Material	mean value	standard deviation	β	α	correlation
PP1	70	2	72.43	19.13	0.94
PP1_1	61	2	62.44	18.04	0.99
PP1_2	61	1	62.26	22.75	0.95
PP1_3	77	3	79.58	13.10	0.97
PP1_4	69	2	70.75	17.69	0.97
PP2	60	3	62.63	12.32	0.92
PP2_1	80	5	84.33	10.31	0.91
PP2_2	74	2	76.12	20.50	0.95

The AC breakdown strengths of the materials are presented in Figure 2 with standard deviation bars. Reference materials PP1 and PP2 are marked with light colors and reference AC breakdown strength levels have been marked with broken lines. Mixture 2 (darkest bars: PP1_3, PP1_4, PP2_1 and PP2_2) seemed to increase the AC breakdown strength of polypropylene more than mixture 1 (light grey bars: PP1_1 and PP1_2). Samples PP2_1 and PP2_2 (based on PP2) had slightly higher AC breakdown strengths than samples PP1_3 and PP1_4, which were based on PP1.

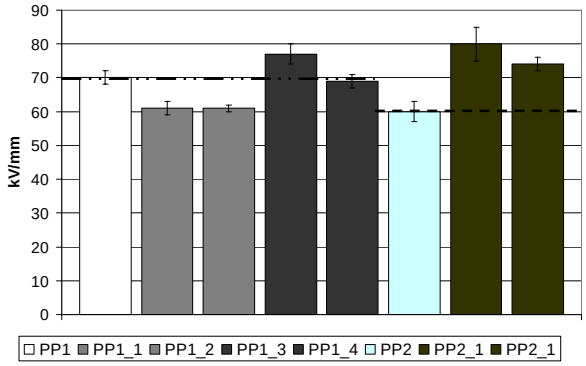

Fig. 2 - AC breakdown strengths of the materials with standard deviation bars.

In Figs. 3-6 the measurement results are presented in Weibull probability plots. 90 % confidence intervals

were plotted with dots on the both sides of the straight Weibull fitting line. Measurement points were marked with small crosses and circles. In Fig. 3 two reference materials, PP1 and PP2, were compared. PP1 material gave better AC breakdown strength results and 90 % confidence intervals did not even cross.

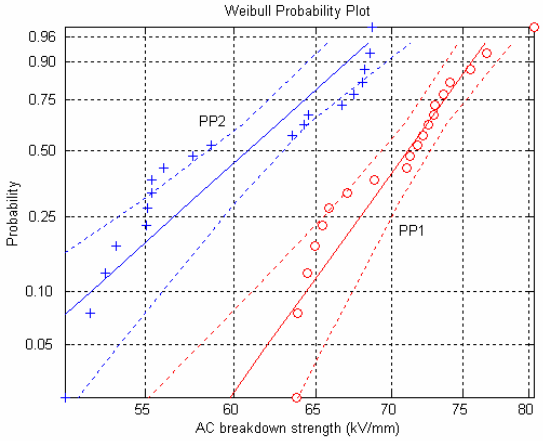

Fig. 3 - AC breakdown test results of materials PP1 and PP2 presented in Weibull probability paper.

In Fig. 4 PP1 and PP1_3 materials are compared. PP1_3 material contained 10 wt-% of $CaCO_3$ mixture 2. 90 % confidence intervals crossed each other at a probability of 0.35. The addition of 10 wt-% of $CaCO_3$ mixture 2 to PP1 increased the mean value of AC breakdown strength by 10 %.

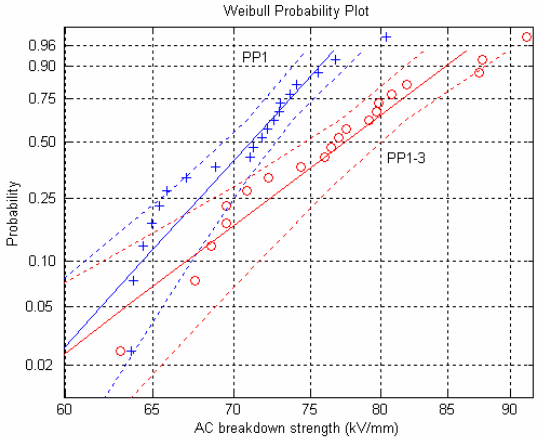

Fig. 4 - AC breakdown test results of materials PP1 and PP1_3 presented in Weibull probability paper.

In Fig. 5 PP2 and PP2_1 materials are compared. PP2_1 material contained 10 wt-% of $CaCO_3$ mixture 2. 90 % confidence intervals crossed each other at a probability of 0.03. PP2_1 material had clearly higher AC breakdown strength than the reference material PP2. The addition of 10 wt-% of $CaCO_3$ mixture 2 to PP2 increased the mean value of AC breakdown strength by 33 %.

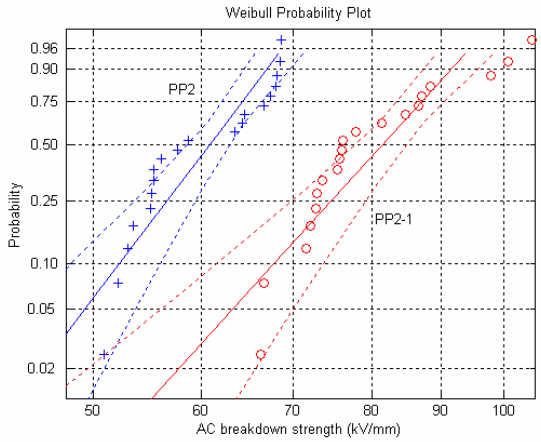

Fig. 5 - AC breakdown test results of materials PP2 and PP2_1 presented in Weibull probability paper.

In Fig. 6 PP2 and PP2_2 materials are compared. PP2_2 material contained 10 wt-% of $CaCO_3$ mixture 2. 90 % confidence intervals did not even cross at lowest probabilities. PP2_2 material had clearly higher AC breakdown strength than the reference material PP2. The addition of 10 wt-% of $CaCO_3$ mixture 2 to PP2 increased the mean value of AC breakdown strength by 23 %.

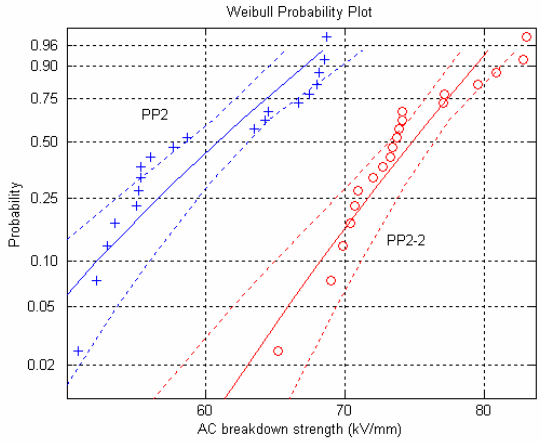

Fig. 6 - AC breakdown test results of materials PP2 and PP2_2 presented in Weibull probability paper.

5. Discussion

According to the reference by Deng and Hackam [4] the melting point was higher in XLPE when $CaCO_3$ was added to polyethylene (PE). The filler particles had a superior resistance to erosion and arc damage due to the much higher melting temperature than PE. This also explains the AC breakdown strength increase in PP as the measurements done in this study indicate (Figs. 4-6).

The reason could be e.g. crystallinity or permittivity changes. The volume fraction of crystallinity may decrease because particles must be segregated in non-crystalline regions by the process of crystallization. As the boundaries between spherulites accept particles, the

resistance to electric breakdown may increase [12].
The rise in the melting point would appear a likely reason for the increase in breakdown strength. The melting point of $CaCO_3$ is 1340 °C [13] and for PP around 160 °C [14]. In breakdown there are high temperatures involved and in higher temperatures material begins to soften and erode more easily.
Processing times seemed to decrease the breakdown strength in two cases of three (PP1_3, PP1_4; PP2_1, PP2_2). The reason for this may be thermal oxidation and degradation.

6. Conclusion

The AC breakdown voltages obtained from reference PP and PP-$CaCO_3$ compounds were analyzed according to Weibull statistical analysis.
This study concluded that $CaCO_3$ could substantially increase the breakdown strength of PP. The addition of 10 wt-% of $CaCO_3$ mixture 2 increased the AC breakdown strength mean value of the materials PP1_3, PP2_1 and PP2_2 by 10 %, 33 % and 23 %, respectively. The Weibull shape parameter values were high and varied between 10.3 and 22.8, showing less scattering of the dielectric strength and consequently good reliability of the AC dielectric breakdown behavior.
Reasonable explanations for the increase in AC breakdown strength are that the particles must be segregated in boundaries between spherulites and the high melting point of $CaCO_3$ leads to high resistance to thermal degradation. Processing times seem to decrease the AC strength of the material, possibly due to thermal oxidation and degradation.
More measurements need to be performed on the materials to obtain more profound knowledge of the materials, also as a function of the amount of $CaCO_3$. Breakdown strength measurements should also be made in lightning impulse voltage and the repeatability of these reported AC measurements should be verified. Dielectric permittivity and loss factor should also be measured given the possible applications of the material.

7. References

[1] H. Deng and R. Hackam, Effects of Calcium Carbonate Filler on the Hydrophobic Property of XLPE, IEEE International Symposium on Electrical Insulation, Pittsburgh, PA USA, 5-8 June 1994, pp. 453-456.

[2] H. Deng and R. Hackam, Loss and Recovery of Hydrophobic Property of XLPE Filled with Calcium Carbonate, IEEE 5th International Conference on Conduction and Breakdown in Solid Dielectrics, 1995, pp. 547-551.

[3] H. Deng and R. Hackam, Hydrophobic Property of XLPE Filled with Calcium Carbonate, IEEE Transactions on Dielectrics and Electrical Insulation, Vol. 3 No. 4, August 1996, pp. 577-586.

[4] H. Deng and R. Hackam, Electrical Salt-Fog Performance of XLPE Insulation with Different Levels of $CaCO_3$, IEEE Transactions on Dielectrics and Electrical Insulation, Vol. 3 No.6, December 1996, pp. 817-826.

[5] H. Deng and R. Hackam, Electrical Performance in Salt-fog of XLPE Containing Different Levels of Calcium Carbonate Filler, IEEE Electrical Insulation and Dielectric Phenomena, 23-26 Oct. 1994, pp. 553-558.

[6] Y. Koshino, I. Umeda, and M. Ishiwari, Deterioration of Silicone Rubber for Polymer Insulators by Corona Discharge and Effect of Fillers, IEEE Electrical Insulation and Dielecric Phenomena, 25-28 Oct. 1998, Vol. 1, pp. 72-79.

[7] IEC Publication 60243-1: Electrical Strength of Insulating Materials – Test Methods – Part 1: Test at Power Frequencies, 1998-01.

[8] IEEE Standard 930: IEEE Guide for the Statistical Analysis of Electrical Insulation Breakdown Data, IEEE Dielectrics and Electrical Insulation Society, 1 April 2005.

[9] M. Cacciari, G. Mazzanti and G.C Montanari, Weibull Statistics in Short-Term Dielectric Breakdown of Thin Polyethylene Films, IEEE Transactions on Dielectrics and Electrical Insulation, 1(1), 1994, 153-159.

[10] P. Salovaara and K. Kannus, Increasing the Dielectric Breakdown Strength of Polypropylene Using Polyaniline Additive, IASTED-conference on Energy and Power Systems, March 29-31, 2006, Chiang Mai, Thailand, pp. 234-239.

[11] L.A. Dissado, & J.C. Fothergill, Electrical Degradation and Breakdown in Polymers, IEE Materials and Devices Series, Peter Peregrinus Ltd., London, UK, 1992.

[12] C. C. Ku and R. Liepins, Electrical Properties of Polymers, Chemical Principles, Hanser Publishers, Munich, Germany, 1987.

[13] G. J. Janz, Molten Salts Handbook, Academic Press, 1967.

[14] Data Sheet, Polypropylene Borclean HB300BF, Polypropylene Homopolymer for Capacitor Film (BOPP), F 0059 06.07.2004 Ed.3.

Publication 3

M. Takala, M. Karttunen, P. Salovaara, S. Kortet, K. Kannus, T. Kalliohaka, Dielectric Properties of Nanostructured Polypropylene-Polyhedral Oligomeric Silsesquioxane Compounds, *IEEE Transactions on Dielectrics and Electrical Insulation*, Vol. 15, No. 1, pp. 40-51, (2008)

© 2008 IEEE. Reprinted, with permission, from IEEE Transactions on Dielectrics and Electrical Insulation.

This material is posted here with permission of the IEEE. Such permission of the IEEE does not in any way imply IEEE endorsement of any of the Tampere University of Technology's products or services. Internal or personal use of this material is permitted. However, permission to reprint/republish this material for advertising or promotional purposes or for creating new collective works for resale or redistribution must be obtained from the IEEE by writing to pubs-permissions@ieee.org. By choosing to view this material, you agree to all provisions of the copyright laws protecting it.

Dielectric Properties of Nanostructured Polypropylene-Polyhedral Oligomeric Silsesquioxane Compounds

M. Takala[1], M. Karttunen[2], P. Salovaara[1], S. Kortet[2], K. Kannus[1] and T. Kalliohaka[2]

[1]Tampere University of Technology
Institute of Power Engineering
P.O. Box 692
FI-33101 Tampere, Finland

[2]Technical Research Centre of Finland
P.O. Box 1607
FI-33101 Tampere, Finland

ABSTRACT

This paper presents the results of the dielectric measurements conducted on polymer nanocompounds consisting of polypropylene (PP) and polyhedral oligomeric silsesquioxane (POSS). The material compounds were analyzed with a scanning electron microscope (SEM) and Raman-atomic force microscope (Raman-AFM). Ac and lightning impulse (LI) breakdown strength of the material compounds were measured. Relative permittivity, loss factor and volume resistivity measurements were also conducted on the material samples. Two types of POSS, octamethyl and isooctyl, were used in different quantities. The thickness of the samples was approximately 600 µm. Statistical analysis was applied to the results to determine the effects of the additive type and amount on the breakdown strength of polypropylene. The paper discusses the possibilities and restrictions in order to achieve advantages in high voltage applications using polyhedral oligomeric silsesquioxanes.

Index Terms — **Dielectric properties, polyhedral oligomeric silsesquioxane, polypropylene, statistical analysis.**

1 INTRODUCTION

THE use of polymers as electrical insulating materials has been growing rapidly in recent decades. The base polymer properties have been developed by adding small amounts of different fillers (e.g. carbon black, talc, quartz and metal oxides) to the polymer material. Recently, great expectations have focused on nano-fillers, e.g. polyhedral oligomeric silsesquioxanes (POSS).

A general overview and the theory of the functionality and morphology of the nanocomposite dielectrics have been described in various articles [1-16]. CIGRE Task Force D1.16.03 [17] has reported that advanced polymer nanocomposite materials have significant potential applications for electrical and electronics insulation.

According to the EU 6th FP report "Nanomaterial roadmap 2015" [18] the demand throughout the industry, in the case of POSS, has begun to increase and market entry in thermal insulators has been predicted by the turn of the decade. The POSS related articles published so far usually deal with the thermal and mechanical properties, including both thermoplastic and epoxy matrices [19-29]. Current applications of POSS have been related to fire retardant materials, electronics [30-34], medical engineering, packaging and space industries.

Few articles related to dielectric properties of POSS materials have been published [35-37]. Horwarth et al. [35, 36] have reported improved corona endurance in polypropylene (PP) and epoxy with the use of POSS. Linnamaa and Kannus [37] have published on the partial discharge endurance and dielectric properties of POSS-XLPE. POSS seemed to inhibit physical degradation caused by the partial discharges on XLPE.

This study concentrates on the dielectric properties of nanostructured PP-POSS compounds since previous research results indicated improved corona endurance. POSS also has good compatibility with PP.

2 EXPERIMENTAL

2.1 MATERIALS USED

Polymer compounds were produced with melt state compounding. The same isotactic polypropylene was used as matrix polymer in all compounds. The polypropylene used is

Manuscript received on 3 August 2007, in final form 31 October 2007.

1070-9878/08/$25.00 © 2008 IEEE

Authorized licensed use limited to: Tampereen Teknillinen Korkeakoulu. Downloaded on March 23,2010 at 04:46:45 EDT from IEEE Xplore. Restrictions apply.

designed for capacitor films and was produced by Borealis Polymers. Two different POSS chemicals, octamethyl and isooctyl POSS, were used with the matrix polymer. The compositions of the materials studied are shown in Table 1. PP1 and PP2 are the reference materials.

Table 1. Composition of the studied materials.

Material	POSS type	wt-%
PP1	-	-
PP1_1	octamethyl	1
PP1_2	octamethyl	2
PP1_3	octamethyl	3
PP1_4	octamethyl	5
PP1_5	octamethyl	10
PP2	-	-
PP2_1	isooctyl	1
PP2_2	isooctyl	3
PP2_3	isooctyl	3.5
PP2_4	isooctyl	5
PP2_5	isooctyl	10

The wt-% of the mixture was calculated from the weight of the polymer. PP and POSS were compounded with a twin screw extruder (Berstorff ZE 25x48D) at the Technical Research Centre of Finland (VTT). PP1 material series was mixed once using a highly mixing screw. PP2 material series was mixed twice using a highly mixing screw with a longer mixing zone than in a screw used for PP1 series. Due to the different thermal history of these series two references (PP1 and PP2) were made. In order to make homogeneous compounds two-stage mixing was made for PP-isooctyl (PP2_1 to PP2_5) materials. All materials were extruded with the Brabender Plasticorder single screw extruder (diameter 18 mm) using a flat die. The cast film was 0.5-0.7 mm thick.

POSS chemicals were purchased from Hybrid Plastics Inc.. The chemical structures of octamethyl and isooctyl POSS chemicals are presented in Figure 1. An octamethyl POSS molecule contains eight methyl groups and an isooctyl POSS molecule contains eight octyl groups. Octamethyl POSS is in the microcrystalline powder form and isooctyl POSS is viscous liquid at room temperature.

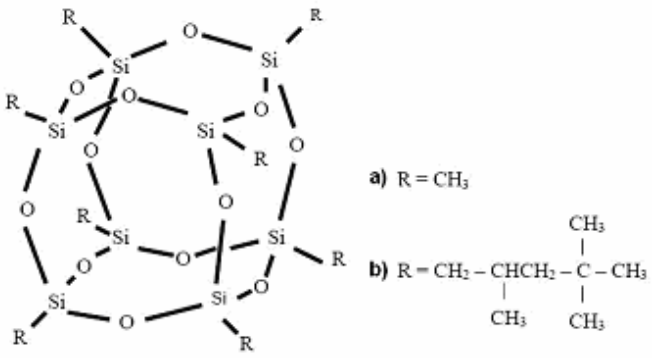

Figure 1. a) octamethyl b) isooctyl POSS cage structures [19, 38].

2.2 AC AND LI BREAKDOWN STRENGTH MEASUREMENTS

ac and lightning impulse (LI) breakdown strength of the test samples were measured at Tampere University of Technology. The measurements were performed at room temperature (~20 °C). The size of the test samples was approximately 4 cm x 4 cm and thickness 500-700 μm. The thickness dependent breakdown strength at these material thicknesses has only a small effect on the results and was ignored because of the small thickness variation in material samples [39]. Rod-like electrodes having a diameter of 12 mm and made of stainless steel were used in the measurements. The electrodes were placed on opposite surfaces of a specimen film. The measurements were performed by immersing the sample and the electrodes in mineral oil (Shell Diala DX) in order to avoid surface discharges and flashovers. In addition, the edges of the electrodes were rounded (r =1 mm) for that reason. The sites of the breakdown were distributed all over the sample area. The measurement bench is presented in Figure 2.

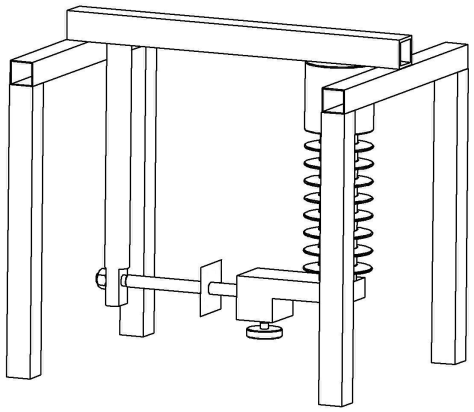

Figure 2. The measurement bench.

The ac breakdown measurements were performed using a high voltage supply (Hipotronics) with a maximum output of 50 kV and 6 A. The voltage applied was ac 50 Hz with 2 kV/s rate increase according to IEC 60243-1 [40] until breakdown occurred. A set of 10 test samples was used with each material.

The LI breakdown measurements were performed using a high voltage impulse generator (Haefely Test, AG) of maximum charging voltage 1000 kV and maximum pulse energy 50 kJ. The wave shape of the impulse voltage was 1.2/50 μs defined according to IEC Standard 60060-1 [41]. The charging voltage of the impulse generator was raised 2 kV after each impulse until breakdown occurred. Negative impulses were used and the time interval between them was 10-20 s. The number of the parallel measurements with LI voltage was 10.

2.3 DIELECTRIC SPECTROSCOPY

The complex impedance of PP-POSS compounds was measured as a function of frequency. The measurements were performed using insulation diagnosis analyzer IDA200. The

Authorized licensed use limited to: Tampereen Teknillinen Korkeakoulu. Downloaded on March 23,2010 at 04:46:45 EDT from IEEE Xplore. Restrictions apply.

frequency range used was from 0.1 Hz to 1 kHz at 140 V_{RMS} voltage. The relative permittivity (ε_r), loss factor (tan δ) and volume resistivity (ρ) were calculated from the measured parallel capacitance and resistance with the following Equations 1-5,

$$\varepsilon' = \frac{C_P}{C_0} - \frac{C_e}{C_0} \quad (1)$$

$$\varepsilon'' = \frac{1}{R_P C_0 \omega} - \frac{C_e}{C_0} \quad (2)$$

$$\varepsilon_r = \sqrt{\varepsilon'^2 + \varepsilon''^2} \quad (3)$$

$$\tan\delta = \frac{\varepsilon''}{\varepsilon'} \approx \frac{1}{R_P C_P \omega} \quad , C_e << C_P \quad (4)$$

$$\sigma = \frac{1}{\rho} = \frac{\varepsilon_0}{R_P C_0} \quad (5)$$

where C_P and R_P respectively are the measured parallel capacitance and resistance at the measurement frequency when the specimen is represented in terms of equivalent parallel circuit (Figure 3), C_0 the vacuum capacitance of the measurement setup, C_e the edge capacitance according to IEC standard 250 [42], ω the angular frequency and ε_0 the vacuum permittivity.

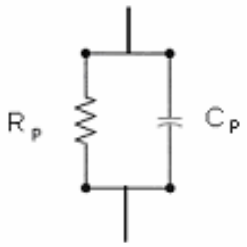

Figure 3. Equivalent RC parallel electrical circuit of dielectric specimens.

Samples were approximately 9 cm x 9 cm wide and 600 μm thick. Aluminum foil electrodes (d=8 cm) attached to the samples with a small amount of silicone grease were used. Three parallel measurements were conducted on the samples.

2.4 STATISTICAL ANALYSIS

Statistical analysis was applied to the breakdown strength measurement results. Results were calculated according to the IEEE standard "IEEE Guide for the Statistical Analysis of Electrical Insulation Breakdown Data" [43] using Microsoft Excel and Matlab programs.

Two-parameter Weibull distribution function was used to process the data derived from the breakdown strength measurements. Distribution parameter estimation was easier and confidence intervals of parameters were smaller with two than with three-parameter Weibull distribution [44]. The quality of data fit was good, even though slight deviations at low or high probability values were sometimes detected [45]. The 2-parameter Weibull cumulative distribution function (Eq. 6) is related to the probability of failure occurring in certain field strength *x* [46].

$$F(x) = 1 - \exp\left\{-\left[\frac{x}{\beta}\right]^{\alpha}\right\} \quad (6)$$

The shape parameter α is related to the shape or the width of the distribution. The spread of the breakdown strengths is narrower when the value of α is higher. There is a smaller scattering of the dielectric strength values and consequently higher reliability of the dielectric behavior of the material when shape parameter is high. Scale parameter β is related to the 63.2 % probability for the sample to break down at electric field strength β [45].

Statistical differences between two materials can be compared, when the sample amount is the same in both materials, by average standard deviation (s_{ave}), which is the average value of the two standard deviations of the materials. The difference between the breakdown strength means (dif) of the materials is compared with meaningful sectors. These sectors are not significant (dif ≤ $1.96\times s_{ave}$), almost significant ($1.96\times s_{ave}$ < dif ≤ $2.58\times s_{ave}$), significant ($2.58\times s_{ave}$ < dif ≤ $3.29\times s_{ave}$) and extremely significant (dif > $3.29\times s_{ave}$) [47]. With these quantiles statistical significance levels can be calculated and differences between the materials evaluated.

3 RESULTS

3.1 MORPHOLOGY

The morphology of the octamethyl and isooctyl POSS PP materials was studied with scanning electron microscope (SEM). Octamethyl PP material was studied also with Raman-atomic force microscope (Raman-AFM). In Figures 4-7 the fracture surfaces of reference PP (PP2), 5 wt-% isooctyl POSS PP (PP2_4), 3 and 10 wt-% octamethyl POSS PP compounds (PP1_3 and PP1_5) are presented. Samples were broken in liquid nitrogen. In both octamethyl POSS PP compounds some relatively large POSS crystals were observed. The maximum size of the POSS crystals was approximately 5 to 10 μm (POSS crystals indicated with arrows.). The fracture surface of pure PP (Figure 4) was more even than the fracture surfaces of octamethyl POSS PP samples. In the fracture surfaces of pure PP and isoctyl POSS PP (Figure 5) samples no particles were observed.

The reference PP (PP1), octamethyl POSS and 10 wt-% octamethyl POSS PP compound (PP1_5) were analyzed also by Raman-AFM. In Figures 8 and 9 the micro Raman video images (surface and depth profiles) and the Raman spectrum of reference PP, octamethyl POSS (only Raman spectrum) and 10 wt-% octamethyl POSS samples are presented. The analyses of these Raman spectra show that the typical peak

Authorized licensed use limited to: Tampereen Teknillinen Korkeakoulu. Downloaded on March 23,2010 at 04:46:45 EDT from IEEE Xplore. Restrictions apply.

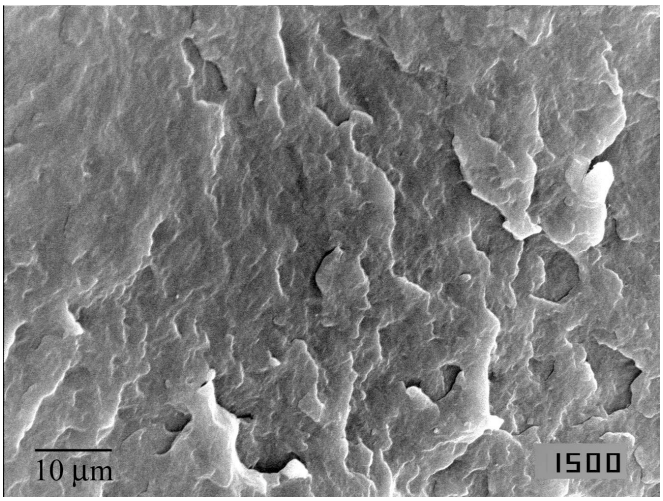

Figure 4. Fracture surface of reference PP (PP2) (1500X).

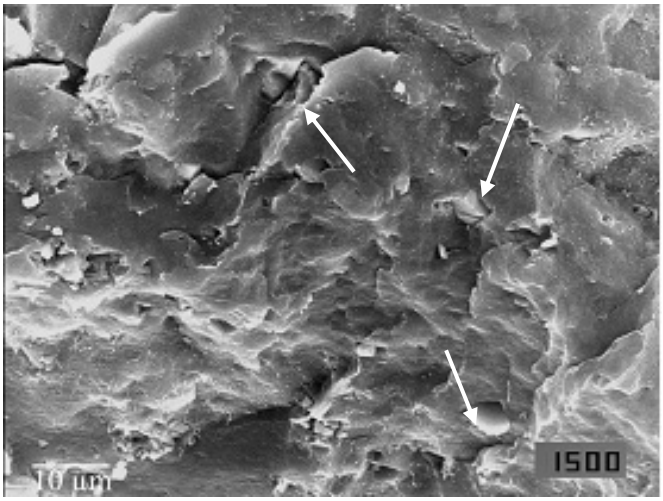

Figure 7. Fracture surface of 10 wt-% octamethyl POSS PP (PP1_5) compound (1500X). POSS crystals indicated with arrows.

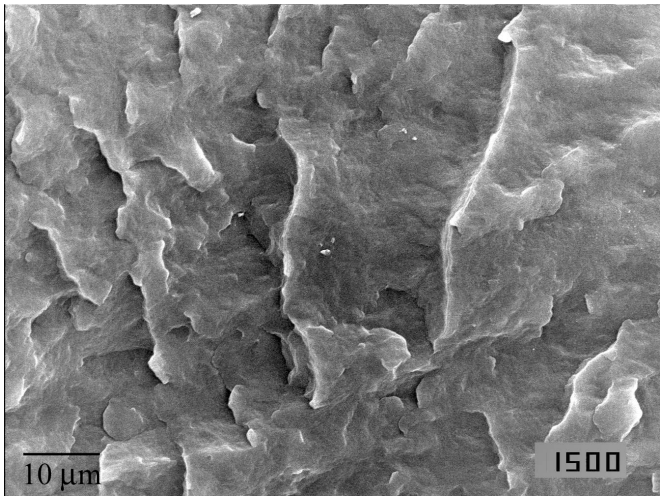

Figure 5. Fracture surface of 5 wt-% isooctyl POSS PP (PP2_4) compound (1500X).

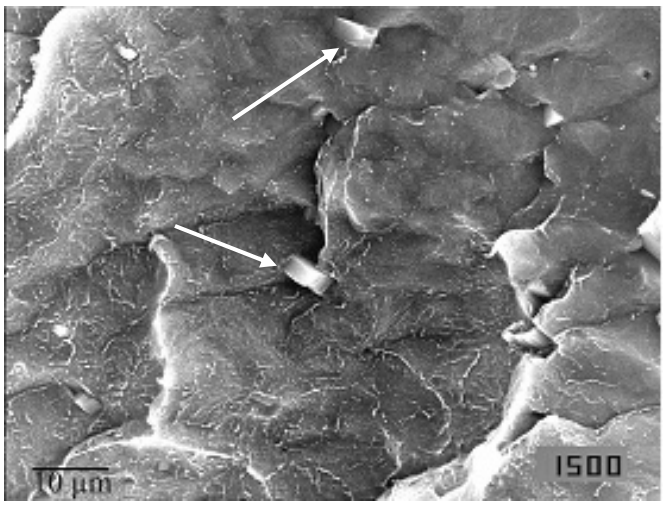

Figure 6. Fracture surface of 3 wt-% octamethyl POSS PP (PP1_3) compound (1500X). POSS crystals indicated with arrows.

(e.g. 413/cm and 853/cm) for octamethyl POSS can be observed also in spectra of POSS-PP compound (PP1_5). In Figure 8b) there are two different areas (light grey and darker, marked with numbers 1 and 2). The averaged Raman spectras of the areas seemed to be almost similar (Figure 9 c)). Differences were visible in the intensity of the Raman lines (compare line at 413/cm and at 820/cm and 853/cm) and also in the shape (compare the CH stretching band around 2800/cm). In Figure 9c) the features showed a double peak at 175/220/cm. The material seemed to be similar but was not really equal. The POSS chemicals were distributed in both areas. It is possible that in the light grey areas the POSS content was higher than in the darker areas. The original size of octamethyl POSS particles is approximately 20 to 30 µm. The shape of the particles in SEM pictures is similar as in POSS powder. The size of the light grey areas in Figure 8b) is approximately 1 µm to 8 µm and the size of the particles in the SEM pictures (Figures 6 and 7) is approximately 5 µm.

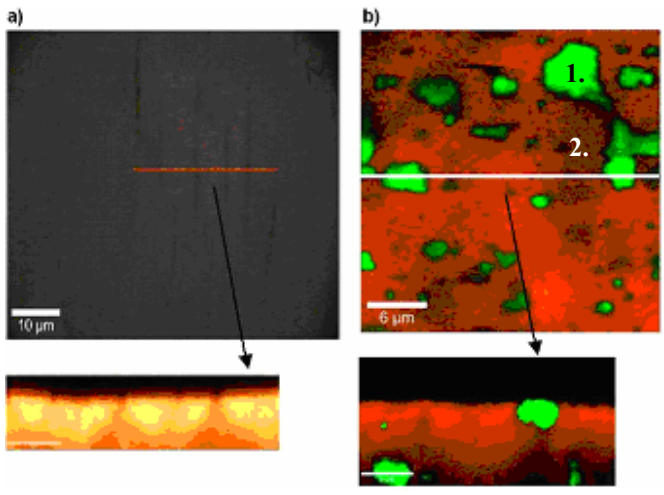

Figure 8. Surface and depth profiles of a) reference PP (PP1) b) 10 wt-% octamethyl POSS PP (PP1_5) compound (light grey and darker areas marked with numbers 1. and 2.).

Authorized licensed use limited to: Tampereen Teknillinen Korkeakoulu. Downloaded on March 23,2010 at 04:46:45 EDT from IEEE Xplore. Restrictions apply.

Therefore it is also possible that in the light grey areas there are large POSS crystals observed in the SEM pictures. Typically the POSS chemicals and PP form a polymer nanocompound. Thus, in the darker areas POSS is probably distributed in nanoparticles.

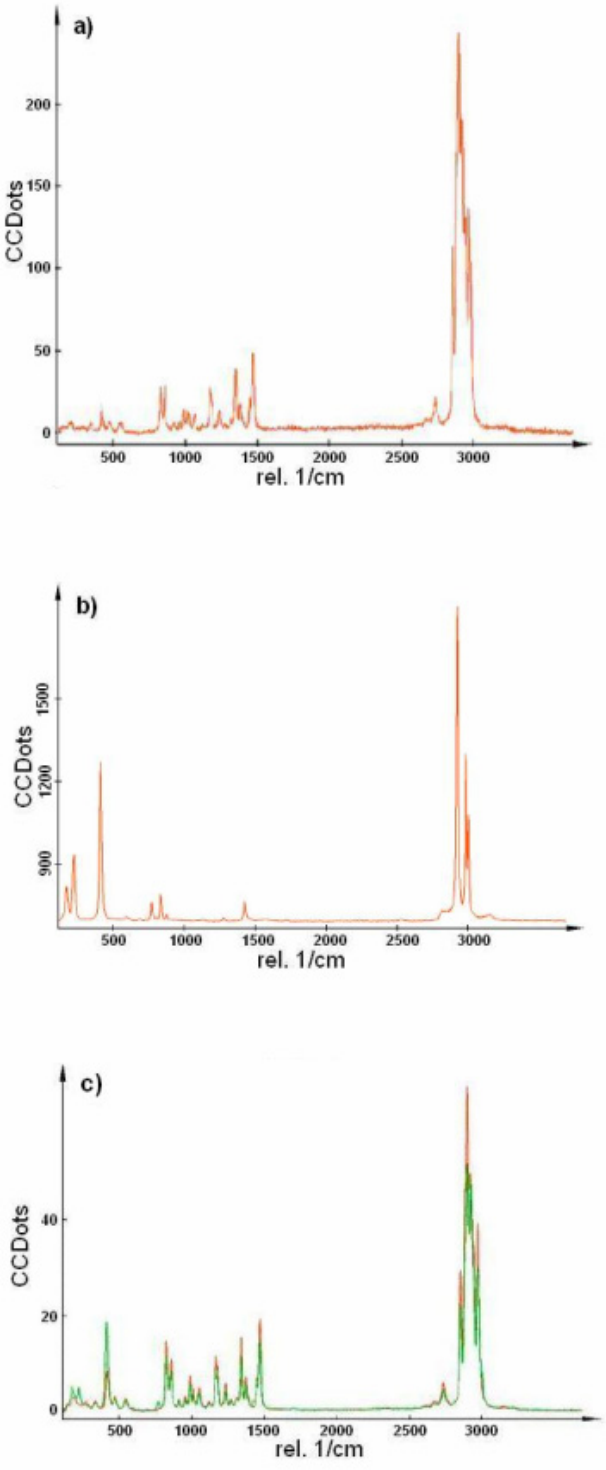

Figure 9. Raman spectrum of a) reference PP (PP1), b) octamethyl POSS and c) 10 wt-% octamethyl POSS PP (PP1_5) compound.

3.2 DISCHARGING TIME

The discharging time of paraffin oil with basic saturated hydrocarbon structure and POSS chemicals was determined according to the standard IEC 61340-2-1 [48]. The sample was pressured against a charging chamber with an earthed ring. The sample was charged by corona discharge. The charging voltage was 8 kV and the charging time was 100 ms. Potential was measured with the electrostatic voltmeter Trek Model 347. The test temperature was 25 °C. The diameter of the sample area was 100 mm and the depth was 0.5 mm.

The charge decay, in this case negative charge, of the paraffin oil, isooctyl and octamethyl POSS is presented in Figure 10. The corona discharging tests indicated that the discharge time of octamethyl and isooctyl POSS is much longer than that of paraffin oil. Firstly, both POSS materials take much higher charge compared to paraffin oil. Secondly, charge stays longer in both POSS materials. Especially, octamethyl POSS powder seems to be stable in this test. The reason for the faster charge decay in liquid (isooctyl POSS) is that particle interfaces are not apparent like in powder (octamethyl POSS). Hence, it may be that POSS chemicals act as electron scavengers in the polymer insulation.

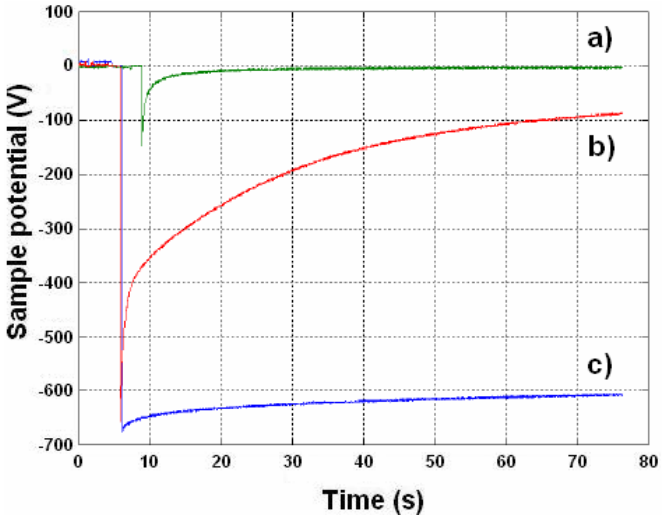

Figure 10. Sample potential as a function of time in a) paraffin oil, b) isooctyl POSS and c) octamethyl POSS.

3.3 AC AND LI BREAKDOWN STRENGTH

The results of the ac and LI breakdown strength measurements are presented in Table 2. The mean value is calculated from 10 measurement results. Uncertainties were estimated with standard deviation. According to the IEEE standard [43] correlation to the data points should be over 0.92 if good enough correlation with 10 measurements using 2-parameter Weibull distribution is achieved. With these measurements 3-parameter Weibull distribution gave lower correlation results than 2-parameter Weibull distribution. Hence, the correlation values of Table 2 were calculated and statistical analysis was conducted using 2-parameter Weibull

Authorized licensed use limited to: Tampereen Teknillinen Korkeakoulu. Downloaded on March 23,2010 at 04:46:45 EDT from IEEE Xplore. Restrictions apply.

distribution. With PP1_2 and PP1_3 the correlation achieved was slightly below the limit.

The breakdown strength measurement results of the PP compounds containing octamethyl POSS are presented in Figures 11 and 12 with standard deviation bars. The greatest ac breakdown strength was achieved with 3 wt-% (Figure 11) and the highest LI breakdown strength with 10 wt-% octamethyl POSS content (Figure 12).

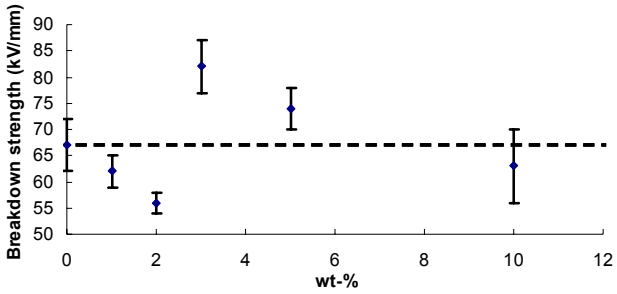

Figure 11. Influence of the octamethyl POSS amount on the ac breakdown strength of PP (reference line dotted).

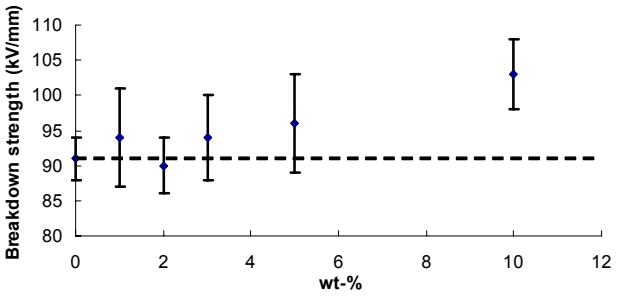

Figure 12. Influence of the octamethyl POSS amount on the LI breakdown strength of PP (reference line dotted).

In Figures 13 and 14 the best octamethyl POSS PP results with ac and LI are presented in Weibull probability plots. 90 % confidence intervals are plotted with dashed lines on the both sides of the straight Weibull fitting line. Measurement points are marked with small crosses and circles. In Figure 13 ac breakdown strength measurements of the reference material (PP1) and 3 wt-% octamethyl POSS PP compound (PP1_3) are presented in the Weibull probability plot. 3 wt-% octamethyl POSS PP compound gave better ac breakdown strength results than the reference PP and 90 % confidence intervals did not cross at even the lowest probabilities (Figure 13). Statistically this difference between the two materials may be considered significant.

In Figure 14 LI breakdown strength measurements of the reference material (PP1) and 10 wt-% octamethyl POSS PP compound (PP1_5) are presented in the Weibull probability plot. 10 wt-% octamethyl POSS PP compound gave better LI breakdown strength results than the reference PP and 90 % confidence intervals crossed at only the very lowest probabilities (Figure 14). Statistically this difference between the two materials may be considered significant.

Table 2. Ac and LI breakdown strength of the test materials.

ac					
Material	mean [kV/mm]	s [kV/mm]	β [kV/mm]	α [kV/mm]	corr
PP1	67	5	69.7	15.0	0.99
PP1_1	62	3	63.4	26.3	0.97
PP1_2	56	2	57.0	34.0	0.91
PP1_3	82	5	84.2	21.9	0.92
PP1_4	74	4	75.4	25.8	0.94
PP1_5	63	7	65.8	10.9	0.99
PP2	54	2	55.3	32.1	0.98
PP2_1	55	2	55.5	37.7	0.97
PP2_2	59	2	59.9	35.7	0.98
PP2_3	59	3	60.0	22.6	0.97
PP2_4	60	2	61.4	32.3	0.96
PP2_5	59	3	59.8	27.6	0.94
LI					
Material	mean [kV/mm]	s [kV/mm]	β [kV/mm]	α [kV/mm]	corr
PP1	91	3	92.0	32.1	0.98
PP1_1	94	7	96.8	16.4	0.93
PP1_2	90	4	91.4	30.0	0.97
PP1_3	94	6	96.1	20.0	0.93
PP1_4	96	7	99.3	17.1	0.99
PP1_5	103	5	104.6	28.6	0.95
PP2	90	7	92.9	14.8	0.99
PP2_1	85	4	87.1	22.7	0.98
PP2_2	80	4	81.7	21.1	0.96
PP2_3	83	5	85.4	20.2	0.99
PP2_4	90	4	92.8	18.4	0.96
PP2_5	84	4	85.6	22.3	0.98

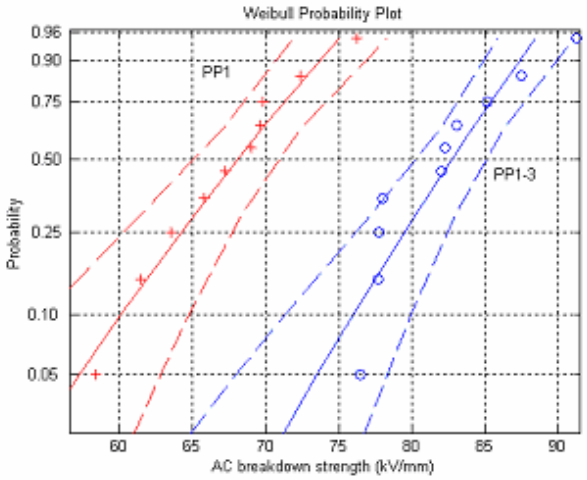

Figure 13. Ac breakdown strength measurements of the reference material (PP1) and 3 wt-% octamethyl POSS PP compound (PP1_3) presented in the Weibull probability plot.

Authorized licensed use limited to: Tampereen Teknillinen Korkeakoulu. Downloaded on March 23,2010 at 04:46:45 EDT from IEEE Xplore. Restrictions apply.

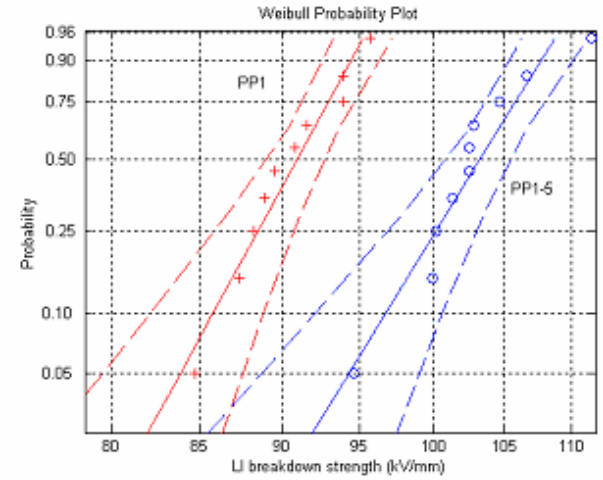

Figure 14. LI breakdown strength measurements of the reference material (PP1) and 10 wt-% octamethyl POSS PP compound (PP1_5) presented in the Weibull probability plot.

The breakdown strength measurement results of the PP compounds containing isooctyl POSS are presented in Figures 15 and 16 with standard deviation bars. From Figure 15 it can be seen that slightly higher ac breakdown strength values than the reference were obtained with POSS quantities 3, 3.5, 5 and 10 wt-%. The highest ac breakdown strength result was obtained with a 5 wt-% sample (PP2_4). From Figure 16 it can be seen that the highest breakdown strength result in LI, same as with the reference sample, was obtained with 5 wt-% sample (PP2_4). Other quantities of isoooctyl POSS slightly decreased the LI breakdown strength of PP.

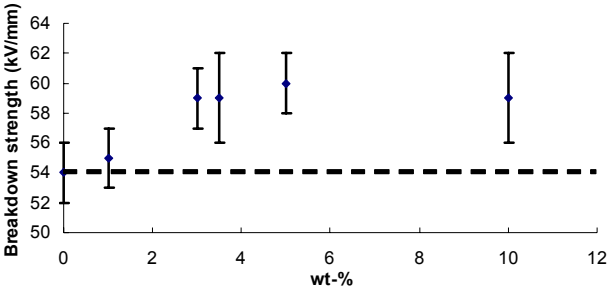

Figure 15. Effect of isooctyl POSS content on the ac breakdown strength of PP (reference line dotted).

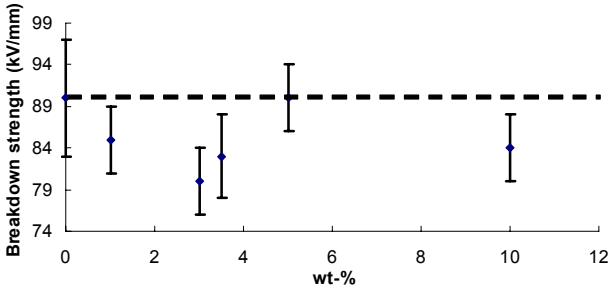

Figure 16. Effect of isooctyl POSS content on the LI breakdown strength of PP (reference line dotted).

Figures 17 and 18 present the best isooctyl POSS PP results with ac and LI in Weibull probability plots. 5 wt-% isooctyl POSS PP compound (PP2_4) gave better ac breakdown strength results than the reference PP (PP2) and 90 % confidence intervals crossed each other only at the lowest probabilities (Figure 17). Statistically this difference between the two materials may be considered significant. In Figure 18 LI breakdown strength measurements of the reference PP (PP2) and 5 wt-% isooctyl POSS PP compound (PP2_4) are presented in the Weibull probability plot. 5 wt-% isooctyl POSS PP compound performed equally well as the reference PP and 90 % confidence intervals crossed each other in all probabilities (Figure 18). Statistically there was no difference between the two materials.

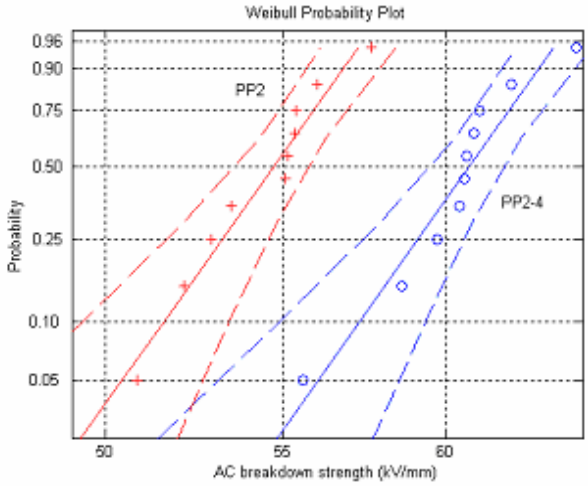

Figure 17. Ac breakdown strength measurements of the reference material (PP2) and 5 wt-% isooctyl POSS PP compound (PP2_4) presented in the Weibull probability plot.

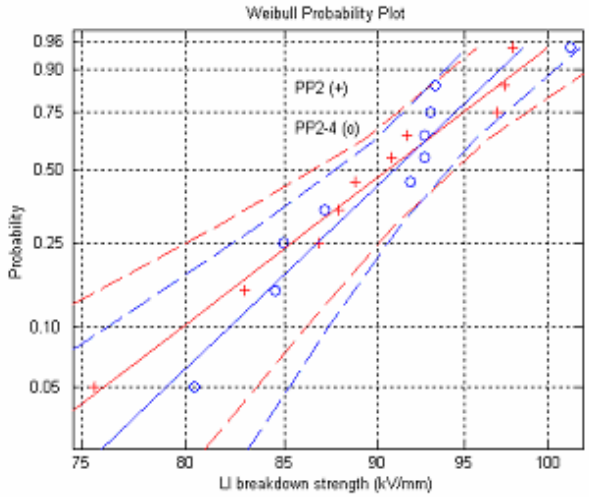

Figure 18. LI breakdown strength measurements of the reference material (PP2) and 5 wt-% isooctyl POSS PP compound (PP2_4) presented in the Weibull probability plot.

Authorized licensed use limited to: Tampereen Teknillinen Korkeakoulu. Downloaded on March 23,2010 at 04:46:45 EDT from IEEE Xplore. Restrictions apply.

3.4 DIELECTRIC PROPERTIES

The relative permittivity, loss factor and volume resistivity of the octamethyl POSS PP compounds are presented in Figures 19-21. According to the measurements, higher permittivity values were obtained with octamethyl POSS PP compounds than with pure PP (Figure 19). At the same time with higher POSS-quantities (3, 5 and 10 wt-%) the loss factor increased compared to the reference sample, but with small quantities (1 and 2 wt-%) losses remained at the same level as the reference (Figure 20). The volume resistivity of the POSS compounds decreased at lower frequencies. At frequencies above 100 Hz loss factor and volume resistivity were too low for the analyzer to measure. The mean standard deviations in the relative permittivity, loss factor and volume resistivity measurements of octamethyl POSS PP compounds varied between 0.005-0.071 %, 0.93-1.98 % and 0.94-2.03 %, respectively.

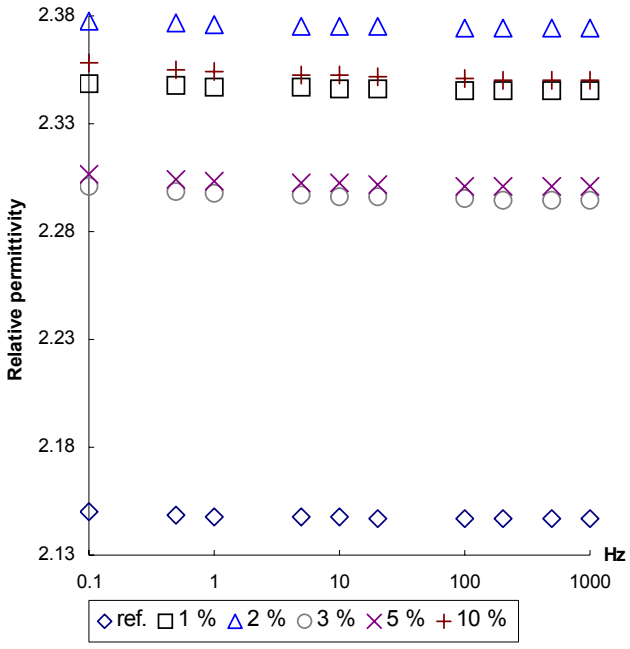

Figure 19. Effect of octamethyl POSS content on the relative permittivity of PP as a function of frequency.

The relative permittivity, loss factor and volume resistivity of the isooctyl POSS PP compounds are presented in Figures 22-24. According to the measurements isooctyl POSS did not affect the relative permittivity of PP. The permittivity of the isooctyl PP POSS compounds is on both sides of the reference material permittivity. Thus, no clear correlation between the isooctyl POSS amount and relative permittivity can be stated. The loss factor and volume resistivity also remained at the same level as the reference material. Similar results regarding the relative permittivity and loss factor changes due isooctyl POSS addition were presented in [37]. The mean standard deviations in the relative permittivity, loss factor and volume resistivity measurements of isooctyl POSS PP compounds varied between 0.004-0.021 %, 1.47-4.30 % and 1.48-4.43 %, respectively.

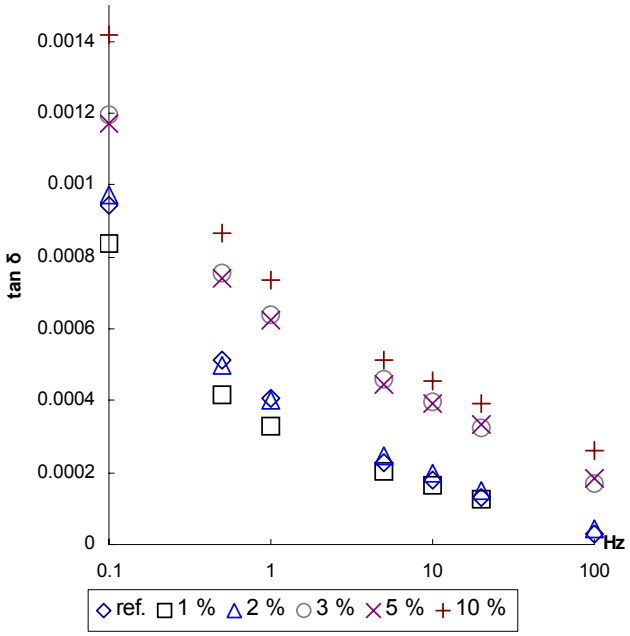

Figure 20. Effect of octamethyl POSS content on the dielectric losses of PP as a function of frequency.

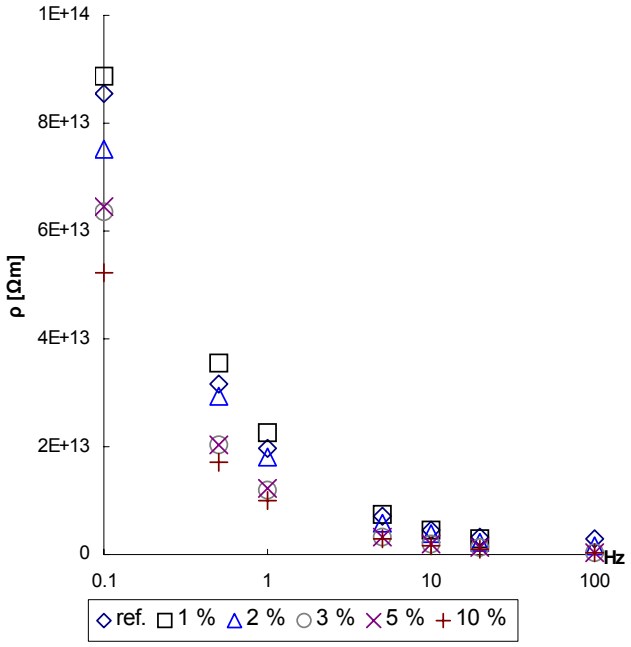

Figure 21. Effect of octamethyl POSS content on the volume resistivity of PP as a function of frequency.

4 DISCUSSION

According to the dielectric measurements presented in this paper, the breakdown strength, both in ac and LI voltages, of pure PP can be improved with the addition of POSS. Statistically these differences were significant. POSS is a new option to increase the breakdown strength of thermoplastic polymers.

Authorized licensed use limited to: Tampereen Teknillinen Korkeakoulu. Downloaded on March 23,2010 at 04:46:45 EDT from IEEE Xplore. Restrictions apply.

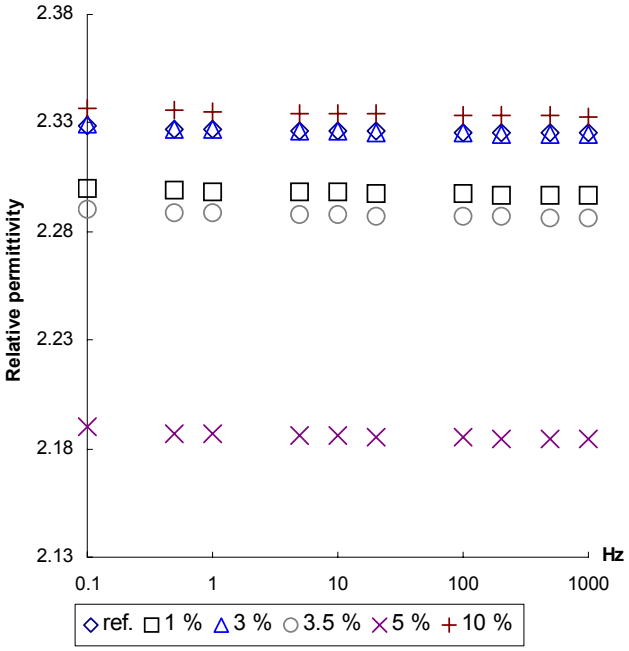

Figure 22. Effect of isooctyl POSS content on the relative permittivity of PP as a function of frequency.

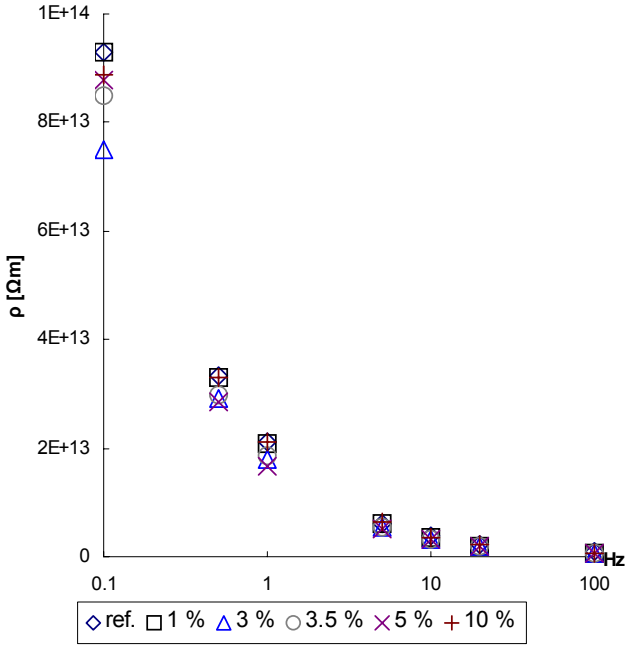

Figure 24. Effect of isooctyl POSS content on volume resistivity of PP as a function of frequency.

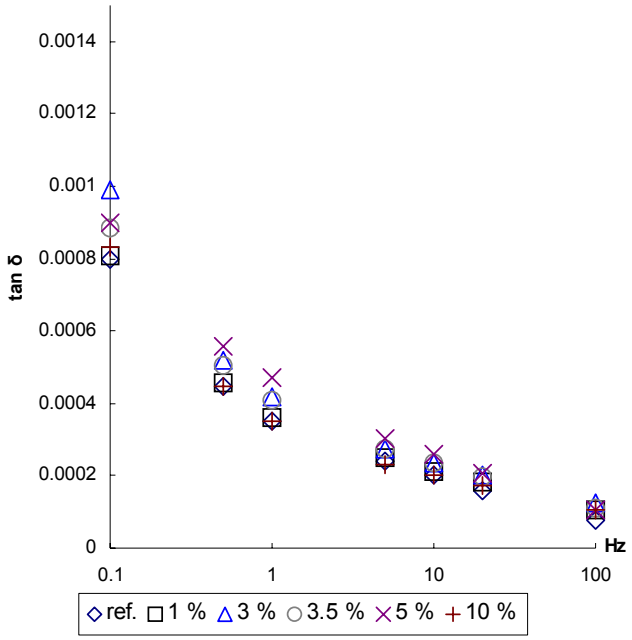

Figure 23. Effect of isooctyl POSS content on the dielectric losses of PP as a function of frequency.

It is generally thought that large filler particles tend to impair the breakdown strength of the insulation. This is problematic, especially with thin layers of insulation, and hence large particles are not desirable. In this study the insulation thicknesses (500-700 μm) were large enough to ensure the functionality of the compounds with these dispersion levels. The POSS molecules were partly distributed on nanoscale and partly in micron sized particles (Figures 4-9). We assume that by improving the dispersion of the compounds more towards nanoscale we can achieve even better dielectric properties for the insulation, also with thinner insulation thicknesses.

POSS molecules on the boundaries of the spherulites can absorb charge temporarily (Figure 10) and therefore impede the insulation against breakdown. POSS molecules can impede the electrons to speed up in the insulation and so prevent the charge from going through the insulation. The charging behavior of liquid and powder POSS can be seen in breakdown strength results. Octamethyl POSS gave better results in breakdown strength measurements than isooctyl POSS. According to the charge decay measurements, the charge stays in octamethyl POSS longer and is a possible reason for the better breakdown strength results for octamethyl POSS PP. The reason for the faster charge decay in liquid is that particle interfaces are not apparent like in powder. Hence, POSS molecules may serve as nanocapacitors in dielectric matrix, and when nanodispersed, even better functionality may be observed.

The melting point of octamethyl POSS is high, 385 °C [49]. For pure PP the melting point is around 160 °C [50]. The rise in the melting point would appear a likely reason for the increase in breakdown strength. In breakdown high temperatures are involved and material begins to soften and erode more easily. In critical places, like spherulite boundaries, increased thermal endurance is advantageous.

The relative permittivity of the octamethyl POSS PP compounds changed with different quantities of POSS. POSS could be distributed in compounds in different ways. The size of the POSS particles could be different depending on the total amount of POSS in the compound. This may be the

Authorized licensed use limited to: Tampereen Teknillinen Korkeakoulu. Downloaded on March 23,2010 at 04:46:45 EDT from IEEE Xplore. Restrictions apply.

reason for the differences in relative permittivity with different filler quantities. Octamethyl POSS also affected dielectric losses and volume resistivity. By contrast, isooctyl POSS did not affect the relative permittivity, dielectric losses and volume resistivity. Similar results regarding the relative permittivity and loss factor changes due isooctyl POSS addition were presented in [37].

It seems that POSS molecules have great potential to achieve advantages in high voltage applications. The mechanical and thermal properties of the compounds should also be ascertained in long-term ageing measurements to see if there are limitations on the use of POSS in high voltage applications.

5 CONCLUSION

Compounded materials were studied with SEM and Raman-AFM. SEM pictures revealed relatively large POSS crystals in octamethyl POSS PP compounds. In surface and depth profiles of the 10 wt-% octamethyl POSS PP compound two different areas could be seen. This suggests that POSS chemicals were distributed in both areas. It may be that the POSS content was higher in one area than in another.

The breakdown strengths with ac and LI obtained from reference PP and PP-POSS compounds were analyzed according to Weibull statistical analysis. This study concluded that octamethyl POSS could substantially increase the breakdown strengths of PP. The addition of 3 wt-% of octamethyl POSS increased the mean value of the ac breakdown strength of PP by 22 % and 10 wt-% of octamethyl POSS increased the LI breakdown strength by 13 %. The increase of breakdown strengths of isooctyl POSS PP compounds was not as high as with octamethyl POSS. The ac breakdown strength of 5 wt-% isooctyl POSS PP compound was 11 % higher compared to the reference. Statistically these achieved differences in materials may be considered significant. Isooctyl POSS did not improve the LI breakdown strength of PP. The correlation values were high enough, showing less scattering of the breakdown strength measurement results and consequently good reliability of the ac and LI dielectric breakdown behavior.

The results of the relative permittivity, loss factor and volume resistivity measurements indicated that octamethyl POSS could have an effect on the dielectric properties of PP. According to the measurements, higher permittivity values were obtained with octamethyl POSS compounds than with pure PP. With higher octamethyl POSS quantities the loss factor increased, but with small quantities losses remained at the same level. The volume resistivity of the octamethyl POSS compounds decreased at lower frequencies. Isooctyl POSS did not significantly affect the relative permittivity, loss factor or volume resistivity of PP.

Reasonable explanations for the increase in ac and LI breakdown strength are that the small size POSS particles are segregated on the boundaries between spherulites and the good ability to scavenge charge leads to good resistance to dielectric breakdown. By improving the mixing in the melt state more uniform compounds without large unwanted particles can be achieved. Still better dielectric strength can be achieved with homogenous POSS nanocomposites.

ACKNOWLEDGMENT

The authors want to thank Mrs. Andrea Jauss from WiTEC GmbH and Mr. Kim Grundström from Cheos Oy for their contribution considering measurement and analysis of the materials by Raman-AFM.

REFERENCES

[1] J. K. Nelson, Y. Hu and J. Thiticharoenpong, "Electrical Properties of TiO_2 Nanocomposites", IEEE Conf. Electr. Insul. Dielectr. Phenomena (CEIDP), pp. 719-722, 2003.

[2] S. Rätzke and J. Kindersberger, "Erosion Behaviour of Nano Filled Silicone Elastomers", XIVth Intern. Sympos. High Voltage Eng. (ISH), pp. 1-6, 2005.

[3] T. J. Lewis, "Interfaces are the Dominant Feature of Dielectrics at the Nanometric Level", IEEE Trans. Dielectr. Electr. Insul., Vol. 11, pp. 739-753, 2004.

[4] M. F. Frechette, M. Trudeau, H. D. Alamdari and S. Boily, "Introductory Remarks on Nanodielectrics", IEEE Conf. Electr. Insul. Dielectr. Phenomena (CEIDP), pp. 92-99, 2001.

[5] G. C. Montanari, D. Fabiani, F. Palmieri, D. Kaempfer, R. Thomann and R. Mülhaupt, "Modification of Electrical Properties and Performance of EVA and PP Insulation through Nanostructure by Organophilic Silicates", IEEE Trans. Dielectr. Electr. Insul., Vol. 11, pp. 754-762, 2004.

[6] J. K. Nelson and Y. Hu, "Nanocomposite Dielectrics-Properties and Implications", J. Phys. D: Appl. Phys., Vol. 38, pp.213-222, 2005.

[7] T. J. Lewis, "Nanometric Dielectrics", IEEE Trans. Dielectr. Electr. Insul., Vol. 1, pp. 812-825, 1994.

[8] S. Pothukuchi, Y. Li and C. P. Wong, "Shape Controlled Synthesis of Nanoparticles and Their Incorporation into Polymers", Electronic Components and Technology Conf., pp. 1965-1967, 2004.

[9] J. K. Nelson and J. C. Fothergill, "Internal Charge Behaviour of Nanocomposites", Nanotechnology, Vol. 15, pp. 586-595, 2004.

[10] T. Tanaka, G. C. Montanari and R. Mülhaupt, "Polymer Nanocomposites as Dielectrics and Electrical Insulation-perspectives for Processing Technologies, Material Characterization and Future Applications", IEEE Trans. Dielectr. Electr. Insul., Vol. 11, pp. 763-784, 2004.

[11] T. Tanaka, M. Kozako, N. Fuse and Y. Ohki, "Proposal of a Multi-core Model for Polymer Nanocomposite Dielectrics", IEEE Trans. Dielectr. Electr. Insul., Vol. 12, pp. 669-681, 2005.

[12] J. K. Nelson, J. C. Fothergill, L. A. Dissado and W. Peasgood, "Towards an Understanding of Nanometric Dielectrics", IEEE Conf. Electr. Insul. Dielectr. Phenomena (CEIDP), pp. 295-298, 2002.

[13] A. L. An and S. A. Boggs, "What is "Nano" in the Context of a Filled Dielectric", IEEE Intern. Sympos. Electr. Insul.(ISEI), pp. 273-276, 2006.

[14] T. Tanaka, "Dielectric Nanocomposites with Insulating Properties", IEEE Trans. Dielectr. Electr. Insul., Vol. 12, pp. 914-928, 2005.

[15] M. Roy, J. K. Nelson, R. K. MacCrone, L. S. Schandler, C. W. Reed, R. Keefe and W. Zenger, "Polymer Nanocomposite Dielectrics: The Role of the Interface", IEEE Trans. Dielectr. Electr. Insul., Vol. 12, pp. 629-643, 2005.

[16] M. F. Frechette and C. W. Reed, "The Emerging Field of Nanodielectrics: an Annotated Appreciation", IEEE Intern. Sympos. Electr. Insul. (ISEI), pp. 458-465, 2006.

[17] T. Tanaka and M. Frechette, "Emerging Nanocomposite Dielectrics", CIGRE Task Force Report, ELECTRA, No. 226, pp.24-32, 2006.

[18] U. Sutter and J. Loeffler, "Roadmap Report Concerning the Use of Nanomaterials in the Energy Sector", 6th Framework Programme, p. 88, 2006.

Authorized licensed use limited to: Tampereen Teknillinen Korkeakoulu. Downloaded on March 23,2010 at 04:46:45 EDT from IEEE Xplore. Restrictions apply.

[19] A. Fina, D. Tabuani, A. Frache and G. Camino, "Polypropylene Polyhedral Oligomeric Silsesquioxanes (POSS) Nanocomposites", Polymer, Vol. 46, pp. 7855-7866, 2005.
[20] S. Phillips, T. Haddad and S. Tomczak, "Developments in Nanoscience: Polyhedral Oligomeric Silsesquioxane (POSS)-Polymers", Solid State and Material Science Vol. 8, pp. 21-29, 2004.
[21] J. Huang, C. He, Y. Xiao, K. Y. Mya, J. Dai and Y. P. Siow, "Polyimide/POSS Nanocomposites: Interfacial Interaction, Thermal Properties and Mechanical Properties", Polymer, Vol. 44, pp. 4491-4499, 2003.
[22] B. X. Fu, M. Namani and A. Lee, "Influence of Phenyl-trisilanol Polyhedral Silsesquioxane on Properties of Epoxy Network Glasses", Polymer, Vol. 44, pp. 7739-7747, 2003.
[23] G. Li, L. Wang, H. Ni and C. U. Pittman, "Polyhedral Oligomeric Silsesquioxane (POSS) Polymers and Copolymers: A Review", Journal of Inorganic and Organometallic Polymers, Vol. 11, No. 3, pp. 123-154, 2001.
[24] H. Dodiuk, S. Kenig, I Blinsky, A. Dotan and A. Buchman, "Nanotailoring of Epoxy Adhesives by Polyhedral-oligomeric-silsesquioxanes (POSS)", Intern. J. Adhesion & Adhesives, Vol. 25, pp. 211-218, 2005.
[25] Y. Ni, S. Zheng and K. Nie, "Morphology and Thermal Properties of Inorganic-organic Hybrids Involving Epoxy Resin and Polyhedral Oligomeric Silsesquioxanes", Polymer, Vol. 45, pp. 5557-5568, 2004.
[26] M. Joshi, B. S. Butola, G. Simon and N. Kukaleva, "Rheological and Viscoelastic Behavior of HDPE/Octamethyl-POSS Nanocomposites", Macromolecules, Vol. 39, pp. 1839-1849, 2006.
[27] G. Pan, J. E. Mark and D. W. Schaeffer, "Synthesis and Characterization of Fillers of Controlled Structure Based on Polyhedral Oligomeric Silsesquioxane Gages and Their Use in Reinforcing Siloxane Elastomers", J. Polymer Sci.: Part B: Polymer Phys., Vol. 41, pp. 3314-3323, 2003.
[28] E. T. Kopesky, T. S. Haddad, R. E. Cohen and G. H. McKinley, "Thermomechanical Properties of Poly(methyl methacrylate)s Containing Tethered and Untethered Polyhedral Oligomeric Silsesquioxanes", Macromolecules, Vol. 37, pp. 8992-9004, 2004.
[29] A. Lee and J. D. Lichtenhan, "Viscoelastic Responses of Polyhedral Oligosilsesquioxane Reinforced Epoxy Systems", Macromolecules, Vol. 31, pp. 4970-4974, 1998.
[30] E. Itoh, H. Karasawa, N. Matsukawa and K. Mivairi, "The Electrical Properties of Glass Like Insulator Prepared by Solution Process and Its Application for Organic Electronic Devices", Intern. Sympos. Electr. Insul. Materials, Kitakyushu, Japan, pp. 646-649, 2005.
[31] Y. Lee, J. Huang, S. Kuo and F. Chang, "Low-dielectric, Nanoporous Polyimide Films Prepared from PEO-POSS Nanoparticles", Polymer, Vol. 46, pp. 10056-10065, 2005.
[32] Y. Lee, J. Huang, S. Kuo, J. Lu and F. Chang, "Polyimide and Polyhedral Oligomeric Silsesquioxane Nanocomposites for Low-dielectric Applications", Polymer, Vol. 46, pp. 173-181, 2005.
[33] M. Vasilopoulou, S. Tsevas, A. M. Douvas, P. Argitis, D. Davazoglou and D. Kouvatsos, "Characterization of Various Low-k dielectrics for Possible Use in Applications at Temperatures below 160 °C", J. Phys.: Conf. Series, 10, pp. 218-221, 2005.
[34] W. W. Zhu, S. Xiao and I. Shih, "Field-effect Mobilities of Polyhedral Oligomeric Silsesquioxanes Anchored Semiconducting Polymers", Appl. Surface Sci., Vol. 221, pp. 358-363, 2004.
[35] J. Horwath and D. Schweickart, "Inorganic Fillers for Corona Endurance Enhancement of Selected Polymers", IEEE, Air Force Research Library, pp. 644-647, 2002.
[36] J. Horwarth, D. Schweickart, G. Garcia, D. Klosterman and M. Galaska, "Improved Performance of Polyhedral Oligomeric Silsesquioxane Epoxies", IEEE Conf. Electr. Insul. Dielectr. Phenomena (CEIDP), pp.155-157, 2005.
[37] L. Linnamaa and K. Kannus, "Effects of Polyhedral Oligomeric Silsesquioxanes on Partial Discharge Endurance and Electrical Properties of XLPE", Nordic Insulation Sympos., pp. 135-138, 2007.
[38] Hybrid Plastics Catalog, 2006.
[39] P. Salovaara, M. Takala and K. Kannus, "Effect of Film Thickness on the Electrical Strength of Polypropylene Compounds", 10th International Electr. Insul. Conf., INSUCON, pp. 131-135, 2006.
[40] IEC Publication 60243-1: "Electrical Strength of Insulating Materials-Test Methods-Part 1: Test at Power Frequencies", 1998.
[41] IEC Publication 60060-1: "High-voltage Test Techniques. Part 1: General Definitions and Test Requirements", 1989.
[42] IEC Publication 250: "Recommended Methods for the Determination of the Permittivity and Dielectric Dissipation Factor of Electrical Insulating Materials at Power, Audio and Radio Frequencies Including Metre Wavelengths", 1969.
[43] IEEE Standard 930: "IEEE Guide for the Statistical Analysis of Electrical Insulation Breakdown Data", IEEE Dielectr. Electr. Insul. Society, 2005.
[44] M. Cacciari, G. Mazzanti and G.C. Montanari, "Weibull Statistics in Short-Term Dielectric Breakdown of Thin Polyethylene Films", IEEE Trans. Dielectr. Electr. Insul., Vol. 1, pp. 153-159, 1994.
[45] P. Salovaara and K. Kannus, "Increasing the Dielectric Breakdown Strength of Polypropylene Using Polyaniline Additive", IASTED Conf. on Energy and Power Systems, pp. 234-239, 2006.
[46] L.A. Dissado and J.C. Fothergill, *Electrical Degradation and Breakdown in Polymers*, IEE Materials and Devices Series, Peter Peregrinus Ltd., London, UK, 1992.
[47] W. Hauschild and W. Mosch, *Statistical Techniques for High-Voltage Engineering*, Peter Peregrinus Ltd., London, UK, 1992.
[48] IEC 61340-2-1: "Electrostatics-Part 2-1: Measurement methods in electrostatics-Test methods to measure ability of materials and products to dissipate static electric charge", 2000.
[49] Hybrid Plastics, Inc., Material Safety Data Sheet, OctaMethyl POSS, MS0830, 2004.
[50] Data Sheet, Polypropylene Borclean HB300BF, Polypropylene Homopolymer for Capacitor Film (BOPP), F 0059 06.07.2004 Ed.3, 2004.

Markus Takala was born in Vaasa, Finland in 1980. He graduated with a M.Sc. (Eng.) degree in electrical power engineering, Tampere University of Technology (TUT), Tampere, Finland in 2005. Since 2005 he has been a researcher in the High Voltage Laboratory at TUT. His research interests include topics in new electrical insulation materials. He has published articles on dielectric properties of PP compounds, the main research topics being nano- and microstructured epoxy and PP.

Mikko Karttunen was born in Tampere, Finland in 1955. He received the M.Sc. (Eng.) and Licentiate of Technology degrees in material science and plastics technology from Tampere University of Technology (TUT), in 1980 and 1986, respectively. From 1980 to 1985 he was a research scientist at TUT. From 1985 to 1988 he worked at Neste Oy as a researcher. From 1988 to 1991 he was a research scientist at the Technical Research Centre of Finland (VTT) and since 1991 he has been a senior research scientist at VTT. His research interest is in electrically conductive polymer compounds, compliant electrodes and polymer nanocomposites for electromechanical films and electrical insulation materials.

Pauliina Salovaara was born in Mouhijärvi, Finland in 1980. She graduated with an M.Sc. (Eng.) degree from the Department of Electrical Power Engineering, Tampere University of Technology, Tampere, Finland in 2004. Since 2004 she has been a researcher in the High Voltage Laboratory at TUT. She has published articles on the dielectric properties of PP compounds. Her research interests include new dielectric material compounds and high voltage engineering.

Authorized licensed use limited to: Tampereen Teknillinen Korkeakoulu. Downloaded on March 23,2010 at 04:46:45 EDT from IEEE Xplore. Restrictions apply.

Satu Kortet was born in Tampere, Finland in 1977. She received the B.Sc. degree in chemical engineering from Tampere Polytechnic University of Applied Sciences, Tampere, Finland in 2001. She will start her M.Sc studies at Tampere University of Technology (TUT) in autumn 2007. Since 2001 she has been a Research Engineer at the Technical Research Centre of Finland (VTT). Her research interests include high temperature elastomers, hybrid polymers and nanocomposites for electromechanical films and electrical insulation applications.

Kari Kannus was born in Längelmäki, Finland, on 17 May 1957. He received the M.Sc. (Eng.), Licentiate of Technology and doctoral degrees in electrical engineering from Tampere University of Technology (TUT) in 1981, 1987 and 1998, respectively. From 1982 to 1988 he was a teaching and research assistant and from 1988 to 1992 he was a laboratory manager at the Institute of Power Engineering of TUT. From 1993 to 1998 he was a researcher and since 1999 he has been a senior researcher at TUT. Since 2002 he has been an Adjunct Professor of High Voltage Engineering at TUT. His main research interests are in the field of high voltage technology, especially overvoltage protection and surge arresters, new polymeric materials and environmental testing.

Tapio Kalliohaka was born in Helsinki, Finland, on 31 March 1972. He received the M.Sc. degree in Department of Automation from Tampere University of Technology. After graduation he worked as a researcher in the Laboratory of electromagnetism in Tampere University of Technology. His research field was in superconductivity and in cryogenics. After that he has been working on VTT Technical Research Center of Finland since 2001, where he is currently working as a research scientist. Main work areas are related to electrostatic hazards and electrostatic measurements.

Authorized licensed use limited to: Tampereen Teknillinen Korkeakoulu. Downloaded on March 23,2010 at 04:46:45 EDT from IEEE Xplore. Restrictions apply.

Publication 4

M. Takala, T. Sallinen, P. Nevalainen, J. Pelto and K. Kannus, Surface Degradation of Nanostructured Polypropylene Compounds Caused by Partial Discharges, In *Proceedings of IEEE International Symposium on Electrical Insulation* (ISEI 2008), Vancouver, Canada, June 8-11, pp. 205-209, (2008)

© 2008 IEEE. Reprinted, with permission, from the proceedings of IEEE International Symposium on Electrical Insulation.

This material is posted here with permission of the IEEE. Such permission of the IEEE does not in any way imply IEEE endorsement of any of the Tampere University of Technology's products or services. Internal or personal use of this material is permitted. However, permission to reprint/republish this material for advertising or promotional purposes or for creating new collective works for resale or redistribution must be obtained from the IEEE by writing to pubs-permissions@ieee.org. By choosing to view this material, you agree to all provisions of the copyright laws protecting it.

Surface Degradation of Nanostructured Polypropylene Compounds Caused by Partial Discharges

M. Takala[1], T. Sallinen[1], P. Nevalainen[1], J. Pelto[2] and K. Kannus[1]
[1]Tampere University of Technology
Department of Electrical Energy Engineering
P.O. Box 692
FI-33101 Tampere, Finland

[2]Technical Research Centre of Finland
P.O. Box 1607
FI-33101 Tampere, Finland

Abstract- **This paper presents the results of the surface degradation measurements conducted on nanostructured polymer compounds consisting of polypropylene (PP), polyaniline (PANI) and acrylic acid (AA). According to prior investigations the chosen additives have improved the electrical performance of polypropylene e.g. dielectric breakdown strength and relative permittivity. Materials were subjected to high voltage stress leading to partial discharges (PD). Surface degradation was measured with optical profilometry. The partial discharge activity during corona bombardment was also measured. The measurements were conducted at the high voltage laboratory of Tampere University of Technology. Statistical analysis was applied to the results to determine the effects of the additive on the surface degradation and PD activity of polypropylene.**

I. Introduction

The use of polymers as electrical insulating materials has increased rapidly in recent decades. The base polymer properties have been developed by adding small amounts of different fillers (e.g. carbon black, talc, quartz and metal oxides) to the polymer material. In material development process a variety of properties have to be ensured e.g. electrical, mechanical and thermal.

PP is the most used material in capacitor insulations. It is important to study the surface properties of the materials, not only the dielectric properties (e.g. breakdown strength, relative permittivity and dielectric losses). Surface degradation due to partial discharges of polymers e.g. epoxy, polyamide (PA), polyimide (PI), polyethylene (PE), PP has been studied in various articles [1-11].

According to earlier studies by the authors the chosen additives indicated good AC and lightning impulse (LI) breakdown strength in PP. The relative permittivity and dielectric loss measurements of the compounds were likewise promising. This study concentrates on the surface degradation of nanostructured PP compounds including surface profilometry analysis and PD activity measurements.

II. Experimental

A. Materials studied

Polymer compounds were produced with melt state compounding. The same isotactic polypropylene was used as matrix polymer in all materials. The polypropylene used was designed for capacitor films and was produced by Borealis Polymers (HC318BF). The compositions of the materials studied are shown in Table I.

TABLE I
Composition Of The Studied Materials

Material	Additive	wt-%
PP	-	-
PP_1	Polyaniline+ LGA	0.5+1.3
PP_2	Acrylic acid	1

The wt-% of the mixture was calculated from the weight of the polymer. PP and the additives were mixed with a twin screw compounder (Berstorff ZE 25x48D) at the Technical Research Centre of Finland (VTT). Materials were extruded with the Brabender Plasticorder single screw extruder (diameter 18 mm) using a flat die. The cast film thickness varied between 0.5-0.7 μm.

The dispersion of the PP_1 material was studied with transmission electron microscope (TEM). Fig. 1 shows that part of the PANI is dispersed on the nanometer length scale. The diffuse boundary layer between the PANI and PP is due to the effects of lauryl gallate (LGA) plasticizer which renders the PANI compatible with PP because it is otherwise insoluble in the PP matrix.

978-1-4244-2092-6/08/$25.00 ©2008 IEEE

Authorized licensed use limited to: Tampereen Teknillinen Korkeakoulu. Downloaded on March 23,2010 at 04:50:09 EDT from IEEE Xplore. Restrictions apply.

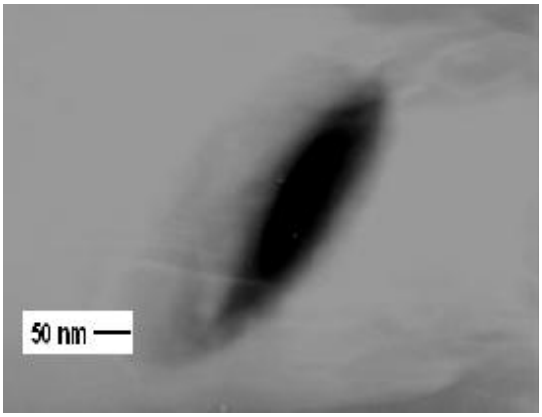

Fig. 1. Transmission electron micrograph of PP_1 compound. Magnification 100 000X.

B. Surface degradation test

Surface degradation tests were carried out for the PP sheets. Fig. 2 presents the test setup used. Materials were placed between six electrodes and a metallic plane (IEC (b)) [8,9] and a constant AC voltage (50 Hz) of 9 kV (RMS) was applied to the sheets. The test cycle was arranged so that three samples were collected at each time (1h, 2h, 4h and 5h).

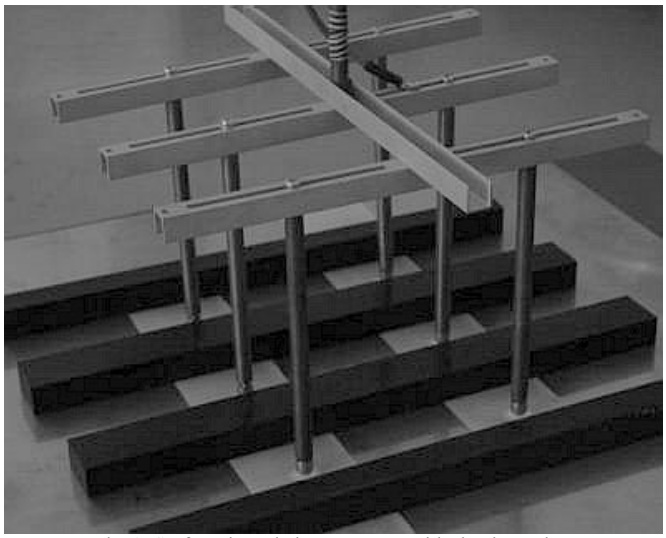

Fig. 2. Surface degradation test setup with six electrodes.

C. Partial discharge activity measurement

The partial discharge (PD) levels were measured during the 6-hour voltage stress. The PD measuring system used consists of material samples, a high voltage generator, a coupling capacitor, an IEC 60270 bandpass filter and amplifier, an acquisition card with sampling frequency of 5 MS/s and a PC with a Matlab based software for the analysis of the PD pulses. The acquisition card records periodically one-second samples during the measurement. The software calculates the largest repeatedly occurring pulse (LROP) from the samples according to the IEC 60270 standard and makes a report of the measurements. The construction of the PD measuring system is presented in Fig. 3.

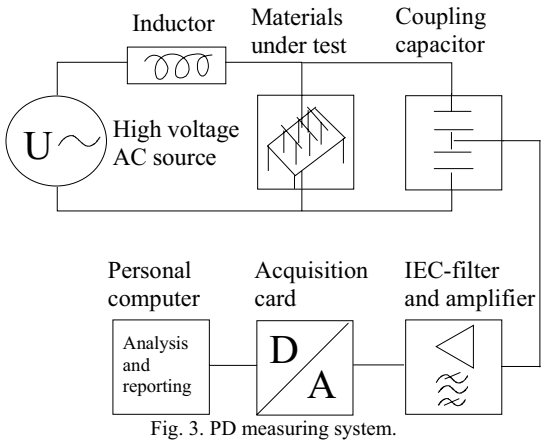

Fig. 3. PD measuring system.

When a 9kV AC voltage was applied to the material samples partial discharges occurred smoothly around each of the six rods and on the material sheets. No large sliding discharges were observed. The discharge distribution can be seen in Fig. 4. The discharge patterns of all the materials studied were uniform around the electrodes.

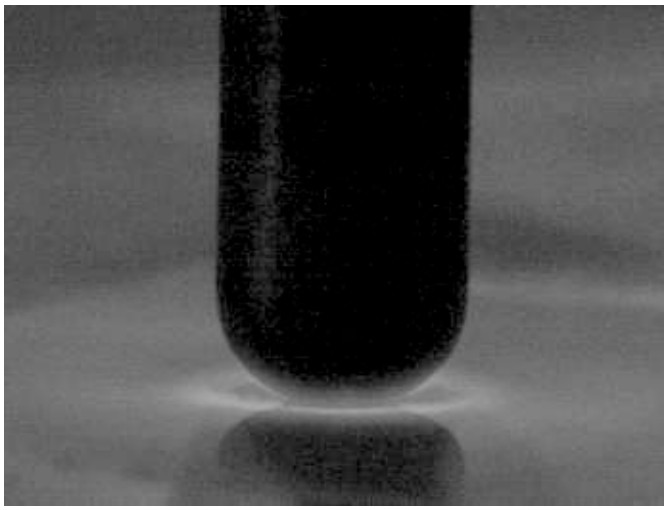

Fig. 4. Partial discharges around the electrode and material sheet.

D. Optical profilometry

The surface degradation of the material samples was analyzed optically with Wyco NT1100 surface profiler after the surface degradation test and partial discharge activity measurement. The measuring method used was vertical scanning interferometry (VSI), in which the surface is mapped by peak-contrast interference fringes of white light as the focus point is slowly moved vertically.

The area measured was 1.2 X 0.9 mm. At each time stamp (0, 1, 2, 4 and 5 h) a total of 10 measurements were made from the three parallel samples. Measurements were made from the degraded area at 90° intervals (Fig. 5.).

Authorized licensed use limited to: Tampereen Teknillinen Korkeakoulu. Downloaded on March 23,2010 at 04:50:09 EDT from IEEE Xplore. Restrictions apply.

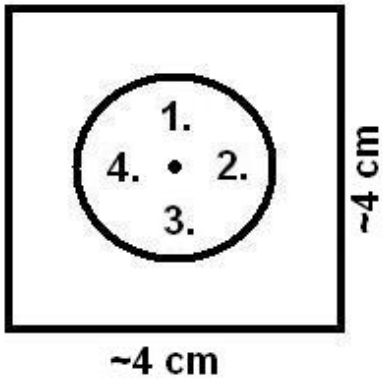

Fig. 5. Optical profilometry measurement procedure.

E. Statistical analysis

Statistical analysis was applied to evaluate the differences in materials caused by surface degradation. Statistical differences between two materials can be compared when the sample amount is the same in both materials by average standard deviation (save), being the average value of the two standard deviations of the materials. The difference between the breakdown strength means (dif) of the materials is compared with meaningful sectors. These sectors are: not significant (dif $\leq$ 1.96×save), almost significant (1.96×save < dif $\leq$ 2.58×save), significant (2.58×save < dif $\leq$ 3.29×save) and extremely significant (dif > 3.29×save) [12]. With these quantiles statistical significance levels can be calculated and differences between the materials evaluated.

III. Results

A. Surface degradation

The surface degradation of the materials was studied with optical profilometry. Figs. 6 and 7 present photographs of the PP_1 material samples. The degraded areas were rounded, about 2 cm in diameter. Fig. 8 shows a three dimensional surface profile of material PP_1. The surface roughness is smaller at the centre of the sample where the electrode was attached and increases quickly after the edge of the electrode where the electric field strength is at its largest. At the centre of the sample no apparent degradation was found (Figs. 6-8).

In Figs. 9-11 the average surface roughness of the materials (PP, PP_1 and PP_2) as a function of degradation time is presented with standard deviation bars. The reference roughness level is marked with a dashed line. With pure PP the average surface roughness remained at the same level with the non-stressed reference. With pure PP the surface roughness was initially about 200 nm and slightly larger with materials PP_1 and PP_2, possibly because of the additives. With PP_1 and PP_2 materials the average surface roughness increased slightly as degradation time increased. With both materials the time stamp 5 h gave the highest roughness values.

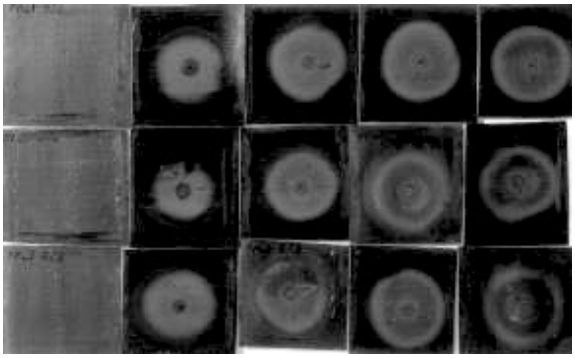

Fig. 6. Reference and all degraded samples of material PP_1 in order of degradation time (0, 1, 2, 4 and 5 h). Three samples of each time stamp.

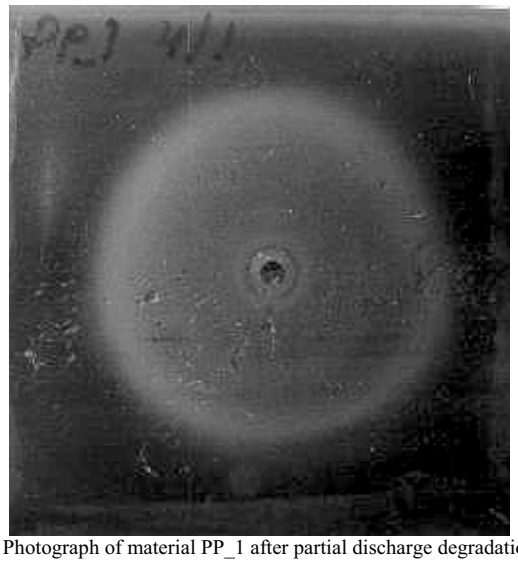

Fig. 7. Photograph of material PP_1 after partial discharge degradation test. Dimensions 40 X 40 mm.

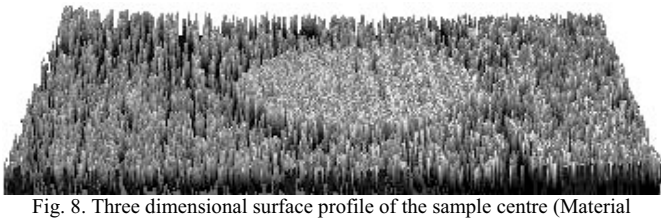

Fig. 8. Three dimensional surface profile of the sample centre (Material PP_1). Dimensions 1.9 X 2.4 X 0.013 mm.

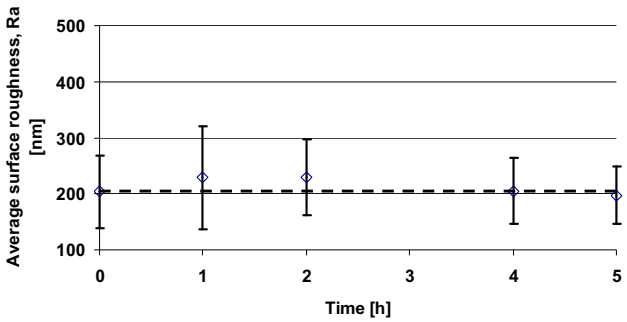

Fig. 9. Average surface roughness of PP as a function of time with standard deviation bars.

Authorized licensed use limited to: Tampereen Teknillinen Korkeakoulu. Downloaded on March 23,2010 at 04:50:09 EDT from IEEE Xplore. Restrictions apply.

Statistically only with PP_1 were the changes in surface roughness almost significant (with time stamps 2, 4 and 5 h).

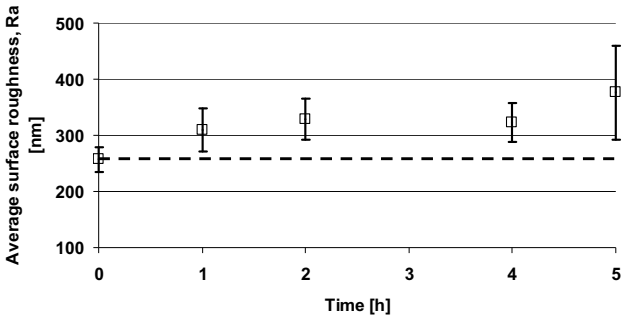

Fig. 10. Average surface roughness of PP_1 as a function of time with standard deviation bars.

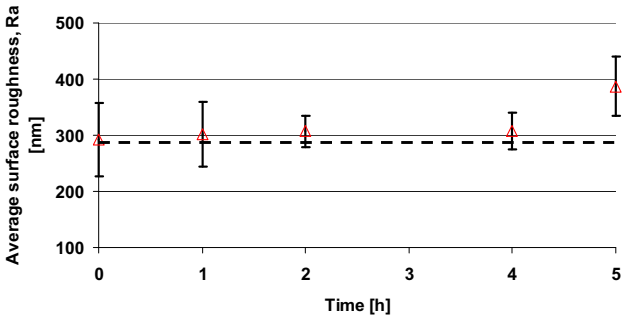

Fig. 11. Average surface roughness of PP_2 as a function of time with standard deviation bars.

B. Partial discharge activity

The results of average partial discharge levels of the materials studied are presented in Fig. 12. The average LROP level and standard deviation were calculated from the measuring data for each material for three time periods; first hour, second hour and four last hours of the total 6 hours voltage stress. The slope of the trendline was also calculated for each material and time period to depict the development of the LROP values (Table II).

According to the results, pure PP had the smallest PD activity compared to materials PP_1 and PP_2. The slope of the trendline was also initially negative and settled later to a value of 0.1. This indicates that the PD activity did not considerably increase or decrease as a function of time. Both PP_1 and PP_2 had higher PD activity and also greater standard deviation of the LROP values compared to pure PP. When considering Fig. 12 and the slope of trendline in Table II, it can be seen that the PD level of materials PP_1 and PP_2 increases as a function of time. With PP_1 and PP_2 the changes in LROP values were almost significant (with time period 2-6 h).

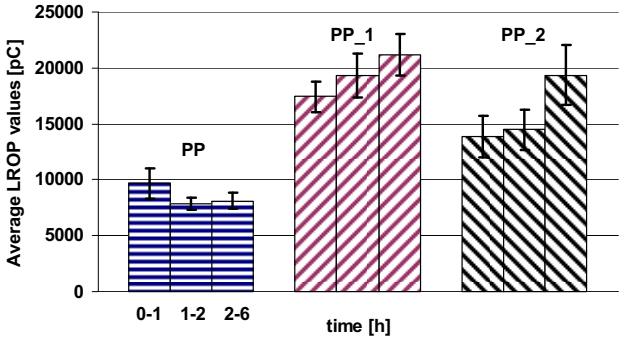

Fig. 12. Average partial discharge levels of the studied materials with standard deviation bars.

TABLE II
SLOPE OF THE TRENDLINE WITH EACH TIME PERIOD

Material	Time period [h]	Slope of the trendline [pC/sample]
PP	0-1	-65
	1-2	-8.0
	2-6	0.1
PP_1	0-1	7.5
	1-2	7.5
	2-6	2.2
PP_2	0-1	-12
	1-2	65
	2-6	18

IV. DISCUSSION

The reason for these continuing studies of the materials PP_1 and PP_2 was to confirm other dielectric properties than e.g. breakdown strength, relative permittivity and dielectric losses of the materials.

Degradation time was 6 hours with each material. Statistically small changes could be seen with the surface roughness and PD activity within the last hours of the test (Figs. 9-12). This indicates that the measurement time should maybe have been longer. Then the effect of time would probably have been more easily seen. However, these reported tests were fast to execute and showed the behavior of the materials under partial discharge stress.

The materials selected did not perform well under the PD stress. This indicates that properties like breakdown strength give short-term data on the material but the reality even in a few hours of testing could be different. It is important also to study even longer performance of the materials to obtain extensive knowledge of the material properties.

Further improvements for the measurement procedure have already been planned and interesting materials to be studied as an additive in these kinds of studies are polyhedral oligomeric silsesquioxanes (POSS). Dielectric properties of PP-POSS nanocompounds are presented in [13].

Authorized licensed use limited to: Tampereen Teknillinen Korkeakoulu. Downloaded on March 23,2010 at 04:50:09 EDT from IEEE Xplore. Restrictions apply.

V. Conclusion

According to surface degradation test and partial discharge measurements presented in this paper, the surface degradation, of pure PP cannot be improved with polyaniline or acrylic acid (Figs. 9-12). Moreover, surface profilometry and partial discharge activity measurements both supported this observation. Degradation and partial discharge activity increased as a function of time with materials PP_1 and PP_2. Correspondingly, with pure PP degradation and PD activity remained at the reference level and no clear relation to the time of stress could be seen.

References

[1] A. J. Shields and I. J. Kemp, "Degradation and breakdown of mica under partial discharge stressing", *IEE Proc.-Sci. Meas. Technol.*, Vol. 147, No. 3, May 2000, pp. 105-109.

[2] D. M. Hepburn, I. J. Kemp, A. J. Shields and J. Cooper, "Degradation of epoxy resin by partial discharges", *IEE Proc.-Sci. Meas. Technol.*, Vol. 147, No. 3, May 2000, pp. 97-104.

[3] M. Kozako, R. Kido, N. Fuse, Y. Ohki, T. Okamoto and T. Tanaka, "Difference in surface degradation due to partial discharges between polyamide nanocomposite and microcomposite", *IEEE Annual Report Conference on Electrical Insulation and Dielectric Phenomena*, 2004, pp. 398-401.

[4] J. Horwath and D. Schweickart, "Electrical, physical and chemical measurements on electric field degraded polyethylene", *Electrical Insulation Conference and Electrical Manufacturing & Coil Winding Conference*, 1999, pp. 99-102.

[5] B. Thomas and R. S. Nema, "Partial discharge degradation and breakdown studies in polypropylene films", *Conference Record of the 1996 IEEE International Symposium on Electrical Insulation*, Montreal, Quebec, Canada, June 16-19, 1996, pp. 521-524.

[6] H. Ichikawa, K. Itoh, Y. Suzuoki, T. Mizutani and K. Uchida, "Partial discharge patterns and their temporal change in polyethylene and polyimide", *IEEE Annual Report Conference on Electrical Insulation and Dielectric Phenomena*, 1994, pp. 143-148.

[7] N. Fuse, M. Kozako, T. Tanaka, S. Murase and Y. Ohki, "Possible mechanism of superior partial-discharge resistance of polyamide nanocomposites", *IEEE Annual Report Conference on Electrical Insulation and Dielectric Phenomena*, 2004, pp. 322-325.

[8] M. Kozako, N. Fuse, K. Shibata, N. Hirai, Y. Ohki, T. Okamoto and T. Tanaka, "Surface change of polyamide nanocomposite caused by partial discharges", *IEEE Annual Report Conference on Electrical Insulation and Dielectric Phenomena*, 2003, pp. 75-78.

[9] M. Kozako, N. Fuse, Y. Ohki, T. Okamoto and T. Tanaka, "Surface degradation of polyamide nanocomposites caused by partial discharges using IEC (b) electrodes", *IEEE Trans. Dielectr. Electr. Insul.*, Vol. 11, No. 5, 2004, pp. 833-839.

[10] M. Kozako, R. Kido, T. Imai, T. Ozaki, T. Shimizu and T. Tanaka, "Surface roughness change of epoxy/TiO2 nanocomposites due to partial discharges", *Proceedings of 2005 International Symposium on Electrical Insulating Materials*, June 5-9, 2005, Kitakyushu, Japan, pp. 661-664.

[11] T. Ishida and M. Nagao, "Time variation of partial discharge current waveforms with degradation of insulators", *Proceedings of 2005 International Symposium on Electrical Insulating Materials*, June 5-9, 2005, Kitakyushu, Japan, pp. 494-497.

[12] W. Hauschild and W. Mosch, *Statistical Techniques for High-Voltage Engineering*, Peter Peregrinus Ltd., London, UK, 1992.

[13] M. Takala, M. Karttunen, P. Salovaara, S. Kortet, K. Kannus and T. Kalliohaka, "Dielectric properties of nanostructured polypropylene-polyhedral oligomeric silsesquioxane compounds", *IEEE Trans. Dielectr. Electr. Insul.*, Vol. 15, No. 1, 2008, pp. 40-51.

Authorized licensed use limited to: Tampereen Teknillinen Korkeakoulu. Downloaded on March 23,2010 at 04:50:09 EDT from IEEE Xplore. Restrictions apply.

Publication 5

M. Takala, M. Karttunen, J. Pelto, P. Salovaara, T. Munter, M. Honkanen, T. Auletta and K. Kannus, Thermal, Mechanical and Dielectric Properties of Nanostructured Epoxy-Polyhedral Oligomeric Silsesquioxane Composites, *IEEE Transactions on Dielectrics and Electrical Insulation*, Vol. 15, No. 5, pp. 1224-1235, (2008)

© 2008 IEEE. Reprinted, with permission, from IEEE Transactions on Dielectrics and Electrical Insulation.

This material is posted here with permission of the IEEE. Such permission of the IEEE does not in any way imply IEEE endorsement of any of the Tampere University of Technology's products or services. Internal or personal use of this material is permitted. However, permission to reprint/republish this material for advertising or promotional purposes or for creating new collective works for resale or redistribution must be obtained from the IEEE by writing to pubs-permissions@ieee.org. By choosing to view this material, you agree to all provisions of the copyright laws protecting it.

Thermal, Mechanical and Dielectric Properties of Nanostructured Epoxy-polyhedral Oligomeric Silsesquioxane Composites

M. Takala[1], M. Karttunen[2], J. Pelto[2], P. Salovaara[1], T. Munter[2], M. Honkanen[1], T. Auletta[3], and K. Kannus[1]

[1]Tampere University of Technology
Institute of Power Engineering
P.O. Box 692
FI-33101 Tampere, Finland

[2]Technical Research Centre of Finland
P.O. Box 1607
FI-33101 Tampere, Finland

[3]ABB Corporate Research
Power Technologies
SE 721 78 Västerås, Sweden

ABSTRACT

This paper presents the results of the thermal, mechanical and dielectric measurements conducted on polymer nanocomposites consisting of epoxy and polyhedral oligomeric silsesquioxane (POSS). The material composites were analyzed with a scanning electron microscope (SEM), an atomic force microscope (AFM) and a transmission electron microscope (TEM). Glass transition temperatures of the composites were measured with differential scanning calorimeter (DSC). Stress, strain, modulus and impact strength of epoxy nanocomposites were tested. Ac and lightning impulse (LI) breakdown strength of the composites were measured. Relative permittivity, loss factor and volume resistivity measurements were also conducted on the material samples. Two types of POSS, glycidyl and octaglycidyldimethylsilyl, were used in different quantities. Statistical analysis was applied to the measurement results to determine the effects of the additive type and amount on the properties of epoxy. The paper discusses the possibilities and restrictions in order to achieve advantages in high voltage applications using polyhedral oligomeric silsesquioxanes.

Index Terms — **Epoxy, polyhedral oligomeric silsesquioxane, thermal, mechanical and dielectric properties.**

1 INTRODUCTION

THE use of polymers as electrical insulating materials has been growing rapidly in recent decades. The base polymer properties have been developed by adding small amounts of different fillers (e.g. carbon black, talc, quartz and metal-oxides) to the polymer material. Recently, great expectations have focused on nano-fillers, e.g. polyhedral oligomeric silsesquioxanes (POSS).

A general overview and the theory of the functionality and morphology of the nanocomposite dielectrics have been reported in various articles [1-16]. CIGRE Task Force D1.16.03 [17] has reported that advanced polymer nanocomposite materials have significant potential applications for electrical and electronics insulation.

According to the EU 6th FP report "Nanomaterial roadmap 2015" [18] the demand throughout the industry, in the case of POSS, has begun to increase and market entry in thermal insulators has been predicted by the turn of the decade. The POSS related articles published so far usually deal with the thermal and mechanical properties, including both thermoplastic and epoxy [19-22] matrices. Current applications of POSS have been related to fire retardant materials, electronics [23-27], medical engineering, packaging and space industries.

Manuscript received on 8 May 2008, in final form 27 August 2008.

1070-9878/08/$25.00 © 2008 IEEE

Authorized licensed use limited to: Tampereen Teknillinen Korkeakoulu. Downloaded on March 23,2010 at 04:49:17 EDT from IEEE Xplore. Restrictions apply.

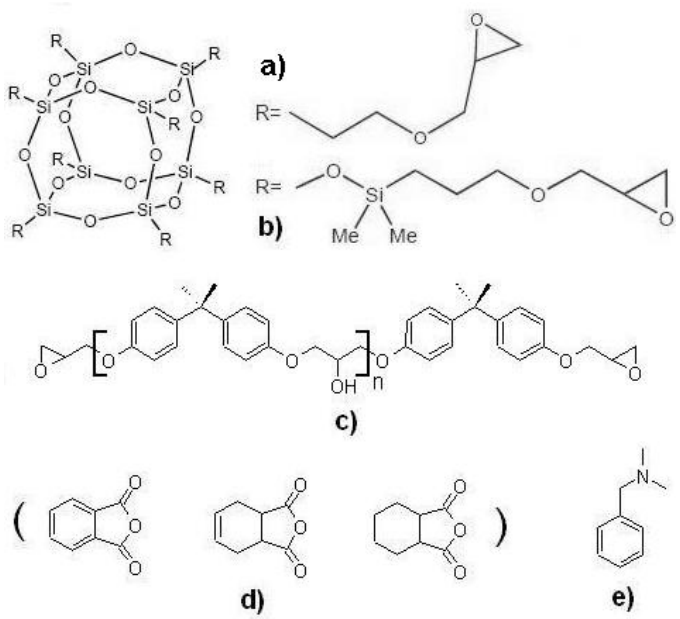

Figure 1. a) octaglycidyl POSS, b) octaglycidyldimethylsilyl POSS, c) diglycidyl ether of bisphenol A (Araldite® F), d) anhydride hardener (Aradur® HY 905), e) tertiary amine catalyst, *N, N*-dimethylbenzylamine (DY 062) [32].

Few articles related to dielectric properties of POSS materials have been published [28-31]. Horwarth et al have reported improved corona endurance in PP [28] and epoxy [29] with the use of POSS. Linnamaa and Kannus [30] have published on the partial discharge endurance and dielectric properties of POSS-XLPE. POSS seemed to inhibit physical degradation caused by the partial discharges on XLPE.

This study concentrates on the thermal, mechanical and dielectric properties of nanostructured epoxy-POSS composites.

2 EXPERIMENTAL

2.1 MATERIALS USED

POSS® chemicals were purchased from Hybrid Plastics Inc. Hattiesburg, MS, USA. Diglycidyl ether of bisphenol A (DGEBA epoxy resin, Araldite®F, CAS No. 25068-38-6), anhydride hardener (Aradur®HY 905, CAS No. 85-42-7, 85-43-8, 85-44-9, and 2210-79-9) and the tertiary amine catalyst (*N,N*-dimethylbenzylamine, DY 062, CAS No. 103-83-3) were purchased from Huntsman Advanced Materials, Basel, Switzerland. Glycidyl POSS (EP0409) is a oil cage mixture of octa-, deca- and dodecaglycidyl POSS. These molecules have an average size of 15, 16 and 17 Å respectively. Octaglycidyldimethylsilyl POSS (EP0435) is a viscous liquid and the molecule contains-two methyl groups and one glycidyl group on each of the eight side chains, and the average molecular diameter is 16 Å. The chemical structures of the chemicals used are presented in Figure 1.

Two POSS chemicals, glycidyl and octaglycidyldimethylsilyl, were used in combination with the pure epoxy resin. The epoxy polymer used is designed for indoor insulators for medium and high voltage. The compositions of the materials studied are shown in Table 1. Epoxy polymer (without added POSS compound, EP) is reference material. The planning of nanocomposite recipes, preparation of test samples and thermal and mechanical characterization were made at Technical Research Centre of Finland.

Table 1. Composition of the studied materials.

Material	POSS-type	wt-%
EP	-	-
EP1_1	glycidyl	1.0
EP1_2	glycidyl	3.0
EP1_3	glycidyl	4.8
EP2_1	octaglycidyldimethylsilyl	1.0
EP2_2	octaglycidyldimethylsilyl	3.0
EP2_3	octaglycidyldimethylsilyl	4.8
EP2_4	octaglycidyldimethylsilyl	9.6

In sample preparation the liquid POSS chemicals were mixed properly with the epoxy resin. The anhydride hardener was mixed with the epoxy resin-POSS mixture. The tertiary amine catalyst was then added last. The mixing rate of epoxy resin and hardener was same in all specimens. The mixing was done manually using a glass rod. The mixing time was 30 min. The mixed sample was then put in a vacuum oven for 30 minutes at 60 ºC. After degassing, the sample was injected into the polymethyl pentene (TPX) moulds. Epoxy resins with small amount of POSS used in this study didn't change the processability of resin into the mould. The viscosity of epoxy-POSS mixture is suitable for injection. For preparation of impact test samples the mould with dimension of 100 mm x 20 mm with thickness of 4.0 mm was used. The dimension of mould used for tensile test samples was 60 mm x 60 mm with thickness of 1.0 mm. The mould for breakdown test samples was 60 mm x 60 mm with thickness of 0.5 mm. Pre-curing of samples were done at 80 ºC for 7 h and curing at 130 ºC for 11 h (atmospheric pressure). The largest wt-% concentration of glycidyl POSS was neglected because shortage of the additive.

2.2 DSC

A differential scanning calorimeter (DSC) analysis was made on the epoxy samples (TA Instruments MDSC 2920). The heating and cooling rate was 10 ºC/min and heating was stopped at 200 ºC. With each recipe three measurements were made. DSC analysis was made for 0.5 mm thick samples.

2.3 MECHANICAL TESTING

Tensile tests were made by Instron 4505 tensile testing machine according to ISO 527 standard [33]. Tensile strength, elongation at break and elastic module were measured during the tensile test. Minimum of 5 tests were made with each composition. Specimen thickness was 1.0 mm. Moulded plates were milled into the form of tensile test samples.

Authorized licensed use limited to: Tampereen Teknillinen Korkeakoulu. Downloaded on March 23,2010 at 04:49:17 EDT from IEEE Xplore. Restrictions apply.

The impact strength of epoxy nanocomposites was tested by the Charpy method (ISO 179) [34] with instrumented impact tester Ceast Resil 5.5. In the Charpy method the specimen is loosely laid horizontally on supports and then broken by the pendulum swinging against the middle. Tests were made at 25 ºC/50 % R.H. Minimum of 4 tests were made with each composite. Specimens were milled to dimensions 80 mm x 9 mm x 4 mm. Unnotched samples were used.

2.4 AC AND LI BREAKDOWN STRENGTH MEASUREMENTS

ac and lightning impulse (LI) breakdown strength of the test samples were measured at Tampere University of Technology. The measurements were performed at room temperature (~20 °C). The size of the test samples was approximately 5 cm x 5 cm and thickness 500 µm. The thickness dependent breakdown strength at these material thicknesses has only a small effect on the results and was ignored because of the small thickness variation in material samples [35]. Rod-like electrodes having a diameter of 12 mm and made of stainless steel were used in the measurements. The electrodes were placed on opposite surfaces of a specimen. The measurements were performed by immersing the sample and the electrodes in mineral oil (Shell Diala DX) in order to avoid surface discharges and flashovers. In addition, the edges of the electrodes were rounded (r =1 mm) for that reason. The sites of the breakdown were distributed all over the sample area.

The ac breakdown measurements were performed using a high voltage supply (Hipotronics) with a maximum output of 50 kV and 6 A. The voltage applied was ac 50 Hz with 2 kV/s rate of increase according to IEC 60243-1 [36] until breakdown occurred. A set of 10 test samples was used with each material. The LI breakdown measurements were performed using a high voltage impulse generator (Haefely Test, AG) of maximum output voltage 980 kV and maximum pulse energy 50 kJ. The wave shape of the impulse voltage was 1.2/50 µs defined according to IEC Standard 60060-1 [37]. The output voltage of the impulse generator was raised 2 kV after each impulse until breakdown occurred. Negative impulses were used and the time interval between them was 10-20 s. The number of the parallel measurements with LI voltage was 10.

2.5 DIELECTRIC SPECTROSCOPY

The complex impedance of epoxy-POSS composites was measured as a function of frequency. The measurements were performed using insulation diagnosis analyzer IDA200. The frequency range used was from 0.1 Hz to 1 kHz at 140 V_{RMS} voltage. The relative permittivity (ε_r), loss factor (tan δ) and volume resistivity (ρ) were calculated from the measured parallel capacitance and resistance with the following Equations 1-5,

$$\varepsilon' = \frac{C_P}{C_0} - \frac{C_e}{C_0} \tag{1}$$

$$\varepsilon'' = \frac{1}{R_P C_0 \omega} - \frac{C_e}{C_0} \tag{2}$$

$$\varepsilon_r = \sqrt{\varepsilon'^2 + \varepsilon''^2} \tag{3}$$

$$\tan\delta = \frac{\varepsilon''}{\varepsilon'} \approx \frac{1}{R_P C_P \omega} \quad , C_e << C_P \tag{4}$$

$$\sigma = \frac{1}{\rho} = \frac{\varepsilon_0}{R_P C_0} \tag{5}$$

where C_P and R_P respectively are the measured parallel capacitance and resistance at the measurement frequency when the specimen is represented in terms of equivalent parallel circuit (Figure 2), C_0 the vacuum capacitance of the measurement setup, C_e the edge capacitance according to IEC standard 250 [38], ω the angular frequency and ε_0 the vacuum permittivity. Samples were approximately 5 cm x 5 cm wide and 500 µm thick. Aluminum foil electrodes (d=4.6 cm) attached to the samples with a small amount of silicone grease were used. Three parallel measurements were conducted on the samples.

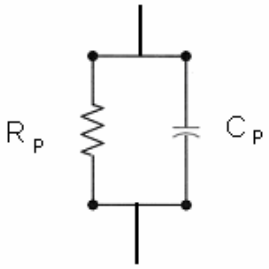

Figure 2. Equivalent RC parallel electrical circuit of dielectric specimens.

2.6 STATISTICAL ANALYSIS

Statistical analysis was applied to the measurement results. Results were calculated according to the IEEE standard "IEEE Guide for the Statistical Analysis of Electrical Insulation Breakdown Data" [39] using Microsoft Excel and Matlab programs.

Two-parameter Weibull distribution function was used to process the data derived from the breakdown strength measurements. Distribution parameter estimation was easier and confidence intervals of parameters were smaller with two than with three-parameter Weibull distribution [40]. The quality of data fit was good, even though slight deviations at low or high probability values were sometimes detected [41]. The 2-parameter Weibull cumulative distribution function (Eq. 6) is related to the probability of failure occurring in certain field strength *x* [42].

$$F(x) = 1 - \exp\left\{-\left[\frac{x}{\beta}\right]^{\alpha}\right\} \tag{6}$$

Authorized licensed use limited to: Tampereen Teknillinen Korkeakoulu. Downloaded on March 23,2010 at 04:49:17 EDT from IEEE Xplore. Restrictions apply.

The shape parameter α is related to the shape or the width of the distribution. The spread of the breakdown strengths is narrower when the value of α is higher. There is a smaller scattering of the dielectric strength values and consequently higher reliability of the dielectric behavior of the material when shape parameter is high. The scale parameter β is related to the 63.2 % probability for the sample to break down at electric field strength β [41].

Statistical differences between two materials can be compared by average standard deviation (s_{ave}), which is the weighted average value of the two standard deviations of the materials. The difference between the means (dif) of the materials is compared with meaningful sectors. These sectors are not significant (dif $\leq 1.96\times s_{ave}$), almost significant ($1.96\times s_{ave} <$ dif $\leq 2.58\times s_{ave}$), significant ($2.58\times s_{ave} <$ dif $\leq 3.29\times s_{ave}$) and extremely significant (dif $> 3.29\times s_{ave}$) [43]. With these quantiles statistical significance levels can be calculated and differences between the materials evaluated.

3 RESULTS

3.1 THERMAL CURE REACTIONS

The samples were prepared by thermal curing of a mixture of epoxy resin and various epoxy functionalised POSS compounds with anhydride in the presence of a tertiary amine. The reaction mechanisms for curing epoxy resins with anhydrides in the presence of a base have been studied by Matějka et al [44] and Rocks et al [45]. The suggested reaction mechanism is presented in Figure 3. Initially, the tertiary amine reacts with the epoxide groups of the epoxy resin and the POSS compound and forms a zwitterion (**3**) containing a quaternary nitrogen atom and an alkoxide ion. The alkoxide group reacts further with an anhydride, forming a carboxylate ion (**5**). In the next step, the reaction of the carboxylate ion with **1** results in ring opening of the epoxide and a new alkoxide ion (**6**) is formed. The carboxylate ion (**7**) is formed by reaction of an anhydride with the alkoxide group of **6**.

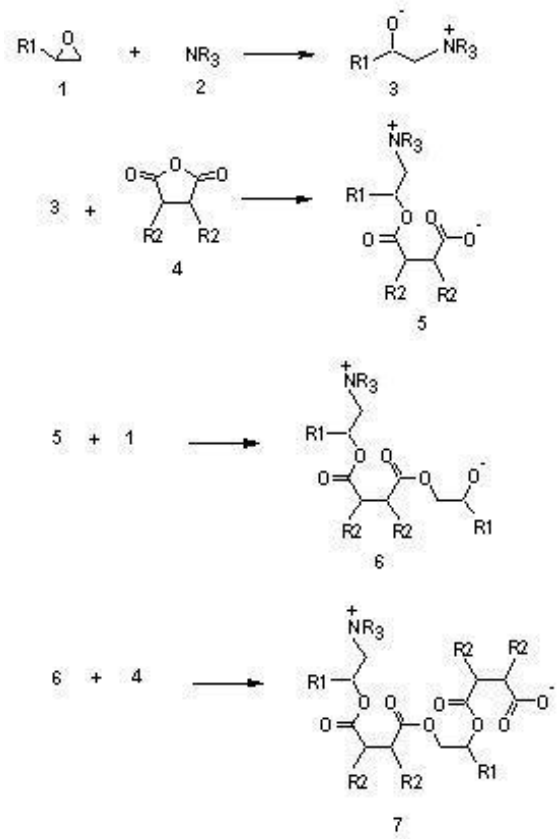

Figure 3. Curing reactions of epoxy resin and POSS with anhydride. Compounds: **1** mixture of epoxy resin (Araldite® F) and POSS compound; **2** *N,N*-dimethylbenzylamine (DY 062); **4** anhydride hardener (Aradur® HY 905).

3.2 MORPHOLOGY

The morphology of the reference epoxy and octaglycidyldimethylsilyl POSS epoxy materials was studied with scanning electron microscopy (SEM), atomic force microscopy (AFM) and transmission electron microscopy (TEM).

The moulded epoxy samples were broken in liquid nitrogen and the fracture surface was analyzed by SEM. The fracture surfaces of reference epoxy and 1.0 wt-% octaglycidyldimethylsilyl POSS epoxy (EP and EP2_1) composites with different magnifications are presented in Figures 4 and 5. The fracture surface of the octaglycidyldimethylsilyl POSS epoxy nanocomposite is different from the fracture surface of the reference epoxy sample (Figure 4 a) and b)). In one part of the sample the rough fracture area was observed. In one area of the nanocomposite also small, approximately 150 nm particles were seen.

AFM was applied directly to the surface of the molded reference epoxy and 1 wt-% octaglycidyldimethylsilyl POSS epoxy sample (EP2_1) in air (Figures 6-8). For the imaging, Digital Instruments Dimension 3100 system operating in non-contact Tapping Mode™, with standard silicon cantilever from NSC15 Micromasch was utilized. The normal height image contained little additional information to the SEM imaging. The phase imaging, however, revealed the two-phase granular-like morphology of the surface. The contrast in the phase image is due to differences in the energy dissipation of the oscillating cantilever in the tip-sample interaction. The phase image is sensitive to compositional differencies on the surface and below the surface. It commonly reveals morphological features that are not visible in the topographical (Height) image. The Phase signal sums all the effects of the local energy dissipation on the shape of the tip-displacement force curve i.e. the surface chemistry and the viscoelastic properties of the material under the oscillating tip. The instruments were operated in soft tapping regime to ensure nondestructive tip-sample interaction and to prevent switching between the different resonant modes of the cantilever, a well known experimental artifact producing high contrast phase images.

Authorized licensed use limited to: Tampereen Teknillinen Korkeakoulu. Downloaded on March 23,2010 at 04:49:17 EDT from IEEE Xplore. Restrictions apply.

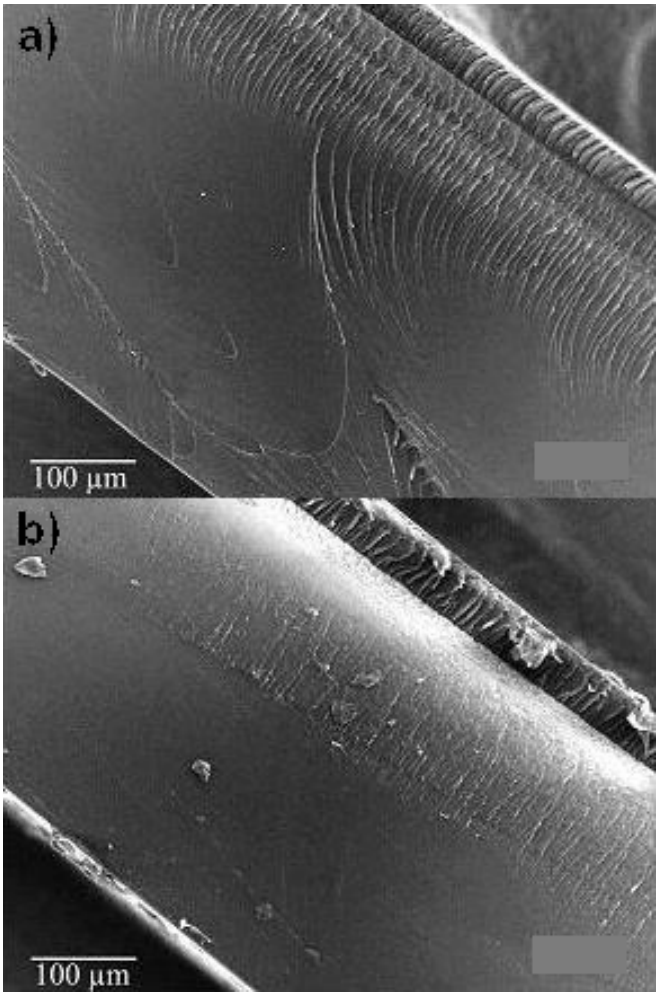

Figure 4. Fracture surfaces of a) reference epoxy (EP) b) 1 wt-% octaglycidyldimethylsilyl POSS epoxy (EP2_1) composites.

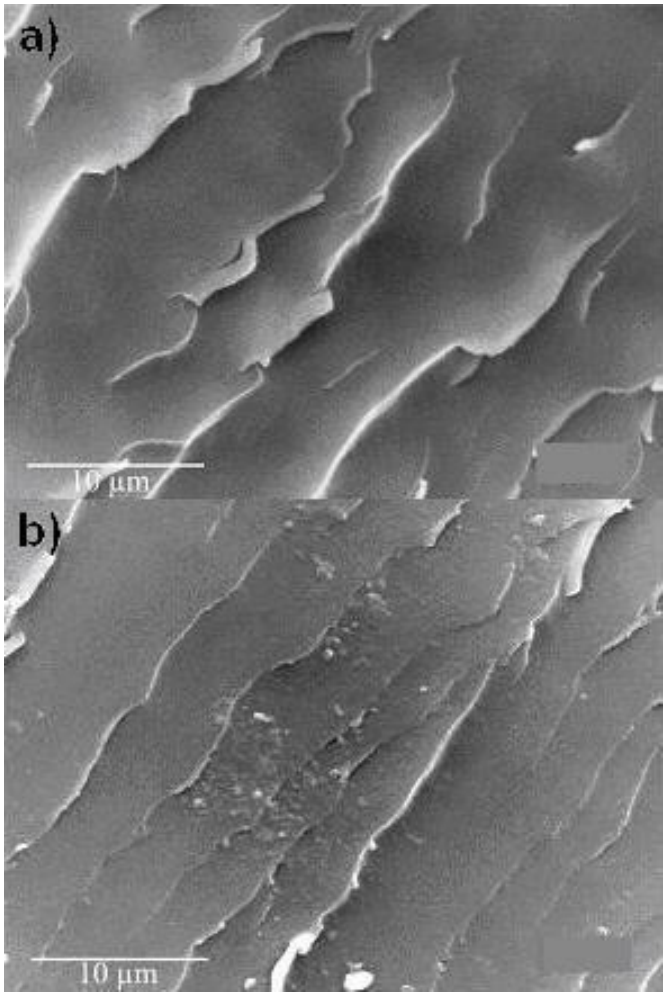

Figure 5. Fracture surfaces of a) reference epoxy (EP) b) 1 wt-% octaglycidyldimethylsilyl POSS epoxy (EP2_1) composites.

The tapping mode AFM phase images of 1 wt-% octaglycidyldimethylsilyl POSS epoxy (EP2_1) nanocomposite are presented in Figures 7 (1500 nm scan) and 8 (500 nm scan). The darker contrast corresponds to the viscoelastically "stiffer" phase or lower attractive interaction force between the tip and the sample, respectively. It is noteworthy to notice that during AFM imaging in air, there is always an adsorbed layer of water and gases present on the surface. This adsorbed layer will contribute to the tip-sample force in air and it probably dominates the tip-sample interaction curve sensitive to the surface chemistry in every non-contact imaging in air. Figure 8 of the nanocomposite indicates that there are two at least slightly differing nanostructured (both with roughly 50 % surface coverage) phases in the sample. The bright-contrast phase appears to consist of approximately 20 nm interconnected round areas.

The Phase contrast is well below 20° which suggests two-phase morphology: The AFM Phase image does not suggest complete miscibility of POSS and epoxy but rather two phases with differing compositions. This kind of compositional contrast is not present in the AFM images of the reference epoxy sample, presented in Figure 6 and recorded under identical experimental conditions. Neither has this kind of phase separated morphology been reported in related epoxy-POSS studies by Liu et Al [46] who, according to their AFM imaging, suggested truly uniform morphology. Based on our current observations it is not clear into what extent the POSS is partitioned between the observed phases. Correlating to the fact that the bridging groups of POSS particles tend to decrease the glass transition temperature of the composite (3.3 Glass transition temperature), the regions exhibiting higher phase angles are more likely to be rich in POSS i.e. having softer character.

In Figure 9 the TEM (Jeol, JEM 2010) bright field image of the 1.0 wt-% octaglycidyldimethylsilyl POSS epoxy (EP2_1) is presented. The acceleration voltage used was 120 kV. The TEM sample is a thin, stained slice cut of the bulk sample. The contrast in the image is relatively low. However, higher contrast is observed in irregularly shaped clusters, consisting of round areas (particles) with roughly the same 20 nm pattern. Isolated POSS nanoparticles are not visible in the AFM or the TEM images, but rather aggregates containing at least tens of the particles.

Authorized licensed use limited to: Tampereen Teknillinen Korkeakoulu. Downloaded on March 23,2010 at 04:49:17 EDT from IEEE Xplore. Restrictions apply.

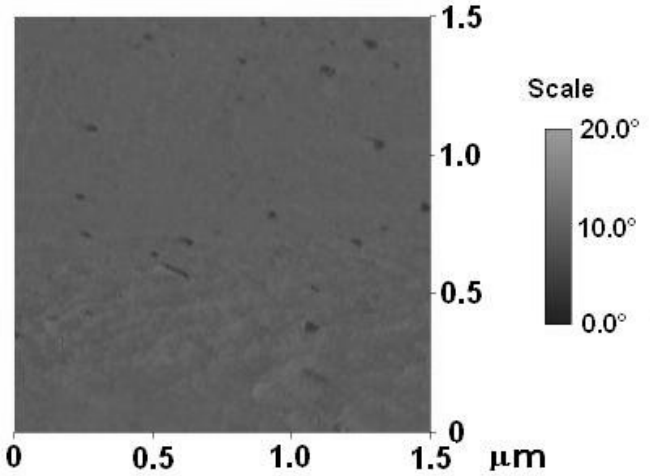

Figure 6. AFM Phase image of the reference epoxy. The few dark areas correspond to topographical extremities or dust particles on the surface and are present in the corresponding Height image (not shown).

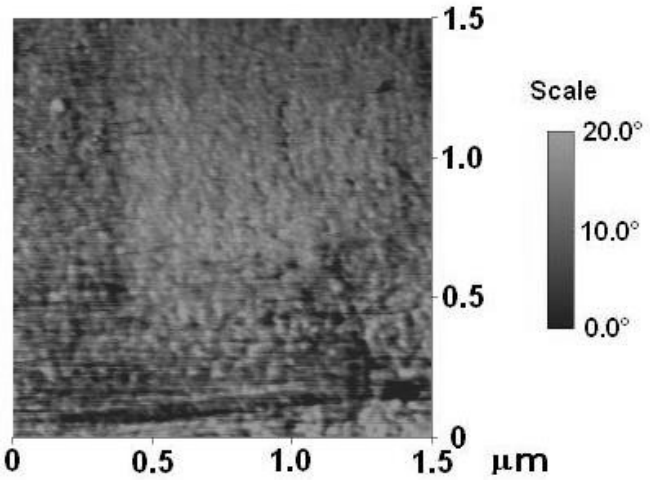

Figure 7. AFM Phase image of 1 wt-% octaglycidyldimethylsilyl POSS epoxy nanocomposite (EP2_1), 1500 nm scan. Areas with dark contrast appear throughout the scan area and are likely to present a POSS deficit phase.

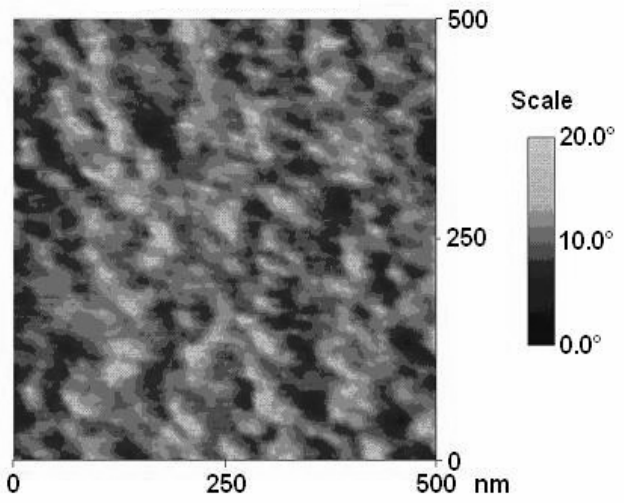

Figure 8. AFM Phase image of 1 wt-% octaglycidyldimethylsilyl POSS epoxy nanocomposite (EP2_1), 500 nm scan. The phase with darker contrast consists of 20 nm round interconnected areas.

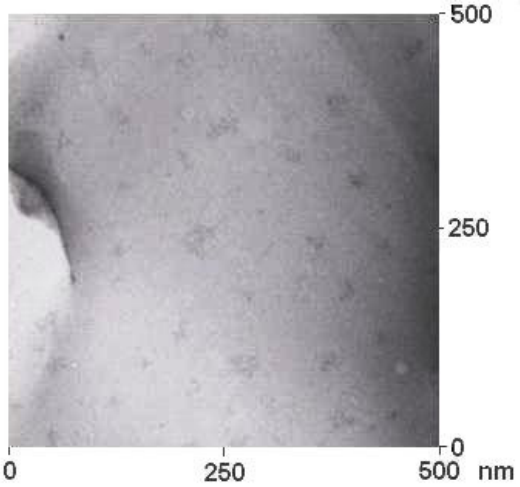

Figure 9. TEM bright field analysis of 1 wt-% octaglycidyldimethylsilyl POSS epoxy nanocomposite (EP2_1). The darker area is likely to consist of small aggregates of POSS nanoparticles. The weak constrast is due to relatively small differencies in the average atomic weight of the two phases.

3.3 GLASS TRANSITION TEMPERATURE

The results of the glass transition temperature measurements of the epoxy composites are presented in Figure 10 as a function of POSS contents. According to the DSC analysis the T_g of test samples containing glycidyl and octaglycidyldimethylsilyl POSS decrease as a function of the POSS content (Figure 10). Statistically these changes were extremely significant (except with 3 wt-% glycidyl POSS almost significant). Standard deviation bars of the measurements are presented with each material composition. Long side chains of glycidyl and octaglycidyldimethylsilyl POSS soften the material and increase molecular mobility and therefore decrease the glass transition temperature of epoxy nanocomposite.

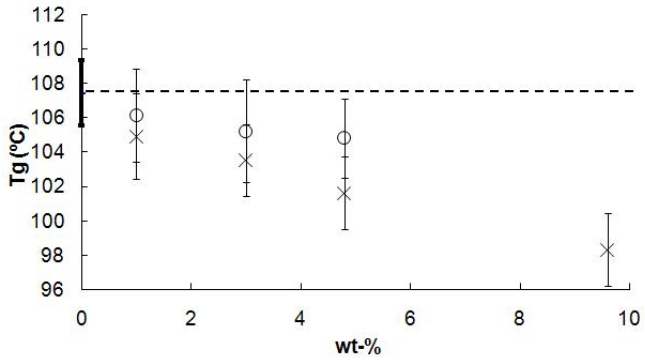

Figure 10. The DSC glass transition temperature of epoxy-POSS nanocomposites as a function of POSS content (glycidyl POSS O and octaglycidyldimethylsilyl POSS ×, reference line dotted).

3.4 MECHANICAL PROPERTIES

The results of the mechanical properties measurements are presented in Figures 11-14. Octaglycidyldimethylsilyl POSS epoxy nanocomposites have slightly lower tensile strength and strain than the base epoxy. The differences were significant with 3 and 4.8 wt-% composites and extremely significant

Authorized licensed use limited to: Tampereen Teknillinen Korkeakoulu. Downloaded on March 23,2010 at 04:49:17 EDT from IEEE Xplore. Restrictions apply.

with 9.6 wt-% composite. With 1 wt-% of octaglycidyldimethylsilyl POSS mechanical properties remained near the reference level. Standard deviation bars of the measurements are presented with each material composition. Long side chains of octaglycidyldimethylsilyl POSS soften the material and increase mobility and therefore the stress and strain are weakened with 3, 4.8 and 9.6 wt-% composites. Modulus and Charpy impact strength of octaglycidyldimethylsilyl POSS epoxy composites remained near the reference level with all compositions.

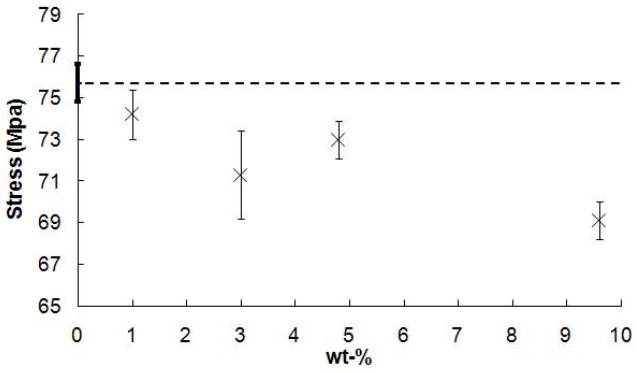

Figure 11. Tensile strength of octaglycidyldimethylsilyl POSS epoxy nanocomposites as a function of POSS content (reference line dotted).

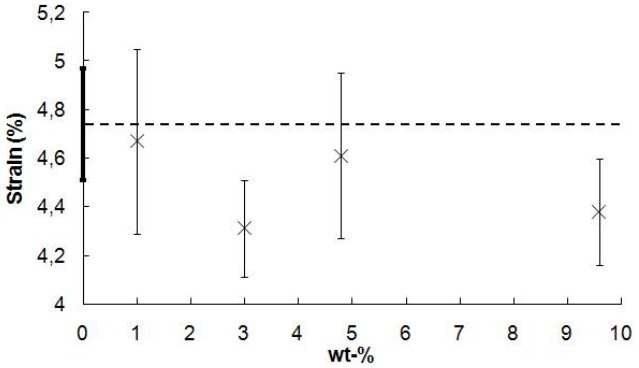

Figure 12. Strain (elongation at break) of octaglycidyldimethylsilyl POSS epoxy nanocomposites as a function of POSS content (reference line dotted).

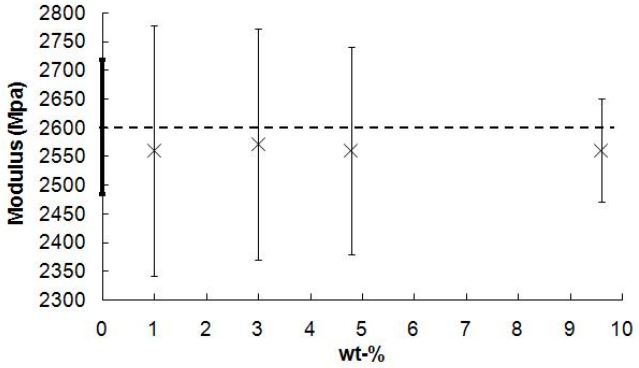

Figure 13. Modulus of octaglycidyldimethylsilyl POSS epoxy nanocomposites as a function of POSS content (reference line dotted).

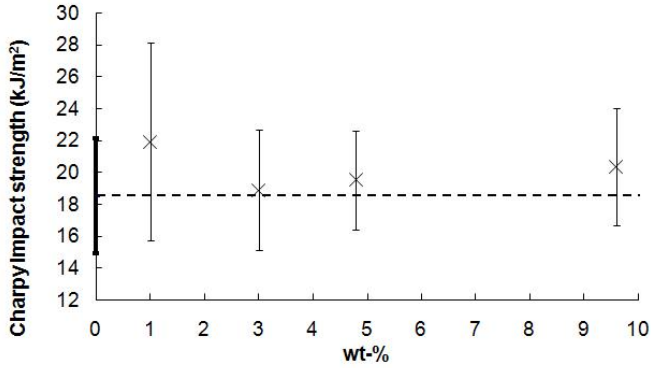

Figure 14. Charpy impact strength of octaglycidyldimethylsilyl POSS epoxy nanocomposites as a function of POSS content (reference line dotted).

3.5 AC AND LI BREAKDOWN STRENGTH

The results of the ac and LI breakdown strength measurements are presented in Table 2. The mean value is calculated from 10 measurement results. Uncertainties were estimated with standard deviation. According to the IEEE standard [39] correlation to the data points should be over 0.92 if good enough correlation with 10 measurements using 2-parameter Weibull distribution is achieved. With these measurements 3-parameter Weibull distribution gave lower correlation results than 2-parameter Weibull distribution. Hence, the correlation values of Table 2 were calculated and statistical analysis was conducted using 2-parameter Weibull distribution. With samples EP2_1 (ac), EP1_3 (LI) and EP2_2 (LI) the correlation achieved was below the limit and no further statistical analysis was done for those samples.

Table 2. Ac and LI breakdown strength of the test materials.

ac					
Material	mean [kV/mm]	s [kV/mm]	β [kV/mm]	α [kV/mm]	corr
EP	61	5	63.5	14.7	0.93
EP1_1	66	5	68.4	17.5	0.93
EP1_2	66	7	68.9	11.3	0.95
EP1_3	62	5	64.5	14.4	0.98
EP2_1	58	4	59.7	20.8	0.91
EP2_2	60	4	61.6	17.5	0.96
EP2_3	65	4	66.9	18.8	0.98
EP2_4	63	6	65.7	13.1	0.98
LI					
Material	mean [kV/mm]	s [kV/mm]	β [kV/mm]	α [kV/mm]	corr
EP	129	23	137.6	7.3	0.92
EP1_1	108	11	112.3	12.9	0.93
EP1_2	101	17	107.3	8.0	0.92
EP1_3	104	19	110.1	7.9	0.86
EP2_1	162	26	173.4	6.7	0.97
EP2_2	131	40	140.6	5.4	0.82
EP2_3	112	27	121.8	5.3	0.95

Authorized licensed use limited to: Tampereen Teknillinen Korkeakoulu. Downloaded on March 23,2010 at 04:49:17 EDT from IEEE Xplore. Restrictions apply.

The ac and LI breakdown strength measurement results of the epoxy composites containing glycidyl and octaglycidyldimethylsilyl POSS are presented in Figures 15 and 16. The greatest ac breakdown strengths were achieved with 1 and 3 wt-% glycidyl POSS (Figure 15) and the highest LI breakdown strength with 1 wt-% octaglycidyldimethylsilyl POSS content (Figure 16). In LI breakdown measurements of 1 wt-% octaglycidyldimethylsilyl POSS epoxy composite seven samples of 10 did not break. When voltage was raised high enough a flashover occurred in transformer oil. It can be thought that the true LI breakdown strength of 1 wt-% octaglycidyldimethylsilyl POSS epoxy composites is even higher than presented in Figure 16. With reference epoxy only one sample did not break. Statistically these differences in the breakdown strength of the materials were not significant because of the relatively high standard deviations in the measurements.

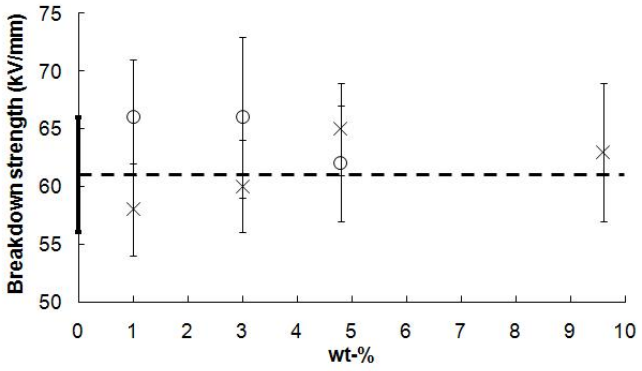

Figure 15. Effect of the POSS type and content on the AC breakdown strength of epoxy (glycidyl POSS O and octaglycidyldimethylsilyl POSS ×, reference line dotted).

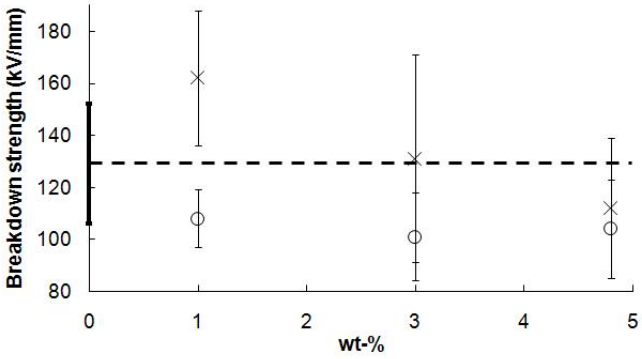

Figure 16. Effect of the POSS type and content on the LI breakdown strength of epoxy (glycidyl POSS O and octaglycidyldimethylsilyl POSS ×, reference line dotted).

In Figures 17 and 18 the best epoxy-POSS breakdown strength results with ac (EP1_1) and LI (EP2_1) are presented in the Weibull probability plots. 90 % confidence intervals are plotted with dashed lines on both sides of the straight Weibull fitting line. Measurement points are marked with small crosses and circles. These nanostructured composites gave better ac and LI breakdown strength results than the reference epoxy but 90 % confidence intervals did cross at low probabilities (Figures 17 and 18).

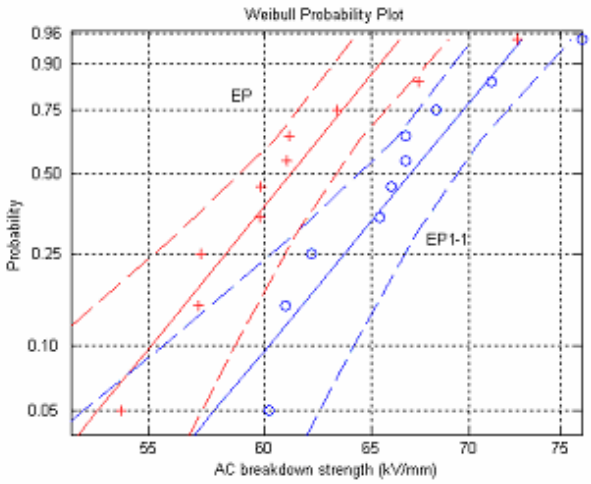

Figure 17. AC breakdown strength measurements of the reference epoxy (EP) and 1 wt-% glycidyl POSS epoxy composite (EP1_1) presented in the Weibull probability plot.

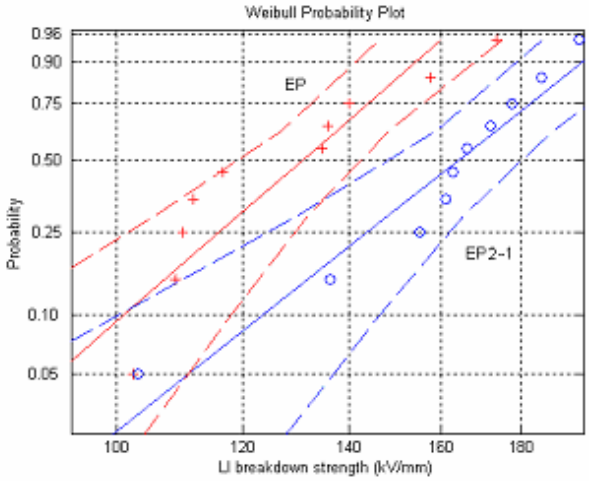

Figure 18. LI breakdown strength measurements of the reference epoxy (EP) and 1 wt-% octaglycidyldimethylsilyl POSS epoxy composite (EP2_1) presented in the Weibull probability plot.

3.6 DIELECTRIC PROPERTIES

The relative permittivity, loss factor and volume resistivity of the glycidyl POSS epoxy composites are presented in Figures 19-21. According to the measurements, higher permittivity values were obtained with 3 and 4.8 wt-% glycidyl POSS epoxy composites (EP1_2, EP1_3) than with pure epoxy. At the same time loss factor and volume resistivity remained at the same level as reference epoxy. The mean standard deviations in the relative permittivity, loss factor and volume resistivity measurements of glycidyl POSS epoxy composites varied between 0.003-0.010 %, 0.17-0.65 % and 0.17-0.65 %, respectively.

The relative permittivity, loss factor and volume resistivity of the octaglycidyldimethylsilyl POSS epoxy composites are presented in Figures 22-24. According to the measurements octaglycidyldimethylsilyl POSS did not significantly affect the relative permittivity of epoxy. The loss factor and volume resistivity also remained at the same level as the reference epoxy. The mean standard deviations in the relative

Authorized licensed use limited to: Tampereen Teknillinen Korkeakoulu. Downloaded on March 23,2010 at 04:49:17 EDT from IEEE Xplore. Restrictions apply.

permittivity, loss factor and volume resistivity measurements of octaglycidyldimethylsilyl POSS epoxy composites varied between 0.003-0.015 %, 0.21-0.30 % and 0.21-0.31 %, respectively.

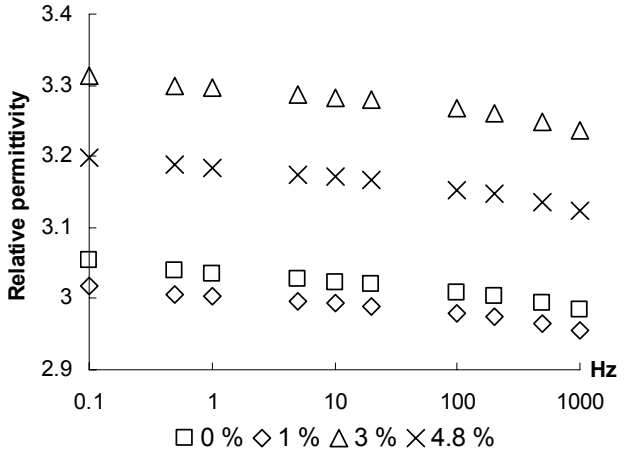

Figure 19. Effect of glycidyl POSS content on the relative permittivity of epoxy as a function of frequency.

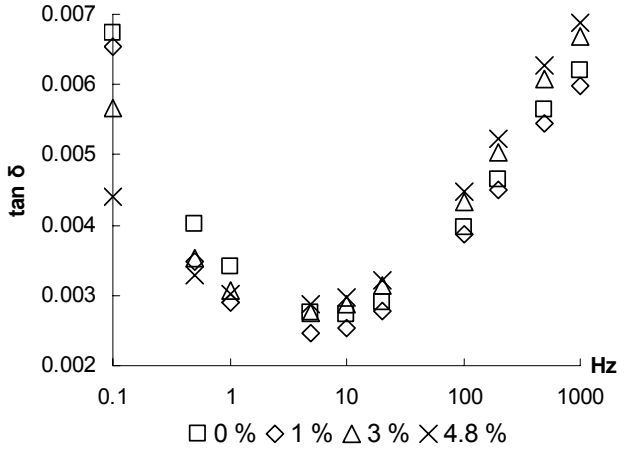

Figure 20. Effect of glycidyl POSS content on the dielectric losses of epoxy as a function of frequency.

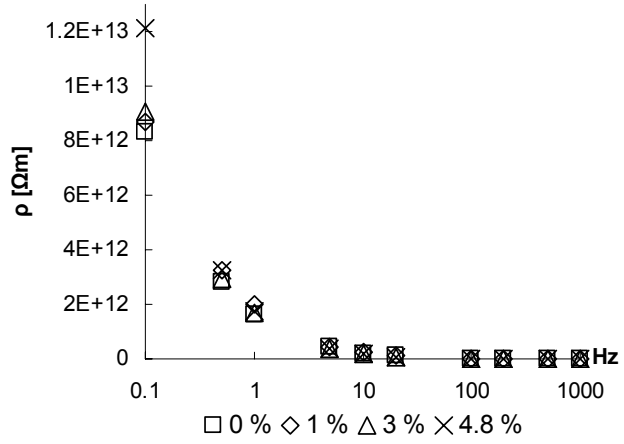

Figure 21. Effect of glycidyl POSS content on the volume resistivity of epoxy as a function of frequency.

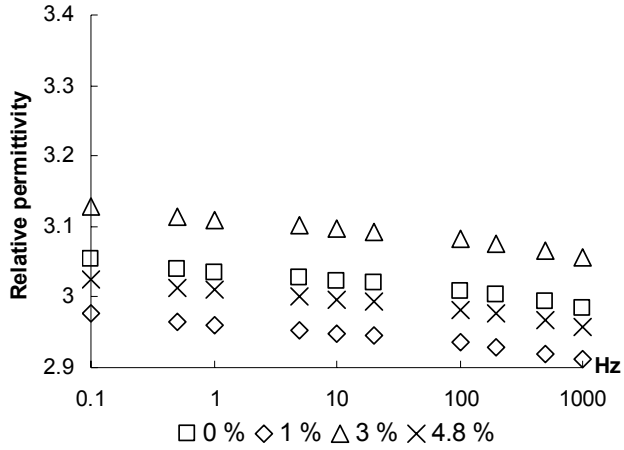

Figure 22. Effect of octaglycidyldimethylsilyl POSS content on the relative permittivity of epoxy as a function of frequency.

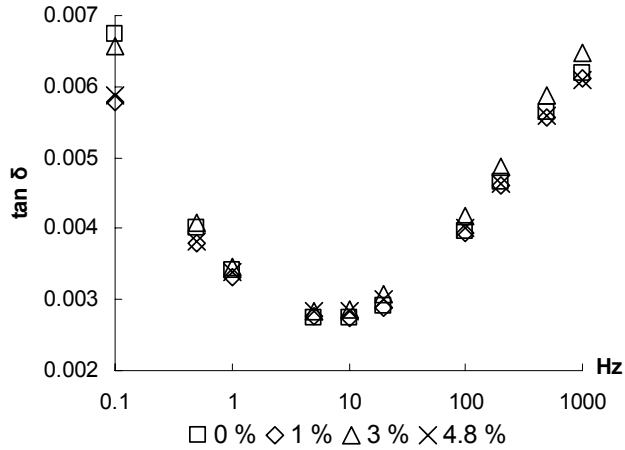

Figure 23. Effect of octaglycidyldimethylsilyl POSS content on the dielectric losses of epoxy as a function of frequency.

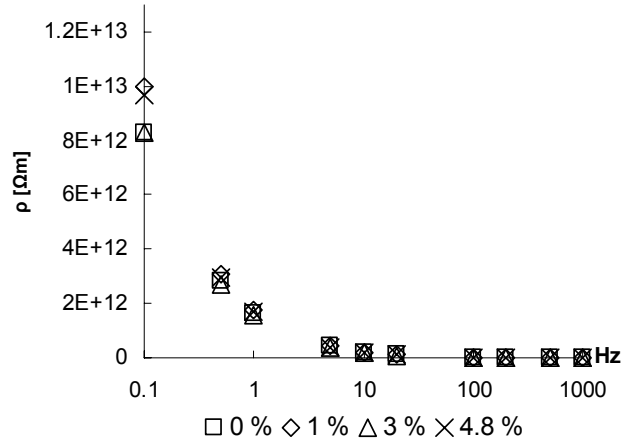

Figure 24. Effect of octaglycidyldimethylsilyl POSS content on the volume resistivity of epoxy as a function of frequency.

4 DISCUSSION

According to the dielectric measurements presented in this paper, the breakdown strength of pure epoxy can be improved with the addition of POSS. The most interesting results were the

Authorized licensed use limited to: Tampereen Teknillinen Korkeakoulu. Downloaded on March 23,2010 at 04:49:17 EDT from IEEE Xplore. Restrictions apply.

flashovers in the LI measurements. Seven flashovers occurred in LI breakdown measurements of 1 wt-% octaglycidyldimethylsilyl POSS epoxy nanocomposite (EP2_1) and in reference epoxy (EP) only one, showing clearly higher LI breakdown strength of the POSS nanocomposite material.

It is possible that POSS can strengthen epoxy under the high electric field by scavenging charges temporarily. POSS molecules may hinder the electrons from speeding up in the insulation and so prevent the charge from going through the insulation. POSS molecules may serve as nanocapacitors in dielectric matrix. We assume that by still improving the dispersion of the compounds more towards nanoscale we can achieve even better dielectric properties for the insulation.

The relative permittivity of the glycidyl POSS composites increased with 3 and 4.8 wt-% composites (EP1_2, EP1_3). It is not just the loading which affects the properties. POSS could be distributed in compounds in different ways. The size of the POSS particles could be different depending on the total amount of POSS in the composite. This may be the reason for the differences in relative permittivity with different filler quantities. There are also other references where a property of an epoxy POSS nanocomposite does not follow the change of loading, e. g. in [47].

Mechanical properties of 1 wt-% octaglycidyldimethylsilyl POSS epoxy nanocomposite were near the base epoxy. Tensile properties are slightly lower and impact strength is slightly higher than that of reference epoxy. The glass transition temperature decreased appr. 2 °C with 1 wt-% composite. In summary, the profile of properties of 1 wt-% octaglycidyldimethylsilyl POSS nanocomposite is very promising for the use of that type of material in high voltage applications.

It seems that POSS molecules have potential to achieve advantages in high voltage applications. According to our studies with XLPE-POSS [30], PP-POSS [31] and epoxy-POSS it seems that POSS materials are applicable for both indoor insulators and high voltage apparatuses also in very harsh environmental and electrical stresses. It also seems that with small quantities (< 3 wt-%) of an additive property changes can already be seen. This is an advantage when material costs are under consideration. The properties of the composites should also be ascertained in long-term ageing measurements.

5 CONCLUSION

Epoxy composites were studied with SEM, AFM and TEM. SEM pictures revealed that the fracture surface of the octaglycidyldimethylsilyl POSS epoxy nanocomposite is different from the fracture surface of the reference epoxy sample. In one part of the sample the rough fracture area was observed. In one area of the nanocomposite small, approximately 150 nm particles were also seen.

The AFM phase imaging revealed the two-phase granular-like morphology of the surface. Figure 8 of the nanocomposite indicates that there are two at least slightly differing nanostructured (both with roughly 50 % surface coverage) phases in the sample. The bright-contrast phase appears to consist of approximately 20 nm interconnected round areas. The Phase contrast is well below 20° which suggests two-phase morphology: the AFM Phase image does not suggest complete miscibility of POSS and epoxy but rather two phases with differing compositions. This kind of compositional contrast is not present in the AFM images of the reference epoxy sample, presented in Figure 6. In TEM analysis a higher contrast is observed in irregularly shaped clusters, consisting of round areas (particles) with roughly the same 20 nm pattern. However, individual POSS nanoparticles are not visible in the AFM or the TEM images, but rather aggregates containing at least tens of the particles.

Glass transition temperature of test samples containing glycidyl and octaglycidyldimethylsilyl POSS decreased as a function of the POSS content. With 1 wt-% octaglycidyldimethylsilyl POSS composite the glass transition temperature decreased appr. 2 °C. The mechanical properties of 1 wt-% octaglycidyldimethylsilyl POSS epoxy composite remained near the base epoxy.

The breakdown strengths with ac and LI obtained from reference epoxy and epoxy-POSS composites were analyzed according to Weibull statistical analysis. This study concluded that glycidyl and octaglycidyldimethylsilyl POSS did not statistically increase or decrease the breakdown strengths of epoxy. Remarkably, in LI breakdown measurements of 1 wt-% octaglycidyldimethylsilyl POSS epoxy composite seven samples of 10 did not break. When voltage was raised high enough a flashover occurred in transformer oil. It can be thought that the true LI breakdown strength of 1 wt-% octaglycidyldimethylsilyl POSS epoxy composites is even higher than presented in Figure 16. With reference epoxy only one sample did not break. This phenomen suggests that it is possible to achieve improvement in breakdown strength with a certain amount of POSS and epoxy.

The results of the relative permittivity, loss factor and volume resistivity measurements indicated that glycidyl POSS could have an effect on the relative permittivity of epoxy. Higher permittivity values were obtained with 3 and 4.8 wt-% glycidyl POSS composites (EP1_2, EP1_3) than with pure epoxy. The loss factor and volume resistivity remained at the same level as reference epoxy. Octaglycidyldimethylsilyl POSS did not affect the relative permittivity, loss factor or volume resistivity of epoxy.

REFERENCES

[1] J. K. Nelson, Y. Hu and J. Thiticharoenpong, "Electrical Properties of TiO2 Nanocomposites", IEEE Conf. Electr. Insul. Dielectr. Phenomena (CEIDP), pp. 719-722, 2003.

[2] S. Rätzke and J. Kindersberger, "Erosion Behaviour of Nano Filled Silicone Elastomers", XIVth Intern. Sympos. High Voltage Eng. (ISH), pp. 1-6, 2005.

[3] T. J. Lewis, "Interfaces are the Dominant Feature of Dielectrics at the Nanometric Level", IEEE Trans. Dielectr. Electr. Insul., Vol. 11, pp. 739-753, 2004.

[4] M. F. Frechette, M. Trudeau, H. D. Alamdari and S. Boily, "Introductory Remarks on Nanodielectrics", IEEE Conf. Electr. Insul. Dielectr. Phenomena (CEIDP), pp. 92-99, 2001.

[5] G. C. Montanari, D. Fabiani, F. Palmieri, D. Kaempfer, R. Thomann and R. Mülhaupt, "Modification of Electrical Properties and Performance of EVA and PP Insulation through Nanostructure by Organophilic Silicates", IEEE Trans. Dielectr. Electr. Insul., Vol. 11, pp. 754-762, 2004.

[6] J. K. Nelson and Y. Hu, "Nanocomposite Dielectrics-Properties and Implications", J. Phys. D: Appl. Phys., Vol. 38, pp.213-222, 2005.

[7] T. J. Lewis, "Nanometric Dielectrics", IEEE Trans. Dielectr. Electr. Insul., Vol. 1, pp. 812-825, 1994.

[8] S. Pothukuchi, Y. Li and C. P. Wong, "Shape Controlled Synthesis of Nanoparticles and Their Incorporation into Polymers", Electronic Components and Technology Conf., pp. 1965-1967, 2004.

[9] J. K. Nelson and J. C. Fothergill, "Internal Charge Behaviour of Nanocomposites", Nanotechnology, Vol. 15, pp. 586-595, 2004.

Authorized licensed use limited to: Tampereen Teknillinen Korkeakoulu. Downloaded on March 23,2010 at 04:49:17 EDT from IEEE Xplore. Restrictions apply.

[10] T. Tanaka, G. C. Montanari and R. Mülhaupt, "Polymer Nanocomposites as Dielectrics and Electrical Insulationperspectives for Processing Technologies, Material Characterization and Future Applications", IEEE Trans. Dielectr. Electr. Insul., Vol. 11, pp. 763-784, 2004.
[11] T. Tanaka, M. Kozako, N. Fuse and Y. Ohki, "Proposal of a Multicore Model for Polymer Nanocomposite Dielectrics", IEEE Trans. Dielectr. Electr. Insul., Vol. 12, pp. 669-681, 2005.
[12] J. K. Nelson, J. C. Fothergill, L. A. Dissado and W. Peasgood, "Towards an Understanding of Nanometric Dielectrics", IEEE Conf. Electr. Insul. Dielectr. Phenomena (CEIDP), pp. 295-298, 2002.
[13] A. L. An and S. A. Boggs, "What is "Nano" in the Context of a Filled Dielectric", IEEE Intern. Sympos. Electr. Insul.(ISEI), pp. 273-276, 2006.
[14] T. Tanaka, "Dielectric Nanocomposites with Insulating Properties", IEEE Trans. Dielectr. Electr. Insul., Vol. 12, pp. 914-928, 2005.
[15] M. Roy, J. K. Nelson, R. K. MacCrone, L. S. Schandler, C. W. Reed, R. Keefe and W. Zenger, "Polymer Nanocomposite Dielectrics: The Role of the Interface", IEEE Trans. Dielectr. Electr. Insul., Vol. 12, pp. 629-643, 2005.
[16] M. F. Frechette and C. W. Reed, "The Emerging Field of Nanodielectrics: an Annotated Appreciation", IEEE Intern. Sympos. Electr. Insul. (ISEI), pp. 458-465, 2006.
[17] T. Tanaka and M. Frechette, "Emerging Nanocomposite Dielectrics", CIGRE Task Force Report, ELECTRA, No. 226, pp.24-32, 2006.
[18] U. Sutter and J. Loeffler, "Roadmap Report Concerning the Use of Nanomaterials in the Energy Sector", 6th Framework Programme, p. 88, 2006.
[19] B. X. Fu, M. Namani and A. Lee, "Influence of Phenyl-trisilanol Polyhedral Silsesquioxane on Properties of Epoxy Network Glasses", Polymer, 44, pp. 7739-7747, 2003.
[20] H. Dodiuk, S. Kenig, I Blinsky, A. Dotan and A. Buchman, "Nanotailoring of Epoxy Adhesives by Polyhedral-oligomeric-sil-sesquioxanes (POSS)", Intern. J. Adhesion & Adhesives, Vol. 25, pp. 211-218, 2005.
[21] Y. Ni, S. Zheng and K. Nie, "Morphology and Thermal Properties of Inorganic-organic Hybrids Involving Epoxy Resin and Polyhedral Oligomeric Silsesquioxanes", Polymer, Vol. 45, pp. 5557-5568, 2004.
[22] A. Lee and J. D. Lichtenhan, "Viscoelastic Responses of Polyhedral Oligosilsesquioxane Reinforced Epoxy Systems", Macromolecules, Vol. 31, pp. 4970-4974, 1998.
[23] E. Itoh, H. Karasawa, N. Matsukawa and K. Mivairi, "The Electrical Properties of Glass Like Insulator Prepared by Solution Process and Its Application for Organic Electronic Devices", Intern. Sympos. Electr. Insul. Materials, Kitakyushu, Japan, pp. 646-649, 2005.
[24] Y. Lee, J. Huang, S. Kuo and F. Chang, "Low-dielectric, Nanoporous Polyimide Films Prepared from PEO-POSS Nanoparticles", Polymer, Vol. 46, pp. 10056-10065, 2005.
[25] Y. Lee, J. Huang, S. Kuo, J. Lu and F. Chang, "Polyimide and Polyhedral Oligomeric Silsesquioxane Nanocomposites for Low-dielectric Applications", Polymer, Vol. 46, pp. 173-181, 2005.
[26] M. Vasilopoulou, S. Tsevas, A. M. Douvas, P. Argitis, D. Davazoglou and D. Kouvatsos, "Characterization of Various Low-k dielectrics for Possible Use in Applications at Temperatures below 160 °C", J. Phys.: Conf. Series, Vol. 10, pp. 218-221, 2005.
[27] W. W. Zhu, S. Xiao and I. Shih, "Field-effect Mobilities of Polyhedral Oligomeric Silsesquioxanes Anchored Semiconducting Polymers", Appl. Surface Sci., Vol. 221, pp. 358-363, 2004.
[28] J. Horwath and D. Schweickart, "Inorganic Fillers for Corona Endurance Enhancement of Selected Polymers", IEEE, Air Force Research Library, pp. 644-647, 2002.
[29] J. Horwarth, D. Schweickart, G. Garcia, D. Klosterman and M. Galaska, "Improved Performance of Polyhedral Oligomeric Silsesquioxane Epoxies", IEEE Conf. Electr. Insul. Dielectr. Phenomena (CEIDP), pp.155-157, 2005.
[30] L. Linnamaa and K. Kannus, "Effects of Polyhedral Oligomeric Silsesquioxanes on Partial Discharge Endurance and Electrical Properties of XLPE", Nordic Insul. Sympos., pp. 135-138, 2007.
[31] M. Takala, M. Karttunen, P. Salovaara, S. Kortet, K. Kannus and T. Kalliohaka, "Dielectric properties of nanostructured polypropylene-polyhedral oligomeric silsesquioxane compounds", IEEE Trans. Dielectr. Electr. Insul., Vol. 15, pp. 40-51, 2008.
[32] *Hybrid Plastics Catalog*, 2006.
[33] ISO 527-1,-2: "Tensile Properties", 1996.
[34] ISO 179-1: "Determination of Charpy Impact Properties", 2000.
[35] P. Salovaara, M. Takala and K. Kannus, "Effect of Film Thickness on the Electrical Strength of Polypropylene Compounds", 10th Intern. Electr. Insul. Conf., INSUCON, pp. 131-135, 2006.
[36] IEC Publication 60243-1: "Electrical Strength of Insulating Materials-Test Methods-Part 1: Test at Power Frequencies", 1998.
[37] IEC Publication 60060-1: "High-voltage Test Techniques. Part 1: General Definitions and Test Requirements", 1989.
[38] IEC Publication 250: "Recommended Methods for the Determination of the Permittivity and Dielectric Dissipation Factor of Electrical Insulating Materials at Power, Audio and Radio Frequencies Including Metre Wavelengths", 1969.
[39] IEEE Standard 930: "IEEE Guide for the Statistical Analysis of Electrical Insulation Breakdown Data", IEEE Dielectr. Electr. Insul. Society, 2005.
[40] M. Cacciari, G. Mazzanti and G.C. Montanari, "Weibull Statistics in Short-Term Dielectric Breakdown of Thin Polyethylene Films", IEEE Trans. Dielectr. Electr. Insul., Vol. 1, pp. 153-159, 1994.
[41] P. Salovaara and K. Kannus, "Increasing the Dielectric Breakdown Strength of Polypropylene Using Polyaniline Additive", IASTED Conf. on Energy and Power Systems, pp. 234-239, 2006.
[42] L.A. Dissado and J.C. Fothergill, *Electrical Degradation and Breakdown in Polymers*, IEE Materials and Devices Series, Peter Peregrinus Ltd., London, UK, 1992.
[43] W. Hauschild and W. Mosch, *Statistical Techniques for High-Voltage Engineering*, Peter Peregrinus Ltd., London, UK, 1992.
[44] L. Matějka, J. Lövy, S. Pokorný, K. Bouchal and K. Dušek, "Curing epoxy resins with anhydrides. Model reactions and reaction mechanism", J. Pol. Sci., Polymer Chemistry Edition, Vol. 21, pp. 2873-2885, 1983.
[45] J. Rocks, L. Rintoul, F. Vohwinkel and G. George, "The kinetics and mechanism of cure of an amino-glycidyl epoxy resin by a co-anhydride as studied by FT-Raman spectroscopy", Polymer, Vol. 45, pp. 6799-6811, 2004.
[46] Y. Liu, S. Zheng and K. Nie, "Epoxy Nanocomposites with Octa(propylglycidyl ether) Polyhedral Oligomeric Silsesquioxanes", Polymer 46, pp. 12016-12025, 2005.
[47] I. K. Jones, Y. Zhou and S. Jeelani, "Thermal and Mechanical Properties of Polyhedral-oligomeric-sil-sesquioxanes (POSS) modified SC-15 epoxy", Report, Tuskegee University's Center for Advanced Materials (T-CAM), 2007.

Markus Takala was born in Vaasa, Finland in 1980. He graduated with M.Sc. (Eng.) degree in electrical power engineering from Tampere University of Technology (TUT), Tampere, Finland, 2005. Since 2005 he has been a researcher in the High Voltage Laboratory at TUT. His research interests include topics in new electrical insulation materials. He has published articles on dielectric properties of PP compounds, the main research topics being nano- and microstructured epoxy and PP.

Mikko Karttunen was born in Tampere, Finland in 1955. He received the M.Sc. (Eng.) and Licentiate of Technology degrees in material science and plastics technology from Tampere University of Technology (TUT), in 1980 and 1986, respectively. From 1980 to 1985 he was a research scientist at TUT. From 1985 to 1988 he worked at Neste Oy as a researcher. From 1988 to 1991 he was a research scientist at the Technical Research Centre of Finland (VTT) and since 1991 he has been a senior research scientist at VTT. His research interest is in electrically conductive polymer compounds, compliant electrodes and polymer nanocomposites for electromechanical films and electrical insulation materials.

Authorized licensed use limited to: Tampereen Teknillinen Korkeakoulu. Downloaded on March 23,2010 at 04:49:17 EDT from IEEE Xplore. Restrictions apply.

Jani Pelto was born in Tampere, Finland in 1976. He received the M.Sc. (Eng.) degree in material science and plastics technology from Tampere University of Technology (TUT) in 2001. Since 2001 he has been working as a research scientist at the Technical Research Center of Finland (VTT). His main research interests are synthesis, processing and characterization (AFM, electrochemistry and spectroscopy) of new conductive inherently conductive polymers such as polyanilines, polypyrroles, organic polymer nanocomposites and their applications.

Pauliina Salovaara was born in Mouhijärvi, Finland in 1980. She graduated with M.Sc. (Eng.) degree from the Department of Electrical Power Engineering, Tampere University of Technology, Tampere, Finland in 2004. Since 2004 she has been a researcher in the High Voltage Laboratory at TUT. She has published articles on the dielectric properties of PP compounds. Her research interests include new dielectric material compounds and high voltage engineering.

Tony Munter was born in Porvoo, Finland in 1968. He received the M.Sc. (Eng.) degree in chemistry in 1993 and the Ph.D. degree in organic chemistry in 2000 from Åbo Akademi University, Turku, Finland. From 2001 to 2003 he has been a postdoctoral researcher at the University of Newcastle upon Tyne, UK and from 2003 to 2005 at the Syngenta Central Toxicology Laboratory, Macclesfield, UK. Since 2005 he has been working as a research scientist at the Technical Research Center of Finland (VTT). His main research interests are organic synthesis and surface chemistry.

Mari Honkanen was born in Kangasala, Finland in 1976. She graduated with M.Sc. (Eng.) degree in materials science, Tampere University of Technology (TUT), Tampere, Finland in 2002. Since 2002, she has been a researcher in the Department of Materials Science at TUT. Her current research interest is microscopical characterization (TEM, SEM, AFM) of composites and especially metal-plastic hybrids.

Tommaso Auletta was born in Palermo, Italy in 1972. He received the M.Sc. degree in chemistry in 1995 from the University of Catania, Italy and the Ph.D. degree in chemistry and nanotechnology from the University of Twente, The Netherlands in 2003. From 2003 to 2005 he was Postdoctoral Fellow at The Royal Institute of Technology of Stockholm and from 2005 to 2007 he was a Scientist at ABB Corporate Research, Power Technology Division, in Västerås, Sweden dealing with polymeric nanocomposites and nanofluids for electrical insulation.

Kari Kannus was born in Längelmäki, Finland, on 17 May 1957. He received the M.Sc. (Eng.), Licentiate of Technology and Doctoral degrees in electrical engineering from Tampere University of Technology (TUT) in 1981, 1987 and 1998, respectively. From 1982 to 1988 he was a teaching and research assistant and from 1988 to 1992 he was a laboratory manager at the Institute of Power Engineering of TUT. From 1993 to 1998 he was a researcher and since 1999 he has been a senior researcher at TUT. Since 2002 he has been an Adjunct Professor of High Voltage Engineering at TUT. His main research interests are in the field of high voltage technology, especially overvoltage protection and surge arresters, new polymeric materials and environmental testing.

Authorized licensed use limited to: Tampereen Teknillinen Korkeakoulu. Downloaded on March 23,2010 at 04:49:17 EDT from IEEE Xplore. Restrictions apply.

Publication 6

M. Takala, H. Ranta, J. Pelto, S. Virtanen, V. Koivu, M. Pettersson and K. Kannus, Dielectric Properties of Polypropylene-Silica Nanocomposites, In *Proceedings of Nordic Insulation Symposium* (NORD-IS09), Gothenburg, Sweden, June 15-17, pp. 31-35, (2009)

© 2009 NORD-IS. Reprinted, with permission, from the proceedings of Nordic Insulation Symposium.

Dielectric Properties of Polypropylene-Silica Nanocomposites

M. Takala[1], H. Ranta[1], J. Pelto[2], S. Virtanen[3], V. Koivu[4], M. Pettersson[3] and K. Kannus[1]
[1]*Department of Electrical Energy Engineering, Tampere University of Technology, Tampere, Finland*
[2]*Advanced Materials, Technical Research Centre of Finland, Tampere, Finland*
[3]*Nanoscience Center, Department of Chemistry, University of Jyväskylä, Finland*
[4]*Department of Physics, University of Jyväskylä, Finland*

Abstract

This paper presents the results of the dielectric measurements conducted on polypropylene (PP)-silica nanocomposites. AC and DC breakdown strength of the approximately 20 µm thick material was measured. Relative permittivity, loss factor and volume resistivity measurements were conducted on samples of 500 µm thickness. Statistical analysis was applied to the results to determine the effects of the additive on the dielectric properties of the composite.

The morphology of the material was analyzed with micro-Raman spectroscopy, X-ray tomography and transmission electron microscopy (TEM).

The applicability of the material in high voltage equipment is discussed and evaluated.

1. Introduction

It has been often claimed that high voltage engineering and especially insulation technology is a mature field of research. This means that by implementing new technology, great achievements are possible. Nanotechnology is expected to have an impact on many areas of research. Nanotechnology refers to the use of 1 to 100 nm particle size additives in different applications.

In this paper dielectric properties are presented for silica PP nanocomposites. Earlier research results regarding nanosilica used for purposes of insulation mostly deal with epoxy [1-5], polyimide [6-7], polyamide [7], polyetherimide [8], cross-linked polyethylene [9] and silicone [1-2, 10] as a matrix polymer. One paper [11] presents the use of the smallest form of silica – polyhedral oligomeric silsesquioxane (POSS), in PP matrix. The results of the papers [1-11] indicate that silica nanocomposites are promising materials for the field of insulation e.g. improved voltage endurance, partial discharge resistance and breakdown strength have been reported.

The aim of this study is to determine the dielectric properties of PP-silica nanocomposite and the applicability of the material in high voltage equipment.

2. Materials studied

2.1. Processing

The processing of materials was conducted at the Technical Research Centre of Finland. Borealis HC318BF polypropylene homopolymer was used as a matrix polymer. The premixed materials, polymer powder and 5 wt-% of silica filler (primary particle size 12 nm, surface area 200 m^2/g) were fed into the first zone of the compounder by gravimetric twin screw feeder. Typical parameters in the compounding were: temperature (profile) +180…+200 °C, 300 rpm and torque 60-70 %. High shear screw geometry was used in mixing. The materials were processed into 100 mm x 0.5 mm sheets with minimum orientation in the machine direction. The samples were then biaxially oriented with Brückner KARO IV sheet stretching machine (+162 °C, 471 %/s, draw ratio 5.6 x 5.6, simultaneously). The biaxially oriented sample thickness varied from 10 µm to 22 µm.

2.2. Morphology

The PP-silica composite was characterized with several methods using material which was not biaxially oriented. The nanoscale dispersion of silica in the PP matrix was investigated with TEM. Ultrathin sections of the sample were obtained using a diamond knife at room temperature on a Leica Reichert Ultracut S ultramicrotome. The sections of 95 nm thickness were collected on a copper grid and observed with JEOL-JEM-1200EX electron microscope at 60 kV acceleration voltage. From Fig. 1 b) it can be clearly seen that the nanoparticles are gathered together to form clusters of a few tens to hundreds of particles. The agglomerates are nevertheless mostly in the <100 nm size range. Fig. 1 a) shows that these clusters are dispersed evenly in the polymer matrix.

Particles of several microns were also seen by inspection with an optical microscope. With micro-Raman spectroscopy these particles were identified to be calcite mineral ($CaCO_3$), a contamination presumably from the compounder. A three dimensional

image of the composite structure was obtained by SkyScan 1172 X-ray microtomography device with detail detectability of 0.9 µm. Structure analysis based tomographic images revealed the average volume of the micro-sized particles to comprise 0.8 % of the total sample volume, which corresponds to ~2.3 wt-% assuming the density of calcite to be 2.71 g/cm^3.

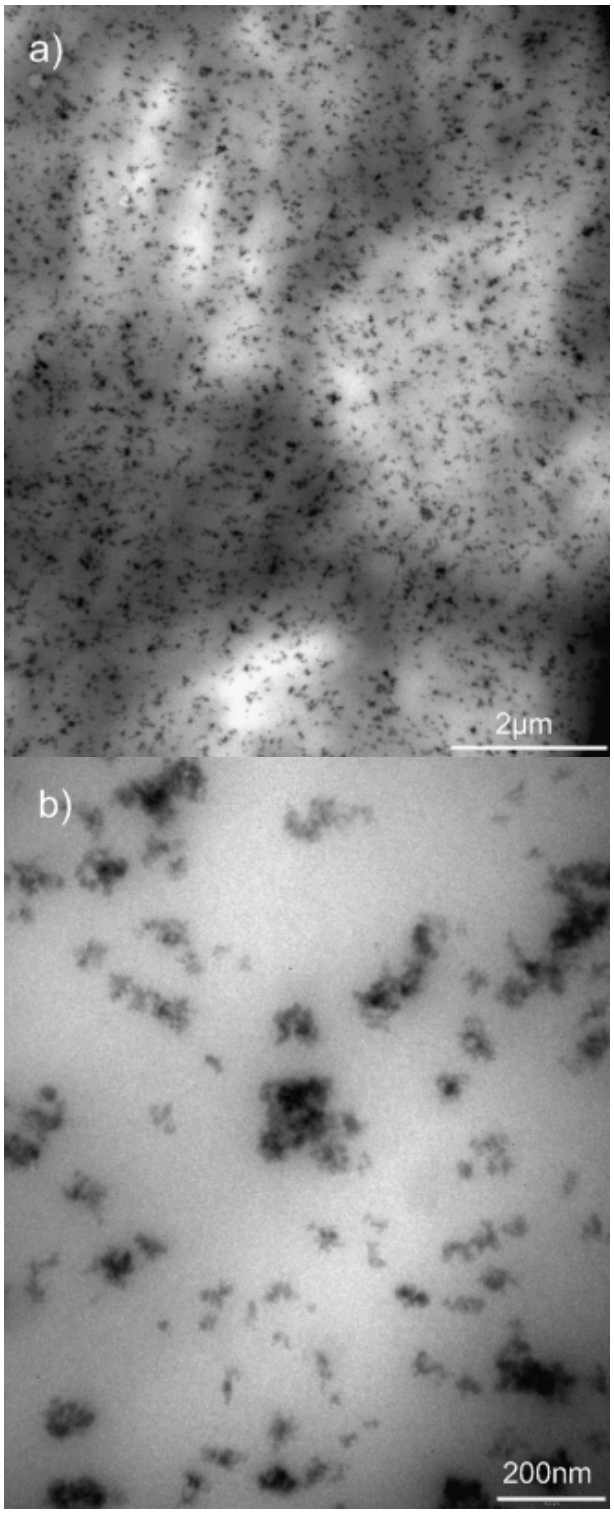

Fig. 1 - TEM micrographs of ultrathin sections of the PP-silica composite.

3. Dielectric measurements and statistical analysis

3.1. Breakdown strength

The AC and DC breakdown strengths of the PP thin films were measured with the same kind of measurement setup. The measurements were conducted with small ∅ 12 mm electrodes (approx. 1 cm^2). The measurements were conducted at room temperature (20 °C) and the samples were immersed in mineral oil (Shell Diala oil DX). Graphite layers between the samples and steel electrodes were used to smoothe the contact to the sample. The samples were manually fixed to the electrode setup. Each sample was stressed with steadily increasing AC (50 Hz) or DC voltage until the breakdown occurred. The voltage ramp used was approximately 400 V/s [12]. The thickness of the samples was measured before immersing the sample in oil. A set of 20 test samples was used with both materials and voltage shapes.

3.2. Dielectric spectroscopy

The complex impedance of PP and PP silica compound was measured as a function of frequency. The measurements were performed using an insulation diagnosis analyzer IDA 200. The frequency range used was from 0.1 Hz to 1 kHz at 140 V_{RMS} voltage. The real part and the imaginary part of the complex permittivity (ε' and ε''), relative permittivity (ε_r) and loss factor (tan δ) were calculated from the measured parallel capacitance and resistance with Equations (1-4).

$$\varepsilon' = \frac{C_P}{C_0} - \frac{C_e}{C_0} \tag{1}$$

$$\varepsilon'' = \frac{1}{R_P C_0 \omega} - \frac{C_e}{C_0} \tag{2}$$

$$\varepsilon_r = \sqrt{\varepsilon'^2 + \varepsilon''^2} \tag{3}$$

$$\tan\delta = \frac{\varepsilon''}{\varepsilon'} \approx \frac{1}{R_P C_P \omega}, C_e << C_P \tag{4}$$

where C_P and R_P, respectively, are the measured parallel capacitance and resistance, C_0 the vacuum capacitance of the measurement setup, C_e the edge capacitance according to IEC standard 250 [13], ω the angular frequency. The thickness of the specimens was determined as an average value of eight measurements. The thickness of the samples varied 380-670 µm.

Table 1. AC and DC breakdown strength measurement results of the pure PP and PP silica compound. From left there are shown number of parallel measurements, mean (kV/mm or V/µm) and two standard deviations (other calculated using Student's T-distribution 95 % confidence intervals). In the next section there are scale α and shape β parameters of Weibull distribution (according to IEEE standard 930), electric field strength corresponding to 95 % breakdown probability and correlation value to 2-parameter Weibull distribution. All parameters representing electric field strength are RMS values.

	n	mean	s	± 95 % confidence	α	β	95 %	cor
AC		V/µm	V/µm	V/µm	V/µm	V/µm	V/µm	
PP ref.	20	361	89	39	400	3.62	542	0.85
silica	20	432	57	25	458	8.62	520	0.97
DC								
PP ref.	20	511	93	41	552	5.75	668	0.92
silica	20	778	89	39	817	10.03	912	0.91

A ∅ 8 cm aluminum foil electrodes were attached to the samples with a small amount of silicone grease according to IEC standard 250 [13].

3.3. Statistical analysis

All the measurement results were transferred to equal the breakdown strength of 9 µm thick film using the power law (Eq. 5) relationship between the breakdown field and the film thickness in order to obtain comparable results.

$$E_2 = E_1\left[d_2 / d_1\right]^{-0.4} \tag{5}$$

In the equation E_2 is the breakdown strength at thickness d_2 (9 µm) and E_1 is the measured value of the film of which the thickness is d_1.

The dielectric breakdown voltage data was plotted on the Weibull probability plots according to a two-parameter Weibull distribution, stating a zero location parameter. The 2-parameter Weibull cumulative distribution function (Eq. 6) is related to the probability of failure occurring in certain field strength x [14].

$$F(x) = 1 - \exp\left\{-\left(\frac{x}{\alpha}\right)^{\beta}\right\} \tag{6}$$

The shape parameter β is related to the shape or the width of the distribution. The spread of the breakdown strengths is narrower when the value of β is greater. Scale parameter α is related to the 63.2 % probability for the sample to break down at electric field strength α [15].

Statistical differences between two materials can be compared by average standard deviation (s_{ave}), which is the weighted average value of the two standard deviations of the materials. The difference between the means (dif) of the materials is compared with relevant sectors. These sectors are not significant (dif ≤ $1.96\times s_{ave}$), almost significant ($1.96\times s_{ave}$ < dif ≤ $2.58\times s_{ave}$), significant ($2.58\times s_{ave}$ < dif ≤ $3.29\times s_{ave}$) and highly significant (dif > $3.29\times s_{ave}$). With these quantiles statistical significance levels can be calculated and the differences between the materials evaluated [16-17].

4. Results of the dielectric measurements

4.1. AC and DC breakdown strength

Table 1 shows the AC and DC breakdown strength measurement results of the pure PP and PP silica compound. The same results are presented graphically in Fig. 2. Silica compound gave higher AC and DC dielectric strengths than the polypropylene reference (per cent values 20 and 52, respectively calculated from the mean values). The value of the critical correlation coefficient for 20 parallel samples is approximately 0.9375 (according to IEEE standard 930) [17]. The correlation values, presented in Table 1 are close to the critical correlation coefficient for all samples. The correlation value for PP reference is low because in two samples breakdown occurred with very low electric field (AC). Without these two measurements the correlation to 2-parameter Weibull distribution would have been 0.99. But the weak samples also have to be taken into account.

The Weibull probability plots with 90 % confidence bounds are shown in Figs. 3 and 4 for pure PP and silica-PP composite with AC and DC voltages. Relative standard deviation in the measurements was 7.4 %. Especially with DC breakdown strength measurements the confidence intervals are quite narrow. Breakdown strength measurements with silica-PP composite are shifted towards higher electric field strengths (to the right). Statistically the changes in AC and DC breakdown strengths were respectively not significant and significant.

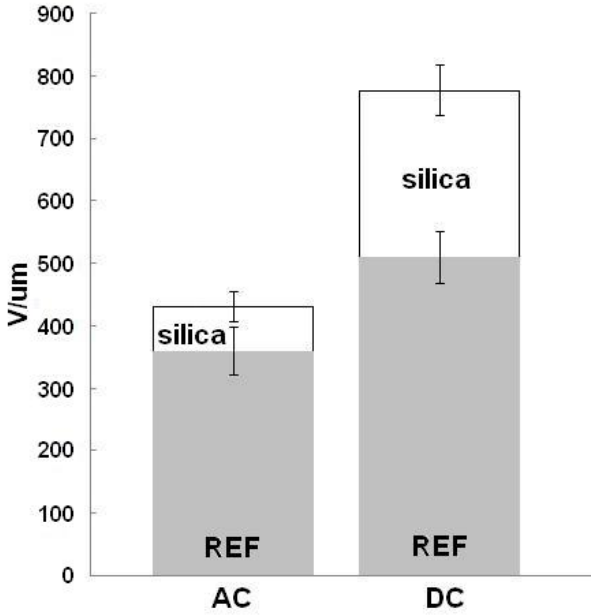

Fig. 2 - AC and DC breakdown strengths (V/µm, RMS) of pure PP and silica-PP composite with their 95 % confidence limits.

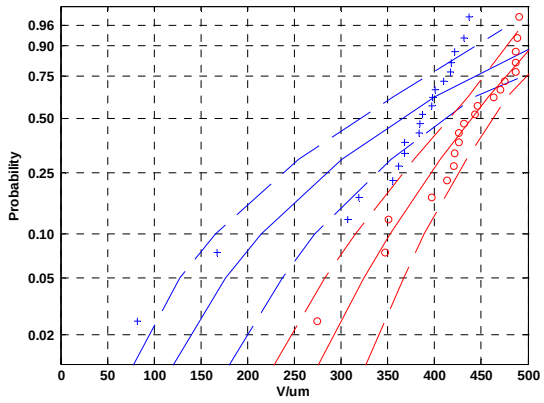

Fig. 3 - AC breakdown strength (V/µm, RMS) measurements of the PP reference (+) and silica-PP composite (o) presented in Weibull probability plot.

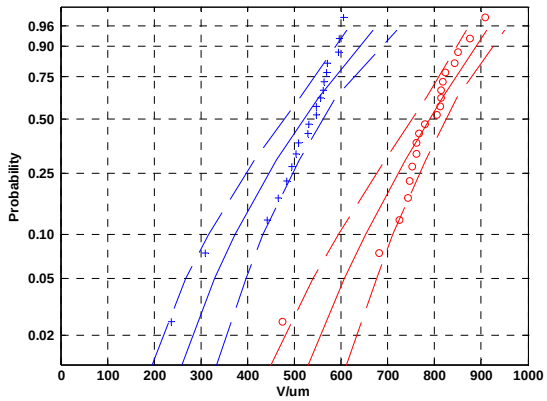

Fig. 4 - DC breakdown strength (V/µm, RMS) measurements of the PP reference (+) and silica-PP composite (o) presented in Weibull probability plot.

4.2. Dielectric spectroscopy

The results of relative permittivity, loss factor and volume resistivity measurements of pure PP and PP silica compound are presented in Figs. 5-7. Three parallel measurements were done on all samples in order to determine the deviation. Relative deviations in permittivity, loss factor and volume resistivity varied between 0.01-0.04 %, 2.2-18.4 % and 2.2-18.4 % respectively. Relative permittivity increased 2.3 % at 50 Hz with silica-PP composite compared to pure PP and at the same time the dielectric losses remained as low as with pure PP. Thus, considering the relative permittivity increase and losses remaining at the same level with the reference, the dielectric properties of the silica-PP composite are indeed encouraging.

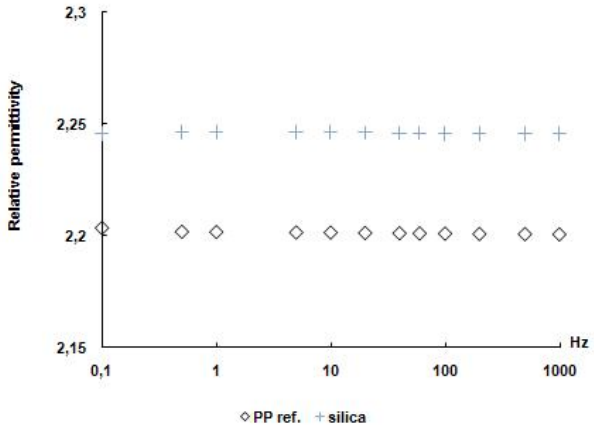

Fig. 5 - Relative permittivity of pure PP and silica-PP composite as a function of frequency.

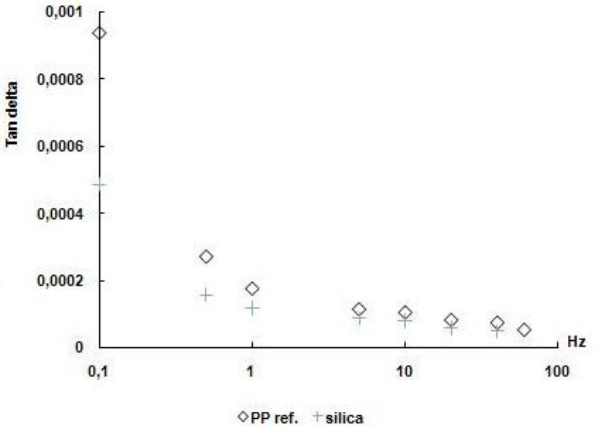

Fig. 6 - Loss factor of pure PP and silica-PP composite as a function of frequency.

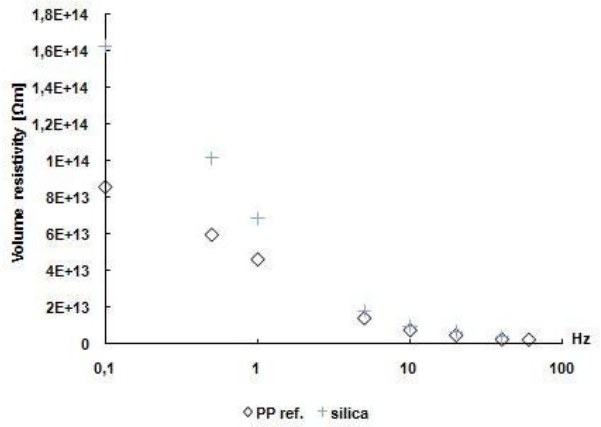

Fig. 7 - The volume resistivity of pure PP and silica-PP composite as a function of frequency.

5. Conclusion

PP containing silica nanoparticles showed a promising combination of dielectric properties compared to pure PP. The AC and DC breakdown strength of silica-PP composite increased 20 % and 52 % respectively. Usually the dielectric losses have also increased hand in hand with breakdown strength, but with silica-PP composite losses remained comparable to pure PP. The relative permittivity of the silica-PP composite increased by 2.6 % compared to the reference material. Further repetitive studies are still needed to confirm these promising results.

Acknowledgment

The authors want to thank Specialized Research Mechanicians Raija Vassinen and Paavo Niutanen at Department of Biological and Environmental Science in University of Jyväskylä, for their indispensable contribution considering TEM analysis.

6. References

[1] T. Tanaka and M. Frechette, "Emerging Nanocomposite Dielectrics", CIGRE Task Force Report, ELECTRA, No. 226, pp.24-32, 2006.
[2] T. Tanaka, "Dielectric Nanocomposites with Insulating Properties", IEEE Trans. Dielectr. Electr. Insul., Vol. 12, No. 5, pp. 914-928, 2005.
[3] K. Jiang, L. Cheng, L. Zheng, Z. Yao, G. Li and Q. Yin, "The Unique Dielectric Behaviour of Nanosilica Epoxy Composites", Proceedings of the 7th IEEE International Conference on Nanotechnology, Hong Kong, 2-5 August 2007, pp. 1101-1106, 2007.
[4] T. Imai, G. Komiya, K. Murayama, T. Ozaki, F. Sawa, T. Shimizu, M. Harada, M. Ochi, Y. Ohki and T. Tanaka, "Improving Epoxy-based Insulating Materials with Nano-fillers toward Practical Application", IEEE International Symposium on Electrical Insulation, Vancouver, Canada, 8-11 June 2008, pp. 201-204, 2008.
[5] T. Tanaka, Y. Ohki, M. Ochi, M. Harada and T. Imai, "Enhanced Partial Discharge Resistance of Epoxy/Clay Nanocomposite Prepared by Newly Developed Organic Modification and Solubilization Methods", IEEE Trans. Dielectr. Electr. Insul., Vol. 15, No. 1, pp. 81-89, 2005.
[6] M. Zhang, S. Zeng, T. Dong, Y. Fan and Q. Lei, "Study on the Dielectric Properties of Polyimide/Silica Nanocomposite Films", 8th International Conference on Properties and Applications of Dielectric Materials, 26-30 June 2006, pp. 733 – 735, 2006.
[7] F. Guastavino, E. Torello, A. Dardano, S. Bono, M. Pellegrini and L. Vignati, "A comparison of the short and long term behaviour of nanostructured enamels with the performances of conventional insulation" IEEE International Symposium on Electrical Insulation, Vancouver, Canada, 8-11 June 2008, pp. 659-662, 2008.
[8] B. Chen, J. Du and C. Hou, "The Effects of Chemical Structure on the Dielectric Properties of Polyetherimide and Nanocomposites" IEEE Trans. Dielectr. Electr. Insul., Vol. 15, No. 1, pp. 127-133, 2008.
[9] C. Zou, J. C. Fothergill, M. Fu and J. K. Nelson, "Improving the Dielectric Properties of Polymers by Incorporating Nano-particles", 10th International Electrical Insulation Conference, INSUCON, Birmingam, UK, May 24-26 2006, pp. 125-130, 2006.
[10] S. Rätzke and J. Kindersberger, "Erosion Behaviour of Nano Filled Silicone Elastomers", XIVth Intern. Sympos. High Voltage Eng. (ISH), pp. 1-6, 2005.
[11] M. Takala, M. Karttunen, P. Salovaara, S. Kortet, K. Kannus and T. Kalliohaka, "Dielectric Properties of Nanostructured Polypropylene-Polyhedral Oligomeric Silsesquioxane Compounds", IEEE Trans. Dielectr. Electr. Insul., Vol. 15, No. 1, pp. 40-51, 2008.
[12] IEC Publication 60243-1: "Electrical Strength of Insulating Materials-Test Methods-Part 1: Test at Power Frequencies", 1998.
[13] IEC Publication 250: "Recommended Methods for the Determination of the Permittivity and Dielectric Dissipation Factor of Electrical Insulating Materials at Power, Audio and Radio Frequencies Including Metre Wavelengths", 1969.
[14] L.A. Dissado and J.C. Fothergill, "Electrical Degradation and Breakdown in Polymers", IEE Materials and Devices Series, Peter Peregrinus Ltd., London, UK, 1992.
[15] P. Salovaara and K. Kannus, "Increasing the Dielectric Breakdown Strength of Polypropylene Using Polyaniline Additive", IASTED Conf. on Energy and Power Systems, pp. 234-239, 2006.
[16] W. Hauschild and W. Mosch, Statistical Techniques for High-Voltage Engineering, Peter Peregrinus Ltd., London, UK, 1992.
[17] IEEE Standard 930: "IEEE Guide for the Statistical Analysis of Electrical Insulation Breakdown Data", IEEE Dielectr. Electr. Insul. Society, 2005.

Publication 7

M. Takala, B. Sonerud, H. Ranta, J. Pelto, S. Ahonen, M. Pettersson and K. Kannus, Effect of Low Amount of Nanosilica on Dielectric Properties of Polypropylene, In *Proceedings of IEEE International Conference on Solid Dielectrics* (ICSD 2010), Potsdam, Germany, July 4-9, pp. 187-191, (2010)

© 2010 IEEE. Reprinted, with permission, from the proceedings of IEEE International Conference on Solid Dielectrics.

This material is posted here with permission of the IEEE. Such permission of the IEEE does not in any way imply IEEE endorsement of any of the Tampere University of Technology's products or services. Internal or personal use of this material is permitted. However, permission to reprint/republish this material for advertising or promotional purposes or for creating new collective works for resale or redistribution must be obtained from the IEEE by writing to pubs-permissions@ieee.org. By choosing to view this material, you agree to all provisions of the copyright laws protecting it.

Effect of Low Amount of Nanosilica on Dielectric Properties of Polypropylene

M. Takala[1], B. Sonerud[2], H. Ranta[1], J. Pelto[3], S. Ahonen[4], M. Pettersson[4] and K. Kannus[1]

[1]Tampere University of Technology, Department of Electrical Energy Engineering
Tampere, Finland

[2]Chalmers University of Technology, Department of Materials and Manufacturing Technology
Gothenburg, Sweden

[3]VTT Technical Research Centre of Finland, Advanced Materials
Tampere, Finland

[4]University of Jyväskylä, Department of Chemistry, Nanoscience Center
Jyväskylä, Finland

Abstract- **This paper presents the results of the dielectric properties measurements conducted on Silica-Polypropylene (PP) nanocomposites. According to prior investigations by the authors silica nanoparticles have improved the performance of the dielectric material considering capacitor applications. Especially breakdown strengths with ac and dc voltages and resistance against surface degradation have increased. The relative permittivity and dielectric losses have also been comparable to reference PP. In this paper the results of the dielectric measurements conducted on composites with 1-2 wt-% silica are compared with reference PP. Silica dispersion in PP was confirmed with transmission electron microscopy (TEM). Weibull analysis was applied to the breakdown strength measurement results with dc voltage. Capacitance and loss factor measurements were conducted as a function of temperature to study thermal behavior. The measurements were conducted at the high voltage laboratories of Tampere University of Technology and Chalmers University of Technology. Statistical analysis was applied to the results to determine the significance of the differences between the materials.**

Keywords-nanodielectric, polypropylene, silica, dielectric properties

I. INTRODUCTION

The use of nanoadditives in dielectric materials has made great progress in the last few years. Nanosilica has mostly been used in other matrices than in PP. Earlier research results regarding nanosilica used for purposes of insulation mostly deal with epoxy [1-8] and silicone [9-12] but other matrices such as polyimide [13-14], polyamide [14], polyetherimide [15] and cross-linked polyethylene [16] have also been used. One paper [17] presents the use of the smallest form of silica – polyhedral oligomeric silsesquioxane (POSS), in PP matrix. The results of the papers [1-17] indicate that silica nanocomposites are emerging materials in the field of insulation: improved voltage endurance, partial discharge resistance and breakdown strength have been reported.

This study concentrates on the dielectric properties of PP nanocomposites. Nanosilica contents of 1 and 2 wt-% were chosen because small amounts are more easily dispersed in nanoscale in the matrix. The paper discusses the applicability of nanocomposite material in high voltage equipment. This study is a continuation of the work published in [18].

II. EXPERIMENTAL

A. Materials used

The materials were processed at the Technical Research Centre of Finland (VTT). Polypropylene homopolymer (MFR 3.2, ISO 1133) from Borealis Polymers N. V. was used as a matrix polymer. The polypropylene used was designed for capacitor films. The silica filler used was Aeroxide LE2 hydrophobic fumed silica from Evonik Degussa GmbH. Silica-PP nanocomposites with 1 and 2 wt-% of silica filler were processed. The premixed materials, polymer powder and silica filler were fed into the first zone of the compounder (Berstorff ZE 25x48D) by a gravimetric twin screw feeder. Parameters in the compounding were: temperature +200 °C, 300 rpm, torque 60-70%. High shear screw geometry was used for mixing. The wt-% of the mixture was calculated from the weight of the polymer. The materials were processed into 100 mm x 0.5 mm sheets with minimum orientation in the machine direction with Brabender Plasticorder single screw extruder (∅ 18 mm) using a flat die. The samples were then bi-axially oriented with a sheet stretching machine (Brückner KARO IV). The thickness of the biaxially oriented samples varied from 17 µm to 27 µm.

978-1-4244-7944-3/10/$26.00 ©2010 IEEE

B. Dc breakdown strength measurements

Dc breakdown strength of the test samples was measured at Tampere University of Technology. The measurements were performed at RT (20 °C). The size of the test samples was approximately 3 cm x 3 cm. Rod-like electrodes having a diameter of 12 mm and made of stainless steel were used in the measurements. Graphite layers between the samples and steel electrodes were used to smooth the contact to the sample. The samples were manually fixed to the electrode setup (Fig. 1.). The measurements were performed by immersing the sample and the electrodes in mineral oil (Shell Diala DX) in order to avoid surface discharges and the edges of the electrodes (r =1 mm) were also rounded for that reason. The thickness of the samples was measured before immersing the sample in oil. Each sample was stressed with steadily increasing dc voltage until breakdown occurred. The voltage ramp used was approximately 400 V/s [19]. A set of 20 test samples was used with all materials.

C. Dielectric response

Dielectric response of the samples was measured using Arbitrary Waveform Impedance Spectroscopy (AWIS) presented in [20]. The measurements were conducted at Chalmers University of Technology. The measurement system (Fig. 2.) was designed to measure dielectric response using arbitrary repetitive voltage signals. Both the applied voltage signal and the current response were measured by a data acquisition card (DAC) and Fourier transformed into the frequency domain where a dielectric response spectrum can be extracted. The system demands careful calibration procedures to be accurate [20]. In the present study, AWIS was used as a low voltage Frequency Domain Spectroscopy (FDS) instrument in order to perform dielectric response measurements on low impedance (i.e. high capacitance), low loss test objects not easily characterized by commercial instruments. The measurement setup used is similar to that presented in [21], where aluminum bars are used as connectors in order to reduce series resistance and inductance.

A ∅ 3 cm silver electrodes were painted on film samples in order to ensure good contact to the material. After painting the samples were heat treated at 60 °C for 18 h under compressive stress in order to avoid creasing of the film. Creasing of the film can cause cracking of the silver paint layer, distorting the measurements. One advantage of the heat treatment is also to exclude the moisture from the insulation. Three samples of each material were measured and three data points were collected at each frequency and temperature (43 Hz…43 kHz; RT (22 °C), 40 °C, 60 °C, 80 °C and 100 °C). The voltage used was 4 V_{peak}.

D. Statistical analysis

Statistical analysis was applied to the breakdown strength measurement results. Results were calculated according to the IEEE standard "IEEE Guide for the Statistical Analysis of Electrical Insulation Breakdown Data" [23] using Microsoft Excel and Matlab programs. All the measurement results were transferred to equal the breakdown strength of 9 µm thick film using the power law (Eq. 1) relationship between the breakdown field and the film thickness in order to obtain comparable results.

$$E_2 = E_1\left[d_2 \big/ d_1\right]^{-0.4} \tag{1}$$

In the equation E_2 is the breakdown strength at thickness d_2 (9 µm) and E_1 is the measured value of the film the thickness of which is d_1 [23]. The dielectric breakdown voltage data was plotted on the Weibull probability plot according to a two-parameter Weibull distribution, stating a zero location parameter. The 2-parameter Weibull cumulative distribution function (Eq. 2) is related to the probability of failure occurring in certain field strength x.

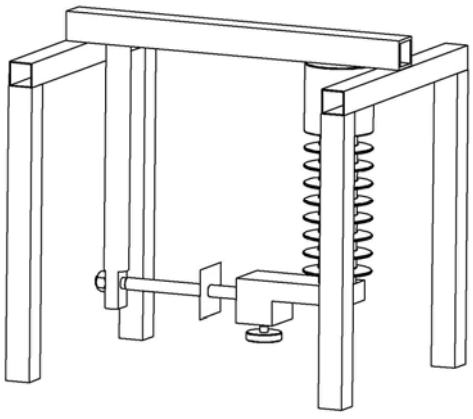

Fig. 1. Measurement bench for breakdown strength measurements.

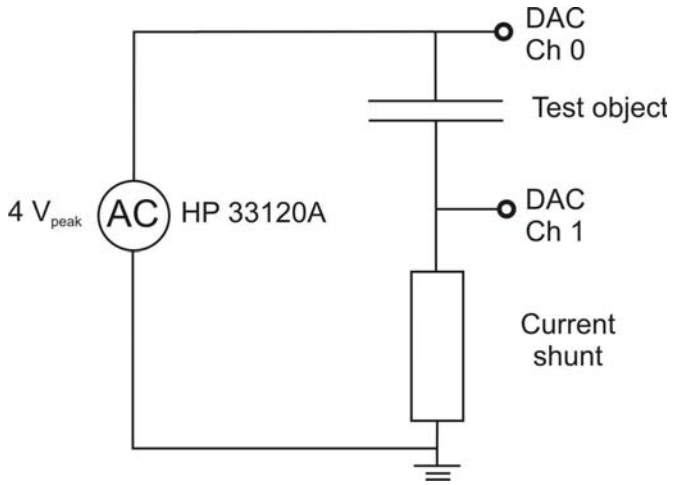

Fig. 2. Measurement setup for dielectric response measurements.

$$F(x) = 1 - \exp\left\{-\left[\frac{x}{\beta}\right]^{\alpha}\right\} \quad (2)$$

The shape parameter β is related to the shape or the width of the distribution. The spread of the breakdown strengths is narrower when the value of β is higher. There is a smaller scattering of the dielectric strength values and consequently higher reliability of the dielectric behavior of the material when the shape parameter is high. Scale parameter α is related to the 63.2 % probability that the sample will break down at electric field strength α [24].

Statistical differences between two materials can be compared by average standard deviation (s_{ave}), which is the weighted average value of the two standard deviations of the materials. The difference between e. g. the breakdown strength means (dif) of the materials is compared with relevant sectors. These sectors are not significant (dif $\leq 1.96\times s_{ave}$), almost significant ($1.96\times s_{ave} <$ dif $\leq 2.58\times s_{ave}$), significant ($2.58\times s_{ave} <$ dif $\leq 3.29\times s_{ave}$) and extremely significant (dif $> 3.29\times s_{ave}$). With these quantiles statistical significance levels can be calculated and differences between the materials evaluated [23-24].

III. Results

A. Morphology

The nanoscale dispersion of silica in the PP matrix was investigated with TEM at the University of Jyväskylä. Approximately 100 nm thick slices of the samples were cut at room temperature with Reicher-Jung Ultracut ultramicrotome using a glass knife. The sections were collected on a copper grid and observed with JEOL-JEM-1200EX electron microscope at a 60 kV acceleration voltage. The smallest particle size is about 10 nm for the 1 wt-% silica-PP nanocomposite. From Fig. 3 it can be seen that the particles form agglomerates mostly in <100 nm size range and these agglomerates are dispersed evenly in the polymer matrix.

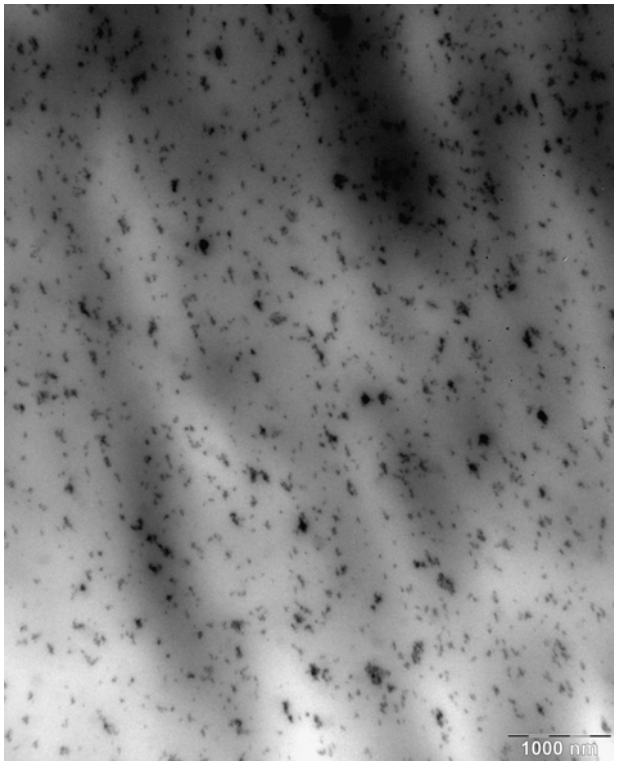

Fig. 3. TEM micrograph of ultrathin section of the 1 wt-% Silica-PP nanocomposite.

B. Dc breakdown strength

The results of dc breakdown strength measurements are presented in Figs. 4-5. As usual with nanocomposites the dc breakdown strength is positively affected [18]. 1 wt-% Silica-PP nanocomposite gave slightly higher dc breakdown strength results than the reference material. It is equally important that the β value of the nanocomposite is higher than with the reference, an indicator of smaller standard deviation and homogeneous material. This phenomenon has an interesting impact on insulation system design, because safety margins can be reduced. The results also suggest that with even low amount of nanofiller addition changes can be observed. By still improving the dispersion of nanosilica advantages can be seen with even lower wt-% values. The Weibull probability plot with 90 % confidence bounds is shown in Fig. 5 for measured materials with dc voltage. With 1 wt-% Silica-PP nanocomposite dc breakdown strength values are shifted to higher electric field strength values. Statistically the change between reference PP and 1 wt-% Silica-PP nanocomposite was not significant.

C. Dielectric response

The results of dielectric response measurements (capacitance and loss factor) of reference PP and Silica-PP nanocomposites are presented in Figs. 6-9. Three different samples of each composition were used and the average dielectric response is presented. Relative deviation in repeated capacitance measurements of the same sample was less than 0.3 ‰ (Fig. 6.) and in loss factor measurements in the order of 10^{-4} (Figs. 7-9). The largest deviations were achieved with the lowest frequencies (<100 Hz) due to small capacitive current (microamperes at 43 Hz) in the circuit. At higher frequencies (>10 kHz) reliable results are not available due to line inductances. Normalized capacitance did decrease with all materials as a function of temperature. It has also been reported in [25] that PP capacitors have a negative temperature coefficient. The capacitance of 1 and 2 wt-% Silica-PP nanocomposites remain higher at 80 °C and 100 °C compared to reference PP. At 100 °C the capacitance of 1 wt-% Silica-PP nanocomposite is 1.5 % higher than with PP reference. Loss factors with all materials behaved in the same way with increasing temperature. Measurements at 40 °C and 80 °C were omitted from Figs. 7-9 to show the differences more clearly. It seems that with respect to standard deviations in the

measurements the loss factor of 1 wt-% Silica-PP nanocomposite is slightly lower than with reference PP. The loss factor of 2 wt-% Silica-PP nanocomposite is slightly higher than with 1 wt-% Silica-PP nanocomposite. At low nanofiller concentrations the large volume fraction of interfaces and polymer chain entanglements decrease the motion of charge carriers, thereby reducing dielectric losses [26].

V. Conclusion

Dielectric properties measurements were performed for silica-PP nanocomposites. TEM pictures from the samples revealed that silica is well distributed in the matrix and no large agglomerates of the additive could be found (Fig. 3.).

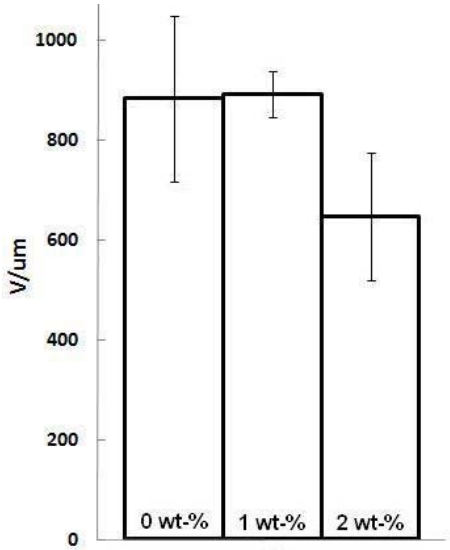

Fig. 4. Breakdown strength mean and standard deviation of the studied materials at dc voltage.

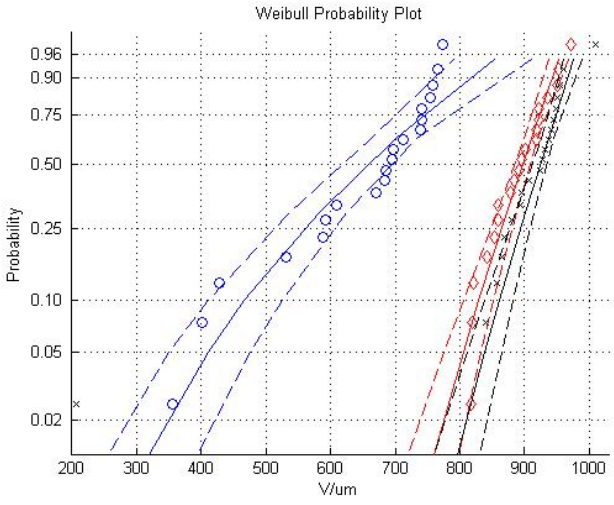

Fig. 5. Breakdown strength of the studied materials (PP Ref. 'X', 1 wt-% Silica-PP '◊' and 2 wt-% Silica-PP 'O') at dc voltage presented in Weibull probability plot.

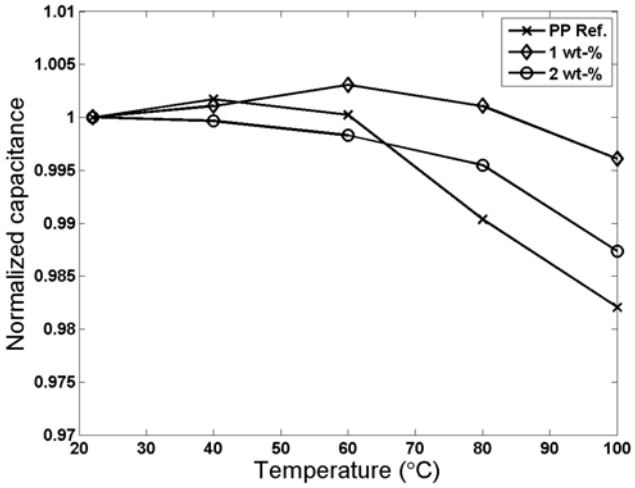

Fig. 6. Normalized capacitance of the studied materials as a function of temperature.

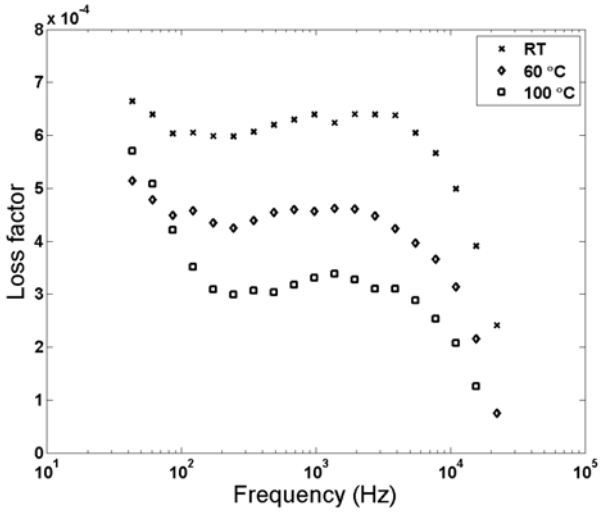

Fig. 7. Dielectric losses for PP Ref. at RT, 60 °C and 100 °C.

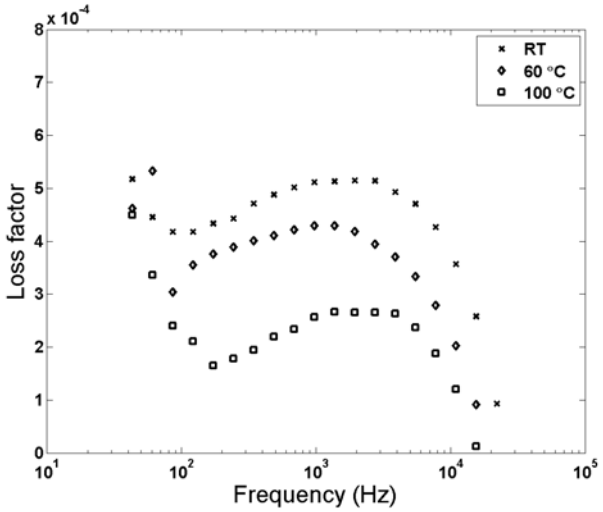

Fig. 8. Dielectric losses for 1 wt-% Silica-PP nanocomposite at RT, 60 °C and 100 °C.

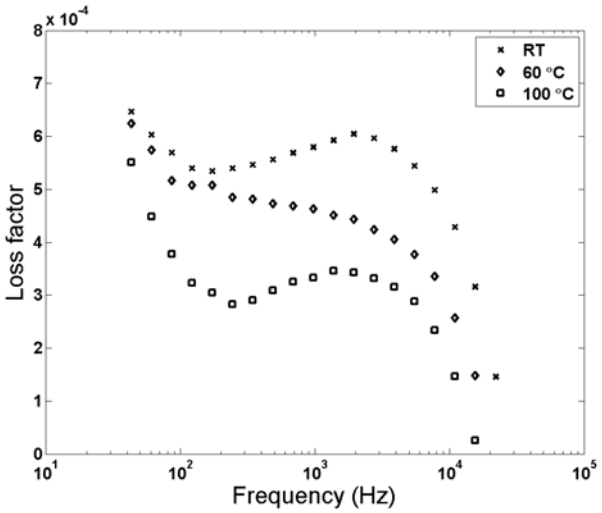

Fig. 9. Dielectric losses for 2 wt-% Silica-PP nanocomposite at RT, 60 °C and 100 °C.

The dc breakdown strength of 1 wt-% Silica-PP nanocomposite was slightly higher than with reference PP. It is equally important that the β value of the nanocomposite is higher than in the reference, an indicator of smaller standard deviation and homogeneous material. The capacitance of 1 and 2 wt-% Silica-PP nanocomposites remain higher at 80 °C and 100 °C compared to reference PP. It also seems that with respect to standard deviations in the measurements the loss factor of 1 wt-% Silica-PP nanocomposite is lower than with reference PP.

REFERENCES

[1] T. Tanaka and M. Frechette, "Emerging Nanocomposite Dielectrics", CIGRE Task Force Report, ELECTRA, No. 226, pp. 24-32, 2006.

[2] K. Jiang, L. Cheng, L. Zheng, Z. Yao, G. Li and Q. Yin, "The Unique Dielectric Behaviour of Nanosilica Epoxy Composites", Proceedings of the 7th IEEE International Conference on Nanotechnology, pp. 1101-1106, 2007.

[3] T. Imai, G. Komiya, K. Murayama, T. Ozaki, F. Sawa, T. Shimizu, M. Harada, M. Ochi, Y. Ohki and T. Tanaka, "Improving Epoxy-based Insulating Materials with Nano-fillers toward Practical Application", Conf. Record of the 2008 IEEE International Symposium on Electr. Insul., pp. 201-204, 2008.

[4] T. Tanaka, Y. Ohki, M. Ochi, M. Harada and T. Imai, "Enhanced Partial Discharge Resistance of Epoxy/Clay Nanocomposite Prepared by Newly Developed Organic Modification and Solubilization Methods", IEEE Trans. Dielectr. Electr. Insul., Vol. 15, pp. 81-89, 2005.

[5] T. Imai, F. Sawa, T. Nakano, T. Ozaki, T. Shimizu, M. Kozako and T. Tanaka, "Effects of Nano- and Micro-filler Mixture on Electrical Insulation Properties of Epoxy Based Composites", IEEE Trans. Dielectr. Electr. Insul., Vol. 13, pp. 319-326, 2006.

[6] T. Iizuka, K. Uchida and T. Tanaka, "Different Voltage Endurance Characteristics of Epoxy/silica Nanocomposites Prepared by Two Kinds of Dispersion Methods", IEEE Conf. Electr. Insul. Dielectr. Phenomena (CEIDP), pp. 236-239, 2007.

[7] T. Tanaka, Y. Matsuo and K. Uchida, "Partial Discharge Endurance of Epoxy/SiC Nanocomposite", IEEE Conf. Electr. Insul. Dielectr. Phenomena (CEIDP), pp. 13-16, 2008.

[8] T. Iizuka, Y. Ohki and T. Tanaka, "Effects of Coupling Agents and Filler Dispersion on V-t Characteristics of Epoxy/Silica Nanocomposites", Proceedings of International Symposium on Electrical Insulating Materials, pp. 60-63, 2008.

[9] I. Ramirez, E. A. Cherney, S. Jayaram and M. Gauthier, "Silicone Rubber Nanocomposites for Outdoor Insulation Applications", IEEE Conf. Electr. Insul. Dielectr. Phenomena (CEIDP), pp. 384-387, 2007.

[10] I. Ramirez, S. Jayaram, E. A. Cherney, M. Gauthier and L. Simon, "Erosion Resistance and Mechanical Properties of Silicone Nanocomposite Insulation", IEEE Trans. Dielectr. Electr. Insul., Vol. 16, pp. 52-59, 2009.

[11] N. A. Perez, A. Sylvestre, J. L. Auge, M. T. Do and S. Rowe, "Dielectric Spectroscopy in Silicone Rubber Incorporating Nanofillers", IEEE Conf. Electr. Insul. Dielectr. Phenomena (CEIDP), pp. 453-456, 2006.

[12] A. H. El-Hag, L. C. Simon, S. H. Jayaram and E. A. Cherney, "Erosion Resistance of Nano-filled Silicone Rubber", IEEE Trans. Dielectr. Electr. Insul., Vol. 13, pp. 122-128, 2006.

[13] M. Zhang, S. Zeng, T. Dong, Y. Fan and Q. Lei, "Study on the Dielectric Properties of Polyimide/Silica Nanocomposite Films", 8th International Conference on Properties and Applications of Dielectric Materials, pp. 733 – 735, 2006.

[14] F. Guastavino, E. Torello, A. Dardano, S. Bono, M. Pellegrini and L. Vignati, "A Comparison of the Short and Long Term Behaviour of Nanostructured Enamels with the Performances of Conventional Insulation" Conf. Record of the 2008 IEEE International Symposium on Electr. Insul., pp. 659-662, 2008.

[15] B. Chen, J. Du and C. Hou, "The Effects of Chemical Structure on the Dielectric Properties of Polyetherimide and Nanocomposites" IEEE Trans. Dielectr. Electr. Insul., Vol. 15, pp. 127-133, 2008.

[16] C. Zou, J. C. Fothergill, M. Fu and J. K. Nelson, "Improving the Dielectric Properties of Polymers by Incorporating Nano-particles", 10th International Electrical Insulation Conference, INSUCON, Birmingam, UK, May 24-26 2006, pp. 125-130, 2006.

[17] M. Takala, M. Karttunen, P. Salovaara, S. Kortet, K. Kannus and T. Kalliohaka, "Dielectric Properties of Nanostructured Polypropylene-Polyhedral Oligomeric Silsesquioxane Compounds", IEEE Trans. Dielectr. Electr. Insul., Vol. 15, pp. 40-51, 2008.

[18] M. Takala, H. Ranta, J. Pelto, S. Virtanen, V. Koivu, M. Pettersson, K. Kannus, "Dielectric Properties of Polypropylene-Silica Nanocomposites", 21st Nordic Insulation Symposium, NORD-IS09, Gothenburg, Sweden, June 15-17 2009, pp. 31-35, 2009.

[19] IEC Publication 60243-1: "Electrical Strength of Insulating Materials-Test Methods-Part 1: Test at Power Frequencies", 1998.

[20] B. Sonerud, T. Bengtsson, J. Blennow, and S. M. Gubanski, "Dielectric response measurements utilizing semi-square voltage waveforms", IEEE Trans. Dielectr. Electr. Insul., Vol. 15, pp. 920-926, 2008.

[21] B. Sonerud, T. Bengtsson, J. Blennow, and S. M. Gubanski, "High voltages with high harmonic content: The influence on dielectric heating" in Proceedings of the 16th International Symposium of High Voltage Engineering (ISH 09), Cape Town, South Africa, 2009.

[22] IEC 60270: "High-Voltage Test Techniques - Partial Discharge Measurements", 2000.

[23] IEEE Standard 930: "IEEE Guide for the Statistical Analysis of Electrical Insulation Breakdown Data", IEEE Dielectr. Electr. Insul. Society, 2005.

[24] W. Hauschild and W. Mosch, Statistical Techniques for High-Voltage Engineering, Peter Peregrinus Ltd., London, UK, 1992.

[25] P. K. Bun and S. P. Kang, "Temperature Coefficient and Capacitance Retrace of Polypropylene Film Capacitors", IEEE Trans. Electr. Insul., Vol. EI-9, pp. 5-11, 1974.

[26] S. Singha and M. J. Thomas, "Dielectric Properties of Epoxy Nanocomposites", IEEE Trans. Dielectr. Electr. Insul., Vol. 15, pp. 12-23, 2008.

Publication 8

M. Takala, H. Ranta, P. Nevalainen, P. Pakonen, J. Pelto, M. Karttunen, S. Virtanen, V. Koivu, M. Pettersson, B. Sonerud and K. Kannus, Dielectric Properties and Partial Discharge Endurance of Polypropylene-Silica Nanocomposite, *IEEE Transactions on Dielectrics and Electrical Insulation*, Vol. 17, No. 4, pp. 1259-1267, (2010)

© 2010 IEEE. Reprinted, with permission, from IEEE Transactions on Dielectrics and Electrical Insulation.

This material is posted here with permission of the IEEE. Such permission of the IEEE does not in any way imply IEEE endorsement of any of the Tampere University of Technology's products or services. Internal or personal use of this material is permitted. However, permission to reprint/republish this material for advertising or promotional purposes or for creating new collective works for resale or redistribution must be obtained from the IEEE by writing to pubs-permissions@ieee.org. By choosing to view this material, you agree to all provisions of the copyright laws protecting it.

Dielectric Properties and Partial Discharge Endurance of Polypropylene-Silica Nanocomposite

M. Takala[1], H. Ranta[1], P. Nevalainen[1], P. Pakonen[1], J. Pelto[2], M. Karttunen[2], S. Virtanen[3], V. Koivu[3], M. Pettersson[3], B. Sonerud[4] and K. Kannus[1]

[1]Tampere University of Technology
FI-33101 Tampere, Finland

[2]Technical Research Centre of Finland
FI-33101 Tampere, Finland

[3]University of Jyväskylä
FI-40014 Jyväskylä, Finland

[4]Chalmers University of Technology
SE-41296 Gothenburg, Sweden

ABSTRACT

This paper presents the results of the dielectric properties and partial discharge endurance measurements conducted on polypropylene (PP)-silica nanocomposite. The material compounds were analyzed with micro-Raman spectroscopy, X-ray tomography and transmission electron microscopy (TEM). ac and dc breakdown strength of the materials was measured. Dielectric response, capacitance and loss factor of the film samples were measured as a function of temperature and frequency. Partial discharge (PD) endurance of the reference PP and PP Silica nanocomposite was studied as a function of ac voltage. Material surfaces were analyzed after PD stress with optical microscopy. All dielectric measurements were done for oriented thin films with a thickness of 11-23 μm. The results were analyzed statistically to determine the effects of the additive on the properties of PP. The paper discusses the potential of PP Silica nanocomposite with a view to high voltage applications, especially power capacitors.

Index Terms — **Dielectric properties, partial discharge, silica, polypropylene, nanocomposite.**

1 INTRODUCTION

THE use of nanoadditives in dielectric materials has made great progress in the last few years. Many papers discussing the general overview, theory and the functionality of nanocomposite dielectrics have been published [1-16]. Nanosilica has mostly been used in other matrices than in PP. Earlier research results regarding nanosilica used for purposes of insulation mostly deal with epoxy [17-24] and silicone [25-28] but other matrices such as polyimide [29-30], polyamide [30], polyetherimide [31] and cross-linked polyethylene [32] have also been used. One paper [33] presents the use of the smallest form of silica –polyhedral oligomeric silsesquioxane (POSS), in PP matrix. The results of the papers [17-33] indicate that silica nanocomposites are emerging materials for the field of insulation: improved voltage endurance, partial discharge resistance and breakdown strength have been reported.

This study concentrates on the morphology characterization, dielectric properties and partial discharge endurance of PP Silica nanocomposite and discusses the applicability of the material in high voltage equipment. This paper is a continuation of the work published in [34].

2 EXPERIMENTAL

2.1 MATERIALS USED

The processing of materials was conducted at the Technical Research Centre of Finland (VTT). Polypropylene homopolymer (HC318BF) from Borealis Polymers N. V. was used as a matrix polymer. The polypropylene used is designed for capacitor films. The silica filler used was Aeroxide LE2 hydrophobic fumed silica from Evonik Degussa GmbH.

Manuscript received on 12 September 2009, in final form 19 April 2010.

1070-9878/10/$25.00 © 2010 IEEE

Authorized licensed use limited to: Tampereen Teknillinen Korkeakoulu. Downloaded on August 09,2010 at 09:03:35 UTC from IEEE Xplore. Restrictions apply.

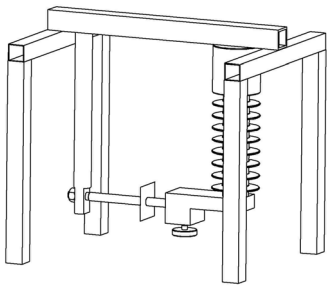

Figure 1. Measurement bench for breakdown strength measurements.

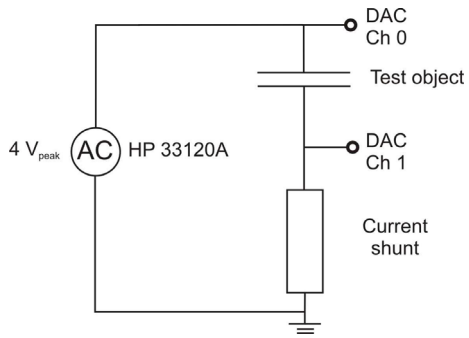

Figure 2. Measurement setup for dielectric response measurements.

The premixed materials, polymer powder and 5 wt-% of silica filler (primary particle size 12 nm, surface area 200 m^2/g) were fed into the first zone of the compounder (Berstorff ZE 25x48D) by a gravimetric twin screw feeder. Parameters in the compounding were: temperature (profile) +180…+200 °C, 300 rpm and torque 60-70 %. High shear screw geometry was used for mixing. The wt-% of the mixture was calculated from the weight of the polymer. The materials were processed into 100 mm x 0.5 mm sheets with minimum orientation in the machine direction with Brabender Plasticorder single screw extruder (∅ 18 mm) using a flat die. The samples were then bi-axially oriented with sheet stretching machine (Brückner KARO IV, +162 °C, 471 %/s, draw ratio 5.6 x 5.6, simultaneously). The thickness of the bi-axially oriented samples varied from 11 µm to 23 µm.

2.2 AC AND DC BREAKDOWN STRENGTH MEASUREMENTS

ac and dc breakdown strength of the test samples were measured at Tampere University of Technology. The measurements were performed at room temperature (~20 °C). The size of the test samples was approximately 3 cm x 3 cm. Rod-like electrodes having a diameter of 12 mm and made of stainless steel were used in the measurements. Graphite layers between the samples and steel electrodes were used to smooth the contact to the sample. The samples were manually fixed to the electrode setup (Figure 1). The measurements were performed by immersing the sample and the electrodes in mineral oil (Shell Diala DX) in order to avoid surface discharges and the edges of the electrodes (r =1 mm) were also rounded for that reason. The thickness of the samples was measured before immersing the sample in oil. Each sample was stressed with steadily increasing ac (50 Hz) or dc voltage until breakdown occurred. The voltage ramp used was approximately 400 V/s [35]. A set of 20 test samples was used with both materials (PP Reference and PP Silica composite) and voltage shapes.

2.3 DIELECTRIC RESPONSE

Dielectric response of the samples was measured using Arbitrary Waveform Impedance Spectroscopy (AWIS) presented in [36]. The measurements were conducted at Chalmers University of Technology. The measurement system (Figure 2) is designed to measure dielectric response using arbitrary repetitive voltage signals. Both the applied voltage signal and the current response were measured by a data acquisition card (DAC) and Fourier transformed into the frequency domain where a dielectric response spectrum can be extracted. The system demands careful calibration procedures to be accurate, and they are also presented in [36]. In the present study, AWIS was used as a low voltage FDS (Frequency Domain Spectroscopy) instrument in order to perform dielectric response measurements on low impedance (i.e. high capacitance), low loss test objects not easily characterized by commercial instruments. The measurement setup used is similar to that presented in [37], where aluminum bars are used as connectors in order to reduce series resistance and inductance.

Silver electrodes (d=3 cm) were painted on biaxially oriented thin film samples in order to ensure good contact to the material. After painting the samples were heat treated at 60 °C for 18 h under compressive stress in order to avoid creasing of the film. Creasing of the film can cause cracking of the silver paint layer, distorting the measurements. Heat treatment also excludes the moisture from the insulation. One sample of both materials was measured and three data points were collected at each frequency and temperature (43 Hz…43 kHz; RT (22 °C), 40 °C, 60 °C, 80 °C and 100 °C). The voltage used was 4 V_{peak}.

2.4 PARTIAL DISCHARGE MEASUREMENTS

PD levels were measured during PD endurance tests conducted at Tampere University of Technology. Tests were carried out at 2, 3, 3.5, 4, 4.5 and 5 kV_{RMS} voltage levels (50 Hz) until breakdown occurred. Eight parallel samples were measured with PP and PP Silica composite at each voltage level. Erosion speeds were calculated for each measurement dividing the breakdown time by the thickness of the sample. The electrode setup used was a conical rod-plane arrangement (Figure 3) and the rod was barely in contact with the test object. A conical rod electrode was chosen to simulate small, puncture-like flaws in the insulation material or in the electrodes. Those weak spots determine e.g. the electric fields used in capacitors and in general impair the reliability of insulation systems.

The PD measuring system used consisted of a material sample, a high voltage transformer, a coupling capacitor, an IEC 60270 [38] bandpass filter (bandwith: 45-430 kHz) and amplifier, an acquisition card with sampling frequency of 5 MS/s and a PC with Matlab based software for the analysis of the PD pulses. The acquisition card takes samples periodically

Authorized licensed use limited to: Tampereen Teknillinen Korkeakoulu. Downloaded on August 09,2010 at 09:03:35 UTC from IEEE Xplore. Restrictions apply.

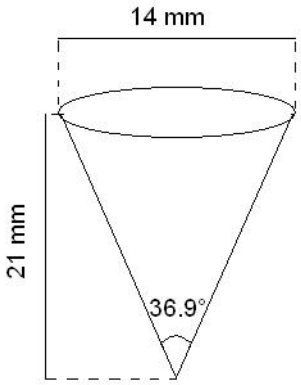

Figure 3. Sketch of the conical rod electrode used in the partial discharge measurements.

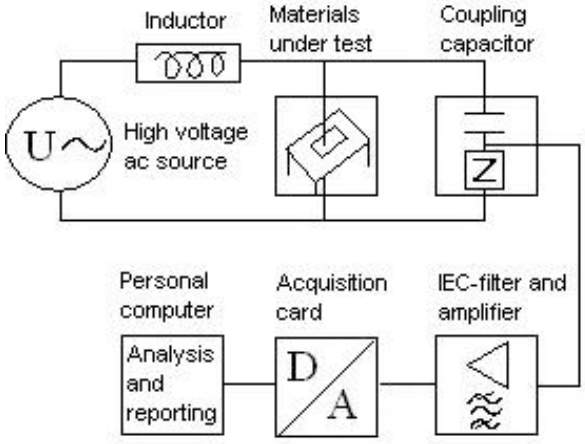

Figure 4. PD measuring system.

one per second during the measurement. The software calculates the largest repeatedly occurring pulse (LROP) from the samples according to the IEC 60270 standard and makes a report of the measurements. The PD measuring system is presented in Figure 4.

2.5 SURFACE ANALYSIS

After PD endurance tests material surfaces were analyzed with optical microscopy at University of Jyväskylä. Both non-stressed and stressed areas were studied for PP Reference and PP Silica composite at the various voltage levels used.

2.6 STATISTICAL ANALYSIS

Statistical analysis was applied to the breakdown strength measurement results. Results were calculated according to the IEEE standard "IEEE Guide for the Statistical Analysis of Electrical Insulation Breakdown Data" [39] using Microsoft Excel and Matlab programs.

All the measurement results were transferred to equal the breakdown strength of 9 μm thick film using the power law (Eq. 1) relationship between the breakdown field and the film thickness in order to obtain comparable results.

$$E_2 = E_1\left[d_2 / d_1\right]^{-0.4} \quad (1)$$

In the equation E_2 is the breakdown strength at thickness d_2 (9 μm) and E_1 is the measured value of the film of which the thickness is d_1 [39].

The dielectric breakdown voltage data was plotted on the Weibull probability plots according to a two-parameter Weibull distribution, stating a zero location parameter. The 2-parameter Weibull cumulative distribution function (Eq. 2) is related to the probability of failure occurring in certain field strength x.

$$F(x) = 1 - \exp\left\{-\left[\frac{x}{\beta}\right]^{\alpha}\right\} \quad (2)$$

The shape parameter β is related to the shape or the width of the distribution. The spread of the breakdown strengths is narrower when the value of β is higher. There is a smaller scattering of the dielectric strength values and consequently higher reliability of the dielectric behavior of the material when the shape parameter is high. Scale parameter α is related to the 63.2 % probability for the sample to break down at electric field strength α [40].

Statistical differences between two materials can be compared by average standard deviation (s_{ave}), which is the weighted average value of the two standard deviations of the materials. The difference between the breakdown strength means (dif) of the materials is compared with relevant sectors. These sectors are not significant (dif $\leq 1.96\times s_{ave}$), almost significant ($1.96\times s_{ave} <$ dif $\leq 2.58\times s_{ave}$), significant ($2.58\times s_{ave} <$ dif $\leq 3.29\times s_{ave}$) and extremely significant (dif $> 3.29\times s_{ave}$). With these quantiles statistical significance levels can be calculated and differences between the materials evaluated [39-40].

3 RESULTS

3.1 MORPHOLOGY

The PP Silica composite was characterized at the University of Jyväskylä. The nanoscale dispersion of silica in the PP matrix was investigated with TEM. Ultrathin sections of the sample were obtained using a diamond knife at room temperature on a Leica Reichert Ultracut S ultramicrotome. The sections of 95 nm thickness were collected on a copper grid and observed with JEOL-JEM-1200EX electron microscope at 60 kV acceleration voltage. From Figure 5b) it can be seen that the nanoparticles are gathered together to form clusters of a few tens to hundreds of particles. The agglomerates are nevertheless mostly in the <100 nm size range. Figure 5a) shows that these clusters are dispersed evenly in the polymer matrix.

Authorized licensed use limited to: Tampereen Teknillinen Korkeakoulu. Downloaded on August 09,2010 at 09:03:35 UTC from IEEE Xplore. Restrictions apply.

Table 1. ac and dc breakdown strength measurement results of PP Reference and PP Silica nanocomposite.

	n	mean	s	± 95 % confidence	α	β	95 %	cor
AC		V/μm	V/μm	V/μm	V/μm	V/μm	V/μm	
PP ref.	20	361	89	39	400	3.62	542	0.85
silica	20	432	57	25	458	8.62	520	0.97
DC								
PP ref.	20	511	93	41	552	5.75	668	0.92
silica	20	778	89	39	817	10.03	912	0.91

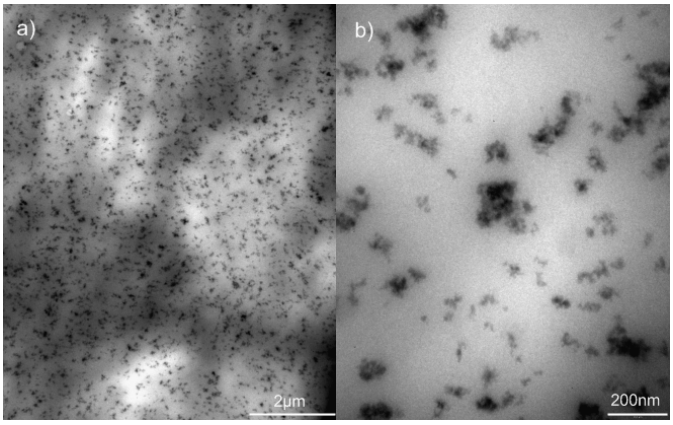

Figure 5. TEM micrographs of ultrathin sections of the PP Silica composite.

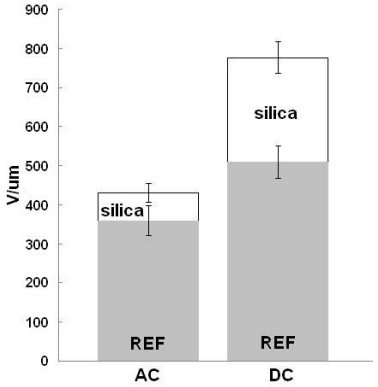

Figure 6. Ac and dc breakdown strengths (V/μm, RMS) of PP Reference and PP Silica composite with their 95 % confidence limits.

Micrometer sized particles were also seen by inspection with an optical microscope. With micro-Raman spectroscopy these particles were identified to be calcite mineral ($CaCO_3$), a contamination presumably from the compounder. A three-dimensional image of the composite structure was obtained by SkyScan 1172 X-ray microtomography device with detail detectability of 0.9 μm. Structure analysis based tomographic images revealed the average volume of the micro-sized particles to comprise 0.8 % of the total sample volume, which corresponds to ~2.3 wt-% assuming the density of calcite to be 2.71 g/cm^3.

3.2 AC AND DC BREAKDOWN STRENGTH

Table 1 shows the ac and dc breakdown strength measurement results of PP Reference and PP Silica nanocomposite. The same results are presented graphically in Figures 6-8. Silica composite gave higher ac and dc dielectric strengths than PP Reference (per cent values 19.9 and 52.3, respectively calculated from the mean values, Figure 6). Equally important is that with both voltage shapes the β value of the nanocomposite is higher than with PP Reference, an indicator of smaller standard deviation and homogeneous material (Figure 5). These results have an interesting impact on insulation system design, because safety margins and insulation thicknesses can be reduced.

The value of the critical correlation coefficient for 20 parallel samples is approximately 0.94 (according to IEEE Standard 930) [39]. The correlation (R^2) values presented in Table 1 are close to the critical correlation coefficient for all the samples. The correlation value for PP Reference is low because in two samples ac breakdown occurred with very low

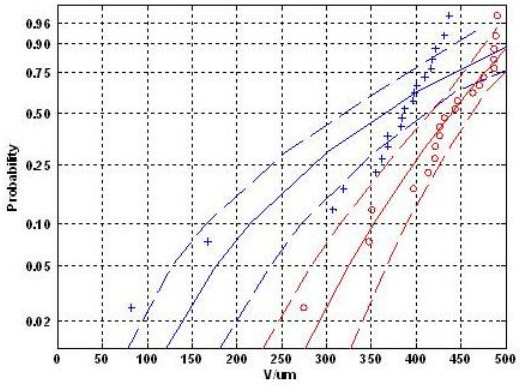

Figure 7. Ac breakdown strength measurements of PP Reference (+) and PP Silica composite (O) presented in the Weibull probability plot.

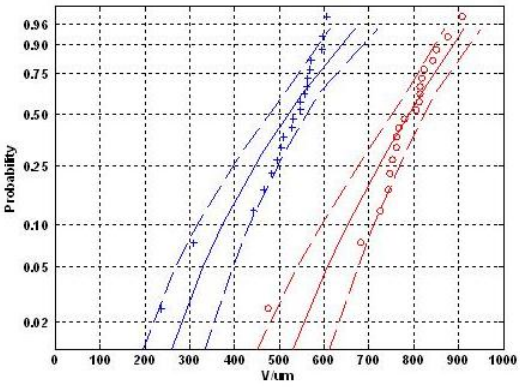

Figure 8. Dc breakdown strength measurements of PP Reference (+) and PP Silica composite (O) presented in the Weibull probability plot.

Authorized licensed use limited to: Tampereen Teknillinen Korkeakoulu. Downloaded on August 09,2010 at 09:03:35 UTC from IEEE Xplore. Restrictions apply.

electric field (82 V/μm, 167 V/μm, Figure 7). Without these two measurements the correlation to 2-parameter Weibull distribution would have been 0.99. With thin film samples (10-30 μm) the quality of the dielectric material can be seen more clearly compared to thicker samples (0.1-1 mm). The weak spots of the dielectric material are emerging and thus data scatter at low probability.

The Weibull probability plots with 90 % confidence bounds are shown in Figures 7 and 8 for PP Reference and PP Silica nanocomposite with ac and dc voltages, respectively. The average standard deviation in the measurements was 7.4 %. Especially with dc breakdown strength measurements the confidence bounds are narrow. Breakdown strength measurements with PP Silica nanocomposite are shifted towards higher electric field strengths (to the right). Statistically the changes in ac and dc breakdown strengths were not significant and significant, respectively.

3.3 DIELECTRIC RESPONSE

The results of dielectric response, capacitance and loss factor, measurements of PP Reference and PP Silica nanocomposite are presented in Figures 9-11. Relative deviations in capacitance measurements were less than 0.3 ‰ (Figure 9) and in loss factor measurements in the order of 10^{-4} (Figures 10 and 11). The highest deviations were achieved with the lowest frequencies (<100 Hz) due to small capacitive current (microamperes at 43 Hz) in the circuit. At higher frequencies (>10 kHz) reliable results are not available due to line inductances. Normalized capacitance did decrease with the same trend in both materials until 80 °C but at 100 °C differences can be seen. It has also been reported in [41] that PP capacitor has a negative temperature coefficient. There may be changes in electrodes or PP Ref. sample, which cause the increase of capacitance at 100 °C. Loss factors for both materials were at the same level and behaved in the same way with increasing temperature. Measurements at 40 °C and 80 °C were omitted from Figures 10 and 11 to show the differences more clearly. It seems that with respect to standard deviations in the measurements capacitance and loss factor behavior as a function of temperature is the same with PP Reference and PP Silica nanocomposite, at temperatures from RT (22 °C) to 80 °C. This is important considering e.g. power capacitors, which operate at 50-60 °C temperature region. There is no capacitance change compared to PP Reference and no additional heat is produced due to low loss factor.

3.4 PARTIAL DISCHARGE ENDURANCE

When ac voltage was applied to the material samples, partial discharges occurred smoothly around the electrode and material sheets. No large sliding discharges were observed. The discharge patterns of the materials studied were uniform around the electrode.

The results of the partial discharge endurance measurements are presented in Figures 12-14. In Figure 12 the erosion speed of PP Reference and PP Silica nanocomposite are presented as a function of ac voltage. When the probability for breakdown increases with voltage the deviation bars also

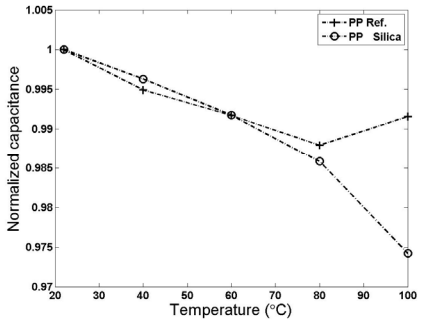

Figure 9. Normalized capacitance of PP Reference and PP Silica nanocomposite as a function of temperature (43 Hz).

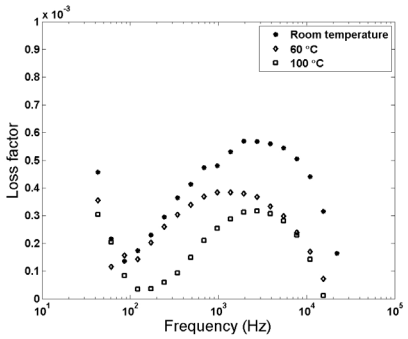

Figure 10. Dielectric losses of PP Reference as a function of frequency at different temperatures.

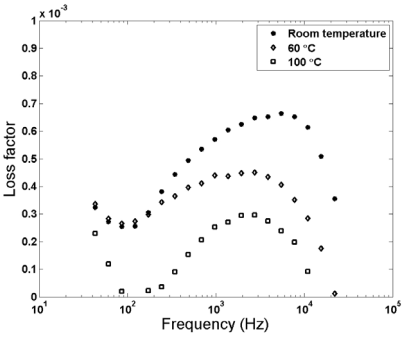

Figure 11. Dielectric losses of PP Silica composite as a function of frequency at different temperatures.

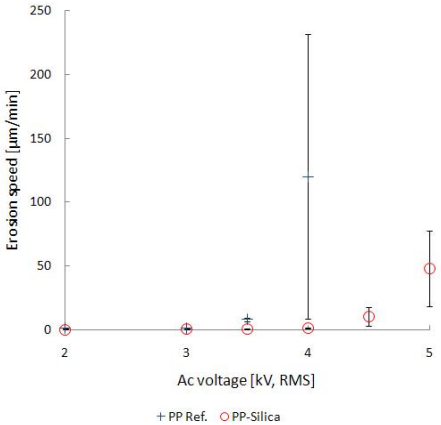

Figure 12. Erosion speeds and 95 % confidence limits of PP Reference and PP Silica nanocomposite as a function of voltage.

increase. For PP Reference 4 kV caused large scattering of erosion speeds and breakdowns occurred shortly after applying the voltage (on average 149 s). Thus, PD endurance

Authorized licensed use limited to: Tampereen Teknillinen Korkeakoulu. Downloaded on August 09,2010 at 09:03:35 UTC from IEEE Xplore. Restrictions apply.

of PP Reference could not be measured at voltages above 4 kV. For PP Silica nanocomposite 5 kV was enough to cause wide scattering. When a few measurement spots (PP Reference 4 kV and PP Silica 5 kV) are taken away from the Figure 12, we can get a better view of the situation at lower voltages and see the differences there (Figure 13). The erosion speeds of PP Reference were 8.2, 2.6, 7.0 and 68 times higher than with PP Silica nanocomposite at 2, 3, 3.5 and 4 kV, respectively. Statistically, these changes in erosion speed as a function of voltage were extremely significant, almost significant, extremely significant and not significant, respectively. Wide deviation at 4 kV with PP Reference material caused this difference to be not significant.

The partial discharge levels were measured during the partial discharge endurance tests. Figure 14 presents the partial discharge levels as a function of time at voltage levels 2 kV and 3.5 kV. The average breakdown times can be seen from Figure 14 for PP Reference and PP Silica nanocomposite. Average breakdown times were at 2 kV level 464 s and 6340 s and at 3.5 kV level 120 s and 1284 s. Partial discharge patterns seemed to stabilize according to Figure 14, but when closer to breakdown the PD level increased. On the other hand with rising voltage the deviation in the partial discharge levels also increased because of the growing probability of surface discharge channels. Standard deviations for PP Reference and PP Silica were 385 pC and 451 pC at 2 kV and 980 pC and 503 pC at 3.5 kV, respectively. The smallest detectable discharge was 74 pC on average in all PD endurance measurements. From the partial discharge measurements it can be concluded that the same erosion behavior for PP Silica nanocomposite was achieved with 1 kV higher ac voltage compared to PP Reference. Also, the partial discharge level at the same voltages was higher with PP Reference material than with PP Silica nanocomposite. The results of the PD endurance measurements indicate that the speed of surface erosion and PD level of PP Silica nanocomposite are lower than with PP Reference. Imperfections in the insulation material or in the electrodes cause concentration of electric field and impair the reliability of insulation systems during their lifetime.

3.5 SURFACE ANALYSIS

Figures 15 and 16 present the optical microscope pictures of the surface analysis of PP Reference and PP Silica. Figure 15a presents the non-stressed PP Reference material and Figures 15b, 15c and 15d present the stressed PP Reference material after PD stress at 2 kV, 3 kV and 4 kV voltages, respectively. The stressed areas were approximately 4 mm in diameter depending on the voltage used. In PP Reference material dots or "craters" formed on the surface of the material because of PD stress. "Craters" were few μm in diameter, but located in all over the stressed area. These spots are probable initial spots of the total breakdown of the sample.

By contrast, PP Silica nanocomposite looked totally different after PD stress. Round and whitish layers were formed on the surface on the nanocomposite during the stress and "craters" could not be found in that scale as with PP Reference. Whitish layers may protect the PP Silica composite from degradation

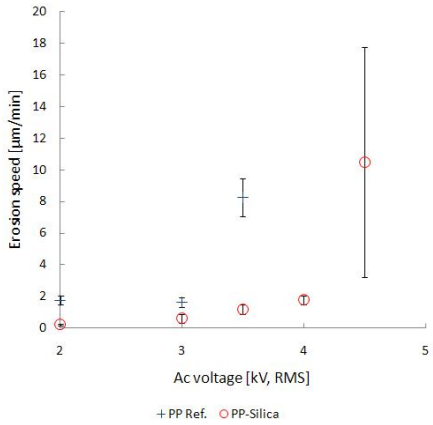

Figure 13. Erosion speeds and 95 % confidence limits of PP Reference and PP Silica nanocomposite as a function of voltage.

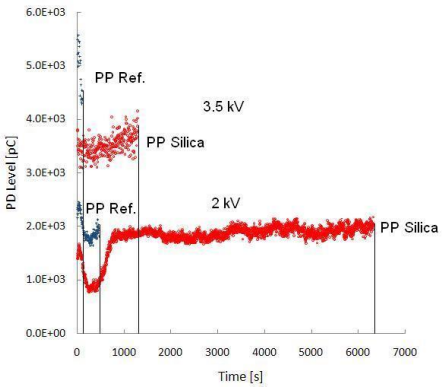

Figure 14. Partial discharge levels of PP Reference and PP Silica nanocomposite as a function of time at 2 kV and 3.5 kV ac voltages.

and lengthen the life-time of the sample. This shielding behavior is significant because whitish layers are formed due to PD stress to critical spots of insulation. Hydrophobic silica also forms a hydrophobic surface for the material and therefore better surface current resistance is achieved.

Bi-axially oriented PP films have exfoliated surface structures (Figures 15a and 16a) with average roughness about 600 nm (measured area 100 μm^2). The highest electric field and PDs exist inside the surface blisters, where the distance to the ground potential is shortest. This is clearly visible at 2 kV and partly also at 3 kV (Figures 16b and 16c). From Figure 16b (after 2 kV voltage stress) it seems that whitish layers formed in a round shape but in Figures 16c and 16d the layers are evenly distributed due to higher voltage stresses (3 and 4 kV).

4 DISCUSSION

Nanodispersion of the silica filler is a prerequisite for improved dielectric behavior of PP Silica nanocomposite. Nanodispersion relates further to scattering and reduced space charge accumulation, which have an effect on ac and dc behavior of the nanocomposite. These phenomena are related to increased short-term breakdown strength results [42]. Nanodispersion of silica also ensures low loss factor of the nanocomposite. The large fraction of interface volume and polymer chain entanglement keep the motion of charge carriers limited. The lower speed of erosion and PD level are related to scattering phenomenon and shielding effect at the surface of the nanocomposite. PD stress is segmented into

Authorized licensed use limited to: Tampereen Teknillinen Korkeakoulu. Downloaded on August 09,2010 at 09:03:35 UTC from IEEE Xplore. Restrictions apply.

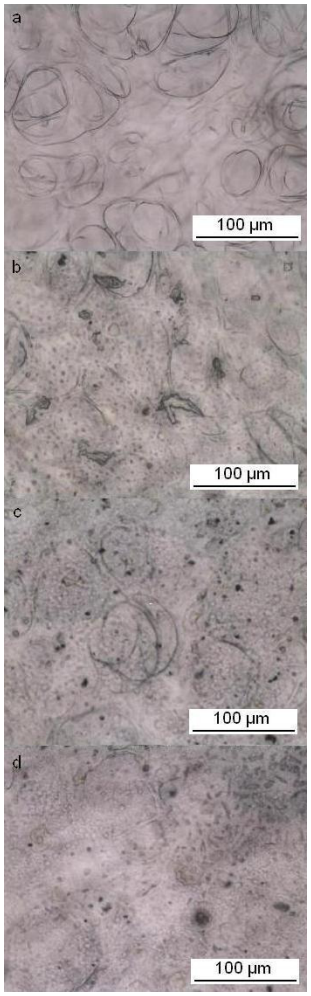

Figure 15. Optical microscope pictures from PP Reference. a) from non-stressed area, b) stressed area at 2 kV, c) stressed area at 3 kV and d) stressed area at 4 kV.

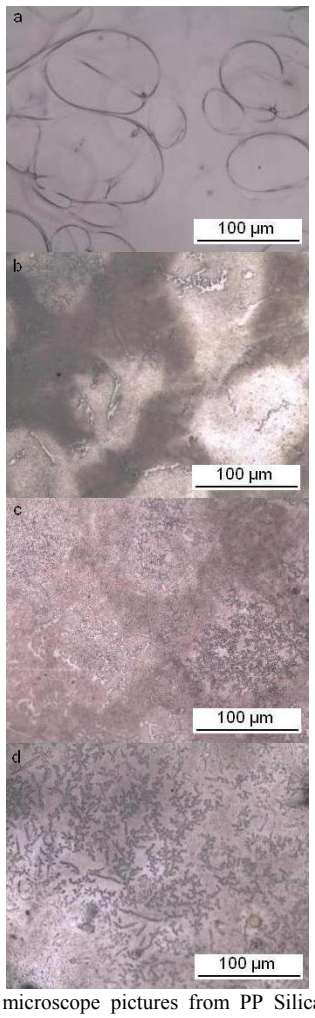

Figure 16. Optical microscope pictures from PP Silica nanocomposite. a) from non-stressed area, b) stressed area at 2 kV, c) stressed area at 3 kV and d) stressed area at 4 kV.

nanoscale and large interfacial area provides barriers against erosion [42]. In addition, it seems that shield is developed at the surface of the nanocomposite to resist degradation of the material and especially the inter-filler space.

5 CONCLUSION

PP Silica nanocomposite was studied with TEM. TEM pictures revealed that silica is well distributed in the matrix and no large agglomerates of the additive could be found. Proper nanodispersion reflects to improved dielectric behavior of PP Silica nanocomposite. PP Silica nanocomposite showed a promising combination of dielectric properties considering especially ac and dc power capacitors.

The ac and dc breakdown strength of PP Silica nanocomposite increased 19.9 % and 52.3 %, respectively. Equally important is that with both voltage shapes the β value of the nanocomposite is higher than with PP Reference, an indicator of smaller standard deviation and homogeneous material. These results have an interesting impact on insulation system design, because safety margins and insulation thicknesses can be reduced.

Usually the dielectric losses also increased hand in hand with breakdown strength, but with PP Silica nanocomposite losses remained comparable to the PP Reference material. Normalized capacitance did decrease by the same trend with both materials until 80 °C. This is important considering e.g. power capacitors, which operate at 50-60 °C temperature region. There is no capacitance change compared to PP Reference and no additional heat is produced due to low loss factor.

In PD endurance measurements the erosion speeds for PP Reference were 8.2, 2.6, 7.0 and 68 times higher than for PP Silica nanocomposite at 2, 3, 3.5 and 4 kV, respectively. Also, the PD levels at the same voltage level were higher for PP Reference than for PP Silica nanocomposite. Surface analysis of the films revealed that a whitish layer formed on the surfaces of the PP Silica nanocomposite during PD stress. Whitish layers may protect the PP Silica composite from degradation and lengthen the life-time of the sample. This shielding behavior is significant because whitish layers are formed due to PD stress to critical spots of insulation.

REFERENCES

[1] J. K. Nelson, Y. Hu and J. Thiticharoenpong, "Electrical Properties of TiO_2 Nanocomposites", IEEE Conf. Electr. Insul. Dielectr. Phenomena (CEIDP), pp. 719-722, 2003.

[2] S. Rätzke and J. Kindersberger, "Erosion Behaviour of Nano Filled Silicone Elastomers", XIVth Intern. Sympos. High Voltage Eng. (ISH), pp. 1-6, 2005.

Authorized licensed use limited to: Tampereen Teknillinen Korkeakoulu. Downloaded on August 09,2010 at 09:03:35 UTC from IEEE Xplore. Restrictions apply.

[3] T. J. Lewis, "Interfaces are the Dominant Feature of Dielectrics at the Nanometric Level", IEEE Trans. Dielectr. Electr. Insul., Vol. 11, pp. 739-753, 2004.

[4] M. F. Frechette, M. Trudeau, H. D. Alamdari and S. Boily, "Introductory Remarks on Nanodielectrics", IEEE Conf. Electr. Insul. Dielectr. Phenomena (CEIDP), pp. 92-99, 2001.

[5] G. C. Montanari, D. Fabiani, F. Palmieri, D. Kaempfer, R. Thomann and R. Mülhaupt, "Modification of Electrical Properties and Performance of EVA and PP Insulation through Nanostructure by Organophilic Silicates", IEEE Trans. Dielectr. Electr. Insul., Vol. 11, pp. 754-762, 2004.

[6] J. K. Nelson and Y. Hu, "Nanocomposite Dielectrics-Properties and Implications", J. Phys. D: Appl. Phys., Vol. 38, pp. 213-222, 2005.

[7] T. J. Lewis, "Nanometric Dielectrics", IEEE Trans. Dielectr. Electr. Insul., Vol. 1, pp. 812-825, 1994.

[8] S. Pothukuchi, Y. Li and C. P. Wong, "Shape Controlled Synthesis of Nanoparticles and Their Incorporation into Polymers", Electronic Components and Technology Conf., pp. 1965-1967, 2004.

[9] J. K. Nelson and J. C. Fothergill, "Internal Charge Behaviour of Nanocomposites", Nanotechnology, Vol. 15, pp. 586-595, 2004.

[10] T. Tanaka, G. C. Montanari and R. Mülhaupt, "Polymer Nanocomposites as Dielectrics and Electrical Insulation- perspectives for Processing Technologies, Material Characterization and Future Applications", IEEE Trans. Dielectr. Electr. Insul., Vol. 11, pp. 763-784, 2004.

[11] T. Tanaka, M. Kozako, N. Fuse and Y. Ohki, "Proposal of a Multi-core Model for Polymer Nanocomposite Dielectrics", IEEE Trans. Dielectr. Electr. Insul., Vol. 12, pp. 669-681, 2005.

[12] J. K. Nelson, J. C. Fothergill, L. A. Dissado and W. Peasgood, "Towards an Understanding of Nanometric Dielectrics", IEEE Conf. Electr. Insul. Dielectr. Phenomena (CEIDP), pp. 295-298, 2002.

[13] A. L. An and S. A. Boggs, "What is "Nano" in the Context of a Filled Dielectric", Conf. Record of the 2006 IEEE Intern. Sympos. Electr. Insul., pp. 273-276, 2006.

[14] T. Tanaka, "Dielectric Nanocomposites with Insulating Properties", IEEE Trans. Dielectr. Electr. Insul., Vol. 12, No. 5, pp. 914-928, 2005.

[15] M. Roy, J. K. Nelson, R. K. MacCrone, L. S. Schandler, C. W. Reed, R. Keefe and W. Zenger, "Polymer Nanocomposite Dielectrics: The Role of the Interface", IEEE Trans. Dielectr. Electr. Insul., Vol. 12, No. 4, pp. 629-643, 2005.

[16] M. F. Frechette and C. W. Reed, "The Emerging Field of Nanodielectrics: an Annotated Appreciation", IEEE Intern. Sympos. Electr. Insul., pp. 458-465, 2006.

[17] T. Tanaka and M. Frechette, "Emerging Nanocomposite Dielectrics", CIGRE Task Force Report, ELECTRA, No. 226, pp. 24-32, 2006.

[18] K. Jiang, L. Cheng, L. Zheng, Z. Yao, G. Li and Q. Yin, "The Unique Dielectric Behaviour of Nanosilica Epoxy Composites", 7th IEEE Intern. Conf. Nanotechnology, pp. 1101-1106, 2007.

[19] T. Imai, G. Komiya, K. Murayama, T. Ozaki, F. Sawa, T. Shimizu, M. Harada, M. Ochi, Y. Ohki and T. Tanaka, "Improving Epoxy-based Insulating Materials with Nano-fillers toward Practical Application", IEEE Intern. Sympos. Electr. Insul., pp. 201-204, 2008.

[20] T. Tanaka, Y. Ohki, M. Ochi, M. Harada and T. Imai, "Enhanced Partial Discharge Resistance of Epoxy/Clay Nanocomposite Prepared by Newly Developed Organic Modification and Solubilization Methods", IEEE Trans. Dielectr. Electr. Insul., Vol. 15, pp. 81-89, 2005.

[21] T. Imai, F. Sawa, T. Nakano, T. Ozaki, T. Shimizu, M. Kozako and T. Tanaka, "Effects of Nano- and Micro-filler Mixture on Electrical Insulation Properties of Epoxy Based Composites", IEEE Trans. Dielectr. Electr. Insul., Vol. 13, pp. 319-326, 2006.

[22] T. Iizuka, K. Uchida and T. Tanaka, "Different Voltage Endurance Characteristics of Epoxy/silica Nanocomposites Prepared by Two Kinds of Dispersion Methods", IEEE Conf. Electr. Insul. Dielectr. Phenomena (CEIDP), pp. 236-239, 2007.

[23] T. Tanaka, Y. Matsuo and K. Uchida, "Partial Discharge Endurance of Epoxy/SiC Nanocomposite", IEEE Conf. Electr. Insul. Dielectr. Phenomena (CEIDP), pp. 13-16, 2008.

[24] T. Iizuka, Y. Ohki and T. Tanaka, "Effects of Coupling Agents and Filler Dispersion on V-t Characteristics of Epoxy/Silica Nanocomposites", Intern. Sympos. Electr. Insulating Materials, pp. 60-63, 2008.

[25] I. Ramirez, E. A. Cherney, S. Jayaram and M. Gauthier, "Silicone Rubber Nanocomposites for Outdoor Insulation Applications", IEEE Conf. Electr. Insul. Dielectr. Phenomena (CEIDP), pp. 384-387, 2007.

[26] I. Ramirez, S. Jayaram, E. A. Cherney, M. Gauthier and L. Simon, "Erosion Resistance and Mechanical Properties of Silicone Nanocomposite Insulation", IEEE Trans. Dielectr. Electr. Insul., Vol. 16, pp. 52-59, 2009.

[27] N. A. Perez, A. Sylvestre, J. L. Auge, M. T. Do and S. Rowe, "Dielectric Spectroscopy in Silicone Rubber Incorporating Nanofillers", IEEE Conf. Electr. Insul. Dielectr. Phenomena (CEIDP), pp. 453-456, 2006.

[28] A. H. El-Hag, L. C. Simon, S. H. Jayaram and E. A. Cherney, "Erosion Resistance of Nano-filled Silicone Rubber", IEEE Trans. Dielectr. Electr. Insul., Vol. 13, pp. 122-128, 2006.

[29] M. Zhang, S. Zeng, T. Dong, Y. Fan and Q. Lei, "Study on the Dielectric Properties of Polyimide/Silica Nanocomposite Films", IEEE 8th Intern. Conf. Properties and Applications of Dielectric Materials (ICPADM), pp. 733 – 735, 2006.

[30] F. Guastavino, E. Torello, A. Dardano, S. Bono, M. Pellegrini and L. Vignati, "A Comparison of the Short and Long Term Behaviour of Nanostructured Enamels with the Performances of Conventional Insulation", IEEE Intern. Sympos. Electr. Insul., pp. 659-662, 2008.

[31] B. Chen, J. Du and C. Hou, "The Effects of Chemical Structure on the Dielectric Properties of Polyetherimide and Nanocomposites" IEEE Trans. Dielectr. Electr. Insul., Vol. 15, pp. 127-133, 2008.

[32] C. Zou, J. C. Fothergill, M. Fu and J. K. Nelson, "Improving the Dielectric Properties of Polymers by Incorporating Nano-particles", 10th Intern. Conf. Electr. Insul., INSUCON, Birmingam, UK, pp. 125-130, 2006.

[33] M. Takala, M. Karttunen, P. Salovaara, S. Kortet, K. Kannus and T. Kalliohaka, "Dielectric Properties of Nanostructured Polypropylene-Polyhedral Oligomeric Silsesquioxane Compounds", IEEE Trans. Dielectr. Electr. Insul., Vol. 15, pp. 40-51, 2008.

[34] M. Takala, H. Ranta, J. Pelto, S. Virtanen, V. Koivu, M. Pettersson, K. Kannus, "Dielectric Properties of Polypropylene-Silica Nanocomposites", 21st Nordic Insulation Symposium, NORD-IS09, Gothenburg, Sweden, pp. 31-35, 2009.

[35] IEC Publication 60243-1: "Electrical Strength of Insulating Materials-Test Methods-Part 1: Test at Power Frequencies", 1998.

[36] B. Sonerud, T. Bengtsson, J. Blennow, and S. M. Gubanski, "Dielectric response measurements utilizing semi-square voltage waveforms", IEEE Trans. Dielectr. Electr. Insul., Vol. 15, pp. 920-926, 2008.

[37] B. Sonerud, T. Bengtsson, J. Blennow, and S. M. Gubanski, "High voltages with high harmonic content: The influence on dielectric heating" in Proceedings of the 16th International Symposium of High Voltage Engineering (ISH 09), Cape Town, South Africa, Paper ID F5, 2009.

[38] IEC 60270: "High-Voltage Test Techniques - Partial Discharge Measurements", 2000.

[39] IEEE Standard 930: "IEEE Guide for the Statistical Analysis of Electrical Insulation Breakdown Data", IEEE Dielectr. Electr. Insul. Society, 2005.

[40] W. Hauschild and W. Mosch, Statistical Techniques for High-Voltage Engineering, Peter Peregrinus Ltd., London, UK, 1992.

[41] P. K. Bun and S. P. Kang, "Temperature Coefficient and Capacitance Retrace of Polypropylene Film Capacitors", IEEE Trans. Electr. Insul., Vol. 9, pp. 5-11, 1974.

[42] M. G. Danikas and T. Tanaka, "Nanocomposites-A Review of Electrical Treeing and Breakdown", IEEE Electr. Insul. Mag., Vol. 25, pp. 19-25, 2009.

Authorized licensed use limited to: Tampereen Teknillinen Korkeakoulu. Downloaded on August 09,2010 at 09:03:35 UTC from IEEE Xplore. Restrictions apply.

Markus Takala was born in Vaasa, Finland in 1980. He graduated with the M.Sc. (Eng.) degree in electrical power engineering, Tampere University of Technology (TUT), Tampere, Finland in 2005. Since 2005 he has been a researcher in the High Voltage Laboratory at TUT. His research interests include topics in new electrical insulation materials. He has published articles on dielectric properties of polymer compounds, the main research topics being nano- and microstructured epoxy and PP.

Hannes Ranta was born in Vantaa, Finland in 1982. He graduated with the M.Sc. (Eng.) degree in electrical power engineering, Tampere University of Technology (TUT), Tampere, Finland in 2008. Since 2008 he has been a researcher in the High Voltage Laboratory at TUT. His main research interests are predicting and testing the long-term properties of new polymeric electrical insulation materials such as PP nanocomposites.

Pekka Nevalainen was born in Tampere, Finland in 1976. He graduated with the M.Sc. (Eng.) degree in electrical power engineering, Tampere University of Technology (TUT), Tampere, Finland in 2002. From 2002 he has been a researcher in the Department of Electrical Energy Engineering (TUT). He has been involved in numerous projects including Partial Discharge (PD) research. His main research work is focused on developing condition monitoring of medium voltage power cables using on-line PD measurements.

Pertti Pakonen was born in Ähtäri, Finland in 1966. He received the M.Sc. (Eng) and doctoral degrees from Tampere University of Technology (TUT) in 1992 and 2007, respectively. From 1992 to 1993 he worked as a teaching assistant, from 1993 to 2007 as a researcher and since 2007 he has worked as a senior researcher at the Department of Electrical Energy Engineering at TUT. His main research interests are in the area of high voltage engineering, especially condition monitoring of electrical insulations using partial discharge measurements (mainly applications in the field of covered conductor lines and MV underground cables) and radio interference measurements of power lines and substations.

Jani Pelto was born in Tampere, Finland in 1976. He received the M.Sc. (Eng.) degree in material science and plastics technology from Tampere University of Technology (TUT) in 2001. Since 2001 he has been working as a research scientist at the Technical Research Center of Finland (VTT). His main research interests are synthesis, processing and characterization (AFM, electrochemistry and spectroscopy) of new conductive inherently conductive polymers such as polyanilines, polypyrroles, organic polymer nanocomposites and their applications.

Mikko Karttunen was born in Tampere, Finland in 1955. He received the M.Sc. (Eng.) and Licentiate of Technology degrees in material science and plastics technology from Tampere University of Technology (TUT), in 1980 and 1986, respectively. From 1980 to 1985 he was a research scientist at TUT. From 1985 to 1988 he worked at Neste Oy as a researcher. From 1988 to 1991 he was a research scientist at the Technical Research Centre of Finland (VTT) and since 1991 he has been a senior research scientist at VTT. His research interest is in electrically conductive polymer compounds, compliant electrodes and polymer nanocomposites for electromechanical films and electrical insulation materials.

Viivi Koivu was born in Anjalankoski, Finland, in 1981. She received the M.Sc. degree in applied physics from the University of Jyväskylä, Finland in 2004. Since 2004 she has been a researcher and doctoral student at that university. Her research interests are material physics, transport properties of porous heterogeneous materials and applications of x-ray micro and nano tomography.

Suvi Virtanen was born in Helsinki, Finland in 1979. She received the M.Sc. degree in organic chemistry from the University of Jyväskylä in 2004 at the international Master's Programme of nanoscience. Since 2004 she has been researcher and Ph.D. student in the same university. Her research interests are nanomaterials and their characterization.

Mika Pettersson was born in Helsinki, Finland in 1969. He received the M.Sc. and Ph.D. degrees in physical chemistry from the University of Helsinki in 1995 and 1998, respectively. He spent a post-doctoral period at the University of California, Irvine during 2000 – 2001 in Prof. V. A. Apkarians laboratory. He was appointed an academy research fellow of the Academy of Finland in 2002 for a 5-year period. He moved to the University of Jyväskylä in 2003 upon appointment as senior lecturer in physical chemistry. Since 2008 he has been an acting professor in physical chemistry at the University of Jyväskylä. His main research area is optical spectroscopy including frequency- time- and spatially resolved techniques.

Björn Sonerud (S'08) was born in Alvesta, Sweden in 1979. He received the M.Sc. degree (automation and mechatronics) in 2004 and the degree of Lic. Eng. (high voltage engineering) in 2007, both from Chalmers University of Technology. In 2009 he received the degree of M.A. (history of ideas and science) from the University of Gothenburg. He is currently pursuing the Ph.D. degree at Chalmers University of Technology. His research interests include dielectric response measurement techniques, material characterization and aging.

Kari Kannus was born in Längelmäki, Finland, on 17 May 1957. He received the M.Sc. (Eng.), Licentiate of Technology and doctoral degrees in electrical engineering from Tampere University of Technology (TUT) in 1981, 1987 and 1998, respectively. From 1982 to 1988 he was a teaching and research assistant and from 1988 to 1992 he was a laboratory manager at the Institute of Power Engineering of TUT. From 1993 to 1998 he was a researcher and since 1999 he has been a senior researcher at TUT. Since 2002 he has been an Adjunct Professor of High Voltage Engineering at TUT. His main research interests are in the field of high voltage technology, especially overvoltage protection and surge arresters, new polymeric materials and environmental testing.

Authorized licensed use limited to: Tampereen Teknillinen Korkeakoulu. Downloaded on August 09,2010 at 09:03:35 UTC from IEEE Xplore. Restrictions apply.